

**Investigations on Hydrodynamic and
Mass Transfer Behavior of
Draft Tube Bubble Columns**

**A thesis submitted to
The Maharaja Sayajirao University of Baroda
for the award of the degree
of**

Doctor of Philosophy
in
Chemical Engineering

By
Piyush B. Vanzara

**Under the supervision of
Prof. Dr. R. Sengupta**



**Chemical Engineering Department
Faculty of Technology and Engineering
The Maharaja Sayajirao University of Baroda
Vadodara - 390 001
January 2013**

CERTIFICATE

This is to certify that the thesis entitled “*Investigations on Hydrodynamic and Mass Transfer Behavior of Draft Tube Bubble Columns*” submitted by **Piyush B. Vanzara** in fulfillment of the requirements of the Degree of **Doctor of Philosophy in Chemical Engineering** is a bonafide record of the investigations carried out by him in the Department of Chemical Engineering, The Maharaja Sayajirao University of Baroda, Vadodara under my supervision and guidance. In my opinion, this thesis has attained the standard fulfilling the requirements of the Degree of Doctor of Philosophy as prescribed in the regulations of the University.

Prof. Dr. R. Sengupta
(Research Supervisor)

Professor in Chemical Engineering,
The Maharaja Sayajirao University of Baroda
Vadodara – 390 001

Head
Chemical Engineering Department,
The M. S. University of Baroda
Vadodara – 390 001

Dean
Faculty of Tech. and Engg.
The M. S. University of Baroda
Vadodara – 390 001

PAPERS PRESENTED

- **Piyush Vanzara** and R. Sengupta. “Assessment of fermenter geometries and flow patterns in the bench scale production of baker’s yeast.” Paper BTBE01, presented at the *International conference on “Recent Advances in Chemical Engineering and Technology” (RACET 2011)*; 10-12 March, 2011; Kochi, India.
- **Piyush Vanzara** and R. Sengupta. “Gas holdup studies in rectangular draft tube bubble column.” Poster 242, presented at the *Indian Chemical Engineering Congress - 2011 (CHEMCON-2011)*; 27-29 December, 2011; Bangalore, India.
- **Piyush Vanzara** and R. Sengupta. “Wastewater treatment using activated sludge in rectangular draft tube bubble column”. Paper TP1-5, presented at the *28th National Convention of Chemical Engineers (28NCCE-2012)*; 7-8 September, 2012; Ahmedabad, India.

Dedicated to my Family

ACKNOWLEDGEMENT

“*A journey of a thousand miles begin with a single step*”, and that step in my case was faith in **GOD**. It is the invisible source that kept me going through all these years which now looking back seems to have been impossible.

Fulfilment of God is in the person who leads you on the right track- my Guide. Words would fall short and could never justify my feelings of gratitude for my Ph. D. Guide **Dr. R. Sengupta**, Professor and Head of chemical engineering department of M.S. University of Baroda. His dedication towards work at this height of achievement and age is really praiseworthy. He has been indeed my friend, philosopher and guide in all terms and from the bottom of my heart I would like to thank him for giving me an opportunity to work under him. Special thanks also to **Prof. Dr. Bina Sengupta** and **Ms. Mira Sengupta** for all the hospitality they have showered on me during my visits.

I blossomed as a student and later as a faculty at V.V.P Engineering College, Rajkot. Honourable Chairman of V.V.P., **Shri Pravinkaka** has always been a source of inspiration for me. He has shown a great deal of interest in my Ph. D. work and has always motivated me to move ahead. Principal of V.V.P., **Prof. Dr. Sachin Parikh** has been instrumental in taking the lead and providing the entire required infrastructure (especially of environment audit laboratory) and other administrative supports from the college. I also would like to thank entire **V.V.P. managing committee** for all the support that they have bestowed upon me.

Chemical and Biotechnology engineering departments of my college have been always elemental in backing me up at all times. A special mention to **Dr. Jyoti Tolia**, former Head of chemical department who had always supported me in all the ways for my Ph.D. work. I would also like to appreciate **Dr. Omprakash Mahadwad**- present HOD, my colleagues-cum-friends **Dr. Sushil Korgaokar**, **Mr. Vyomesh Parsana** and **Mr. Dharmesh Sur** - HOD of biotechnology department, as well as **Mrs. Darshana Bhatti**, **Mr. Jilesh Pandya**, **Mr. Williams Koshy**, **Ms. Jyoti Verma**, **Ms. Rachana Devi** and some Ex-faculty members **Mr. Kiran Varma** and **Mr. Mayur Patel** for all the supports they have rendered to me. Sincere thanks also to **Ritaben Sapariya** and other teaching, semi-teaching and non-teaching staff including peons of my college, without their support and co-operation this thesis would have never been possible.

The M. S. University of Baroda deserves special recognition in this acknowledgment. I extend my sincere thanks to the **Dean, teaching and non-teaching staff of chemical department of MSU** for their generous support and the **librarian** for providing me all the resources and infrastructure.

I am also grateful to **GUJCOST** (Gujarat Council on Science and Technology) for some financial support in this research work by sanctioning a grant under Student Sci-Tech Project during 2009-10.

There were a few stars with me during my research work. - **Mr. Keyur Thaker**, DGM, Sun Pharmaceuticals-Baroda and **Mr Keyur Raval**, Associate Professor, Manipal University are the two names that stand out in this group. These guys have really done a lot, to help me out with various technical know-how. **Mr. Vishal Chavda and Mrs. Pooja Raja** from biotechnology department has also helped me a lot in the areas of fermentation, which was not my cup of tea. My dear **students** who have gone that extra mile to help me in my various works also deserve sincere thanks from my side. I am thankful to **Mr. Kalpesh Ahya** for drawing some figures in AutoCAD. The **officials of Rajkot Municipal Corporation** who were generous enough to provide me the activated sludge for my experiments also deserve due appreciation, I thank all of them.

My thesis required me to move to Baroda quite frequently. During this, I made for myself a family, not of blood relations but of love and affection. Different people who came across in my life in various occasions became my care takers at Baroda. I would like to mention by name **Mr. Ranpariya Hitesh, Mr. Nitin Khuman, Mr. Varun Patel**, my brother-in-law **Mr. Ninad Pujara** and **Mr Dhruv Pathak**, who considered me none other than their family member and arranged for accommodation in Baroda.

Last but not the least, I would like to extend my sincere love and gratitude to my role model my **Father**, my beloved **Mother**, my brother **Dr. Sanjay** and **other family members** for their blessings and the supports they have showered on me. Mentionable especially is **Parita** - my soul mate, who has always been infinitely patient and supporting during this entire course. My Son's education and all other responsibilities were entirely taken care by her, in spite of her hectic work schedule. At times, when I was down and out and was on the verge of giving up, my son **Rajat**'s cheerful smile pumped me up to keep moving till day. My words cannot describe my obligations to them.

Piyush B. Vanzara

INDEX

• LIST OF FIGURES	(i)
• LIST OF TABLES	(v)
• LIST OF SYMBOLS	(vi)
• LIST OF ABBREVIATIONS	(ix)

CONTENTS

CHAPTER 1 : INTRODUCTION	1
1.1 Preamble	2
1.2 Significance of the work	3
1.3 Research objectives	4
1.4 Outline of the thesis	4
CHAPTER 2 : LITERATURE SURVEY	6
2.1 Historical perspective	7
2.2 Operating states in bubble columns	8
2.3 Modified bubble columns	12
2.4 Draft tube bubble columns	12
2.4.1 Introduction	12
2.4.2 Classification of Draft Tube Bubble Columns (DTBC)	13
2.4.3 Bubble columns Vs draft tube bubble columns	14
2.4.5 Applications of draft tube bubble columns	15
2.5 Hydrodynamic and mass transfer features of draft tube bubble columns	17
2.5.1 Gas holdup	17
2.5.2 Specific gas-liquid interfacial area	24
2.5.3 Volumetric mass transfer coefficient	25
2.6 Summary	30

CHAPTER 3 : EXPERIMENTAL SETUP, MATERIALS AND METHODS	31
3.1 Experimental setup	32
3.1.1 Rectangular Draft Tube Bubble Column (RDTBC)	32
3.1.2 Cylindrical Draft Tube Bubble Column-1 (CDTBC-1)	37
3.1.3 Cylindrical Draft Tube Bubble Column-2 (CDTBC-2)	37
3.2 Materials	40
3.3 Methods and experimental techniques	40
3.3.1 Gas holdup and its measurement	40
3.3.1.1 Volume expansion method for measurement of gas holdup	42
3.3.2 Methods for determining specific interfacial area	42
3.3.2.1 Overview of chemical methods	43
3.3.2.2 Determination of interfacial area by sulfite oxidation	47
3.3.3 Volumetric mass transfer coefficient and its measurement	48
3.3.3.1 Methods for the determination of volumetric mass transfer coefficient	49
3.3.3.2 $k_L a$ determination by dynamic gassing-in technique	52
 CHAPTER 4 : HYDRODYNAMIC AND MASS TRANSFER CHARACTERISTICS OF DRAFT TUBE BUBBLE COLUMNS	 55
4.1 Total gas holdup	56
4.1.1 Effect of superficial gas velocity on gas holdup in RDTBC	57
4.1.2 Effect of sparger design on gas holdup in RDTBC	59
4.1.2.1 Effect of number of holes (N_h) in sparger on gas holdup	59
4.1.2.2 Effect of pitch (P_t) of holes in spargers on gas holdup	61

4.1.2.3	Effect of hole diameter (d_h) of sparger on gas holdup	62
4.1.2.4	Effect of row of holes in sparger on gas holdup	64
4.1.2.5	Selection of sparger for characterization and application of RDTBC	66
4.1.3	Effect of draft tube on gas holdup	66
4.1.4	Effect of draft tube height on gas holdup in RDTBC	70
4.1.5	Effect of geometrical shape of DTBC on gas holdup	73
4.1.6	Effect of scale of operations on gas holdup	74
4.1.7	Prediction of gas holdup in draft tube bubble columns	76
4.2	Specific gas-liquid interfacial area	78
4.2.1	Effect of draft tube height on interfacial area for RDTBC	80
4.2.2	Effect of draft tube on interfacial area	81
4.2.3	Effect of geometrical shape of draft tube bubble column on interfacial area	82
4.2.4	Effect of scale of operations on interfacial area	84
4.3	Mass transfer coefficients	86
4.3.1	Effect of superficial gas velocity on $k_L a$	86
4.3.2	Effect of geometrical shape of draft tube bubble columns on $k_L a$	87
4.3.3	Effect of draft tube height on $k_L a$	89
4.3.4	Prediction of $k_L a$ in draft tube bubble columns	90
4.3.5	True mass transfer coefficient, k_L in RDTBC	93
4.4	Conclusions	94
 CHAPTER 5 : WASTEWATER TREATMENT IN DRAFT TUBE BUBBLE COLUMNS		98
5.1	Introduction	99
5.2	Literature survey	100
5.2.1	The necessity of nutrient removal from wastewater	100

5.2.2	Mechanisms of removal of nitrogen and phosphorus from wastewater using activated sludge	100
5.3	Materials and methods	104
5.3.1	Sewage water and its composition	104
5.3.2	Activated sludge and its preparation	104
5.3.3	Chemicals and glassware	106
5.3.4	Synthetic wastewater and its composition	106
5.3.5	Operational methodology	107
5.3.6	Analytical techniques	107
5.3.6.1	Ammoniacal nitrogen estimation	107
5.3.6.2	Phosphorus estimation	109
5.4	Results and discussion	110
5.4.1	Sewage wastewater treatment using activated sludge	110
5.4.1.1	Effect of draft tube in a rectangular bubble column on nitrogen and phosphorus removal	110
5.4.1.2	Effect of draft tube height on nutrient removal in RDTBC	113
5.4.1.3	Effect of air flow rate on nitrogen and phosphorus removal in RDTBC	114
5.4.1.4	Effect of geometrical shape of draft tube bubble column on nutrient removal	116
5.4.1.5	Effect of scale of operation in CDTBC on nutrients removal	118
5.4.2	Synthetic wastewater treatment using activated sludge in rectangular columns	121
5.5	Conclusions	124

CHAPTER 6: FERMENTATION OF BAKER’S YEAST IN DRAFT	126
TUBE BUBBLE COLUMNS	
6.1 Introduction	127
6.2 Literature survey	129
6.2.1 General characteristics of fermentation process	129
6.2.2 Kinetics of batch fermentation	130
6.2.3 Baker’s yeast	131
6.2.4 Yeast metabolism	132
6.2.5 Production of baker’s yeast	133
6.3 Materials and methods	134
6.3.1 Cane sugar solution	134
6.3.2 Chemicals and glassware	134
6.3.3 Experimental procedure	135
6.3.3.1 Primary cultivation and preservation of baker’s yeast	135
6.3.3.2 Medium design, optimization and sterilization	136
6.3.3.3 Inoculum preparation	138
6.3.3.4 Experiment using shake flask	138
6.3.3.5 Trial run using small bubble column	138
6.3.3.6 Production of baker’s yeast in bubble columns and draft tube bubble columns	139
6.3.3.7 Measurement of optical density, calculation of biomass concentration and specific growth rate	140
6.3.3.8 Estimation of total sugar consumption	141
6.4 Results and discussion	141
6.4.1 Effect of aeration and agitation on growth of baker’s yeast	141
6.4.2 Effect of draft tube in a bubble column on cell biomass yield	143
6.4.3 Effect of draft tube height on specific growth rate in RDTBC	145
6.4.4 Effect of air flow rate on baker’s yeast production in RDTBC	147

6.4.5	Effect of shape of draft tube bubble column on biomass production	148
6.4.6	Effect of scale of operation in CDTBC on biomass productivity	150
6.5	Conclusions	152
CHAPTER 7: SUMMARY AND CONCLUSIONS		153
7.1	Introduction	154
7.2	Experimental	154
7.3	Characterization of draft tube bubble columns	155
7.4	DTBC for wastewater treatment	156
7.5	DTBC – as a fermentor	158
7.6	Scope for future work	159
• REFERENCES		161
APPENDICES		
Appendix-I	Iodometric titration	180
Appendix-II	Prediction of diffusivity of oxygen	181
Appendix-III	Justifications of assumptions in dynamic gassing in method	182
Appendix-IV	Calibration of DO probe	185
Appendix-V	Manual phenate method	187
Appendix-VI	Ascorbic acid method	189
Appendix-VII	Cole's method	191

LIST OF FIGURES

Figure No.	Figure caption	Page No.
Fig. 2.1	Simple bubble column	7
Fig. 2.2	Circulation patterns in bubble column	9
Fig. 2.3	Flow regimes in bubble columns	9
Fig. 2.4	Flow regime map for bubble columns	11
Fig. 2.5	Draft tube bubble columns	13
	(a) Internal loop DTBC	13
	(b) External loop DTBC	13
Fig. 2.6	Operating ranges of gas and liquid velocities in bubble columns and airlift loop reactors	14
Fig. 2.7	Gas holdup and fraction of large bubbles	18
Fig. 2.8	Specific interfacial area as a function of superficial gas velocity	25
Fig. 2.9	Comparison of mass transfer coefficients for airlift reactors and bubble columns	26
Fig. 3.1	Schematic of experimental setup of RDTBC	33
Fig. 3.2	Snapshots of rectangular draft tube bubble column and its parts	34
	(a) RDTBC mounted on stand	34
	(b) Draft tube with supports	34
	(c) Sampling valve	34
	(d) Gas distribution chamber	34
Fig. 3.3	Photographs of spargers used in RDTBC	36
Fig. 3.4	Snapshots of cylindrical draft tube bubble column-1 (CDTBC-1) and its parts	38
	(a) CDTBC-1 assembly	38
	(b) Supports on draft tube	38
	(c) Supports for draft tube on sparger	38
	(d) Holes in sparger	38
	(e) Turnings in gas chamber	38
	(f) Oil seal in hole for DO probe	38

Fig. 3.5	Snapshots of cylindrical draft tube bubble column-2 (CDTBC-2) and its parts	39
	(a) CDTBC-2 assembly	39
	(b) Male-female joint in outer column	39
	(c) Sparger with 8 holes and supports for draft tube	39
	(d) Bottom part of column and gas distribution chamber	39
Fig. 3.6	DO probe inserted in RDTBC and connected to DO meter	53
Fig. 3.7	DO Probe and its parts	53
Fig. 4.1	Effect of superficial gas velocity on gas holdup in RDTBC	57
Fig. 4.2	Regime plot of ϵ_g Vs U_{gr} on log scale for sparger C in RDTBC	58
Fig. 4.3	Effect of N_h in sparger on ϵ_g in RDTBC	60
Fig. 4.4	Regime plot of effect of N_h in sparger on ϵ_g in RDTBC	60
Fig. 4.5	Effect of P_t of holes in sparger on ϵ_g in RDTBC	61
Fig. 4.6	Regime plot of effect of P_t of holes in sparger on ϵ_g in RDTBC	62
Fig. 4.7	Effect of d_h of sparger on ϵ_g in RDTBC	63
Fig. 4.8	Regime plot of effect of d_h of sparger on ϵ_g in RDTBC	63
Fig. 4.9	Effect of number of row of holes in sparger on ϵ_g in RDTBC	65
Fig. 4.10	Regime plot of effect of number of row of holes in sparger on ϵ_g in RDTBC	65
Fig. 4.11	Comparison of total gas holdup in RBC and RDTBC	67
Fig. 4.12	Snapshots of bubbling patterns in RDTBC with 70 cm draft tube	68
Fig. 4.13	Effect of draft tube height on gas holdup in RDTBC	71
Fig. 4.14	Regime plot of effect of draft tube height on gas holdup in RDTBC	71
Fig. 4.15	Different hydrodynamic regions in RDTBC	72
Fig. 4.16	Effect of geometrical shape of DTBC on gas holdup	73
Fig. 4.17	Regime plot of effect of geometrical shape of DTBC on gas holdup	73
Fig. 4.18	Effect of scale of operation on gas holdup	75
Fig. 4.19	Regime plot of effect of scale of operation on gas holdup	75
Fig. 4.20	Prediction of gas holdup in RDTBC and CDTBC-1	76
Fig. 4.21	Comparison of predicted and experimental gas holdup profiles in DTBC	77
Fig. 4.22	Prototype interfacial area profile in RDTBC	79
Fig. 4.23	Effect of draft tube height on interfacial area for RDTBC	80

Fig. 4.24	Effect of draft tube on interfacial area for rectangular columns	82
Fig. 4.25	Effect of geometrical shape of DTBC on interfacial area	83
Fig. 4.26	Effect of scale of operation on interfacial area	84
Fig. 4.27	Snapshots of bubble patterns in CDTBC-1	85
Fig. 4.28	Snapshots of bubble patterns in CDTBC-2	85
Fig. 4.29	Effect of superficial gas velocity on $k_L a$ in RDTBC	87
Fig. 4.30	Effect of geometrical shape of draft tube bubble columns on $k_L a$	88
Fig. 4.31	Effect of draft tube height on $k_L a$ for RDTBC	89
Fig. 4.32	Prediction of $k_L a$ in RDTBC and CDTBC-1	91
Fig. 4.33	Comparison of predicted and experimental $k_L a$ of RDTBC	91
	(a) $k_L a$ profiles	91
	(b) Parity plot	91
Fig. 4.34	Comparison of predicted and experimental $k_L a$ profiles of CDTBC-1	92
Fig. 4.35	Effect of draft tube heights on k_L at varying U_{gr} for RDTBC	94
Fig. 5.1	Sample collection point of sewage water in downstream of Athamiya river	105
Fig. 5.2	Location of sewage water sample collection	105
Fig. 5.3	Calibration curve of absorbance Vs ammoniacal nitrogen concentration	108
Fig. 5.4	Calibration curve of absorbance Vs phosphorus concentration	110
Fig. 5.5	Effect of draft tube on ammoniacal nitrogen removal in RBC	111
Fig. 5.6	Effect of draft tube on phosphorus removal in RBC	111
Fig. 5.7	Effect of draft tube height on ammoniacal nitrogen removal in RDTBC	113
Fig. 5.8	Effect of draft tube height on phosphorus removal in RDTBC	113
Fig. 5.9	Effect of air flow rate on ammoniacal nitrogen removal in RDTBC	115
Fig. 5.10	Effect of air flow rate on phosphorus removal in RDTBC	115
Fig. 5.11	Effect of shape of DTBC on ammoniacal nitrogen removal	117
Fig. 5.12	Effect of shape of DTBC on phosphorus removal	117
Fig. 5.13	Effect of scale of CDTBC on nitrogen removal at varying air flow rates	119
Fig. 5.14	Effect of scale of CDTBC on phosphorus removal at varying air flow rates	119

Fig. 5.15	Comparison of synthetic wastewater and sewage water for nitrogen and phosphorus removal in rectangular columns.	122
	(a) RBC	122
	(b) RDTBC with 70 cm draft tube	122
	(c) RDTBC with 60 cm draft tube	122
Fig. 5.16	Ammoniacal nitrogen removal from synthetic wastewater in RBC and RDTBC	123
Fig. 5.17	Phosphorus removal from synthetic wastewater in RBC and RDTBC	123
Fig. 6.1	A generalized schematic representation of a typical fermentation process	129
Fig. 6.2	Typical batch growth curve	130
Fig. 6.3	Colonies of baker's yeast on YEPD agar plates	135
Fig. 6.4	Inoculum on a rotary shaker	138
Fig. 6.5	Snapshots of the small bubble column assembly and its parts	139
	(a) Small bubble column	139
	(b) Sparger	139
	(c) Gas distribution chamber	139
	(d) Bacteria filter for air sterilization	139
Fig. 6.6	Effect of aeration and agitation on growth rate of biomass	142
Fig. 6.7	Effect of aeration and agitation on sugar depletion rate	142
Fig. 6.8	Effect of insertion of draft tube on biomass production for RBC	144
Fig. 6.9	Effect of insertion of draft tube on reducing sugar concentration for RBC	144
Fig. 6.10	Effect of draft tube height on biomass production rate in RDTBC	146
Fig. 6.11	Effect of draft tube height on total sugar consumption in RDTBC	146
Fig. 6.12	Effect of air flow rate on biomass yield for RDTBC	147
Fig. 6.13	Effect of air flow rate on sugar consumption rate for RDTBC	147
Fig. 6.14	Effect of geometrical shape of DTBC on baker's yeast production rate	149
Fig. 6.15	Effect of geometrical shape of DTBC on reducing sugar of fermentation broth	149
Fig. 6.16	Effect of scale of CDTBC on biomass production at varying air flow rates	151
Fig. 6.17	Effect of scale of CDTBC on sugar depletion at varying air flow rates	151

LIST OF TABLES

Table No.	Table caption	Page No.
Table 2.1	Gas holdup correlations for bubble columns	20
Table 2.2	Gas holdup correlations for internal loop draft tube bubble columns	22
Table 2.3	Mass transfer coefficient correlations for bubble columns	28
Table 2.4	Mass transfer coefficient correlations for internal loop draft tube bubble columns	29
Table 3.1	Specifications of columns	32
Table 3.2	Spargers and their specifications for RDTBC	35
Table 4.1	Power law model parameters for different spargers	59
Table 4.2	Comparison of interfacial area of RBC and RDTBC	81
Table 4.3	Calculation of k_L for RDTBC	93
Table 5.1	Analytical composition of sewage wastewater	104
Table 5.2	Composition of synthetic wastewater	107
Table 5.3	Comparison of nutrient removal from synthetic and sewage wastewater	124
Table 6.1	Optimization of carbon content in fermentation broth	136
Table 6.2	Optimization of nitrogen content in fermentation broth	137
Table 6.3	Optimized media for baker's yeast production	137

LIST OF SYMBOLS

a	Specific interfacial area, cm^{-1}
A	Dissolved solute (gas)
A_d	Downcomer cross-sectional area, cm^2
A_r	Riser (draft tube) cross-sectional area, cm^2
B	Reactant in liquid phase
Bo	Bond number
$[B_0]$	Initial concentration of B, kmol/m^3
C^*	Saturation concentration of oxygen in liquid, mg/L
C_A^*	Saturated solubility of A in liquid phase, kmol/m^3 or mol/L
C_0	Distribution parameter
C_{CoSO_4}	Concentration of cobaltous sulfate, kmol/m^3
C_L	Instantaneous concentration of oxygen in liquid, mg/L
C_{L0}	Initial concentration of oxygen in liquid, mg/L
C_s	Solid concentration, mg/L
C_{Sulfite}	Concentration of sulfite solution, kmol/m^3
D	Depth, cm
D_A	Diffusivity of A in liquid phase, cm^2/s
D_{AB}	Diffusivity, cm^2/s
d_b	Bubble diameter, cm
d_h	Hole diameter, mm
D_L	Diffusion coefficient
d_R	Reactor diameter, m
d_s	Sauter mean bubble diameter, cm
d_t	Draft tube diameter, cm
Fr	Froude number
Ga	Galileo number
H	Height, cm
h_d	Height of gas-liquid dispersion, cm
h_l	Un-aerated liquid height, cm
ID	Inside diameter, cm
K	Correlation parameter
k_2	Rate constant of second order reaction, $\text{m}^3/\text{kmol}\cdot\text{s}$

k_L	True liquid phase mass transfer coefficient, cm/s
$k_L a$	Volumetric mass transfer coefficient, min^{-1}
k_{mn}	Rate constant of $m+n$ order reaction
M	Wetted surface parameter
m	Order of reaction with respect to A
Ma	Bubble coalescence parameter
Mo	Morton number
N	Flow index
n	Order of reaction with respect to B
N_h	Number of holes
OD	Outside diameter, cm
P	Pressure, N/m^2
P_G	Power input due to gassing, W
P_{O_2}	Partial pressure of oxygen, atm.
P_t	Pitch, mm
P_V	Energy dissipation rate, W
Q_g	Volumetric gas flow rate, cm^3/s
$R_A a$	Rate of absorption, $\text{kmol/m}^3 \text{ s}$
Re_T	Reynolds number
Sc	Schmidt number
Sh	Sherwood number
T	Thickness, cm
T	Temperature, K
T	Time, sec or hour
t_d	Doubling time, hour
U_1	Superficial liquid velocity, cm/s
U_∞	Terminal rise velocity, cm/s
U_g	Superficial gas velocity based on outer column or bubble column, cm/s
U_{gr}	Superficial gas velocity in riser, cm/s
U_{lr}	Superficial liquid velocity in riser, cm/s
V_b	Volume of bubble, cm^3
V_D	Volume of dispersion, cm^3
V_G	Volume of gas, cm^3
V_L	Volume of liquid, cm^3

v_s	Solid volume fraction
W	Width, cm
W_l	Mass of liquid, kg
W_s	Mass of solid, kg
x	Biomass concentration, gm/L
x_0	Initial biomass concentration, gm/L
z	Stoichiometric coefficient of B

Greek symbols

μ	Specific growth rate, h^{-1}
μ_{ap}	Apparent viscosity, cP
μ_{eff}	Effective viscosity of slurry, cP
μ_g	Viscosity of gas phase, cP
μ_l	Viscosity of liquid phase, cP
μ_{sl}	Viscosity of slurry, cP
μ_w	Viscosity of water, cP
α	Power law model parameter
β	Power law model parameter, velocity index
$\Delta\rho$	Density difference, kg/m^3
ε_{gd}	Downcomer gas holdup
ε_g	Total gas holdup
ε_{gr}	Riser gas holdup
ν_g	Kinematic viscosity of gas, cm^2/s
ν_l	Kinematic viscosity of liquid, cm^2/s
ρ_g	Gas density, kg/m^3
ρ_l	Liquid density, kg/m^3
ρ_s	Solid density, kg/m^3
ρ_{sl}	Slurry density, kg/m^3
σ_l	Liquid-phase surface tension, N/m
σ_w	Surface tension of water, N/m

LIST OF ABBREVIATIONS

LPM	Liters per minute
DTBC	Draft tube bubble column
RBC	Rectangular bubble column
RDTBC	Rectangular draft tube bubble column
CDTBC	Cylindrical draft tube bubble column
CDTBC-1	Cylindrical draft tube bubble column having equivalent draft tube cross-sectional area as RDTBC
CDTBC-2	Cylindrical draft tube bubble column having larger diameter
DT	Draft tube
c.s area	cross-sectional area, cm ²
DO	Dissolved oxygen
NH ₃ -N	Ammoniacal nitrogen
PO ₄ ³⁻ - P	Orthophosphates
APHA	American Public Health Association
YEPD	Yeast Extract Peptone Dextrose

DEFINATION

$$\text{Percentage absolute error} = \frac{1}{n} \left[\sum \left| \frac{\text{Experimental} - \text{Predicted}}{\text{Experimental}} \right| \right] \times 100$$

where, n = number of data points

CHAPTER 1

INTRODUCTION

1.1. PREAMBLE

Bubble columns are gas-liquid contacting devices where gas is dispersed in a deep liquid pool from the bottom, the gas bubbles rise in the pool creating the interfacial area for mass transfer of solute between the gas and the liquid. Bubble columns are widely used as reactors for various synthesis reactions such as oxidation, hydrogenation, halogenation, ammonolysis, ozonolysis, carbonylation, carboxylation, alkylation, Fischer–Tropsch synthesis etc. They are also widely used in wastewater treatment and hydrometallurgical operations but their niche area of application is the fermentation reaction that involves oxygen transfer. Simplicity of construction, ease of operation, low operating costs, effective pneumatic mixing, lack of moving parts, and high degree of freedom to tailor performance characteristics are the reasons for the wide use of bubble columns in process industries.

Bubble columns in spite of numerous advantages suffer from drawbacks such as poor liquid circulation, short residence times for fermentation reactions, low specific interfacial areas, low operating gas velocities etc. Many of these deficiencies found in bubble columns can be eliminated by simply inserting a draft tube within the column. Presence of a draft tube in bubble column leads to stable liquid circulating flow induced by the density difference between the aerated liquid within the draft tube and the liquid in the annulus resulting in enhanced mass transfer rates without high shear force.

In a draft tube bubble column (DTBC) the gases pass through the draft tube that functions as a riser since the cross sectional area of the draft tube is considerably less than the bubble column and the gas velocities in the draft tube even at low gas flow rate are reasonably high. This behavior enhances the gas–liquid interfacial area, stabilizes the liquid flow pattern and increases the mass transfer coefficients. This results in achieving high interfacial area and mass transfer coefficients at relatively lower gas flow rates in comparison with bubble columns.

Draft tube bubble columns have been in existence since 1969 (Hatch et al., 1969; Wang et al., 1971), they were primarily used for single cell protein fermentation. They were mechanically robust, more efficient in features of mass transfer and were more adaptable to fermentation of cultures that are shear sensitive as well as requiring well-defined residence times and monoseptic operation over extended time period. In addition to the above required less energy to operate compared to mechanically agitated stirred tank reactors.

However, due to the commercial rejection of SCP in the food market the draft tube bubble columns also went into hibernation. Nevertheless, the draft tube bubble column remains highly conducive device for waste water treatment and fermentation processes and its applicability and suitability as a contactor needs to be restored in the profession.

1.2 SIGNIFICANCE OF THE WORK

Despite numerous advantages the industrial application of draft tube bubble columns remains limited principally because the basic knowledge of their characteristics is lacking. Even after four decades of conceptualization of draft tube bubble columns, the detailed understanding of the underlying physics of the complex fluid dynamics of these devices is not well understood. A number of factors such as incomplete understanding of their hydrodynamic and mass transfer behavior have been identified as being the bottleneck to the successful commercialization of draft tube bubble columns.

Process engineering information available for the detailed design of draft tube bubble columns is rather limited. Consequently, a reliable design basis is still far from established for draft tube bubble columns. Current knowledge does not permit the design of draft tube bubble column with a high degree of confidence. The uncertainty of performance of draft tube bubble column appears to be the principal factor which restricts wider use of it in industries. The limited information which is accessible frequently shows wide variations and conflicting claims, due to highly empirical, system-specific approaches taken.

Draft tube bubble columns have attracted attention especially in biotechnological processes because of its unique stable flow and liquid circulation patterns. From a hydrodynamic view point, draft tube bubble columns are unique in that the flow of gas initiates the liquid flow. The understanding of gas- induced circulation of liquid in draft tube bubble columns is a critical aspect of their design and operation, the state of knowledge in this area requires an organized study on draft tube bubble columns explaining the effect of geometrical and operational conditions on hydrodynamic and mass transfer behavior and on its important applications viz. wastewater treatment and biomass growth.

1.3 RESEARCH OBJECTIVES

The principle objective of the present investigation is to acquire a fundamental understanding of key parameters such as gas holdup, specific interfacial area, volumetric mass transfer coefficients etc. in draft tube bubble columns and quantify the effect of operational and design parameters such as superficial gas velocity in riser, sparger design, height of draft tube, shape of column, scale of operations on these parameters in DTBC's.

One key research objective was to check the efficacy of draft tube bubble columns of rectangular geometry vis-à-vis the conventional cylindrical geometries. DTBC are gaining greater application in wastewater treatment and wastewater systems usually involve masonry structures since they handle very large liquid volumes, it is convenient to fabricate such masonry equipments in rectangular shape. Hence, rectangular DTBC could be a possibility in near future, the basic investigation done in this work would be a stepping stone to understand and design such columns.

It was intended to test the efficacy of well characterized draft tube bubble columns for

1. Nutrient removal from wastewater using activated sludge process
2. Production of baker's yeast by fermentation

and compare the same with conventional bubble columns and other devices with the objective to establish the veracity of DTBC.

1.4 OUTLINE OF THE THESIS

The thesis is presented in seven chapters; **Chapter 1: Introduction** is devoted to the nature and scope of the investigation. **Chapter 2 : Literature survey** provides a topical review on bubble columns and draft tube bubble columns vis-à-vis historical perspective, operating states, modified bubble columns, types of draft tube bubble columns and their applications etc., it highlights the hydrodynamic and mass transfer fundamentals of draft tube bubble columns along with a comprehensive list of predictive correlations developed by various investigators for prediction of gas holdup and volumetric mass transfer coefficients for bubble columns and draft tube bubble columns.

Chapter 3: *Experimental setup, materials and methods* describes different experimental assemblies of draft tube bubble columns used in the present investigation. It lists the materials used in the present work. It also discusses experimental techniques available for measurement of gas holdup, specific gas-liquid interfacial area and volumetric mass transfer coefficient as well as yardstick for selection of specific techniques adopted and instruments used in the present investigation.

Chapter 4: *Hydrodynamic and mass transfer characteristics of draft tube bubble columns* details the effects of various operating and design parameters such as superficial gas velocities, sparger design, presence of draft tube, height of draft tube, scale of operation etc. on gas holdup, interfacial area, and volumetric mass transfer coefficients of draft tube bubble columns. It also compares the performance of rectangular draft tube columns with cylindrical columns and tests the efficacy of existing correlations for prediction of ε_g and $k_L a$.

Chapter 5: *Wastewater treatment in draft tube bubble columns* reports the basic literature, techniques and methods for removal of nutrients from wastewaters and describes the application of draft tube bubble columns for nutrient removal from sewage water and the effect of various design and operational conditions on extent of removal. It compares nutrient removal in rectangular device with the cylindrical device as well as the bubble column. This chapter also investigates the nutrient removal from synthetic wastewater systems thereby establishing the portability of data from laboratory to field systems.

Chapter 6: *Fermentation of baker's yeast in draft tube bubble columns* explores another application of draft tube bubble column as fermentor for the production of biomass. The fundamentals, materials and methods used as well as effect of various operational, geometrical and design parameters on specific growth rate of biomass and sugar depletion of fermentation broth is described in this chapter. The comparison of shake flask, bubble column and draft tube bubble columns for biomass growth is reported and the effect of scale of operation and scaling parameters are established.

Finally, **Chapter 7: *Summary and conclusions*** summarizes the whole investigation and also suggests the scope for future work on draft tube bubble columns.

CHAPTER 2

LITERATURE SURVEY

Bubble columns are gas-liquid contacting devices where gas is dispersed in the continuous liquid phase in the form of bubbles to achieve either mass transfer or reaction between the species in the interacting gas-liquid phases. In the simplest form of bubble column the gas enters at the bottom of a vertical cylinder through a gas distributor as shown in Fig. 2.1. The liquid phase may be either batch or it may move with or against the flow of the gas phase. The top of the bubble column is often widened to facilitate gas separation. The aspect ratio L/d_R , i.e. the ratio between length and diameter could vary in the range of 3 to 6 and aspect ratios of around 10 are also frequent for laboratory and pilot plant studies. Bubble columns have been used in the chemical industry for many years for hydrogenation, oxidation, chlorination, alkylation and other processes.

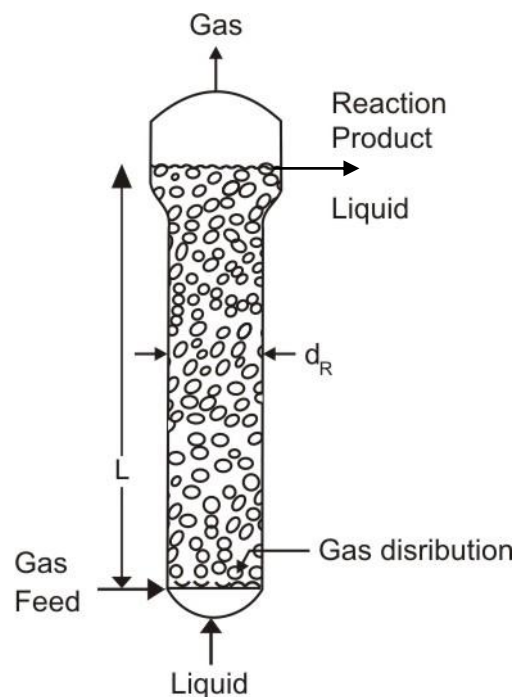


Fig. 2.1 Simple bubble column

2.1 HISTORICAL PERSPECTIVE

Earliest investigations on bubble columns were conducted at the Technical University of Berlin in early 1940's by Kolbel for the development of Fischer-Tropsch synthesis (Deckwer, 1992). Subsequently Yoshida in Japan investigated bubble columns in the mid - 1960's, other than this very little literature was forthcoming from either industry or the universities. The situation changed dramatically during the mid-1970s when all of a

sudden there was an upsurge of interest in bubble columns. The possible reasons for such an increase in interest are attributed to the following:-

- 1) The opening up of new application areas, especially in the field of biotechnology such as single-cell protein production, animal cell culture, antibiotic fermentation, and effluent treatment.
- 2) A revival of interest in coal liquefaction and slurry phase Fisher-Tropsch synthesis, both relying greatly on bubble column technology, resulting from the oil crisis of 1973 and the subsequent search for alternative raw materials and synthetic fuels. Bubble columns also play a role in the development of C_1 chemistry.
- 3) A general recognition of the fundamental advantages of bubble columns e.g. simple in structure and operation, no mechanically moving parts and thus low energy input, cost effective, less space consumption, good heat and mass transfer properties, high thermal stability, etc.

In 1978, more than 10^7 TPA of chemical products were produced in bubble columns. Since then, marked growth has occurred. The scale of operations has also increased dramatically today industrial bubble column reactors for high-tonnage products have capacities of 100 – 300 m^3 while bubble column fermentors for single cell-protein production from methanol have capacities up to 3000 m^3 . The largest units are those used for biological wastewater treatment having capacities of 20 000 m^3 .

2.2 OPERATING STATES IN BUBBLE COLUMNS

In bubble columns the gas bubbles preferentially flows from the center of the column and has significantly lower density than the liquid phase, this leads to an uneven distribution of void fraction and thereby density across the lateral cross-section of the column. This uneven void distribution sets up a global circulation pattern that is primarily density driven as shown in Fig. 2.2. The gas bubbles entrains liquid along with it as it rises in the column after the disengagement of gas from liquid, the liquid moves downwards near the wall of the column, setting up circulation cells.

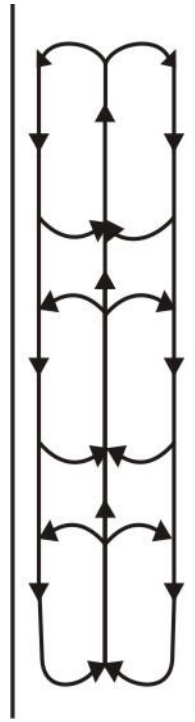


Fig. 2.2 Circulation patterns in bubble column

In bubble columns the hydrodynamics and transport properties such as pressure drop, holdup of gas and liquid phases, gas-liquid interfacial areas and interphase mass and heat transfer coefficients etc. depend strongly on the prevailing flow regime. Wallis (1969) has characterized the upward movement of the bubble swarms into three distinct flow regimes, the homogeneous flow regime, heterogeneous flow and slug flow as shown in Fig. 2.3. These regimes occur in order of increasing gas flow rate.

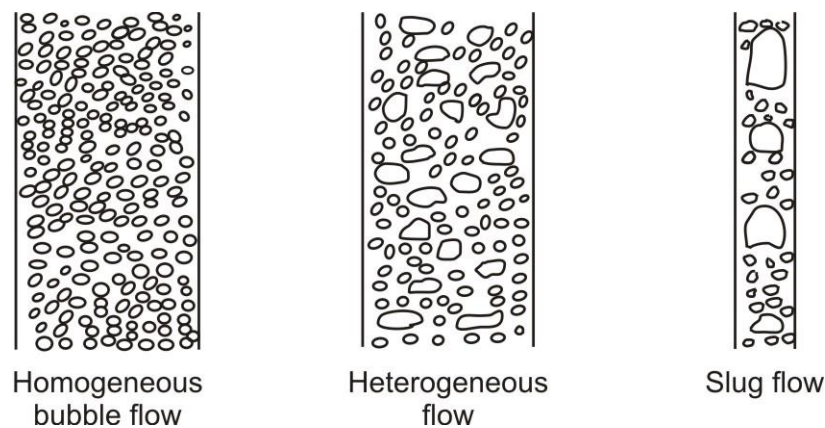


Fig. 2.3 Flow regimes in bubble columns, adopted from Wallis (1969)

- **Bubbly-flow regime or homogeneous flow:-**

This regime is characterized by distinct small bubbles having narrow size distribution which are uniformly distributed in the liquid. Gentle mixing is observed over the entire cross-sectional area of the column. The existence of this

regime is limited to the region of low superficial gas velocities, generally up to 5 cm/s in semi batch columns for a low viscosity liquid similar to water. Practically no bubble coalescence or break-up is observed in this regime.

- ***Churn turbulent flow or heterogeneous regime:-***

At higher superficial gas velocities, homogeneous flow cannot be maintained and bubble aggregates and large bubbles are formed which rise more rapidly than the small bubbles. This type of flow results due to high gas rates, it is referred to as heterogeneous flow and is frequently adopted in industry. As a matter of fact, by bubble coalescence and break-up, a wide bubble size distribution is obtained. In this regime, a large part of the gas is transported through the column in form of large fast ascending bubbles, this amount increases as a function of gas velocity. Heterogeneous flow can also result at low gas velocities if the gas distribution is poor, either when gas is distributed through a single hole or through perforated plate having large holes.

- ***Slugging or Plug Flow regime:-***

Slugging is usually observed in tall and narrow bubble columns of diameter 10 cm or less. The large bubbles in heterogeneous zone are stabilized by the column wall and move upwards through the column in a piston like manner. These elongated bubbles, called slugs, fill practically the whole column cross section and continue to grow by collecting smaller bubbles continuously throughout their upward journey. In slug flow regimes reaction rates and reactor capacities are low and data from such equipment cannot be utilized for larger diameter equipment. Slug flow should be strictly avoided in both laboratory and pilot plant, as test results are of little practical importance.

The detection and investigation of the transition of flow regime from homogeneous to churn-turbulent flow is quite important. As the transition takes place, significant changes are observed in the hydrodynamic behaviour of the system. There exists an onset of upward liquid circulation in the column centre and downward liquid circulation near the column wall. As a result more gas entry takes place in the centre, leading to build-up of transverse holdup-profile that enhances liquid circulation. Thorat and Joshi (2004) reported that the transition gas velocity depends on column diameter, dispersion height, sparger design and physical properties of the system. However, the effect of these parameters has not been thoroughly investigated in literature so far.

Characterization of flow regimes is fuzzy, it is not possible to prescribe definite quantitative range of superficial velocities, investigations done with different systems and operating conditions provide different results for regime boundaries and regime transitions. For instance, Schumpe and Grund (1986) proposed that for superficial velocities lower than 5 cm/s, homogeneous (bubbly) flow prevails, while Bukur and Daly (1987) observed the churn-turbulent flow regime for gas superficial velocities between 2 and 5 cm/s. Pino et al. (1992) proposed that below 4 cm/s superficial velocity a bubbly flow regime prevails. Hyndman et al. (1997) also reported approximately the same velocity for bubbly flow regime.

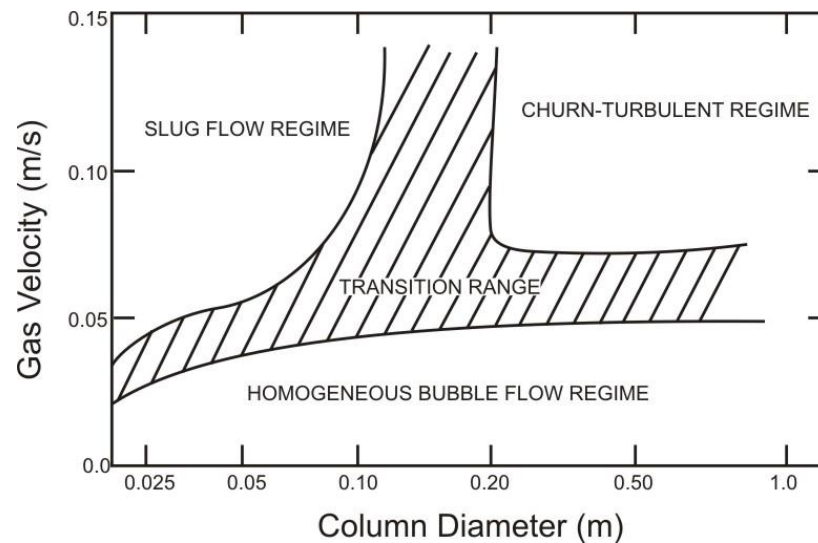


Fig. 2.4 Flow regime map for bubble columns, adopted from Deckwer et al. (1980)

Several flow regime charts have been presented in literature to identify the boundaries of possible flow regimes (Deckwer et al., 1980; Shah et al., 1982; Fan et al., 1985). In Fig. 2.4 one such flow regime map presented by Deckwer et al. (1980) is shown. The map describes quantitatively the dependence of flow regimes on column diameter and superficial gas velocity and is valid for both bubble and slurry bubble columns filled with a batch liquid having low viscosity. The shaded regions in the figure indicate the transition regions between various flow regimes. However, the exact boundaries associated with the transition regions would depend on the system studied. Measurement of flow patterns and flow structures in bubble columns and their hydrodynamic modeling has been investigated by many investigators (Schluter et al., 1992; Joshi et al., 2002; Joshi and Kulkarni, 2004; Joshi et al., 2005). Computational and advanced experimental tools such as CFD and multiresolution analysis of velocity-time series etc. were also applied for the identifications of coherent flow structures and their dynamics in bubble columns.

2.3 MODIFIED BUBBLE COLUMNS

In spite of numerous advantages, bubble columns suffer from a number of deficiencies such as poor and undefined liquid circulation rates, uneven back mixing of liquid and gas phase, uneven radial distribution of the two phases in the column, low operating gas velocities, low specific interfacial area, etc. Many of these deficiencies are eliminated by inserting packings, sieves, static mixers etc. within the column that improves the radial distribution of the gas and liquid, reduces the bubble size and consequently enhances the interfacial area of the column. These modifications have been investigated (Hsu et al., 1975; Maclean et al., 1977; Hofmann, 1982) and tried out industrially, but have not made any significant impact on commercialization of such bubble column devices in the industries.

An interesting development in bubble column devices involved the insertion of a hollow tube known as draft tube in the column that induced a directional flow pattern of the liquid and gas phase in the column resulting in liquid circulation patterns. Such devices are known as draft tube bubble columns or airlift loop reactors and have attracted considerable attention of industrial professionals, academicians and researchers in the last two decades.

2.4 DRAFT TUBE BUBBLE COLUMNS

2.4.1 Introduction

Draft tube bubble columns also known as airlift loop reactors consist of liquid or slurry pool that is divided into two distinct zones of which only one is sparged by gas. The different gas holdup in the gassed and ungassed zones results in difference of bulk densities of the fluid in these regions that causes a well-defined circulation of the liquid in the column by a gas-lift action. The part of the column where the bubble up flow occurs is known as *riser* and the region containing the down flowing fluid is known as the *downcomer*. Bubbles rising through the riser are disengaged at the top (head) and at higher velocities some bubbles may be entrained into the downcomer with the circulating liquor. Since liquid mixing rates are dependent on fluid velocities a knowledge of the flow and mass transfer characteristics of such vessels is required if their performance as chemical reactors or fermentors is to be predicted.

Draft tube bubble columns may be employed for any gas-liquid or gas-liquid-solid contacting process. However, practical application depends on the ability to achieve the

required rates of momentum, heat and mass transfer at acceptable capital and operating costs. The technical and economic feasibility of using draft tube bubble columns has been conclusively established for a number of processes and these devices are finding increasing use for industrial applications requiring solid-suspension without high shear force, such as crystallization, biological treatment of wastewater, aerobic fermentations, cell cultivations and other similar operations. In addition to simplicity of their design and construction (Moresi, 1981), well-defined flow pattern (Chisti and Moo-Young, 1987; Merchuk, 1986) and relatively low power inputs for requisite transport rates make these draft tube bubble columns very attractive. Low shear rates, efficient gas phase disengagement, well controlled and better defined liquid flow, improved mixing, large specific interfacial area, well-defined long residence times, high heat and mass transfer rates at low energy input and extended aseptic operation made possible by the elimination of stirrer shafts, seals and bearings make them superior over all other available bioreactors especially for fermentation applications.

2.4.2 Classification of draft tube bubble columns (DTBC)

Two basic classes of the draft tube bubble columns may be distinguished:

- i. The internal loop draft tube bubble column and
- ii. The external / outer loop draft tube bubble column

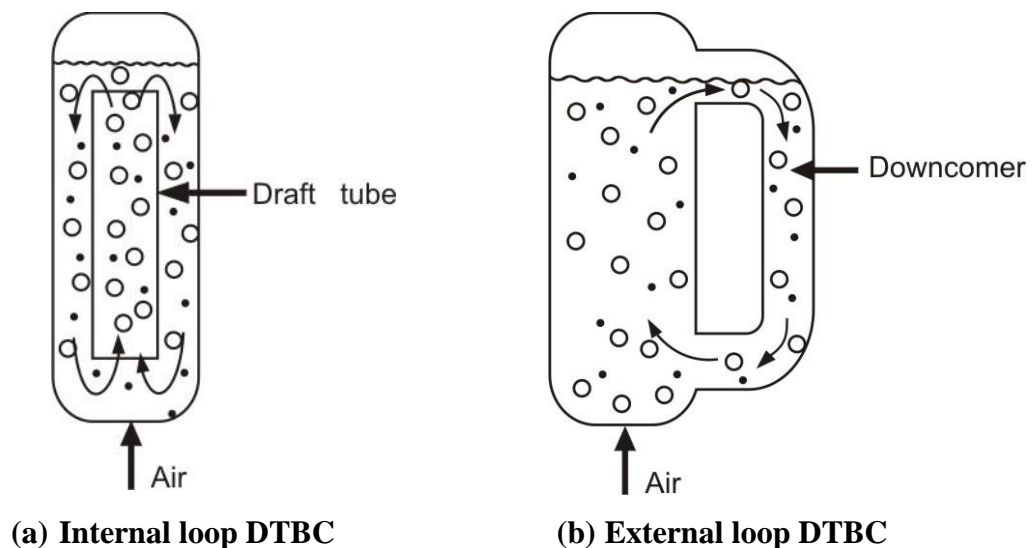


Fig. 2.5 Draft tube bubble columns

The internal loop DTBC shown in Fig.2.5 (a) is split into a riser and a downcomer by a concentric draft tube inside the bubble column. This type of configuration may be sparged with gas either in the annulus or in the draft tube. In the most common mode of operation of internal loop airlift, no gas is injected into the downcomer the gas bubbles present there are dragged in with the liquid flowing into the downcomer at its entrance in the head region of the column. Fig.2.5 (b) shows the external loop draft tube bubble column where the riser and the downcomer are two quite separate tubes connected by horizontal sections near the top and bottom.

Internal and external loop airlift reactors usually have circular cross-sections, but rectangular and square cross-sections, which have practical applications in industry are also a definite option and have been studied by many investigators (Chisti et al., 1987; Chisti and Moo-Young, 1988; Gasner , 1974; Piggott, 1985; Siegel et al., 1986).

2.4.3 Bubble columns Vs draft tube bubble columns

The hydrodynamic behavior of bubble columns and draft tube bubble columns are very different and can be summarized as follows:-

- The main distinction between cocurrent or counter-current bubble columns and draft tube bubble columns is that in the latter the rate of liquid circulation depends strongly on gas flow rate, whereas in bubble columns the type of liquid flow is relatively less dependent on gas flow rate.

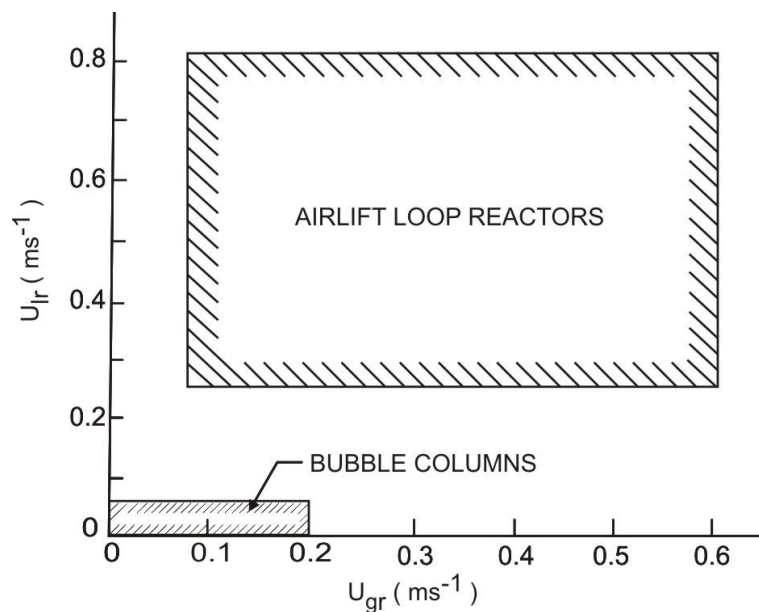


Fig. 2.6 Operating ranges of gas and liquid velocities in bubble columns and airlift loop reactors, adopted from Weiland and Onken (1981)

- To attain the long residence times that are typically required in bioreactors, large liquid throughputs are not possible in bubble columns without significant recycle rates, whereas in draft-tube bubble columns quite high linear liquid velocities may be generated without the need for any external recirculation mechanism.
- The consequent turbulence (generated due to high liquid recirculation) postpones the incipient slugging in the draft tube bubble columns to higher gas velocities than is usual in bubble columns.
- Gas velocities for liquid blow-out condition (i.e. spray formation) are lower in the bubble columns than in draft tube bubble columns (Chisti and Moo-Young, 1987). Hence, the operating range of the draft tube bubble columns in terms of the possible gas and liquid superficial velocities through riser, (U_{gr} and U_{lr} respectively) is much broader (Merchuk, 1986; Weiland and Onken, 1981) than bubble columns as shown in Fig. 2.6.

2.4.5 Applications of draft tube bubble columns

Continuous production of beer, vinegar, citric acid, and biomass from yeasts, bacteria and fungi has been carried out in airlift vessels at different working capacities (Moresi, 1981). The erstwhile USSR and Eastern Europe had extensively employed airlift vessels for SCP yeast cultivation (Blakebrough et al., 1967) and in England the ICI has operated at 1500 m³ (working volume) airlift fermenter for the PRUTEEN process (Westlake, 1986). Ho et al. (1977) have mentioned several currently used industrial scale applications of the airlift fermenters. Malfait et al. (1981) claimed more than 18% (by weight) enhancement in the yield of a filamentous mould *Monascus purpureus* in an external loop airlift (0.055 m³, 0.15 m diameter riser, 0.05 m diameter downcomer) relative to that in a stirred tank (0.100 m³ volume, operated at 1 vvm air flow using 3 six-bladed turbines operated at 300 rpm, 3-4 kWm⁻³ agitation power). This yield improvement was achieved with a 50% reduction in power input leading to a more than 50% reduction in the cost of the biomass produced in the airlift.

Improved productivity of the airlift reactor relative to the stirred vessel was associated with the higher mass transfer coefficient obtained in the airlift (Malfait et al., 1981). Although this was not mentioned, possible shear damage (Markl et al., 1987) to cells in the stirred vessel may have been a contributory factor to its poor performance. Similarly,

Erickson et al. (1983) quoted a report in which novobiocin production using *Streptomyces niveus* in 0.1 to 0.2 m³ airlift fermenters was found to be as good or better compared to the results obtained in stirred tanks. Excellent results have been reported (Koenig et al., 1981) for *Penicillin* fermentation in an external loop device. Several other examples of the successful cultivation of mycelial fungi in airlift reactors have been presented by Erickson et al. (1983).

Fermentations of *candida lipolytica* (Seipenbusch et al., 1976) and *Candida intermedia* (Hatch, 1975) on n-paraffin in internal-loop airlifts have been demonstrated and continuous cultivation of another yeast (*Candida utilis*) in a concentric draught-tube bubble column has been shown to be possible (Huang et al., 1976). Hydrocarbon fermentation in an airlift of external-loop design has also been reported (Blakebrough et al., 1967). Smart and Fowler (1984) demonstrated the feasibility of extended continuous cultivation (~14 days) of plant cell suspensions of *Catharanthus roseus* in a small (~0.010 m³) external-loop airlift reactor.

Successful use has been made of very deep airlift of the internal-loop draught tube bubble column type both for municipal and industrial aerobic sewage treatment (Gallo and Sandford, 1979; Redman, 1987). Such airlifts may be 100-200 m deep and tend to be extremely small in volume compared to conventional activated sludge systems due to the much higher oxygen transfer rates that can be achieved in them. The power economy for the deep shaft plants has been estimated at three times that of a conventional plant. A value of 2.2 kg of O₂ transferred /kWh has been quoted for the former. Further details of airlift reactors for sewage treatment are provided in the papers by Hines et al. (1975), and Redman (1987).

Airlift reactors have been put to use for hybridoma culture for monoclonal antibody production (Wood and Thompson, 1986; Royse, 1987). The relatively low shear tolerances of mammalian cells and their low oxygen demands require that very different reactor operation regimes be used for these fermentations than is conventional for the microbial processes. Industrial use of airlifts in the cell culture applications is increasing exponentially as exemplified by Royse (1987). Shear stress that may be tolerated by animal cells ranges (Wood and Thompson, 1986) from less than 0.05 Nm⁻² to 500 Nm⁻². It has been estimated that at shear stresses of 0.05 Nm⁻² oxygen transfer rates of between 0.6 and 1.0 mmol L⁻¹ h⁻¹ may be achieved in airlift devices.

2.5 HYDRODYNAMIC AND MASS TRANSFER FEATURES OF DRAFT TUBE BUBBLE COLUMNS

The design and scale-up of bubble columns has attracted considerable attention in last two decades to gain an understanding of the complex hydrodynamics of these columns and its influence on the mass transport characteristics. However, the knowledge base of draft tube bubble columns is still scarce and scanty. The construction of these columns is simple but precise design and scale-up requires a thorough understanding of the multiphase fluid dynamics in these devices and their interaction with other transport parameters. More specifically knowledge of the hydrodynamic parameter - ‘gas holdup’ and mass transfer parameters such as ‘specific gas–liquid interfacial area’ and ‘mass transfer coefficients’ is necessary for design. Additionally, the quantification of the effects of operating conditions, physical properties of phases, column dimensions, types of gas distributors, etc. on the hydrodynamic and mass transfer parameters as well as on the overall performance of draft tube bubble columns also merits reflection.

2.5.1 Gas holdup

Gas holdup, ϵ_g is a dimensionless parameter that characterizes the transport phenomena of bubble columns. It is basically defined as the volume fraction of gas phase in the gas-liquid dispersion. It is the key hydrodynamic parameter that directly influences residence time of gas in the column, interfacial area, and indirectly affects the rate of mixing, liquid circulation velocity, rate of mass transfer and ultimately the performance of the column.

Gas holdup depends mainly on gas flow rate, on the gas – liquid system involved and design of gas distributor. For bubble column systems, gas holdup has been found to increase with increasing superficial gas velocity as concluded by several investigators who studied widely different gas- liquid systems (Deckwer et al., 1980; Saxena et al., 1990; Pino et al., 1992; Daly and Bukur, 1992; Krishna et al., 1997; Li and Prakash, 2000; Prakash et al., 2001). This increase has been found to be proportional to superficial gas velocity in the bubbly flow regime (Lockett and Kirkpatrick, 1975; Kara et al., 1982), while in the churn turbulent regime the effect of superficial velocity on gas holdup is less pronounced (Kara et al., 1982; Koide et al., 1984).

Hyndman et al. (1997) analyzed the contribution of small and large bubbles on total holdup. These authors pointed out that in the churn-turbulent regime, as the superficial

velocity increases, the total holdup increases due to an increase in the holdup of large bubbles. The contribution of small bubbles on the total holdup is constant and equal to the transition holdup, i.e. it does not increase with increasing superficial velocity however the large bubble holdup increases with increasing superficial velocity causing an increase in the total holdup. On the other hand in bubbly flow, the small bubble holdup is not constant but increases significantly as the superficial velocity is increased as shown in Fig.2.7.

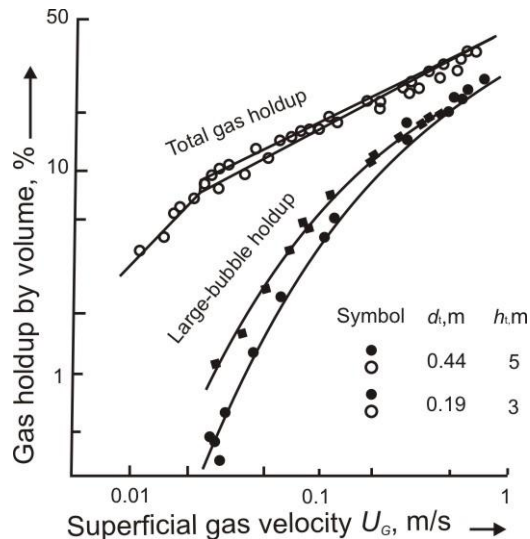


Fig. 2.7 Gas holdup and fraction of large bubbles (system: water-air; gas distributor: perforated plate, $d_h = 3mm$), adopted from Hyndman et al., (1997)

The effects of physical properties on gas holdup are exceedingly complex. Increasing the viscosity of the liquid phase leads to increased bubble coalescence and formation of large bubbles that enhance the bubble rise velocities that brings about a decline in gas holdup as reported by Li and Prakash (1997). It is also reported that adding a small amount of surfactant to water, results in significantly higher gas holdup values. Moreover, the presence of electrolyte or impurities also increases gas holdup (Hikita et al., 1980; Sada et al., 1984).

The effect of column diameter and height on hydrodynamics is also widely investigated in literature. Shah et al. (1982) reported that in bubble columns, the effect of column size on gas holdup is negligible when the column diameter is larger than 10–15 cm. Luo et al. (1999) reported that the influence of the column height is insignificant if the height is above 1–3 m and the aspect ratio is larger than 5.

Gas sparger geometry is an important parameter that can alter bubble characteristics which in turn affects gas holdup values. The sparger used definitely determines the bubble sizes observed in the column. Small orifice diameter plates enable the formation of smaller sized bubbles. Some common types of gas sparger that are reported in literature are dip tube, perforated plate, porous plate, membrane, ring type distributors and jet type dynamic gas distributors etc. Bouaifi et al. (2001) observed that with small orifice gas distributors the gas holdup values were higher, thus they concluded that smaller the bubbles the greater the gas holdup.

In another study by Luo et al. (1999) gas holdup was found to be strongly affected by the type of gas distributor. The effect was more pronounced especially for gas velocities below 6 cm/s. Schumpe and Grund (1986) worked with perforated plate and ring type gas spargers and concluded that with ring type distributor, the total holdup was smaller. They also observed that the small bubble holdup showed a gradual increase with increasing superficial velocity with ring type sparger. Another conclusion about the type of spargers was that the contributions of both small and large bubbles to gas velocity were lower with ring sparger as compared to the perforated plate. In general it is experienced that at low gas velocities, gas holdup also depends on number, pitch and diameter of orifice holes. There exist various correlations in literature to predict the gas holdup in bubble columns and slurry bubble columns as shown in Table 2.1.

Weiland (1984) reported that the gas holdups that occur in draft tube bubble columns with internal loop are only slightly lower than those in bubble columns. In contrast, Bello et al., (1985a) observed that for internal loop draft tube bubble column there is no influence of either the presence of draft tube or its relative area with respect to that of the annulus on the total gas holdup. Thus, the total gas holdup in the internal loop draft tube bubble column is exactly the same as in a corresponding bubble column when the superficial gas velocity based on the entire column cross section was used for comparison. Exactly the same finding was reported for non Newtonian fluid by Kawase and Moo-Young (1986a), in a rectangular internal loop by Piggott (1985) and by Koide et al. (1983) in an internal loop draft tube columns. In Table 2.2, several frequently used gas holdup correlations for internal loop draft tube bubble columns are summarized.

Table 2.1 Gas holdup correlations for bubble columns

Research group	Correlation
Roy et al. (1963)	$\varepsilon_g = 3.88 \times 10^{-3} \left[\text{Re}_T \left(\frac{\sigma_w}{\sigma_l} \right)^{1/3} (1 - v_s)^3 \right]^{0.44}$, for $\text{Re}_T > 500$, $v_s = \frac{W_s/\rho_s}{(W_s/\rho_s) + (W_l/\rho_l)}$
Hughmark (1967)	$\varepsilon_g = \frac{1}{2 + (0.35/U_g)(\rho_l \sigma_l / 72)^{1/3}}$
Akita and Yoshida (1974)	$\frac{\varepsilon_g}{(1 - \varepsilon_g)^4} = \alpha \left(\frac{d_R^2 \rho_l g}{\sigma_l} \right)^{1/8} \left(\frac{g d_R^3 \rho_l^2}{\mu_l^2} \right)^{1/12} \frac{U_g}{\sqrt{g d_R}}$ first term: Bond number, second term: Galilei number, third term: Froude number, $\alpha = 0.2$ for pure liquids and non-electrolyte solutions, $\alpha = 0.25$ for salt solutions
Hikita and Kikukawa (1974)	$\varepsilon_g = 0.505 U_g^{0.47} \left(\frac{0.072}{\sigma_l} \right)^{2/3} \left(\frac{0.001}{\mu_l} \right)^{0.05}$
Lockett and Kirkpatrick (1975)	$\underline{U}_g(1 - \varepsilon_g) + \underline{U}_l \varepsilon_g = V_b \varepsilon_g (1 - \varepsilon_g)^{2.39} (1 + 2.55 \varepsilon_g^3)$
Kumar et al. (1976)	$\varepsilon_g = 0.728 U' - 0.485 U'^2 + 0.0975 U'^3$, $U' = U_g [\rho_l^2 / \{\sigma_l (\rho_l - \rho_g) g\}]^{1/4}$
Joshi and Sharma (1979)	$\varepsilon_g = \frac{U_g}{0.3 + 2U_g}$
Koide et al. (1979)	$\varepsilon_g = \frac{U_g}{31 + \beta(1 - e)\sqrt{U_g}}$, $\beta = 4.5 - 3.5 \exp(-0.064 d_R^{1.3})$; $e = -\frac{0.18 U_g^{1.8}}{\beta}$
Hikita et al. (1980)	$\varepsilon_g = 0.672 f \left(\frac{U_g \mu_l}{\sigma_l} \right)^{0.578} \left(\frac{\mu_l^4 g}{\rho_l \sigma_l^3} \right)^{-0.131} \left(\frac{\rho_g}{\rho_l} \right)^{0.062} \left(\frac{\mu_g}{\mu_l} \right)^{0.107}$, $f = 1$ for pure liquids and non-electrolyte solutions, for ionic solutions f is a function of ionic strength
Godbole et al. (1982)	$\varepsilon_g = 0.239 U_g^{0.634} d_R^{-0.5}$, for viscous media in slug flow regime

Sada et al. (1984)	$\varepsilon_g = 0.32(1 - \varepsilon_g)^4 \text{Bo}^{0.21} \text{Ga}^{0.086} \text{Fr} \left(\frac{\rho_g}{\rho_l} \right)^{0.068}$
Koide et al.(1984)	$\frac{\varepsilon_g}{(1 - \varepsilon_g)^4} = \frac{k_1(U_g \mu_1 / \sigma_1)^{0.918} (g \mu_1^4 / (\rho_1 \sigma_1^3))^{-0.252}}{1 + 4.35 v_s^{0.748} [(\rho_s - \rho_l) / \rho_l]^{0.88} (d_R U_g / \rho_l)^{-0.168}}$
Smith et al. (1984)	$\varepsilon_g = \left[2.25 + \frac{0.379}{U_g} \left(\frac{\rho_l \text{ or } \rho_{sl}}{72} \right)^{0.31} (\mu_l \text{ or } \mu_{sl})^{0.016} \right]^{-1}, \quad \mu_{sl} = \mu_l \exp \left[\frac{(5/3)v_s}{1-v_s} \right]$
Sada et al. (1984)	$\frac{\varepsilon_g}{(1 - \varepsilon_g)^3} = 0.019 U_\infty^{1/16} v_s^{-0.125} U_\infty^{-0.16} U_g$
Reilley et al. (1986)	$\varepsilon_g = 0.009 + 296 U_g^{0.44} (\rho_l \text{ or } \rho_{sl})^{-0.98} \sigma_1^{-0.16} \rho_g^{0.19}$
Grover et al. (1986)	$\varepsilon_g = \left(\frac{1+aP_v}{bP_v} \right) \left(\frac{U_g \mu_1}{\sigma_1} \right)^{0.76} \left(\frac{\mu_1^4 g}{\rho_1 \sigma_1^3} \right)^{-0.27} \left(\frac{\rho_g}{\rho_l} \right)^{0.09} \left(\frac{\mu_g}{\mu_l} \right)^{0.35}, \quad a = 1.1 \times 10^{-4} \text{ and } b = 5 \times 10^{-4}$
Schumpe and Deckwer (1987)	$\varepsilon_g = 0.2 \left(\frac{d_R^2 \rho_l g}{\sigma_1} \right)^{-0.13} \left(\frac{g d_R^3 \rho_l^2}{\mu_{\text{eff}}^2} \right)^{0.11} \left(\frac{U_g}{\sqrt{g d_R}} \right)^{0.54}$ used for highly viscous media and groups vary in the following ranges: $1.4 \times 10^3 \leq \text{Bo} \leq 1.4 \times 10^5$, $1.2 \times 10^7 \leq \text{Ga} \leq 6.5 \times 10^{10}$, $3 \times 10^{-3} \leq \text{Fr} \leq 2.2 \times 10^{-1}$
Kawase and Moo-Young (1987)	$\varepsilon_g = 1.07 \text{Fr}^{1/3}$
Zou et al.(1988)	$\varepsilon_g = 0.17283 \left(\frac{\mu_1^4 g}{\rho_1 \sigma_1^3} \right)^{-0.15} \left(\frac{U_g \mu_1}{\sigma_1} \right)^{0.58} \left(\frac{P+P_v}{P} \right)^{1.61}$
Kawase et al. (1992)	$\frac{\varepsilon_g}{1+\varepsilon_g} = 0.0625 \left(\frac{U_g}{v_l g} \right)^{1/4}$

Table 2.2 Gas holdup correlations for internal loop draft tube bubble columns

Research group	Correlation
Chakravarty et al.(1974)	$\epsilon_{gr} = 0.0057 \left[(\mu_l - \mu_w)^{2.75} - 161 \frac{73.3 - \sigma_l}{79.3 - \sigma_l} \right] U_{gr}^{0.88}$
Koide et al. (1983)	$\frac{\epsilon_{gr}}{(1 - \epsilon_{gr})^4} = 0.16 \left(\frac{U_{gr} \mu_l}{\sigma_l} \right) Mo^{-0.283} \left(\frac{d_t}{d_R} \right)^{-0.222} \left(\frac{\rho_l}{\Delta \rho} \right)^{0.283} [1 - 1.61(1 - e^{-0.00565 Ma})]^{-1}$
Akita and Kawasaki (1983)	$\epsilon_{gr} = 0.364 U_{gr}$
Popovic and Robinson (1984)	$\epsilon_{gr} = 0.465 U_{gr}^{0.65} \left(1 + \frac{A_d}{A_r} \right)^{-1.06} \mu_{ap}^{-0.103}$
Bello et al.(1985a)	$\epsilon_{gr} = 0.16 \left(\frac{U_{gr}}{U_{lr}} \right)^{0.57} \left(1 + \frac{A_d}{A_r} \right),$ $\epsilon_{gd} = 0.79 \epsilon_{gr} - 0.057$
Koide et al. (1985)	$\frac{\epsilon_{gr}}{(1 - \epsilon_{gr})^4} = \frac{0.124 \left(\frac{U_{gr} \mu_l}{\sigma_l} \right)^{0.996} \left(\frac{\rho_l \sigma_l^3}{g \mu_l^4} \right)^{0.294} \left(\frac{d_t}{d_R} \right)^{0.114}}{1 - 0.276(1 - e^{-0.0368 Ma})}$
Vatai and Tekis (1986)	$\epsilon_{gr} = (0.491 - 0.498) U_{gr}^{0.706} \left(\frac{A_d}{A_r} \right)^{-0.254} d_t \mu_{ap}^{-0.0684}$
Chisti et al.(1987)	Rectangular internal loop draft tube bubble column Homogeneous flow regime: $\epsilon_g = (1.488 - 0.496 C_s) U_g^{0.892 \pm 0.075}$ Heterogeneous flow regime: $\epsilon_g = (0.371 - 0.089 C_s) U_g^{0.430 \pm 0.015}$
Kawase and Moo-Young (1986b)	$\epsilon_g = 0.24 n^{-0.6} Fr^{0.84 - 0.14n} Ga$

Miyahara et al.(1986)	$\epsilon_{gr} = \frac{0.4 Fr}{1 + 0.4 Fr \left(1 + \frac{U_{lr}}{U_{gr}}\right)}$
Koide et al. (1988)	$\epsilon_{gr} = \frac{Fr}{0.415 + 4.27 \left(\frac{U_{gr} + U_{lr}}{\sqrt{gd_t}}\right) \left(\frac{g\rho_l d_R^2}{\sigma_l}\right)^{-0.188} + 1.13 Fr^{1.22} Mo^{0.0386} \left(\frac{\Delta\rho}{\rho_l}\right)^{0.0386}}$
Chisti et al.(1988)	$\epsilon_{gr} = 0.65 U_{gr}^{(0.603+0.078C_0)} \left(1 + \frac{A_d}{A_r}\right)^{-0.258},$ $\epsilon_{gd} = 0.46 \epsilon_{gr} - 0.0244$ <p>Where C_0 is distribution parameter, depends mainly on the radial profile of the gas holdup. $C_0 = 1$ for flat profile and 1.5 for parabolic profile.</p>
Cai et al.(1992)	$\epsilon_{gr} = 2.47 U_{gr}^{0.97}$
Li et al.(1995)	$\epsilon_{gr} = 0.441 U_{gr}^{0.841} \mu_{ap}^{-0.135},$ $\epsilon_{gd} = 0.297 U_{gr}^{0.935} \mu_{ap}^{-0.107}$
Kawase et al.(1995)	$\frac{\epsilon_{gr}}{(1-\epsilon_{gr})} = \frac{U_{gr}^{\frac{n+2}{2(n+1)}}}{2^{\frac{3n+1}{n+1}} n^{\frac{n+2}{2(n+1)}} \left(\frac{K}{\rho_l}\right)^{\frac{1}{2(n+1)}} g^{\frac{n}{2(n+1)}} \left(1 + \frac{A_d}{A_r}\right)^{\frac{3(n+2)}{4(n+1)}}$

2.5.2 Specific gas-liquid interfacial area

The area of gas liquid interface is one of the most important process parameters for designing gas-liquid contactors of industrial scale. It is perhaps the most influential factor in determining size of the column and reactor output, especially at high reaction rates i.e. for absorption accompanied by fast chemical reaction, knowledge of this parameter is also necessary for calculating individual mass-transfer co-efficient. Like gas holdup, the value of the interfacial area can vary depending on the type and geometric size of contacting device, operating conditions and the physiochemical properties of gas-liquid system.

Gas holdup and interfacial area per unit volume are related as...

$$a = \frac{A}{V_D} = \frac{A\epsilon_g}{V_G} \quad (2.1)$$

Where the surface area A of bubbles formed within a specific dispersions volume is represented by $\pi \sum n_i d_i^2$ and volume of dispersion V_D can be formulated by $\frac{\pi}{6} \sum n_i d_i^3$, so that a can be written as follows:

$$a = \frac{(\pi \sum n_i d_i^2) \epsilon_g}{\frac{\pi}{6} \sum n_i d_i^3} = \frac{6 \epsilon_g}{\left(\frac{\sum n_i d_i^3}{\sum n_i d_i^2} \right)} \quad (2.2)$$

where d_s is Sauter mean bubble diameter and defined as...

$$d_s = \frac{\sum n_i d_i^3}{\sum n_i d_i^2} \quad (2.3)$$

The interfacial area increases with increasing gas flow rate as shown in Fig. 2.8. An exception occurs when a porous plate sparger is used, interfacial area decreases on transition to the heterogeneous flow regime and then approaches the same values observed with perforated plates. The growth in interfacial area with increasing gas velocity is always greater in the homogeneous than in the heterogeneous flow regime. The reason lies in the formation of large bubbles in the heterogeneous regime; the

interfacial area of large bubbles per unit volume is markedly lower than that of the smaller ones.

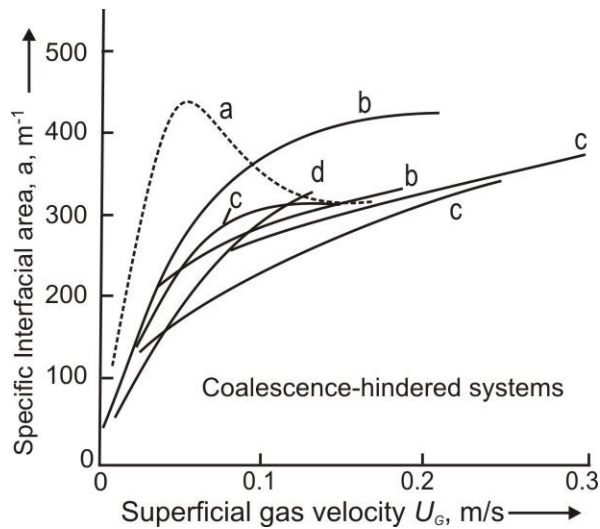


Fig. 2.8 Specific interfacial area as a function of superficial gas velocity

a) $d_i = 0.102$ m; b) $d_i = 0.29$ m; c) $d_i = 0.14$ m; d) $d_i = 0.1$ m; (--- Porous plate; — Perforated plate),
adopted from Deen et al. (2007)

2.5.3 Volumetric mass transfer coefficient

The overall mass transfer rate per unit volume of the dispersion in bubble columns is governed by the liquid-side mass transfer coefficient, $k_L a$ when the gas side resistance is negligible. $k_L a$ is the liquid-phase mass transfer coefficient k_L multiplied by the specific interfacial area a . In bubble columns the variation in $k_L a$ is primarily due to variation in the interfacial area (Fan et al., 1985). The volumetric mass transfer coefficient is a key parameter in the characterization, scale-up and design of industrial gas–liquid reactors.

The mass-transfer coefficient $k_L a$ depends on the gas flow rate, type of sparger, and gas – liquid system like gas holdup and interfacial area, $k_L a$ increases with increasing gas velocity in the same pattern as the gas holdup increased with superficial gas velocity. The dependence of $k_L a$ on superficial velocity is expressed as $k_L a \propto U_g^n$, where n varies between 0.7 and 0.92 (Akita and Yoshida, 1974; Deckwer et al., 1974; Hikita et al., 1981; Kawase et al., 1986a). Experiments performed with viscous liquids showed that the volumetric mass transfer coefficient, $k_L a$, decreases with increasing liquid viscosity (Fukuma et al., 1987; Behkish et al., 2002). Both the teams of investigators pointed out that higher viscosity led to increase of the volume fraction of the large bubbles, leading to much lower gas–liquid interfacial areas. Thus, presence of large bubbles should be

avoided in industrial columns for effective mass transfer. Muller and Davidson (1995) experimented with viscous liquids and studied the effect of surface active agents on the mass transfer in bubble columns, they reported that $k_L a$ values increase in the presence of surfactants. These authors attributed this increase to the creation of small bubbles and reduced bubble coalescence due to surfactants.

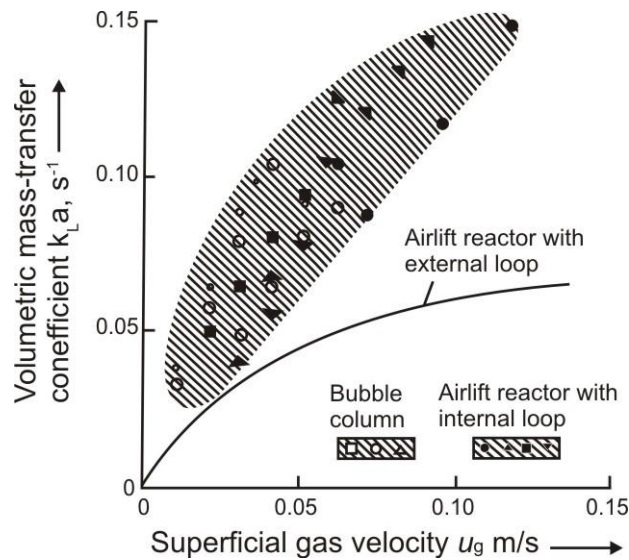


Fig. 2.9 Comparison of mass transfer coefficients for airlift reactors and bubble columns (*System: salt solutions; gas distribution: small bubbles*),
adopted from Koide et al.(1983)

As in the bubble column, the volumetric mass transfer coefficient in draft tube bubble columns also increases with increasing gas flow rate. Airlift reactors with external loop always have lower mass transfer coefficients than bubble columns due to the relatively lower gas holdup in these devices that implies a smaller area for mass transfer. The $k_L a$ values for draft tube bubble columns (internal loop reactors) on the other hand, are similar to the values obtained for bubble columns as shown in Fig. 2.9, because in this case the gas holdups are nearly same (Koide et al., 1983). Further these investigators argue that the difference in $k_L a$ results from differences in interfacial area because the liquid-phase mass transfer coefficients k_L are nearly the same in bubble columns and airlift reactors.

Volumetric mass transfer coefficients experimentally determined by different investigators vary quite widely. However, it is interesting to note that for a given draft tube bubble column, $k_L a$ varies linearly on a log-log scale over a reasonable range of superficial gas velocities (Chen, 1990). Bello et al. (1985a; 1985b) found that the riser

gas holdup and the volumetric mass transfer coefficient in their laboratory airlift reactor depended not only on the superficial gas velocity but also on the circulating liquid velocity in the draft tube. For specified column configuration, sparger type and liquid physiochemical properties the liquid circulation velocity ' U_L ' at a given gas rate is established by the downcomer to riser cross-sectional area. The values of gas holdup and volumetric mass transfer coefficient both increase with increasing gassing power input, but an increase in the circulating liquid velocity, causes both to decrease. Airlift mass transfer performance was poorer than that of bubble column because of the effect of the high circulating liquid velocity in the riser as well as the negligible mass transfer capabilities of the downcomer section.

Kastanek et al., (1993) have reported that increased liquid velocity in aerated sections of the air lift reactors causes partial or complete coalescence suppression even in typically coalescence supporting systems. This phenomena can be explained by the fact that the increased liquid velocity (due to circulation in the internal or external loop) suppresses chaotic motion of bubbles and thus reduces the frequency of their mutual contacts and at the same time facilitates the break-up of extremely large bubbles which may be present in the aerated section. Because high absolute values of liquid circulation velocity cause suppression of coalescence even in essentially coalescing systems, it can be assumed that hydrodynamic behaviour of coalescence promoting and coalescence suppressing systems in airlift reactors will differ substantially less than in common bubble column reactors. Experimental data showed a two-fold increase of $k_L a$, in airlift reactors caused by the addition of coalescence inhibitors to the air-water system, in comparison with the six-fold increase in bubble column reactors under otherwise identical conditions. The decrease in average bubble size leads to the decrease of d_s values. At the same time however gas holdup in airlift reactors also decreases with increasing liquid circulation velocity. Due to the $k_L a$ definition ($k_L a = k_L \frac{6\epsilon_g}{d_s}$), its values are thus contradictorily influenced by changes of d_s and ϵ_g . It has been shown experimentally, that $k_L a$ values in airlift reactors are always rather smaller than in bubble columns.

Various correlations proposed for the prediction of mass transfer coefficients are shown in Tables 2.3 and 2.4 for bubble columns and for internal loop draft tube bubble columns respectively.

Table 2.3 Mass transfer coefficient correlations for bubble columns

Research group	Correlation
Akita and Yoshida (1973)	$\frac{k_1 a d_R^2}{D_{AB}} = 0.6 \left(\frac{v_l}{D_{AB}} \right)^{0.5} \left(\frac{g d_R^2 \rho_l}{\sigma_l} \right)^{0.62} \left(\frac{g d_R^3}{v_l^2} \right)^{0.31} \epsilon_g^{1.1}$
Hikita et al.(1981)	$\frac{k_1 a U_g}{g} = 14.9 \left(\frac{U_g \mu_l}{\sigma_l} \right)^{1.76} \left(\frac{\mu_l^4 g}{\rho_l \sigma_l^3} \right)^{-0.248} \left(\frac{\mu_g}{\mu_l} \right)^{0.243} \left(\frac{\mu_l}{\rho_l D_{AB}} \right)^{-0.604}$
Shah et al. (1982)	$k_1 a = 0.467 U_g^{0.82}$
Schumpe and Grund (1986)	$k_1 a = K U_g^{0.82} \mu_{\text{eff}}^{-0.39},$ K = 0.063 (water/salt solution), K = 0.042 (water, 0.8 M Na ₂ SO ₄)
Ozturk et al. (1987)	$\frac{k_1 a d_b^2}{D_{AB}} = 0.62 \left(\frac{\mu_l}{\rho_l D_{AB}} \right)^{0.5} \left(\frac{g \rho_l d_b^2}{\sigma_l} \right)^{0.33} \left(\frac{g \rho_l^2 d_b^3}{\mu_l^2} \right)$ $\left(\frac{U_g}{\sqrt{g d_b}} \right)^{0.68} \left(\frac{\rho_g}{\rho_l} \right)^{0.04}$ OR $\text{Sh} = 0.62 \text{Sc}^{0.5} \text{Bo}^{0.33} \text{Fr}^{0.68} \left(\frac{\rho_g}{\rho_l} \right)^{0.04}$
Kawase and Moo-Young (1987)	$\frac{k_1 a d_R^2}{D_{AB}} = 0.452 \left(\frac{v_l}{D_{AB}} \right)^{1/2} \left(\frac{d_R U_g}{v_g} \right)^{3/4} \left(\frac{g d_R^2 \rho_l}{\sigma_l} \right)^{3/5} \left(\frac{U_g^2}{d_R g} \right)^{7/60}$
Kang et al. (1999)	$k_1 a = K \times 10^{-3.08} \left(\frac{d_R U_g \rho_g}{\mu_l} \right)^{0.254}$ where K is the correlation dimension

Table 2.4 Mass transfer coefficient correlations for internal loop draft tube bubble columns

Research group	Correlation
Popovic and Robinson (1984)	$k_L a = 1.911 \times 10^{-4} U_{gr}^{0.525} \left[1 + \frac{A_d}{A_r} \right]^{-0.853} \mu_{ap}^{-0.89}$ <p>External loop draft tube bubble column</p>
Koide et al.(1985)	$Sh = 2.66 Sc^{0.5} Bo^{0.715} Ga^{0.25} \left(\frac{d_T}{d_R} \right)^{-0.429} \epsilon_g^{1.34}$
Bello et al. (1985b)	$k_L a = 0.76 \left[1 + \frac{A_d}{A_r} \right]^{-2} U_{gr}^{0.8}$ $k_L a = 5.5 \times 10^{-4} \left[1 + \frac{A_d}{A_r} \right]^{-1.2} (P_G/V_D)^{0.8}$ <p>Bubble column, $A_d/A_r = 0$; External loops, $A_d/A_r = 0.11$ to 0.69; Internal loops draft tube bubble column (annulus sparged); $A_d/A_r = 0.13, 0.35$ and 0.56;</p>
Bello et al.(1985a)	$\frac{k_L a h_D}{U_{lr}} = 2.28 \left[\frac{U_{gr}}{U_{lr}} \right]^{0.90} \left[1 + \frac{A_d}{A_r} \right]^{-1}$ <p>A_d/A_r (external loops) = 0.11 to 0.69; A_d/A_r (internal loops) = $0.13, 0.35$ and 0.56;</p>
Kawase and Moo-Young (1986b)	$\frac{k_L a d_R^2}{D_{AB}} = 0.68 n^{-0.72} \left[\frac{d_R U_g \rho_l}{\mu_{ap}} \right]^{0.38n+0.52} \left[\frac{\mu_{ap}}{D_{AB} \rho_l} \right]^{0.38n-0.14}$ <p>or</p> $Sh = 0.68 n^{-0.72} Fr^{0.38n+0.52} Sc^{0.38n-0.14}$ <p>Also used for Bubble columns</p>
Chisti et al.(1987)	$k_L a = (0.349 - 0.102 C_s) U_{gr}^{0.837} \left[1 + \frac{A_d}{A_r} \right]^{-1}$ <p>External loop draft tube bubble column</p>
Merchuk et al.(1994)	$Sh = 3 \times 10^4 Fr^{0.97} M^{-5.4} Ga^{0.045} \left(1 + \frac{A_d}{A_r} \right)^{-1}$
Li et al.(1995)	$k_L a = 0.0343 U_{gr}^{0.524} \mu_{ap}^{-0.255}$

2.6 SUMMARY

Draft tube bubble columns have been in existence since 1969. In spite of commercial utilization of these devices for large tonnage applications such as SCP production, biomass growth, wastewater treatment etc., the understanding of their hydrodynamic and mass transfer behavior is rather limited.

Literature survey reveals that gas holdup behaviour of these devices have been extensively investigated but till date literature available on the interfacial area of these devices measured by chemical techniques is rare. Information on volumetric mass transfer coefficients is only partially available.

There is a need for systematic investigation on these devices exploring the effect of device geometry on hydrodynamic parameters and mass transfer coefficients, investigating the effect of draft tube length on hydrodynamics and mass transfer, exploring the effect of enhancement of size/scale of operations on hydrodynamic and mass transfer parameters, investigating important applications viz. wastewater treatment and biomass growth in well characterized draft tube bubble column and thereby identifying influence of key parameters on process development.

The investigation chronicled in the subsequent chapters of this thesis is an attempt to address the above mentioned issues.

CHAPTER 3

EXPERIMENTAL SETUP, MATERIALS AND METHODS

The present work was undertaken to investigate the hydrodynamic and mass transfer behaviour of draft tube bubble columns, to investigate the effect of geometry and operating variables on key hydrodynamic and mass transfer parameters and also to explore the application of these devices in wastewater treatment and biomass growth.

3.1 EXPERIMENTAL SETUP

In this investigation three draft tube bubble column assemblies were fabricated using transparent acrylic materials (sheets/cylinders). First one was a rectangular draft tube bubble column and other two were cylindrical draft tube bubble column's having geometrical specifications as mentioned in Table 3.1.

Table 3.1 Specifications of columns

Columns and Notations	Parts	Specifications, cm				c.s. area, cm ²
		W	D	H	T	
Rectangular Draft Tube Bubble column (RDTBC)	Outer column	10.7	4	100	0.5	42.8
	Draft tube-1	8	1	70	0.4	8
	Draft tube- 2	8	1	60	0.4	8
		ID	OD	H	T	
Cylindrical Draft Tube Bubble Column having equivalent draft tube cross-sectional area as RDTBC (CDTBC-1)	Outer column	6.4	7	100	0.3	32.17
	Draft tube	3.2	3.8	70	0.3	8.042
Cylindrical Draft Tube Bubble Column having larger diameter (CDTBC-2)	Outer column	14	15	100	0.5	154
	Draft tube	8	9	70	0.5	50.3

W-Width, D-Depth, H-Height, T-Thickness, ID-Inside Diameter, OD-Outside Diameter.

3.1.1 Rectangular Draft Tube Bubble Column (RDTBC)

The experimental setup of rectangular draft tube bubble column is shown in Fig. 3.1 it consisted of a transparent rectangular outer column and draft tubes having specifications as given in Table 3.1. The draft tube used in this investigation was placed coaxially within the column and held using a bolting mechanism. Care was taken that the gap

between the draft tube and the column was uniform on all sides throughout the length of the draft tube. Small thin circular acrylic pieces were also fixed at some locations on the outer surfaces of draft tube to ensure this coaxial arrangement of draft tube in rectangular geometry as shown in Fig. 3.2(b). The draft tube was mounted 1 cm above the sparger.

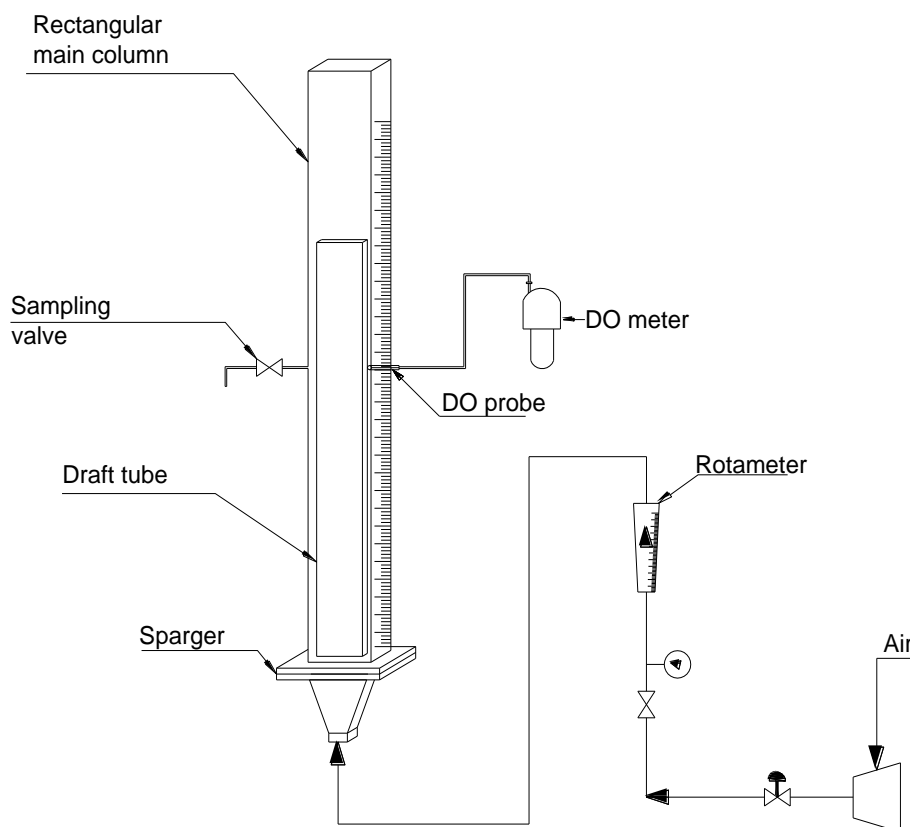


Fig. 3.1 Schematic of experimental setup of RDTBC

Air was sparged into the column through sparger that was fixed at the base of the column using flanged assembly. Holes were drilled and stainless steel bolts were fitted on the all sides of the assembly to tighten the assembly so as to prevent gas and liquid leakage during experiments. This arrangement also helped vertical mounting of the column on the main stand as shown in Fig. 3.2(a). A trapezoidal gas chamber beneath the sparger ensured the uniform distribution of air through sparger as shown in Fig.3.2 (d). A hole was also drilled in the bottom of this gas distribution chamber for the entry of air from compressor into the column.



(a) RDTBC mounted on stand



(b) Draft tube with supports



(c) Sampling valve



(d) Gas distribution chamber

Fig. 3.2 Snapshots of rectangular draft tube bubble column and its parts

The air was supplied by using single stage, two-cylinder, air-cooled compressor. This compressor was equipped with a 0.4 m³ horizontal tank complete with a safety valve, air gauge and drain valve. The maximum compressor capacity was to deliver 0.07 m³/min at 1.5 atm.g. Air flow was regulated at constant pressure, using pressure regulator and measured using calibrated rotameters working in the range of 0.05-1 LPM, 0.5-8 LPM and 6-60 LPM. A scale was mounted behind the column for measurement of liquid level. Liquid samples required for various analyses were drawn through a sampling valve located at the side of the main column at a distance of 0.5 m from the base of the column. Fig.3.2(c) shows the valve, fitted into the turnings made in an acrylic block, which was then fixed on the outer side of the column. A dissolved oxygen probe was introduced at the opposite side of the sampling valve by drilling a hole in the main column. An oil seal and teflon tape was used in the acrylic based cubical mounting assembly of DO probe to avoid any leakage.

Numerous designs of gas spargers exist in the literature as discussed by Chisti and Moo-Young (1987) however, for biotechnological applications the perforated plate and to a lesser extent the porous plates are most commonly used. In this work perforated plate type metal spargers having different number of holes, diameter of holes and pitch were used for hydrodynamic study of air –water system in RDTBC. The specifications of the perforated plate type metal spargers used are given in Table 3.2. Photographs of the same are also shown in Fig.3.3

Table 3.2 Spargers and their specifications for RDTBC

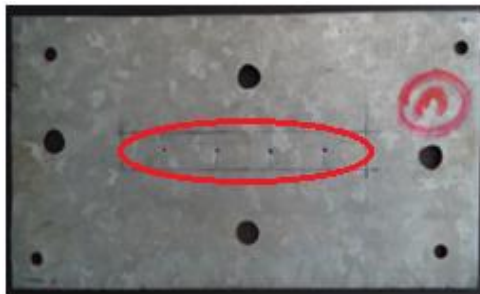
Sparger	Sparger specifications		
	N _h , Number of holes	d _h , Hole diameter, mm	P _t , Pitch, mm
A	1	2	-
B	2	2	20
C	4	1	20
D	6	1	8
E	12	1	6
H	5	1	15
J	4	0.5	20



Sparger A



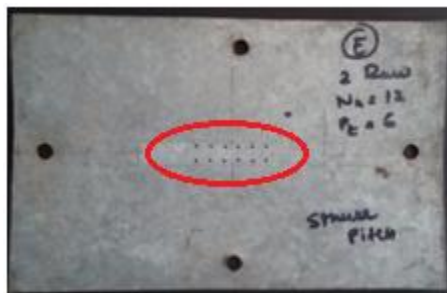
Sparger B



Sparger C



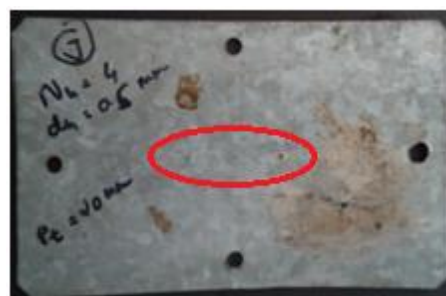
Sparger D



Sparger E



Sparger H



Sparger J

Fig. 3.3 Photographs of spargers used in RDTBC

3.1.2 Cylindrical Draft Tube Bubble Column-1 (CDTBC-1)

A cylindrical draft tube bubble column (CDTBC-1) was fabricated having equivalent circular cross-sectional area of draft tube as that used in the rectangular DTBC as shown in Fig.3.4 (a) and as per the specifications given in Table 3.1. This column was used in this work to compare the effect of geometry (rectangular Vs cylindrical) on hydrodynamic and mass transfer parameters. The draft tube was placed coaxially in the main column stabilized by cut segments of acrylic ring supports on three positions on a plane and at two different vertical locations on the outer side of the draft tube as shown in Fig.3.4 (b). These support segments were obtained by cutting a thin circle that exactly fitted into the annulus space of the assembly. This support assembly ensured that the draft tube snugly fitted in its desired position and did not move under influence of vibrations. The gap between the draft tube and sparger was created by fixing small uniform sized acrylic pieces on the upper surface of the sparger on which the draft tube rested as shown in Fig.3.4 (c). The acrylic sparger used in this CDTBC consisted of 4 holes each of 1 mm diameter and had 15 mm pitch, all the holes in the sparger were drilled on the periphery of a circle of 1.5 cm diameter and with centre of draft tube as the centre of the circle as shown in Fig.3.4 (d). The main column was screwed to the gas chamber that was also fabricated from thick acrylic plates as shown in Fig. 3.4 (e). All other arrangements viz. scale, sampling valve, an oil seal in hole for DO probe (Fig.3.4 f), main stand, rotameters, pressure regulator etc. was similar to that of RDTBC.

3.1.3 Cylindrical Draft Tube Bubble Column-2 (CDTBC-2)

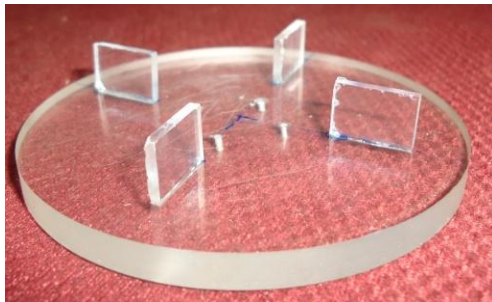
Experiments were also carried out using a 15 cm outer diameter cylindrical draft tube bubble column as shown in Fig.3.5 (a) having specifications as given in Table 3.1. Due to non availability of a seamless acrylic tube having a meters length, the main column was fabricated by joining two different acrylic tubes of length 60 cm and 40 cm respectively having same diameters using male-female joint as shown in Fig.3.5 (b). The sparger used in this investigation had 8 holes each of 1 mm diameter with 2 cm pitch drilled on the corners and midpoints of all sides of a square of 4 cm side length with centre of draft tube as the centre of the square as shown in Fig. 3.5(c). All other arrangements in the assembly of this column were similar to the cylindrical draft tube bubble column (CDTBC-1) described earlier and are shown in Figures 3.5 (d).



(a) CDTBC-1 assembly



(b) Supports on draft tube



(c) Supports for draft tube on sparger



(d) Holes in sparger

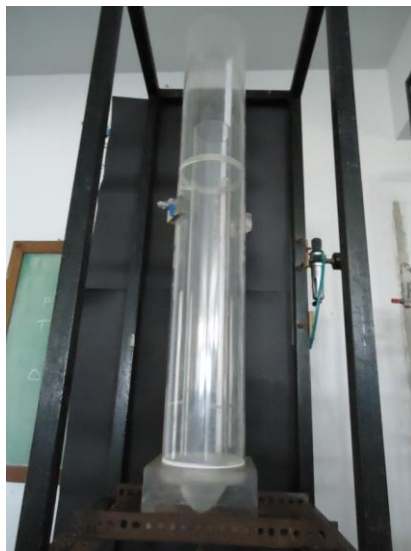


(e) Turnings in gas chamber



(f) Oil seal in hole for DO probe

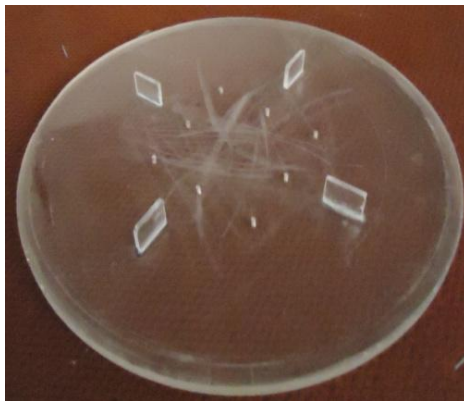
Fig. 3.4 Snapshots of cylindrical draft tube bubble column-1 (CDTBC-1) and its parts



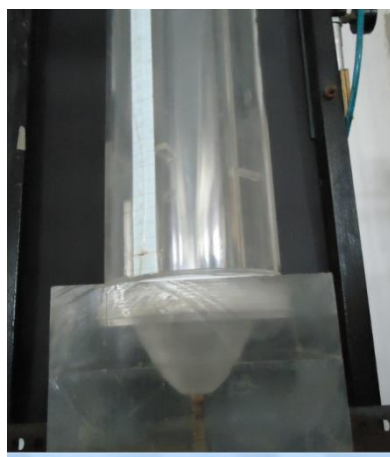
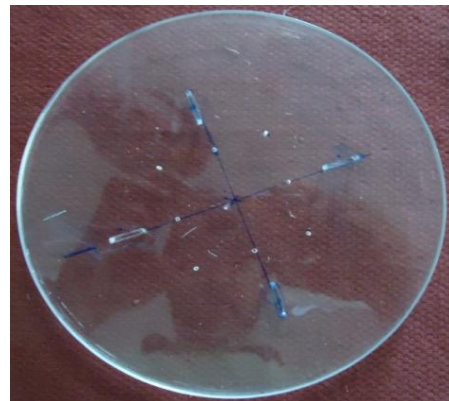
(a) CDTBC-2 assembly



(b) Male-female joint in outer column



(c) Sparger with 8 holes and supports for draft tube



(d) Bottom part of column and gas distribution chamber



Fig. 3.5 Snapshots of cylindrical draft tube bubble column-2 (CDTBC-2) and its parts

3.2 MATERIALS

Atmospheric air and deionized water were the only materials required for the gas holdup measurements. Chemicals used for all the experiments of interfacial area investigations, such as sodium sulfite (97% purity), cobaltous sulfate (99% purity), resublimed iodine (99.5 % purity), potassium iodide ($\geq 99\%$ purity) and soluble starch was the indicator used were of analytical reagent grade and procured from Merck India Pvt. Ltd. De-ionized and de-aerated water was used for preparing the solutions. Sodium sulfite in trace amount, air and deionized water were also required for determination of volumetric mass transfer coefficient. The requirements of materials specific to the applications of DTBC for wastewater treatment and production of Baker's yeast are described in the respective chapters detailing these applications.

3.3 METHODS AND EXPERIMENTAL TECHNIQUES

The gas holdup, interfacial area, volumetric mass transfer coefficients etc. are the important hydrodynamic and mass transfer parameters of draft tube bubble columns which determine the overall performance of the DTBC. The literature abounds with numerous techniques and protocol to determine/ evaluate these parameters. An account on those techniques as well as detailed description of experimental methods used in the present investigation such as volume expansion method for gas holdup measurement, sulfite oxidation technique (Chemical method) for interfacial area determination and dynamic gassing-in method for volumetric mass transfer coefficient incorporating the requirements of chemicals, instruments and techniques are discussed in the following sections. Again, the methods specific to the applications of DTBC for wastewater treatment and production of Baker's yeast are described in the respective chapters detailing these applications.

3.3.1 Gas holdup and its measurement

The volume fraction of gas phase in the gas-liquid dispersion is called the total gas holdup or the gas void fraction, ϵ_g it is based on the total dispersion volume and is defined as

$$\epsilon_g = \frac{V_G}{V_G + V_L} = \frac{V_G}{V_D}$$

Where V_G , V_L and V_D are the gas, liquid and dispersion volumes in the column respectively.

In the draft tube bubble column, the individual riser and down comer gas holdups, ϵ_{gr} and ϵ_{gd} respectively, can also be identified and are related to the over gas holdup via,

$$\epsilon_g = \frac{A_r \epsilon_{gr} + A_d \epsilon_{gd}}{A_r + A_d}$$

Where A_r and A_d are cross-sectional areas of riser (draft tube) and downcomer (annulus) respectively.

A wide range of methods have been proposed for the fractional gas holdup measurements. These methods can be classified as physical methods, optical methods, radiation attenuation methods, electrical capacitance and conductance methods etc. Some methods measure overall average, some measure cross sectional average and some methods measure local fractional phase holdups. The conventional physical methods used to determine the total gas holdup in various pneumatically agitated gas – liquid devices are the manometric technique or using the volume expansion technique as explored by numerous researchers in the past (Akita and Yoshida,1973; Hills,1976; Bello,1981; Kara et al.,1982; Sinha et al.,1984; Kelker et al.,1984; Siegel et al.,1986; Chisti et al.,1987; Kawase and Moo-Young, 1986a; Siegel and Merchuk,1987).

The manometric technique is necessary for the determination of the individual riser (ϵ_{gr}) and the downcomer (ϵ_{gd}) gas holdups. The end of manometers are connected to pressure taps located at two different axial positions either in the riser or in the downcomer of the reactors for the measurements of ϵ_{gr} or ϵ_{gd} respectively. On the other hand, in the volume expansion method the measurement of unaerated, static liquid height (h_l) and the height of gas liquid dispersion (h_d) upon aeration are used to calculate the total gas holdup (ϵ_g). The gas holdup calculated by this method is said to be reproducible within $\pm 10\%$ even at the highest gas flows which induces pronounced fluctuations in the dispersion level.

The reliability and the simplicity of these two techniques- volume expansion and manometric measurements is further attested to by the frequency with which they have been used by many investigators (Fair et al., 1962; Eissa and Schuger, 1975; Hikita et.al, 1980; Kojima et al., 1991; Yamashita, 1994; Wei et al., 2000; Graen-Heedfeld and schlueter, 2000; Ruzicka et al., 2001; Jin and Lant, 2004).

3.3.1.1 Volume expansion method for measurement of gas holdup

In the present investigation, the total gas holdup was determined using the volume expansion technique for all available experimental assemblies with air-water system. In each experimental run the column was first filled with deionized water up to a height (h_l) of 75 cm above the sparger. The total gas holdup (ϵ_g) in the column was determined by measuring the static liquid level (h_l) and the dispersed liquid level (h_d) using equation 3.1.

$$\epsilon_g = \frac{h_d - h_l}{h_d} \quad (3.1)$$

The static liquid height in column was measured by temporarily cutting-off the flow of air for a fraction of time in such a manner that in that duration weeping of liquid in the gas distribution chamber through holes of sparger does not take place. The dispersed liquid height was measured after a steady dispersion height was established and an average value from three measurements was used in the calculation of the total gas holdup.

Total gas holdups were measured over a wide range of superficial gas velocities in the riser for all the DTBC systems using different spargers. The superficial gas velocity in riser (U_{gr}) for various draft tube bubble columns were calculated as

$$U_{gr} = \frac{Q_g}{A_r} \quad (3.2)$$

where Q_g is the volumetric gas flow rate and A_r is the cross section area of the riser (draft tube). In case of bubble columns, the superficial gas velocities (U_g) are calculated based on the entire column cross-sectional area. All experiments for determination of the total gas holdup were conducted at ambient temperature ($30^\circ\text{C} \pm 2^\circ\text{C}$) in semi-batch mode with no liquid throughput.

3.3.2 Methods for determining specific interfacial area

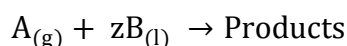
Experimental methods for determining interfacial area in draft tube bubble columns are classified into two categories: *Physical methods* and *Chemical methods*. Physical methods are based on physical measurements of bubble geometry and the holdup of the system; whereas chemical methods are based on the reaction of known kinetics, in which the absorption rate is a function of the gas-liquid interfacial area. The determination of specific interfacial area by physical methods is tedious because it involves the counting of large number of bubbles moreover it is also inaccurate because only bubbles close to the wall can be picked up by the camera. Thus the physical measuring processes at the

best give local values of interfacial area, In recent years investigators have used various image processing software's to estimate bubble diameter in photographic framework but these techniques suffer from the drawback of poor resolution that does not allow the software to identify bubbles in a bubble cluster. (Bui Dinh and Choi, 1999; Buwa and Ranade, 2002; Zaruba et al., 2005a; 2005b), on the other hand, the entire reactor volume can be assessed by using chemical methods.

3.3.2.1 Overview of chemical methods

Chemical methods for determining interfacial area, a was pioneered by Danckwerts and coworkers (Danckwerts et al., 1963; Danckwerts and Sharma, 1966). This technique is discussed in detail by Danckwerts (1970), Doraiswamy and Sharma (1984) and Vazquez et al. (2000). Typical gas – liquid reactions such as CO₂ - aqueous NaOH, CO₂ - aqueous diethanolamine, H₂ - hydrazine, O₂ - sodium sulfite, O₂ - sodium dithionite can be used conveniently as model reactions to determine the specific interfacial area in a gas-liquid contacting device.

For the case of gas-liquid reaction taking place in the liquid phase between the dissolved solute A transferred from the gas phase and reactant B present in the liquid phase the reaction is expressed as follows:-



In the above reaction z is the stoichiometric coefficient and when the solute A is slightly soluble in the liquid phase the entire resistance to mass transfer is considered to exist in the liquid phase.

If the order of above chemical reaction is m with respect to A and n with respect to B then depending on relative rates of diffusion and reaction the kinetics may be classified into different regimes depending upon whether the reaction gets completed in the liquid film or extends to the bulk of the liquid phase (Doraiswamy and Sharma, 1984). In all regimes, the interfacial concentration of species B remains practically the same as that in the bulk liquid phase meaning that is there is no depletion of the species B in the liquid film. In general all chemical methods for determining interfacial area involve fast reactions such that the reaction is completed in the liquid film and the results are independent of k_L .

It would be appropriate to take cognizance of one significant disadvantage of the chemical method - that it can only be used for one particular material system. Hence, it is useful for comparing the interfacial area between various gas-liquid reactors, but cannot help in assessing the effect of material properties. Transfer of results from one mass system to another is always problematical. The use of a specific model reaction can give rise to serious misinterpretation if bubble size distribution is broad. Yet model reactions are available not only for aqueous electrolyte solutions but also for organic solvents (Yoshida and Miura, 1963; Jhaveri and Sharma, 1967; Laddha and Danckwerts, 1981). Based on model reactions, system specific reaction kinetics and operating conditions; different techniques may be adopted to determine the specific interfacial areas using the chemical method such as *Danckwert's plot method*, *Sodium dithionite method*, *Sodium sulfite oxidation method* etc.

- ***Danckwerts' plot method***

This technique applies to cases where the reaction between the diffusing gas A and the liquid phase reactant B is so fast that A gets completely depleted well within the liquid film. Under these conditions the rate of absorption for pseudo m^{th} order reaction, is given as

$$R_A a = a C_A^* \sqrt{\frac{2}{m+1} D_A k_{mn} C_A^{*m-1} [B_0]^n + k_L^2} \quad (3.3)$$

The absorption rate for an overall second order reaction ($m=1$, $n=1$) can then be written as...

$$R_A a = a C_A^* (D_A k_2 [B_0] + k_L^2)^{0.5} \quad (3.4)$$

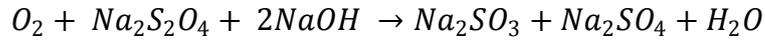
OR

$$(R_A a)^2 = (a C_A^*)^2 D_A k_2 [B_0] + (a C_A^*)^2 k_L^2$$

Plotting $(R_A a)^2$ versus $k_2 [B_0]$ gives a straight line with a slope of $(a C_A^*)^2 D_A$ and an intercept of $(a C_A^*)^2 k_L^2$. When D_A and C_A^* are also known, both interfacial area a and the liquid-side mass transfer coefficient k_L can be simultaneously determined from this plot which is known as the Danckwerts' plot. Interfacial area determination using this method is relatively tedious as many measurements are required to produce one value for a .

- **Sodium dithionite method**

Reaction of oxygen with solutions of sodium dithionite causes the dithionite ion to be oxidized to sulfite and sulfate ions as per the following reaction:-



The rate of reaction is dependent on pH hence continuous adjustment of the pH by the addition of NaOH is necessary to hold the rate of reaction constant as oxidation proceeds.

The oxidation reaction is zero order in $O_2(A)$ and the order of reaction with respect to sodium dithionite (B) depends upon its concentration in the solution. Jhaveri and Sharma (1968) have shown that the reaction is first order with respect to dithionite when the concentration of the latter is less than 0.08 gmole/lit, and is second order with respect to dithionite when concentration of dithionite is more than 0.08 gmole/lit. The rate of absorption is given by equation 3.5 when reaction rate shows first order dependency on the dithionite concentrations

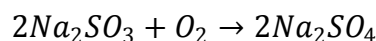
$$R_A a = a \sqrt{2kD_A C_A^* [B_0]} \quad (3.5)$$

Knowing k , D_A and C_A^* the interfacial area, a can be obtained from equation 3.5. The necessary condition to be satisfied for the validity of equation 3.5 is specified in equation 3.6.

$$\frac{\sqrt{2kD_A [B_0] / C_A^*}}{k_L} \ll \frac{[B_0]}{z C_A^*} \quad (3.6)$$

- **Sodium sulfite oxidation method**

The sodium sulfite oxidation technique is the most widely used technique for the determination of specific interfacial area (Yoshida et al., 1960; Dewaal and Okeson, 1966; Miller, 1983; Sada et al., 1987; Popovic and Robinson, 1987; Kulkarni et al., 2001). It has the advantage of acquiring one value of the specific interfacial area from one measurement. The sulfite oxidation method was originally developed by Cooper et al. (1944) to evaluate mass transfer performance of gas-liquid contactors. Sulfite oxidation method employs the oxidation of sodium sulfite (B) to sulfate by dissolved oxygen (A)



The reaction is normally very slow, but it can be catalyzed by the addition of various metallic ions, of which Co^{++} (e.g. CoSO_4) and Cu^{++} (CuSO_4) have received most attention. Cobaltous sulphate as a catalyst was found to be more reproducible, much more effective and more reliable than cupric sulfate (Cooper et.al, 1944; Yoshida et al., 1960; Westerterp, 1963)

Kinetics of sodium sulfite oxidation has received considerable attention in chemical engineering literature. (Schultz and Gaden, 1956; Barron and O'Hern, 1966; Linek, 1971; Linek and Vacek, 1981; Shivaji and Murty, 1982; Zhao et al., 2005). This irreversible reaction has very complex kinetics, according to Astarita et al. (1964), the reaction when catalyzed by CoSO_4 is zero order in O_2 when sulfite concentration is up to 0.06 M; first order when it is 0.25 M and second order when it is 0.25 – 1 M. Alper and Abu-Sharkh (1988) observed that the reaction is independent of sulfite concentration but is second order with respect to oxygen at the oxygen partial pressure range of 0.21 atm., which would, corresponds to interfacial area determination experiments at about atmospheric pressure with air. The oxidation rate depends on the type of catalyst, its concentration, partial pressure of oxygen, temperature, ionic strength of solution, the presence of catalytic impurities and pH of the solution etc. The generalized rate of absorption is given by

$$R_A a = a C_A^* \sqrt{\frac{2}{m+1} D_A k_{mn} C_A^{*m-1} [B_0]^n} \quad (3.7)$$

Rate constants, diffusion coefficients and solubility must all be known prior to calculating interfacial area, a from the measured absorption rate $R_A a$ as in equation (3.7). Here C_A^* and D_A can be estimated with sufficient accuracy, where as there is often a problem in the case of rate constants, especially as regards sulfite oxidation in which the reaction order is a function of operating conditions and kinetic constants depend on pH value and trace level of impurities, therefore it is advisable to use the kinetic data from literature for interfacial area determination by sulfite oxidation. Despite the extensive literature on the sulfite oxidation under various conditions of practical interest, clear and accurate kinetic data is still lacking. Nevertheless, some attractive advantages of the aqueous sulfite system such as its economy for large-scale equipment, cheap and non-corrosive chemicals requirement, lack of toxicity, fire safety etc. have encouraged efforts towards developing a reliable method for mass transfer characteristics determination based upon the use of this system.

3.3.2.2 Determination of interfacial area by sulfite oxidation

In view of the wide applicability and numerous advantages of determining interfacial areas using sulfite oxidation, this method was adopted for determining the interfacial area of the draft tube bubble columns developed in this study. CoSO_4 was used as the catalyst, the initial concentrations of sodium sulfite $[\text{B}_0]$ and CoSO_4 were 0.5 M and 5×10^{-4} M respectively. The source of oxygen was air at 30°C and 1 atm. total pressure. The pH of system was adjusted to 8.5 by addition of NaOH. Under these conditions, the reaction is zero order ($n=0$) with respect to sulfite and second order ($m=2$) with respect to oxygen. The rate of mass transfer in this case is given by equation 3.8

$$R_A a = a \sqrt{\frac{2}{3} D_A k_2 C_A^{*3}} \quad (3.8)$$

The necessary condition to be satisfied for the validity of equation 3.8 is specified in equation 3.9 as

$$\frac{\sqrt{\frac{2}{3} D_A k_2 C_A^*}}{k_L} \ll \frac{[\text{B}_0]}{z C_A^*} \quad (3.9)$$

The decrease of sulfite concentration was determined by iodometric titration (Wood and Weist, 1957) as given in Appendix-1, from which the oxygen transfer rate based on dispersion volume, $R_A a$, was obtained based on the stoichiometry (i.e. one half of the decrease of sulfite concentration) of the reaction. Diffusivity of oxygen in water was determined by the Wilke-Chang equation (Appendix 2), the second order rate constant k_2 was determined by the correlation proposed by Yoshimoto et al. (2007) as shown below in Equation 3.10

$$k_2 = 2.36 \times 10^{19} C_{\text{CoSO}_4} \exp(-5.13 \times 10^7 / RT) \quad (3.10)$$

The oxygen solubility in sulfite solution, C_A^* (mol/l) was determined by equation 3.11 proposed by Linek and Vacek (1981).

$$C_A^* = 5.909 \times 10^{-6} \bar{P}_{\text{O}_2} \exp\left[\frac{1602.1}{T} - \frac{0.9407[\text{B}_0]}{1 + 0.1933[\text{B}_0]}\right] \quad (3.11)$$

Using the above equations, D_A , k_2 and C_A^* were found to be 2.192×10^{-5} cm^2/s , 1.69×10^7 $\text{m}^3/\text{kmol}\cdot\text{s}$ and 1.5987×10^{-4} mol/l respectively at the experimental conditions

mentioned earlier. Substituting the experimental values of oxygen transfer rate, $R_A a$ and the calculated parametric values in equation 3.8, using consistent units gave the value of the interfacial area. In all the experiments of sulfite oxidation method performed in the present investigation, it was required to conduct the experiment for a time duration of approximately 3-4 hours and titration readings were taken at an interval of 10-15 min, for obtaining a single value of interfacial area, a at a given air flow rate.

3.3.3 Volumetric mass transfer coefficient and its measurement

The volumetric mass transfer coefficient is the parameter used to quantify the mass transfer performance of bubble columns and draft tube bubble columns. It is the product of liquid-side mass transfer coefficient k_L and specific interfacial area a . The importance of $k_L a$ implies that the mass transfer is liquid film controlled. In such cases the absorption rate of oxygen $R_A a$ is described by equation 3.12

$$R_A a = \frac{dC_L}{dt} = k_L a (C^* - C_L) \quad (3.12)$$

Where C^* is the saturation concentration (equilibrium concentration) of oxygen in the liquid that is in contact with air or with pure oxygen and C_L is the oxygen concentration in the liquid at any time t .

For the application of draft tube bubble column as fermentor for biomass growth, for the performance evaluation of draft tube bubble column for oxygen transfer in wastewater treatment as well as comparison of draft tube bubble columns with other gas – liquid contactors, knowledge of volumetric mass transfer coefficient $k_L a$ is essential. The effect of various design parameters such as column type and geometry, fluid properties and operational variables such as liquid and gas velocities on $k_L a$ need to be evaluated so that design can be optimized and operational range decided to maximize $k_L a$.

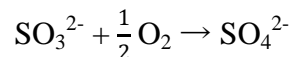
However, enhancement of oxygen transfer can also be achieved to a small extent by manipulating the concentration gradient ($C^* - C_L$). This could be done by increasing the C^* value by increasing either the gas phase mole fraction of oxygen or by increasing the total pressure of the system but these possibilities are not only difficult to implement they are expensive as well and also have other consequences. Thus for the improvement of oxygen transfer in the reactor the best solution is to improve the volumetric mass transfer coefficient, $k_L a$.

3.3.3.1 Methods for the determination of volumetric mass transfer coefficient

The volumetric mass transfer coefficient, k_{La} in bubble column's has been extensively investigated and correlated with various parameters. (Akita and Yoshida, 1973; Deckwer et al, 1982; Heijnen and Van't Riet, 1984; McManamey and Wase, 1986; Kawase et al., 1987; Schumpe and Deckwer, 1987; Kawase and Moo-Young, 1987; 1988). There have been some attempts made to determine k_{La} in draft tube bubble column's as well (Bello et al., 1985a; Chisti, 1989; Shamlou et al., 1995). Measurements taken in the absence of simultaneous chemical reaction are commonly used to determine the volumetric mass transfer coefficients in draft tube bubble columns. In general, the literature suggests that there are six methods to determine k_{La} in gas - liquid contactors they are briefly discussed below highlighting their scope, advantages and limitations (Van't Riet, 1979; Sobotka et al., 1982; Linek et al., 1987)

- **Sulfite oxidation method**

The sulfite oxidation method is based on the consumption of oxygen dissolved in the liquid for the oxidation of sulfite (SO_3^{2-}) to sulfate (SO_4^{2-}) with the aid of either Copper (II) or Cobalt (II) as catalyst.



The rate of sulfite oxidation is a measure of the rate of oxygen transfer to the liquid. The oxidation rate depends on the type of catalyst, its concentration and the pH of the solution. The overall reaction generates H^+ hence pH control is necessary, a decline in pH by ~ 1 unit could decrease the oxidation rate by as much as 10- fold. Careful temperature control is also essential to maintain constant reaction kinetics. Impurities such as iron, manganese and other transition metals in the ppm range affect the reaction.

Sufficiently high sulfite concentration ($\sim 1 \text{ kmol/m}^3$) must be maintained so that oxidation rate becomes independent of sulfite level; the oxygen concentration in the bulk liquid should be zero or close to it. For absence of dissolved oxygen, the k_{La} for sulfite oxidation is nearly equal to the k_{La} for physical absorption and any enhancement of mass transfer due to chemical reaction can be disregarded. Under these conditions, the rate of sulfite consumption is given by equation 3.13

$$-\frac{dC_{\text{sulfite}}}{dt} = k_{La} C^* \quad (3.13)$$

The sulfite consumption rate, which should remain constant, is followed by the liquid samples taken at various times with excess iodine and back titration of the residual iodine with thiosulfate.

The limitations of this technique are significant. High purity chemicals are required in large amounts for large scale experiment, the high ionic strength of the liquid produces a strongly noncoalescing system which may be quite unlike the fluids of interest, the kinetics of sulfite oxidation are sensitive to many variables and sampling and analysis are tedious and slow. Despite these limitations, this method was frequently used by many researchers (Botton et al., 1980; Bhattacharya et al., 1993; Wu and Hsiun, 1996).

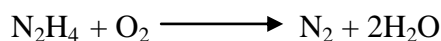
- ***Carbon dioxide absorption method***

The chemical absorption of carbon dioxide into mildly alkaline solutions (Prasher and Wills, 1973) or into an appropriately buffered solution (Kawagoe et al., 1975; Baykara and Ulbrecht, 1978) is another commonly employed technique which is similar in principle to the sulfite oxidation method. Chemical absorption of CO₂ in Na₂CO₃ – NaHCO₃ solution is too slow to be useful for $k_L a$ determination when the ratio of carbonate to bicarbonate concentration in solution is between 3-5 (Kawagoe et al., 1975).

Reaction conditions must also ensure that the enhancement factor is unity. Limitations of the technique are similar to those of sulfite oxidation. In a modification of carbon dioxide absorption, Andre et al. (1981) made use of an infrared analyzer to follow the concentration of carbon dioxide in the gas phase during transient absorption into a previously CO₂ – free liquid under such conditions that the absorption was almost wholly physical. CO₂ is sufficiently soluble in aqueous solutions that a measurable change in its concentration can be readily detected. However the higher solubility of CO₂ also makes this technique sensitive to mixing in the gas phase. Furthermore, this method is limited to pH < 4, if the bicarbonate formation from dissolved CO₂ is to be neglected in the calculations.

- ***The hydrazine method***

The steady state hydrazine (N₂H₄) method introduced by Zlokarnik (1978) makes the use of the reaction to determine $k_L a$



The most favorable conditions for this reaction have been reported to be pH 11 – 12 and 0.01 kmol/m^3 copper sulfate catalyst. With a suitable steady flow of hydrazine into an aerated reactor, the dissolved concentration monitored by a dissolved oxygen (DO) electrode can be held at a constant level. The amount of hydrazine consumed per unit time equals the rate of oxygen absorption. The above reaction does not form any ionic species; therefore, a lower solution ionic strength may be maintained in comparison with sulfite oxidation or carbon dioxide absorption.

- ***Pressure gauge method***

In the pressure gauge method, also proposed by Zlokarnik (1978), the time dependent drop in the pressure of pure oxygen in a gas-space connected to a gas-tight reactor is followed. The volume of liquid is oxygenated by recirculating the gas from the space. The requirement for a reactor vessel designed to conform to the demands of the pressure gauge technique is a limitation.

- ***Enzyme oxidation method***

Oxygen transfer may be followed by the formation of gluconic acid from glucose via oxidation with oxygen in presence of the enzyme glucose oxidase. The rate of absorption of oxygen is calculated from the rate of consumption of alkali which is needed to neutralize the acid. The liquid phase oxygen concentration at steady state is determined with a dissolved oxygen electrode. The cost of the enzyme restricts the method to small scale applications.

- ***Dynamic gassing-in method***

This transient gassing-in method of $k_L a$ determination of gas-liquid contacting devices involve passing air through deaerated water and then tracking the increase in the concentration of dissolved oxygen of water with time. Dynamic gassing-in method is well-known and used by many investigators previously (Sinclair et al., 1971; Koide et al., 1983; 1983a; 1985; Ozturk et al., 1987; Chisti and Moo-Young, 1988 ; Merchuk and Ben-zvi, 1992; Schumpe et al., 1992; Chisti et al., 1990; 1995; Hsiun and Wu, 1995; Laari et al., 1997; Tung et al., 1998; Lu et al., 2000; Han et al., 2005). Since, it is also used in the present investigation; it is described in detail in the following section.

3.3.3.2 $k_L a$ determination by dynamic gassing-in technique

In the present work, dynamic gassing-in technique was employed for the determination of the volumetric mass transfer coefficient, $k_L a$ in air – water system at ambient temperature and pressure in RDTBC and for the cylindrical assemblies as well at different superficial gas velocities.

The rate of oxygen transfer in liquid is related to the volumetric mass transfer coefficient and the concentration driving force by the equation

$$\frac{dC_L}{dt} = k_L a (C^* - C_L) \quad (3.14)$$

Where C_L and C^* are the instantaneous and the saturation concentrations of the dissolved oxygen in the liquid respectively. Under steady state operating conditions the $k_L a$ remains constant hence equation 3.14 can be integrated between the limits $C_L = C_{L0}$ at $t = 0$ and $C_L = C_L$ at $t = t$, which yields

$$\ln \frac{C^* - C_{L0}}{C^* - C_L} = k_L a t \quad (3.15)$$

A plot of left-hand side of equation (3.15) against time gives a straight line with $k_L a$ as the slope. The concentration of dissolved oxygen (DO) in the liquid C_L was determined by using a DO probe. This procedure assumes a constant gas phase composition, a “well mixed” liquid and a negligible effect of the dynamics of the dissolved oxygen electrode, as justified in Appendix-3.

Usually, deaeration of the water is done to maximize the initial concentration gradient for oxygen transfer by passing nitrogen through the liquid in the column prior to oxygenation. In the present investigations dissolved oxygen present in the water was removed by treating the water with trace (stoichiometric) amount of sodium sulfite to enhance the range of dissolution of oxygen, as adopted by Medic et.al (1989) and Bando et al. (1992). No significant change in flow pattern was observed due to the addition of trace quantity of sodium sulfite. In most of the experimental runs, after addition of sodium sulfite, the concentration of dissolved oxygen in the water dropped to 0.1 mg/L which was taken as initial dissolved oxygen concentration in water (C_{L0}) at time $t = 0$. C^* the saturated concentration of dissolved oxygen in the water at atmospheric pressure was taken as 7.5 mg/L from APHA (1998) at operating temperature of 32⁰C in the draft tube bubble columns.



Fig. 3.6 DO probe inserted in RDTBC and connected to DO meter

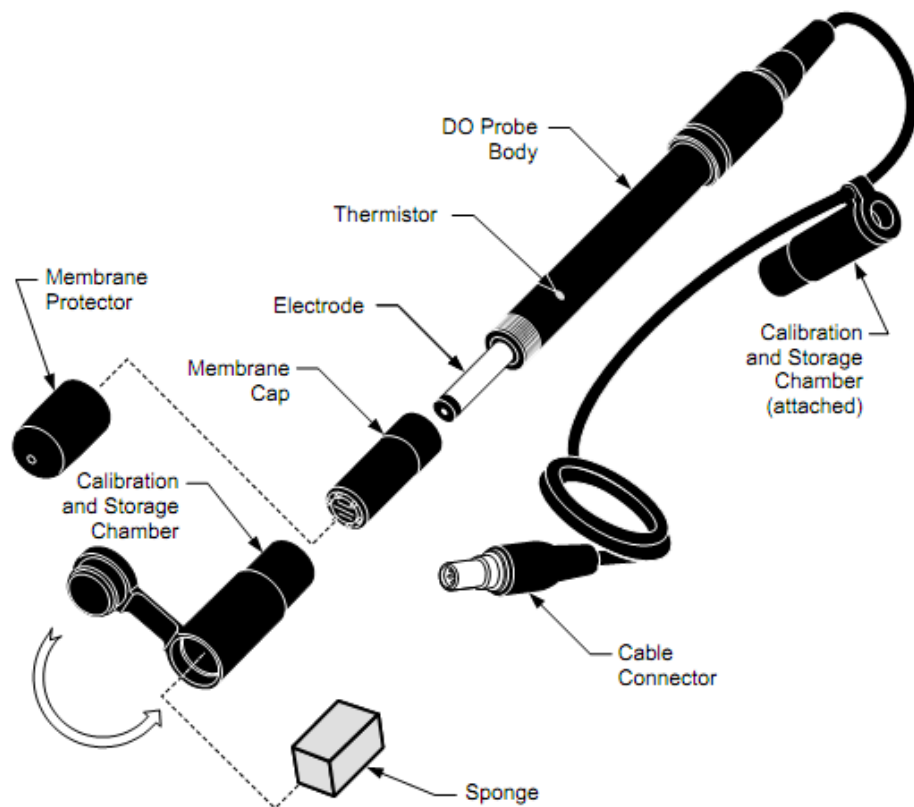


Fig. 3.7 DO Probe and its parts

In all experiments to determine $k_L a$, air at constant superficial gas velocity was bubbled into the deoxygenated water through the sparger into the draft tube for a period of time (generally 3-8 min) to attain saturation. The concentration change of the dissolved oxygen, C_L in water as a function of time was measured using DO probe connected to Sension 156 dissolved oxygen meter (Hach[®], USA). Generally, the readings of C_L in DO meter were noted at time interval of 10-15 seconds. Fig.3.6 shows a snapshot of the DO probe inserted in the RDTBC assembly used in the present investigation, while the DO probe with its parts is shown in Fig.3.7.

The DO probe was plugged into the DO meter through cable connector about one hour prior to use, for polarization to attain a stable reading of dissolved oxygen. A well polished electrode of DO probe was always fully filled with the fresh electrolyte filling solution and fitted with deposits free wet membranes using membrane cap to ensure better performance. It was also ensured that any air bubbles trapped on the probe tip are dislodged before taking readings. The probe was inserted in the column in such a way that the roughness of the outer surface of membrane cap remains in contact with lateral side of draft tube to eliminate any gas bubble impingement effect on the measurement.

DO probe was calibrated (Appendix-4) before each experiment using water saturated air confined in the calibration and storage chamber. Although the electrodes retained calibration for long periods, they were nevertheless recalibrated frequently to obtain accurate readings.

CHAPTER 4

HYDRODYNAMIC AND MASS TRANSFER CHARACTERISTICS OF DRAFT TUBE BUBBLE COLUMNS

Total gas holdup, gas-liquid specific interfacial area, volumetric mass transfer coefficients are the key hydrodynamic and mass transfer parameters for the characterization of draft tube bubble columns. It is known that these parameters vary with gas superficial velocity in the column and are correlated likewise. In the literature there is some discrepancy regarding the usage of superficial gas velocity in the draft tube bubble columns since the superficial velocity could be based on either the cross sectional area of the draft tube i.e. riser or on the total cross sectional area of the column. When draft tube bubble columns are to be compared with bubble columns then the superficial velocities are based on the entire cross sectional area of the column to retain parity in the process. However, for all other purposes ~ to study the effect of parametric dependence on the superficial velocity etc, the gas velocity through the draft tube was taken for reckoning.

4.1 TOTAL GAS HOLDUP

The total gas holdup ϵ_g is an important hydrodynamic parameter in pneumatically agitated gas liquid contact equipments such as bubble columns and draft tube bubble columns. The importance of gas holdup is paramount because it has several direct and indirect influences on the column performance. The direct and the obvious effect is on the column volume since the column must be designed with sufficient volume to accommodate the maximum expected total gas holdup. The indirect influences are also far reaching, the possible spatial variation of ϵ_g , gives rise to pressure variation which results into intense liquid phase motion and thus liquid circulation. These secondary motions govern the rates of mixing, mass transfer and heat transfer etc. Additionally, the gas holdup not only determines the residence time and thus utilization efficiency of the gas in liquid but also in combination with mean bubble size it influences the gas-liquid interfacial area available for mass transfer.

Total gas holdup in case of draft tube bubble column is influenced by superficial gas velocities in riser, sparger as well as height of draft tube, size of column etc. Effect of these geometric and operating variables on total gas holdup of draft tube bubble columns used in the present work is elaborated in the following sections:

4.1.1 Effect of superficial gas velocity on gas holdup in RDTBC

In pneumatically agitated gas liquid devices such as bubble columns and draft tube bubble columns, the superficial gas velocity flowing through the vessel has a dominant influence on gas holdup and through it on other parameters such as specific interfacial area and mass transfer coefficients. The effect of superficial gas velocity on gas holdup in DTBC has been investigated earlier and it is known that with increasing superficial gas velocities in the riser there is a corresponding increase in the total gas holdup (Chisti, 1989; Deckwer 1992; Mouza et al., 2005; 2007). Similar pattern was also observed in the experimental data obtained in this investigation.

The first aspect of this investigation was to examine the behavior of various spargers developed in this study particularly for use with rectangular shaped draft tube bubble columns. The rationale of investigation of rectangular draft tube geometry was to eliminate as far as possible the radial travel of bubbles that in a way reinforces the axial flow of bubbles in the draft tube. Further, industrial draft tube bubble columns having rectangular geometry is not uncommon but there is a paucity of design protocols for such columns.

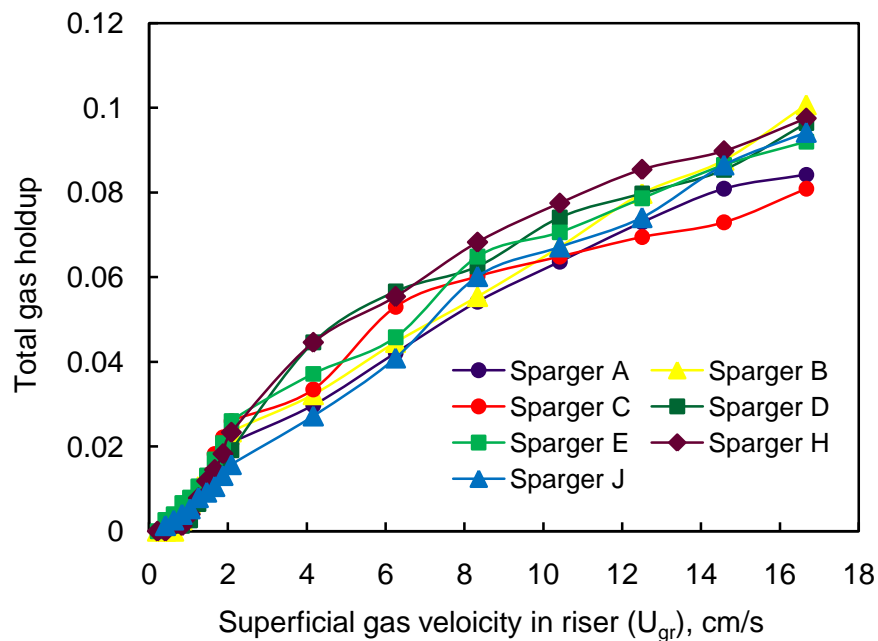


Fig. 4.1 Effect of superficial gas velocity on gas holdup in RDTBC

Fig. 4.1 shows the effect of superficial gas velocity on gas holdup in a rectangular draft tube bubble column having a draft tube height of 70 cm and initial unaerated liquid height 75 cm. Seven different spargers were considered for introducing gas in the draft tubes having openings ranging from 0.785 mm² to 9.425 mm². It is observed from

Fig. 4.1 that with an increase in the superficial gas velocity in the range of 0.2 cm/s to 16.67 cm/s, the total gas holdup increased from nearly zero to 12 % of the total dispersion volume in the RDTBC. It was observed that initially there was a quick rise in the total gas holdup with an increase in the superficial gas velocity, this initial rise in the gas holdup is attributed to the small bubbles rising without interacting with other bubbles in the liquid that is a characteristic of homogeneous regime in draft tube bubble columns.

With further increase in the superficial gas velocities there is a gradual increase of the gas holdup, increased bubble population in the liquid causes an increase in bubble coalescence resulting in the formation of larger and faster moving gas bubbles that reside in the liquid for a shorter while, thus arresting the rapid initial growth of the gas-liquid dispersion ~ a typical characteristic of heterogeneous regime.

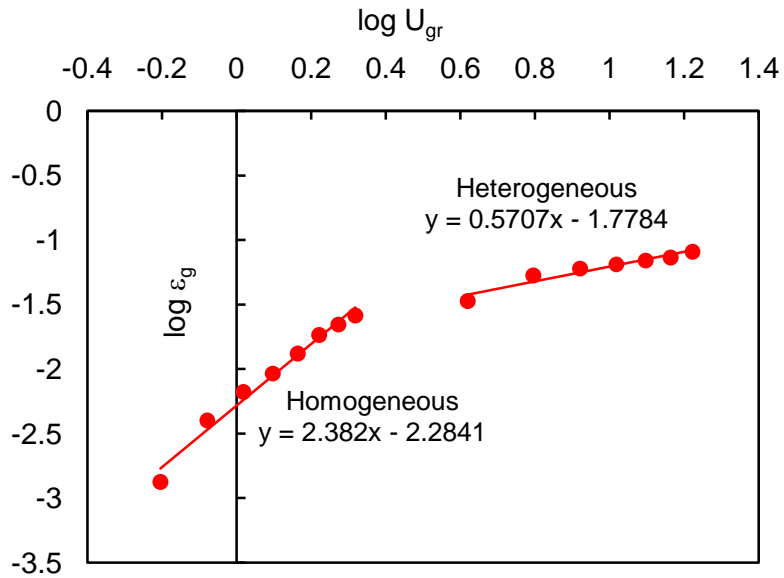


Fig. 4.2 Regime plot of ϵ_g Vs U_{gr} on log scale for sparger C in RDTBC

(DT height = 70 cm; Sparger with $N_h = 4$)

The power law model proposed by Chisti and Moo-Young (1988) equation 4.1 was used to correlate the total gas holdup with the superficial gas velocities for all the spargers used in the RDTBC

$$\epsilon_g = \alpha U_{gr}^\beta \quad (4.1)$$

$$\log \epsilon_g = \log \alpha + \beta \log U_{gr} \quad (4.2)$$

Equation 4.2 suggests linear gas holdup-superficial gas velocity relationship on log scales with β as slope and $\log \alpha$ as intercept. The values of α and β in the power-law

model equation was found to be dependent upon flow regime and sparger specifications for the air-water system.

The homogeneous and heterogeneous regions were segregated in all cases and were represented by different dependencies of α and β for the sparger's investigated. Fig.4.2 illustrates the behavior for sparger C, separate straight lines were obtained for the data generated in the RDTBC with 70 cm draft tube height. Parameters α and β were obtained from the log plots for both the lines representing homogenous and heterogeneous regimes for all the spargers used and are tabulated in Table 4.1.

Table 4.1 Power law model parameters for different spargers

Sparger	Homogeneous		Heterogeneous	
	α	β	α	β
A	0.00499	2.0181	0.01030	0.7672
B	0.00512	2.2114	0.00997	0.8169
C	0.00520	2.3820	0.01670	0.5707
D	0.00255	2.9805	0.02072	0.5369
E	0.00825	1.4107	0.01420	0.6761
H	0.00421	3.2345	0.02609	0.6138
J	0.00518	1.5048	0.00820	0.8826

It is clear from Table 4.1 that the index of gas velocity β is higher (>1) in the homogeneous region for all the spargers than in the heterogeneous region (<1) indicating a strong dependency of holdup on the gas velocities in the homogenous regime.

4.1.2 Effect of sparger design on gas holdup in RDTBC

The influence of sparger design i.e. number of holes, diameter of holes, pitch etc. on gas holdup in RDTBC was investigated in the present study. These experiments were performed in RDTBC having 70 cm draft tube height and with 75 cm of unaerated liquid height.

4.1.2.1 Effect of number of holes (N_h) in sparger on gas holdup

The effect of number of holes (N_h) in spargers on total gas holdup for RDTBC was determined by comparing the gas holdup values at varying superficial gas velocities for sparger A and B having holes of equal diameter of 2 mm ($d_h = 2$ mm) but, there were two holes in sparger B while sparger A had single hole.

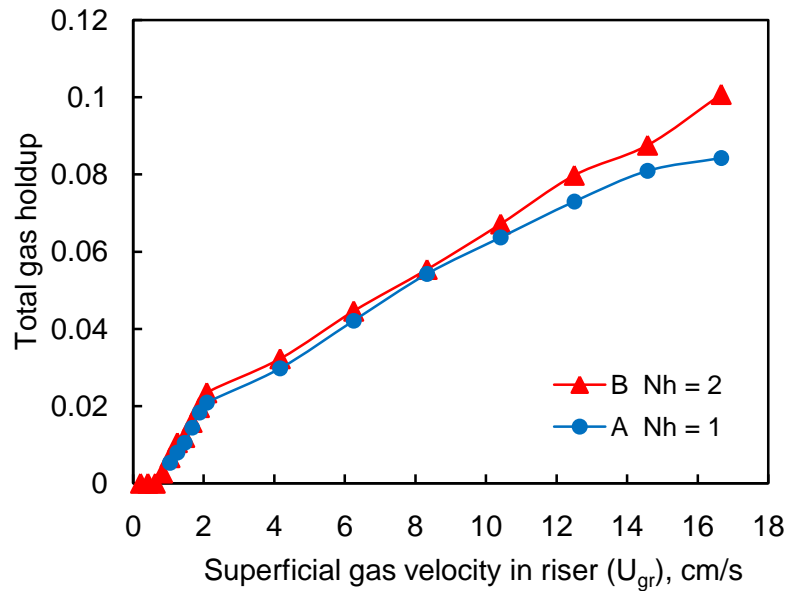


Fig. 4.3 Effect of N_h in sparger on ϵ_g in RDTBC
(DT height = 70 cm)

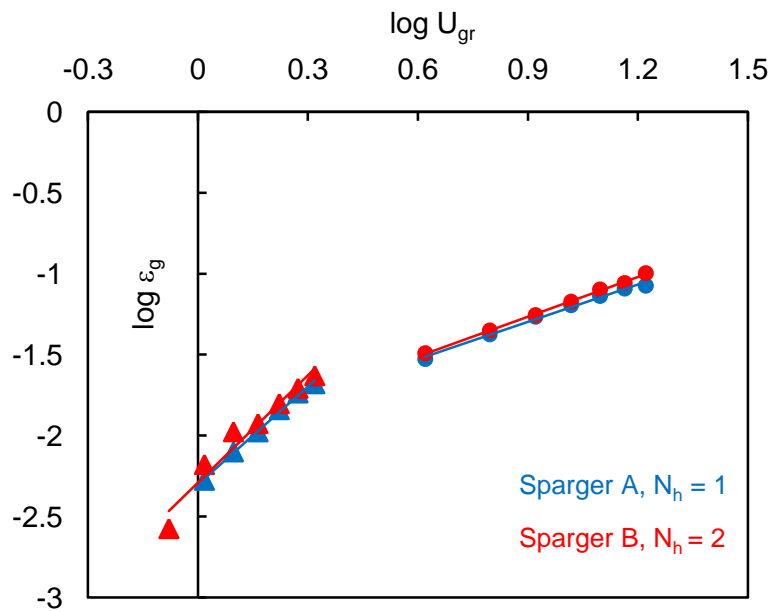


Fig. 4.4 Regime plot of effect of N_h in sparger on ϵ_g in RDTBC
(DT height = 70 cm)

As shown above in Fig.4.3, increasing the number of holes of sparger does not cause any significant increase in total gas hold-up, ϵ_g up to superficial gas velocity of approximately 10 cm/s under these conditions the gas velocity based on the hole diameter was for single hole sparger was 26.5 m/s and 13.3 m/s for the two hole sparger. This corresponded to a bubbling rate of 19904 bubbles/sec and 9952 bubbles/sec for the single hole and two hole sparger respectively considering spherical bubbles having diameter equal to the sparger hole diameter. Beyond $U_{gr} = 10$ cm/s almost 20%

increment in holdup is noted with an increase in gas velocities primarily due to greater degree of circulatory flow that gets established in two hole sparger.

The regime plot is shown in Fig 4.4, as expected the plots of the two spargers almost completely superimpose on each other indicating identical velocity dependencies of gas holdup. These figures help to conclude that in the range of experimentation the number of holes does not contribute much to the gas holdup.

Bubble size distributions in the sparger region was investigated by Polli et al. (2002) for bubble columns, these investigators reported that by decreasing the number of holes the bubble size distribution shifted to smaller sizes. They also showed that increasing the no. of holes in the perforated plate spargers from 7 to 13 at superficial gas velocity of 1 cm/s, did not change gas holdup.

4.1.2.2 Effect of pitch (P_t) of holes in spargers on gas holdup

The dependence of ε_g on P_t , was investigated by comparing the performance of sparger D and H having 6 and 5 holes located at a pitch of 8 mm and 15 mm respectively. The hole diameters were 1 mm for all holes.

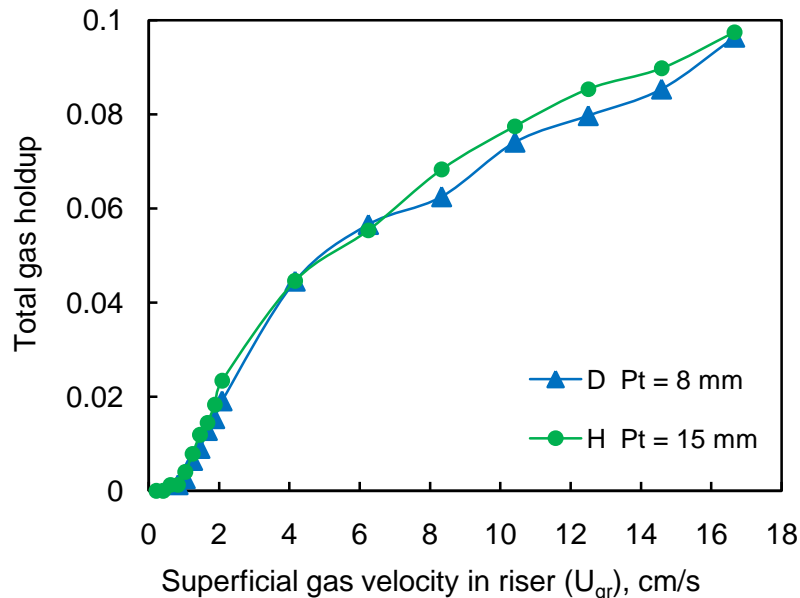


Fig. 4.5 Effect of P_t of holes in sparger on ε_g in RDTBC

(DT height = 70 cm)

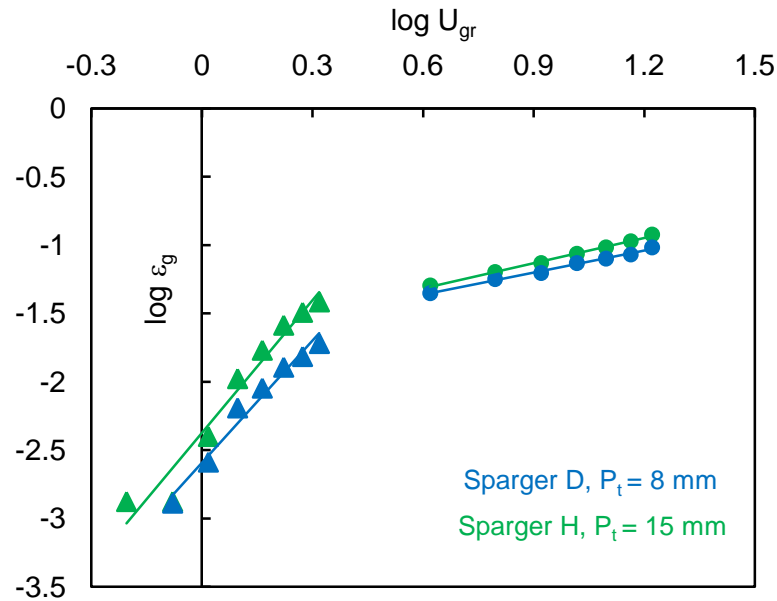


Fig. 4.6 Regime plot of effect of P_t of holes in sparger on ϵ_g in RDTBC

(DT height = 70 cm)

Fig.4.5 shows that changing the pitch of sparger holes does not cause any change in total gas hold-up, ϵ_g up to superficial gas velocity of approximately 7 cm/s under these conditions the gas velocity based on the hole diameter was 10.6 m/s for sparger D and 12.7 m/s for the sparger H. This corresponded to a bubbling rate of 15924 bubbles/sec for sparger D and 19108 bubbles/sec for sparger H, considering spherical bubbles having diameter equal to the sparger hole diameter. The regime plot in Fig. 4.6 show parallel lines in homogeneous regime indicating identical dependence of holdup on gas velocities for both the spargers. Beyond $U_{gr} = 7$ cm/s almost 10% increase in holdup is observed with an increase in gas velocities for sparger H having 15mm pitch compared to sparger D with 8 mm pitch.

The decrease in total gas holdup with a decrease in pitch is attributed to greater coalescence of bubbles in the vicinity of the sparger due to proximity of the bubbles with each other. Buwa and Ranade (2002) have reported increase in bubble diameters due to decrease in the pitch of the sparger. Thus, the formation of large bubbles is finally accountable for decreasing the gas holdup.

4.1.2.3 Effect of hole diameter (d_h) of sparger on gas holdup

The effect of hole diameter (d_h) of perforated plate type metal sparger on total gas holdup in RDTBC was evaluated by measuring the gas holdup over a range of superficial gas velocities in the riser for air-water system using spargers C and J both having four holes ($N_h = 4$) and 20 mm pitch ($P_t = 20$ mm), but the hole diameters were 1 mm and 0.5 mm

for C and J respectively. The holdup pattern is shown in Fig.4.7, it is observed that the value of gas hold-up, ϵ_g almost linearly increases for sparger J while for sparger C having larger holes there is an inflexion in the holdup curve, initially there is a sharp increase in holdup at lower gas velocities but subsequently there is a decline in the rate of increase of the holdup.

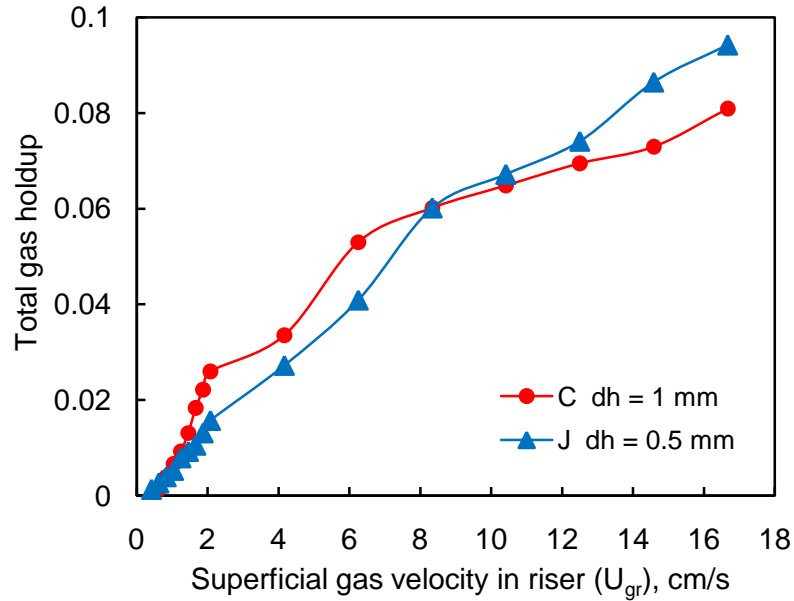


Fig. 4.7 Effect of d_h of sparger on ϵ_g in RDTBC
(DT height = 70 cm)

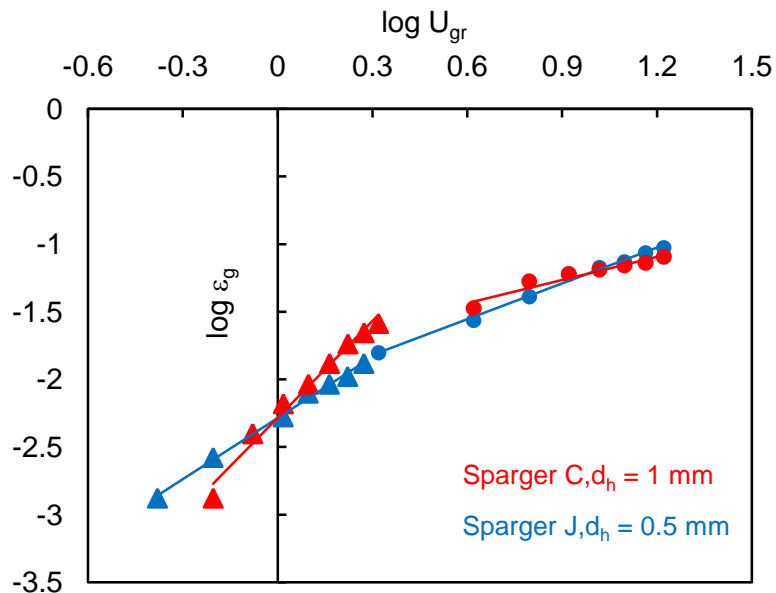


Fig. 4.8 Regime plot of effect of d_h of sparger on ϵ_g in RDTBC
(DT height = 70 cm)

The smaller size of perforations in the sparger J is responsible for higher velocities of bubbles through them such as at superficial gas velocity of 8 cm/s, the gas velocity based on hole diameter was 21.2 m/s for sparger C and 84.9 m/s for sparger J, which corresponded to a bubbling rate of 31847 bubbles/sec and 254777 bubbles/sec for sparger C and sparger J respectively.

These higher bubble velocities in sparger J are accounted for the plug flow behaviour of bubbles rising through draft tube without much interaction and resulted in the linear dependency of holdup on superficial gas velocities. The marginal difference of slope between the homogeneous and heterogeneous regime for sparger J, as shown in Fig 4.8, also confirms linear dependency of holdup on superficial gas velocities over the entire range of experimentation for sparger J.

Regime plot Fig 4.8 shows a large difference in slopes for sparger C and sparger J in the homogeneous region, having the velocity index $\beta = 2.382$ and 1.5048 for sparger C and J respectively. The decrease in holdup of sparger C having larger hole size, particularly in heterogeneous regime at higher superficial gas velocities can be explained by increase in incipient bubble size due to larger hole diameter of sparger as well as formation of larger bubbles with increasing superficial gas velocities. Large bubbles rise faster and decreases the total gas hold-up, ϵ_g .

4.1.2.4 Effect of row of holes in sparger on gas holdup

The effect of number of rows of holes in perforated plate sparger on total gas holdup was investigated for spargers D and E having same hole diameters of 1 mm ($d_h = 1$ mm) but sparger D had a single row of 6 holes with 8 mm pitch, while sparger E had two rows each containing 6 holes with 6 mm pitch.

There is negligible effect of number of rows of holes of sparger on gas holdup as shown in Fig 4.9 this is particularly true in heterogeneous regime at higher superficial gas velocities. It is observed that there is initially quick rise of gas holdup with superficial gas velocities for sparger D with single row compared to sparger E with two rows. At superficial gas velocity of approximately 6 cm/s, the gas velocity based on hole diameter was 10.6 m/s for sparger D and 5.3 m/s for sparger E, which corresponded to a bubbling rate of 15924 bubbles/sec and 7962 bubbles/sec for sparger D and sparger E respectively.

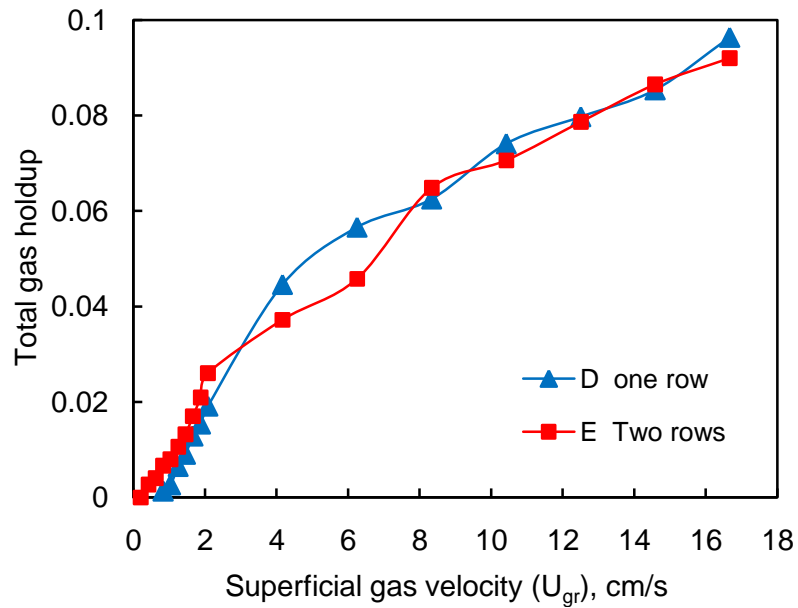


Fig. 4.9 Effect of number of row of holes in sparger on ϵ_g in RDTBC (*DT height = 70 cm*)

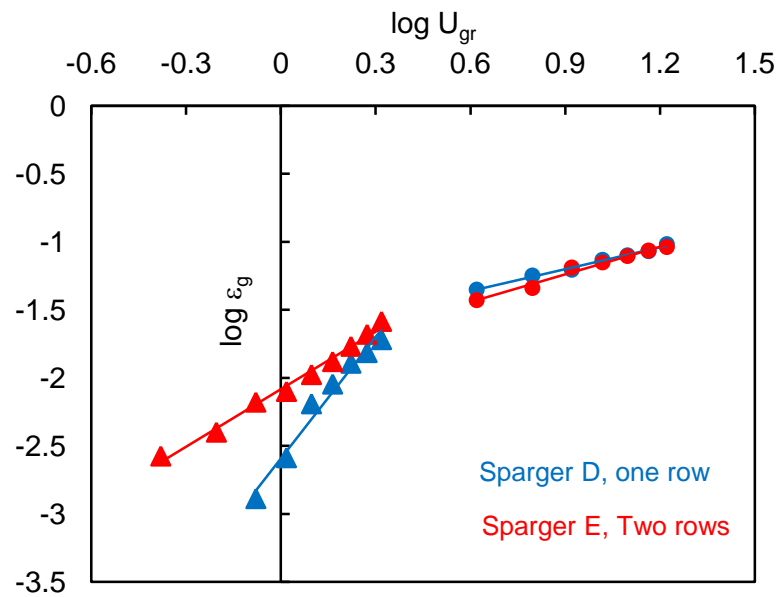


Fig. 4.10 Regime plot of effect of number of row of holes in sparger on ϵ_g in RDTBC (*DT height = 70 cm*)

The superimposition of the lines of heterogeneous regime for the two spargers investigated is shown in Fig. 4.10 which also confirms that the gas holdup in the experimental draft tube bubble column is relatively unaffected by the number of row of sparger holes at higher superficial gas velocities. It is seen from Fig.4.8 that the slope of line for sparger D ($\beta = 2.98$) in homogeneous regime is considerably higher than the slope of sparger E ($\beta = 1.41$), which indicates stronger dependence of gas holdup on

superficial gas velocity for sparger D having one row of holes compared with sparger E having two rows of holes.

4.1.2.5 Selection of sparger for characterization and application of RDTBC

It is well established that the gas holdup in a bubble column influences the specific interfacial area explicitly and the mass transfer coefficients implicitly hence selection of sparger has considerable influence on the overall performance of the RDTBC. Among the various spargers developed in this study it was observed that all except sparger C gave a monotonously increasing gas holdup pattern with increase in the gas velocity in the range of superficial gas velocities encountered in this investigation. Sparger C having four holes of 1mm each at a pitch of 20 mm gave an asymptotic pattern of gas holdup in the range of superficial gas velocities studied. It is seen from Fig. 4.1 that at low gas velocities this sparger gives very large gas holdup almost linearly increasing with gas velocity, as velocities increase and are in the middle range it gives an intermediate value of holdup while at very high velocities it shows saturation with respect to the gas holdup values.

Visual observations revealed that with sparger C there was a uniform distribution of gas bubbles over the entire cross-sectional area of the draft tube and throughout its entire length from bottom to top, thus providing sufficient contact between the gas and liquid. Thus, it was judicious to use sparger C from the available spargers with RDTBC for investigation of hydrodynamic and mass transfer behaviour of as well for the applications of wastewater treatment using activated sludge and the production of baker's yeast.

4.1.3 Effect of draft tube on gas holdup

The insertion of a draft tube in a bubble column, converts the bubble column to a draft tube bubble column and also changes the gas and liquid flow pattern in the column, it also induces a change in the gas holdup in the device. The total gas holdup was measured by the volume expansion technique in the rectangular bubble column and the rectangular draft tube bubble column containing 70 cm draft tube and the RDTBC with a 60 cm draft tube under otherwise identical conditions, using sparger C and unaerated liquid height of 75 cm in all cases. Holdup was evaluated in all three devices and reported as a function of superficial gas velocities U_g based on the cross-sectional area of the outer column, in the range of 0-10 cm/s.

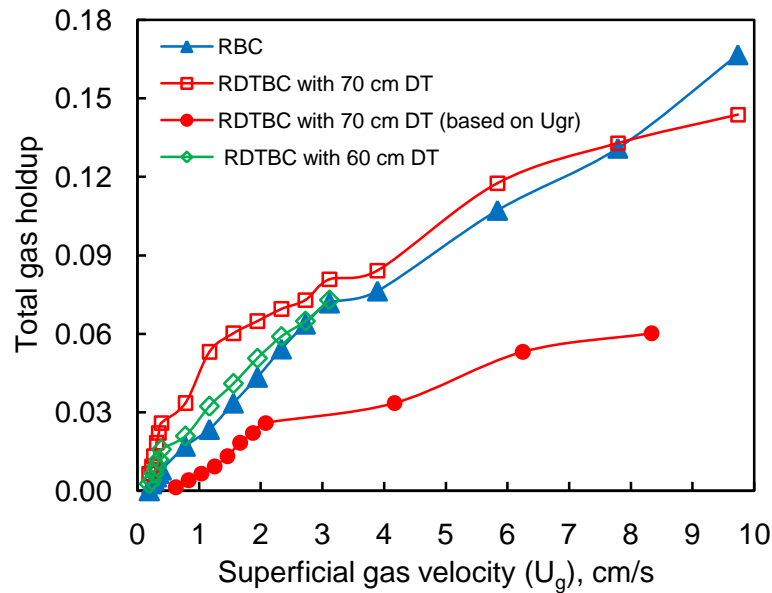


Fig. 4.11 Comparison of total gas holdup in RBC and RDTBC

It is problematic to compare the holdup profiles of RBC and RDTBC, because as a matter of convention the superficial gas velocities in bubble columns is determined based on the entire cross sectional area of the column while in draft tube bubble columns they are evaluated based on the cross sectional area of the draft tube through which the gases rise upwards in the column, the annular region in draft tube bubble columns provides the pathway for circulatory liquid flow, gas bubbles in the annulus arrive over there by virtue of being dragged by the liquid to that region, gas is not sparged in the annulus. Even when the total column cross sectional area of RBC and RDTBC is the same and gas flow rates are also the same the superficial velocity in the draft tube would be substantially larger than a bubble column because the draft tube area is just a fraction of the total column cross sectional area.

The gas holdup values in the RBC and the RDTBC were compared at same gas flow rates and similar values of the superficial gas velocity based on the total column cross-sectional area U_g as shown in Fig. 4.11 for the three devices. Also shown in the figure is the holdup profile based on U_{gr} for RDTBC with 70 cm draft tube. It is observed that the holdup values of RDTBC with 70 cm draft tube is substantially larger than RBC under identical conditions up to $U_g = 3$ cm/s thereafter the difference in holdup is marginal. At high gas velocities above 8 cm/s the gas holdup in RBC exceeds that in the RDTBC.

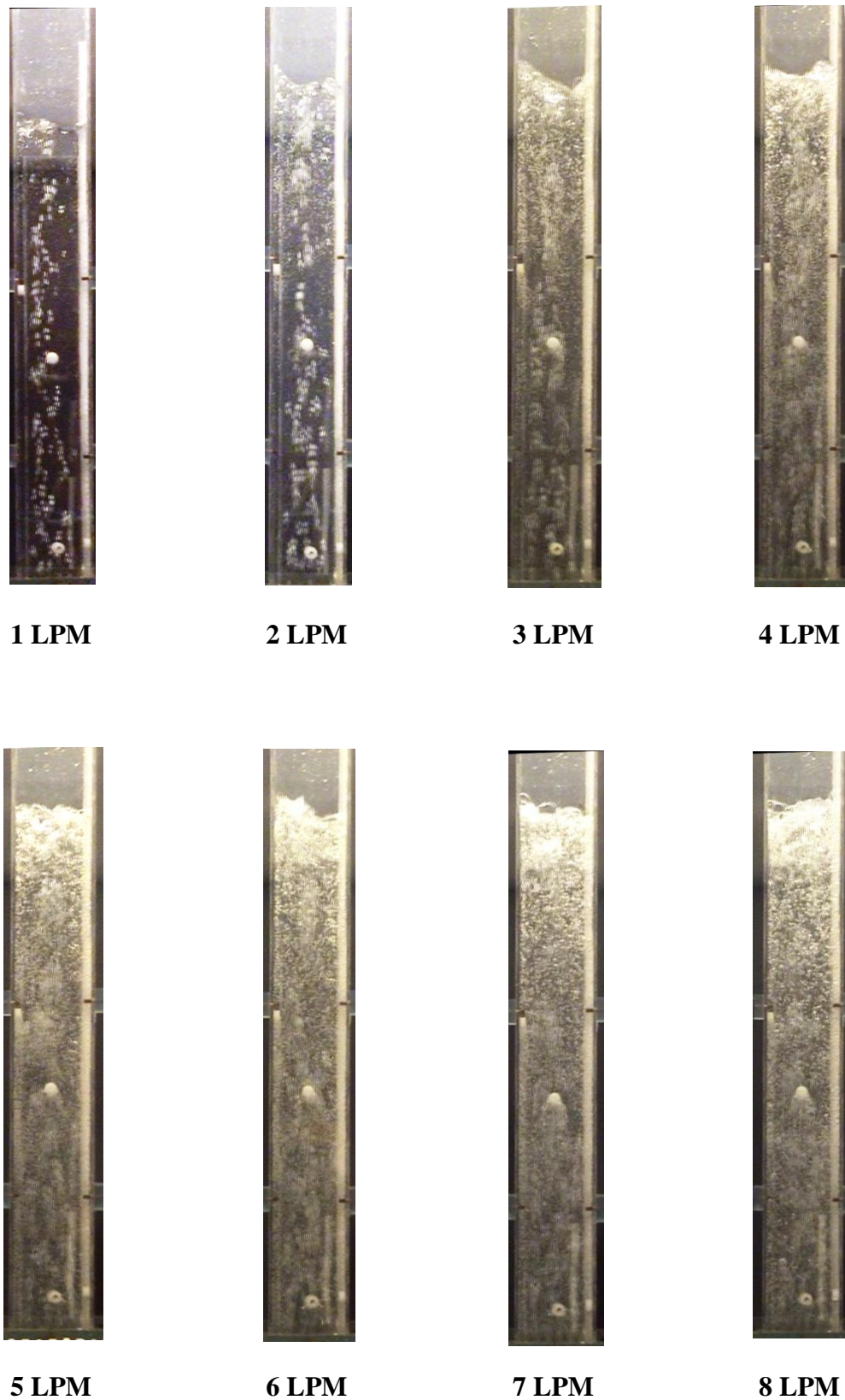


Fig. 4.12 Snapshots of bubbling patterns in RDTBC with 70 cm draft tube
(1 LPM = 2.0833 cm/s of U_{gr})

The holdup profile obtained for the RDTBC with 60 cm draft tube, although slightly more than RBC, closely approximates the holdup profile observed in the RBC for U_g ranging from 0 to 3 cm/s. In Fig. 4.11, the holdup profile of RDTBC with 70 cm DT as a function of U_{gr} is also shown, it is seen that using U_{gr} the curve shifts to right and spreads out in view of expanded range of superficial gas velocity that scales by a factor of 5.35, which is the ratio of the column cross-sectional area and the draft tube cross-sectional area.

The positioning of the curves i.e. holdup profiles based on U_g in Fig. 4.11 provides an insight in the holdup patterns of these devices. It is understood that holdup of gases increase in a gas-liquid system when the gases are unable to disengage from the liquid therefore, holdup increases when gas flow rate increases. Introducing more volume of gas in a liquid mass is bound to increase the gas holdup, in case of a foaming liquid the gas holdup increases tremendously. Gas holdup also tends to increase if in a restricted liquid volume more amount of gas is introduced. The difference in bubble column and draft tube bubble column is on these lines. In a bubble column gas is introduced into the entire mass of liquid while in a draft tube column gas is introduced in a small volume of liquid necessarily the holdup will be more under identical conditions.

It may be argued that the draft tube is immersed in the liquid and the gases escape from the top of the column where the cross sectional area is same for both draft tube column and the bubble column. *Then why is there any difference in holdup in a RBC and RDTBC?* The plausible answer to such an argument lies in the length of Region 2 above the draft tube. When this length is moderately large the gases have enough space and time like bubble column to expand into this region and disengage from the liquid in the usual manner without much crowding, but if this length is small the gas bubbles arriving at Region 2 though they expand over the entire cross sectional area of the column, they tend to crowd in the liquid mass near the interface and take some time before disengaging from the liquid this enhances the gas holdup in the device.

In RDTBC with 70 cm draft tube the gap between the clear liquid level (unaerated liquid level) and the upper edge of draft tube is just 5 cm. Hence, bubbles emerging from draft tube will crowd in that region and find it difficult to disengage easily. Hence, there is a sharp increase in gas holdup even at low gas velocities, while with the 60 cm long draft tube column the gas holdup profile are almost the same as the RBC implying that 15 cm of free space in Region 2 is sufficient to avoid the crowding of the bubbles in the upper

region. Snapshots of bubbling patterns in RDTBC with 70 cm draft tube at increasing air flow rates are shown in Fig. 4.12 for visualization of bubble crowding mechanism as discussed above.

The increased gas holdup observed in the 70 cm draft tube column is attributed to these particular reasons. Since a dominant fraction of gas holdup is concentrated at the upper region of the column at almost all velocities it is unlikely to contribute much towards enhancing the mass transfer parameters of the draft tube column.

4.1.4 Effect of draft tube height on gas holdup in RDTBC

The influence of draft tube cross-sectional geometry and ratio of cross-sectional area of draft tube to that of the annulus on hydrodynamics and mass transfer behavior of draft tube bubble columns has been investigated by many investigators in the past (Koide et al., 1983a; Merchuk et al., 1994; Farizoglu and Keskinler, 2007).

The effect of bottom clearance between the draft tube and the sparger on column hydrodynamics and mass transfer aspects has also been investigated (Koide et al., 1984; 1988; Pironti et al, 1995; Gouveia et al., 2003; Kilonzo et al., 2007).

However, the effect of the height of the draft tube on the overall performance of draft tube bubble column is yet to be appropriately quantified. The present investigation attempts to quantify the effect of the draft height not only on the total gas holdup but also on specific interfacial area and volumetric mass transfer coefficient as well in rectangular draft tube bubble columns.

In the present investigation, the effect of draft tube height on gas holdup was studied by using two draft tubes one of 60 cm height and the other of 70 cm while keeping same bottom clearance of 1 cm between the draft tube and sparger as well as the same unaerated liquid height of 75 cm in both cases. Thus, the top clearance between liquid surface and draft tube ranges from 5 cm for the 70 cm draft tube to 15 cm for the 60 cm draft tube. Sparger C with 4 holes each of 1 mm diameter with 20 mm pitch was used in both cases. The gas holdup was measured as a function of superficial gas velocity for both the draft tubes under investigation.

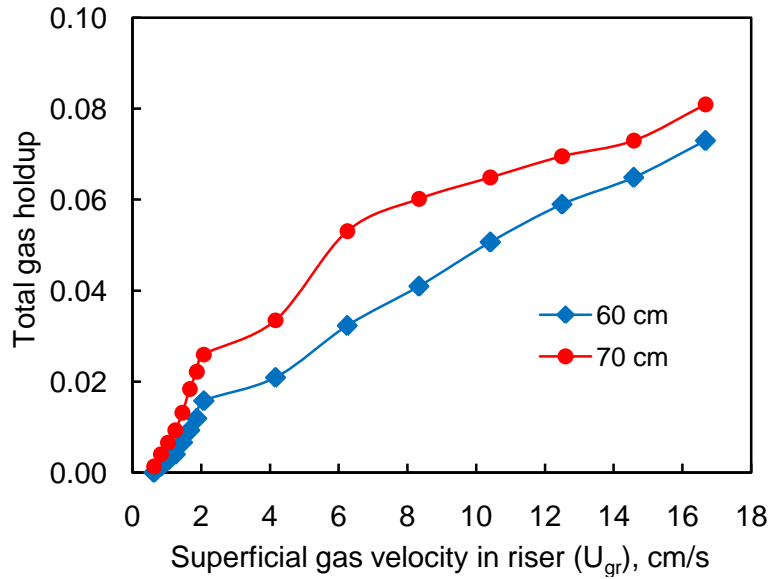


Fig. 4.13 Effect of draft tube height on gas holdup in RDTBC

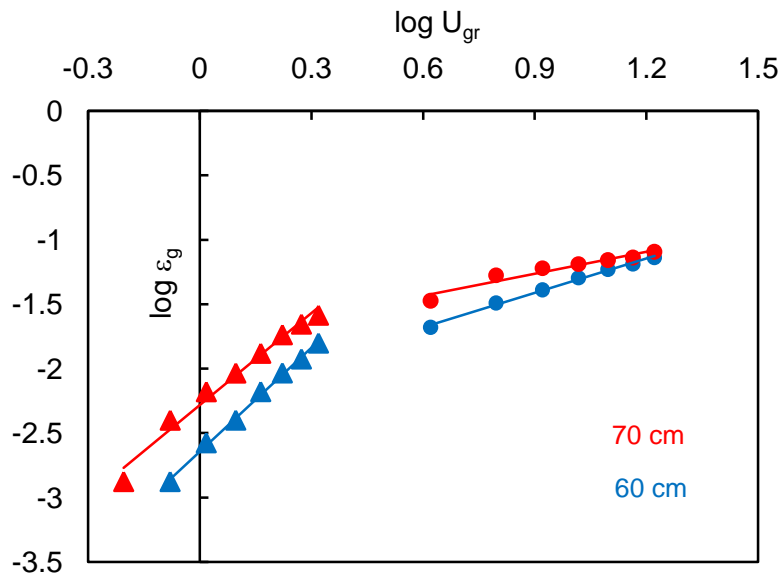


Fig. 4.14 Regime plot of effect of draft tube height on gas holdup in RDTBC

The 70 cm draft tube gave consistently more gas holdup in comparison with the 60 cm draft tube at the same U_{gr} values as shown in Fig. 4.13. The difference in holdup was particularly prominent in the mid range of operating velocities ranging from 2 cm/s to 14 cm/s the maximum difference in the gas holdup in these devices was at U_{gr} values of 6 to 8 cm/s.

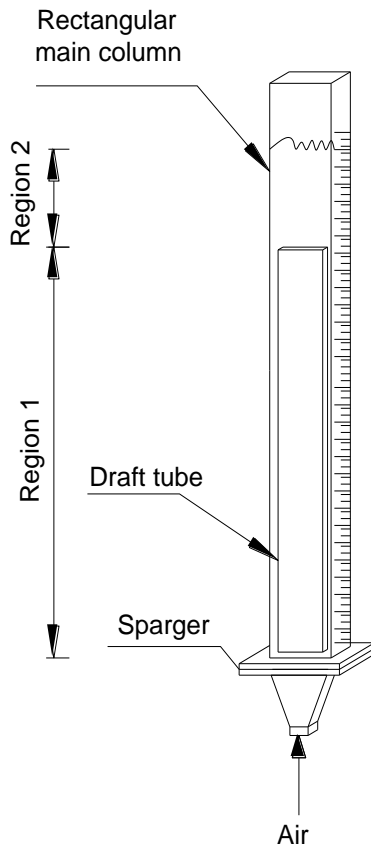


Fig. 4.15 Different hydrodynamic regions in RDTBC

In a draft tube bubble column, two distinct hydrodynamic regions can be identified as shown in Fig. 4.15. Region 1 is from the gas sparger up to the height of the draft tube, in this region due to restriction of space the gas bubbles move upwards in a directed fashion almost in a plug flow pattern with negligible recirculation of the bubbles. Region 2 extends from the upper edge of the draft tube up to the dispersed liquid level, in this region the draft tube bubble column behaves just like an ordinary bubble column with intense backmixing at the high velocities, there is a sudden expansion of space and the bubbles emerging from the draft tube encounter the circulating liquid flow patterns existing in bubble columns.

Due to recirculation of both gas and liquid the coalescence of bubbles gets facilitated leading to formation of larger bubbles that rise very rapidly. Increasing the length of Region 2 would facilitate greater coalescence and quick removal of the bubbles and result in a decline in the gas holdup.

This behavior was evident in the experimental results obtained. At maximum superficial gas velocities of 16.67 cm/s the height of Region 2 to be crossed over by the bubbles in 60 cm draft tube was 20.9 cm while in the 70 cm draft tube it was only 11.6 cm, necessarily in the 60 cm long draft tube extent of bubble coalescence in Region 2 was more due to enhanced space available resulting in lowering the gas holdup in comparison to the 70 cm long draft tube. Fig. 4.14 shows the regime plot from which it is inferred that in the heterogeneous regime the dependency of the holdup on gas velocity is much more prominent for the case of 60 cm draft tube than the 70 cm one.

The consistently higher gas holdup values obtained in the 70 cm draft tube justified its use for further investigations in rectangular as well as cylindrical draft tube bubble columns.

4.1.5 Effect of geometrical shape of DTBC on gas holdup

Effect of column and draft tube geometry on the total gas holdup values were assessed by comparing the holdup profiles obtained for rectangular columns with draft tube, and circular columns with draft tube in identical range of superficial gas velocities U_{gr} . Both the draft tube columns were equipped with four holes sparger (sparger C) having hole diameter of 1 mm.

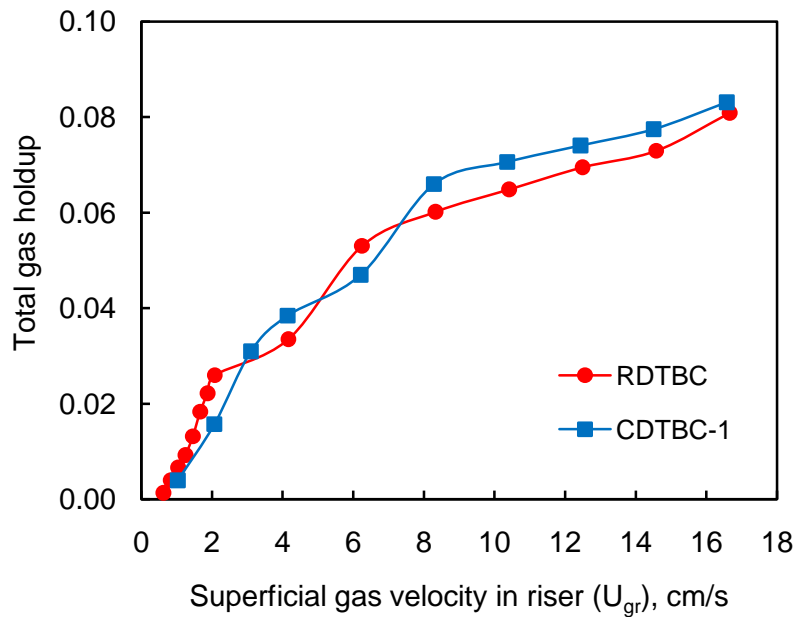


Fig. 4.16 Effect of geometrical shape of DTBC on gas holdup
(DT height = 70 cm; $N_h = 4$ in sparger; $A_r = 8 \text{ cm}^2$)

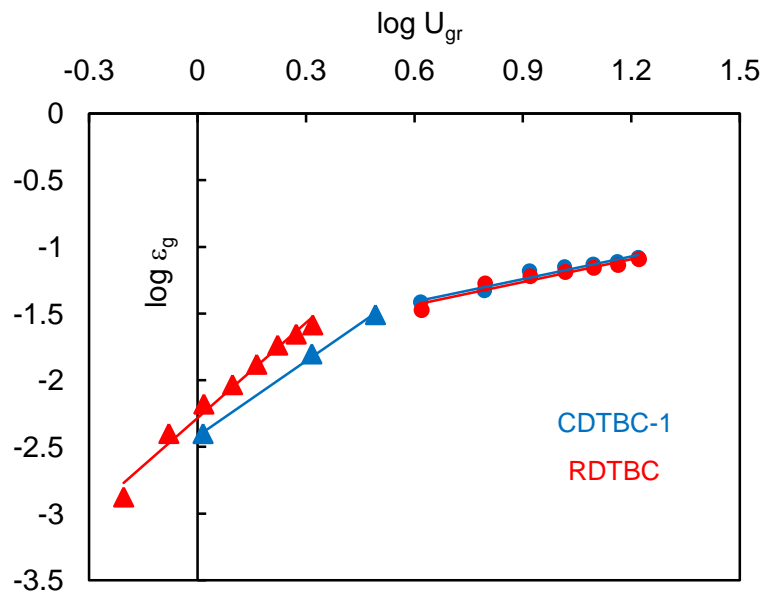


Fig. 4.17 Regime plot of effect of geometrical shape of DTBC on gas holdup
(DT height = 70 cm; $N_h = 4$ in sparger; $A_r = 8 \text{ cm}^2$)

Care was taken that the cross-sectional area of the rectangular as well as the cylindrical draft tube were identical 8 cm^2 and 8.042 cm^2 for rectangular and cylindrical respectively hence at same flow rates similar gas velocities were obtained in both devices. Draft tube height in both cases was 70 cm and the unaerated liquid height was 75 cm.

Total gas holdup profiles for the rectangular device RDTBC and the cylindrical device CDTBC-1 is shown in Fig.4.16. The profiles are quite close, which indicate that there is no considerable effect of the cross-sectional shape -whether circular or rectangular – on gas holdup values in the draft tube bubble columns. At lower superficial gas velocities the RDTBC shows consistently greater gas holdup than the CDTBC-1 while at larger values of U_{gr} CDTBC-1 returns greater values of gas holdup. Akita and Yoshida (1973) has found insignificant effect on gas holdup by changing shape of cross-section of bubble column from circular to square cross-section.

Regime plot for the devices shown in Fig. 4.17 indicate that the difference in the two devices are more pronounced in the homogenous regime and the transition from homogenous to heterogeneous regime occurs at greater values of U_{gr} in CDTBC-1. The dependence on velocity of RDTBC is more pronounced than the CDTBC-1 in the homogenous regime. These effects are attributed to the nature of flow in RDTBC, which is directed and almost plug like over the entire velocity range facilitated by the narrow width of the rectangular draft tube that gives a two dimensional nature and axial direction to the bubble chains flowing through the machine. Such flows were not expected in the cylindrical DTBC hence at lower velocities it returns lower gas holdup in comparison to RDTBC.

4.1.6 Effect of scale of operations on gas holdup

The effect of column size on gas holdup was investigated by comparing experimental results obtained under identical conditions in cylindrical draft tube bubble columns of different diameters as shown in Fig. 4.18. Column CDTBC-1 had a column ID of 6.4 cm and draft tube ID of 3.2 cm the cross-sectional area of draft tube was 8.042 cm^2 , while column CDTBC-2 had an ID of 14 cm and draft tube ID of 8 cm the cross-sectional area of draft tube was 50.3 cm^2 . CDTBC-1 was equipped with a sparger with 4 holes of 1 mm diameter each while CDTBC-2 had a sparger with 8 holes of 1 mm diameter each. The height of column in both the cases was 1 meter and draft tube height was 70 cm.

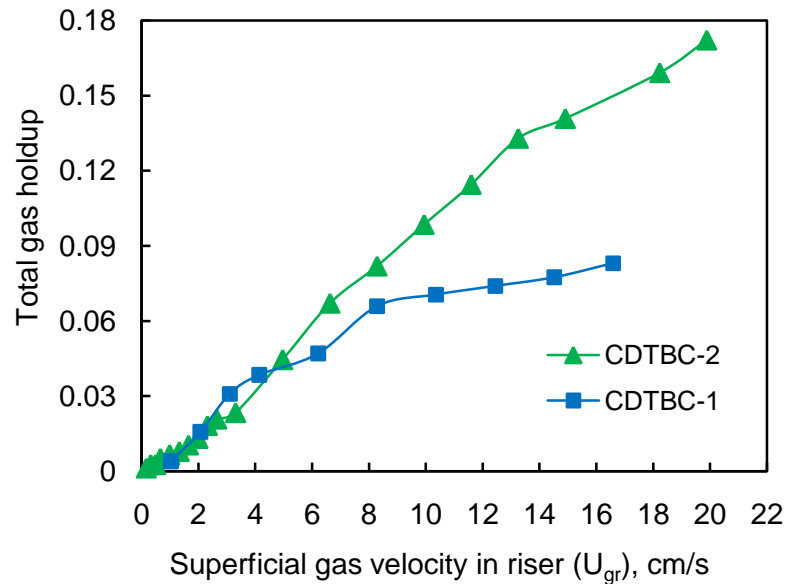


Fig. 4.18 Effect of scale of operation on gas holdup

(DT height = 70 cm; A_r of CDTBC-1 = 8.42 cm²; A_r of CDTBC-2 = 50.3 cm²)

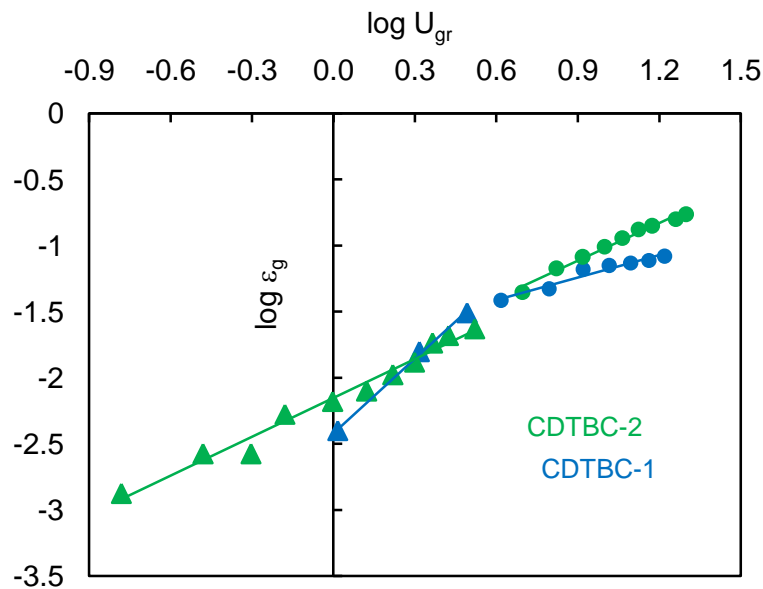


Fig. 4.19 Regime plot of effect of scale of operation on gas holdup

(DT height = 70 cm; A_r of CDTBC-1 = 8.42 cm²; A_r of CDTBC-2 = 50.3 cm²)

The gas holdup profiles in the DTBC are shown in Fig. 4.18 they tend to superimpose at low gas flow rates up to superficial gas velocities of 2 cm/s, while at higher gas flow rates there is considerable increase in gas holdup values in CDTBC-2 compared to CDTBC-1. At a superficial gas velocity of 2 cm/s, in these two draft tube bubble columns, the gas velocity based on hole diameter is 5.3 m/s CDTBC-1 and 15.9 m/s for CDTBC-2, which corresponded to an idealized bubbling rate of 7962 bubbles/sec and 23885 bubbles/sec for CDTBC-1 and for CDTBC-2 respectively, while at a higher superficial gas velocity of 15 cm/s, in these two draft tube bubble columns, the gas

velocity based on hole diameter is 37.2 m/s CDTBC-1 and 119.3 m/s for CDTBC-2, which corresponded to an idealized bubbling rate of 55732 bubbles/sec and 179140 bubbles/sec for CDTBC-1 and for CDTBC-2 respectively.

The gas holdup profile of CDTBC-1 shows tendency to flatten out on attainment of ~ 8% gas holdup similar behavior was not noticed in CDTBC-2 that showed a monotonically increasing holdup profile. This behavior is attributed to the larger scale of operation in CDTBC-2. The total volume of liquid feed in CDTBC-2 was 10.5 liter while in CDTBC-1 it was only 2.2 liter; necessarily there was greater possibility of dispersion formation in CDTBC-2 than in CDTBC-1. From the regime plot Fig. 4.19, it is observed that the homogeneous and heterogeneous regimes are distinctly identifiable in CDTBC-1, but it is not so in CDTBC-2, the effect of velocity on gas holdup appears to be same in the homogeneous and heterogeneous regimes in CDTBC-2.

The gas holdup profiles in draft tube bubble columns are sensitive to the scale of operations; the magnitude of gas holdup in small columns is of the order of around 10% while in larger scale column it can increase to almost double the values. Plateau in gas holdup values was observed in CDTBC-1 but they were not observed in the larger CDTBC-2.

4.1.7 Prediction of gas holdup in draft tube bubble columns

A number of correlations exist to predict the gas holdup in draft tube bubble columns that are listed in Table 2.2. The efficacy of these equations was tested vis-à-vis the experimental data obtained in this work.

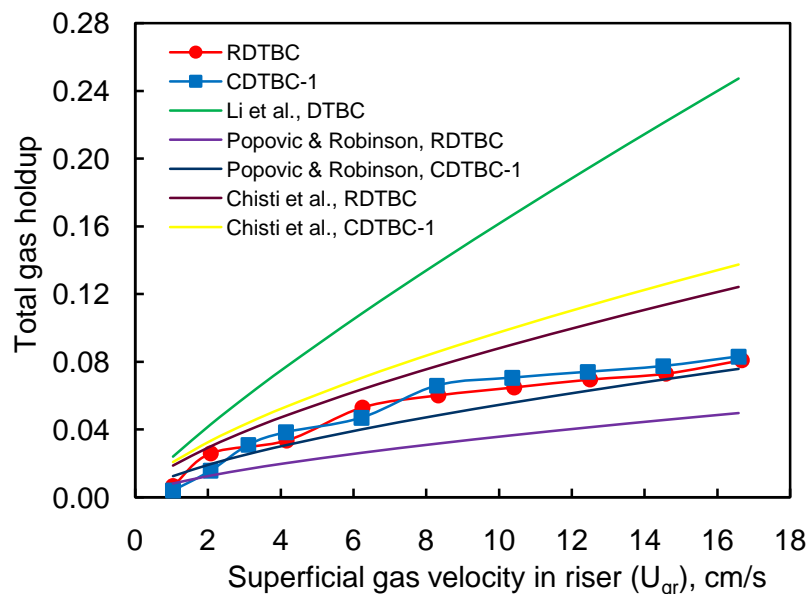


Fig. 4.20 Prediction of gas holdup in RDTBC and CDTBC-1

Different degree of agreement was observed between experimental and predicted values of gas holdup as shown in Fig. 4.20.

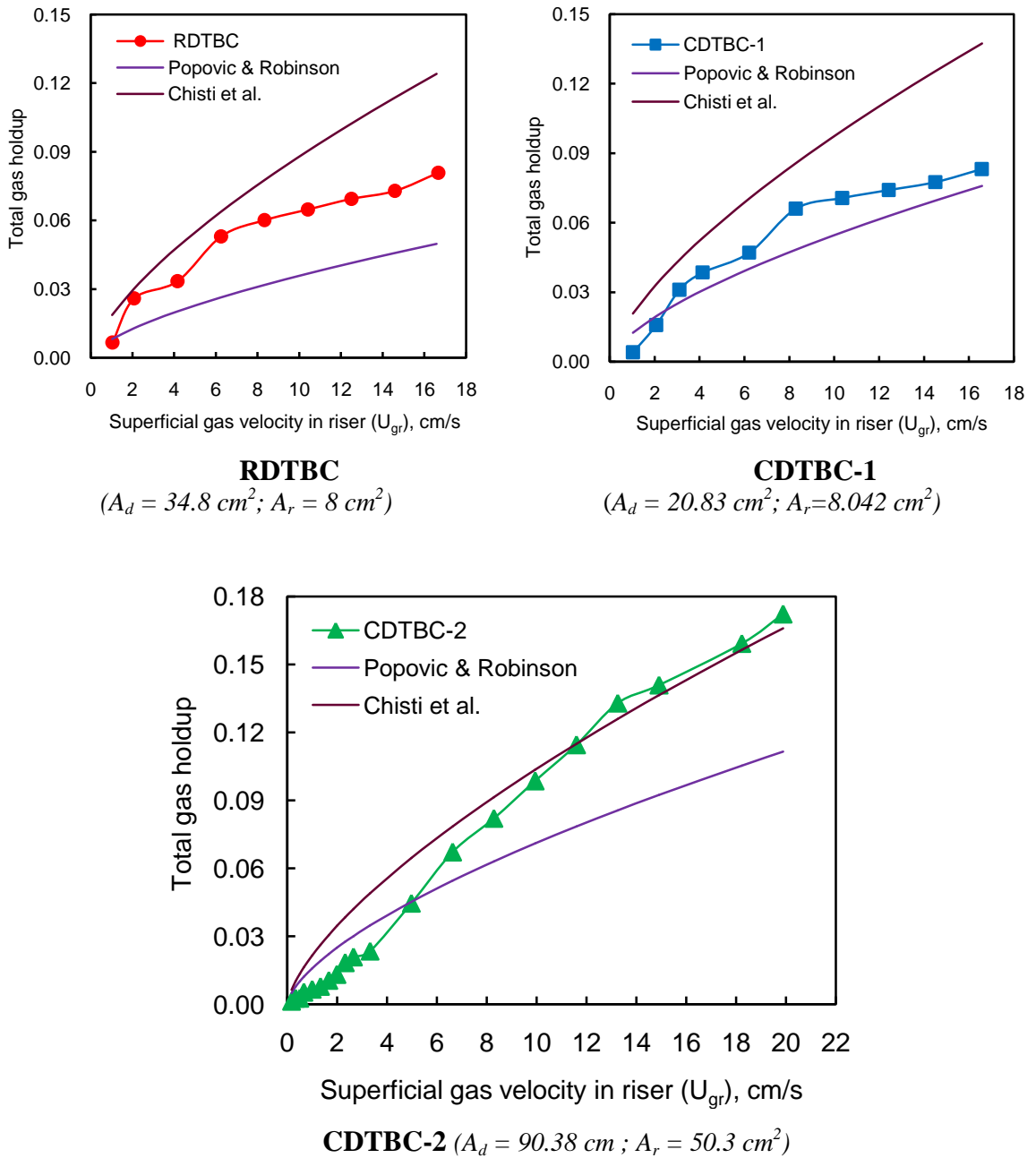


Fig. 4.21 Comparison of predicted and experimental gas holdup profiles in DTBC
(DT height = 70 cm)

It is apparent that the correlations by Popovic and Robinson (1984) and Chisti et al. (1988) gave the closest prediction of the holdup values. These correlations are listed as follows:

Popovic and Robinson:

$$\varepsilon_{gr} = 0.465U_{gr}^{0.65} \left(1 + \frac{A_d}{A_r}\right)^{-1.06} \mu_{ap}^{-0.103}$$

Chisti et al.:

$$\varepsilon_{gr} = 0.65U_{gr}^{(0.603+0.078C_0)} \left(1 + \frac{A_d}{A_r}\right)^{-0.258}$$

Where the distribution parameter $C_0 = 1$. In these equations, A_d and A_r are downcomer and riser cross-sectional areas respectively.

It is observed in Fig. 4.21, that the Popovic and Robinson equation consistently under predicts the holdup values irrespective of the geometry and the scale of operations with the exception in CDTBC-2 at low gas velocities while the Chisti et al. correlation over predicts the holdup for all cases except in CDTBC-2. It is observed that in CDTBC-2 at high values of U_{gr} Chisti's correlation gives a reasonable fit for the holdup data, while CDTBC-1 data was best predicted by Popovic and Robinson correlation. The overall statistical analysis of these correlations with different devices is listed below; there is considerable scope to develop new correlations for superior prediction of gas holdup in draft tube bubble columns.

Percentage absolute errors

Device	Popovic and Robinson	Chisti et al.
RDTBC	41.3	54.1
CDTBC-1	37.3	38.1
CDTBC-2	87	125

4.2 SPECIFIC GAS-LIQUID INTERFACIAL AREA

The interfacial area of the draft tube bubble columns as well as bubble column was determined using sulfite oxidation technique. All runs were performed with an amount of initial solution that gave an unaerated liquid height of 75 cm. It is well known that interfacial area increases with superficial gas velocity which in case of a draft tube bubble column is the superficial gas velocity in the riser. Prior to exploring the effect of various parameters on the interfacial area a few test runs were performed to obtain prototype profile of specific interfacial area with respect to the superficial gas velocities. For this purpose the RDTBC with 70 cm draft tube was the chosen device equipped with sparger C having 4 holes of 1 mm diameter.

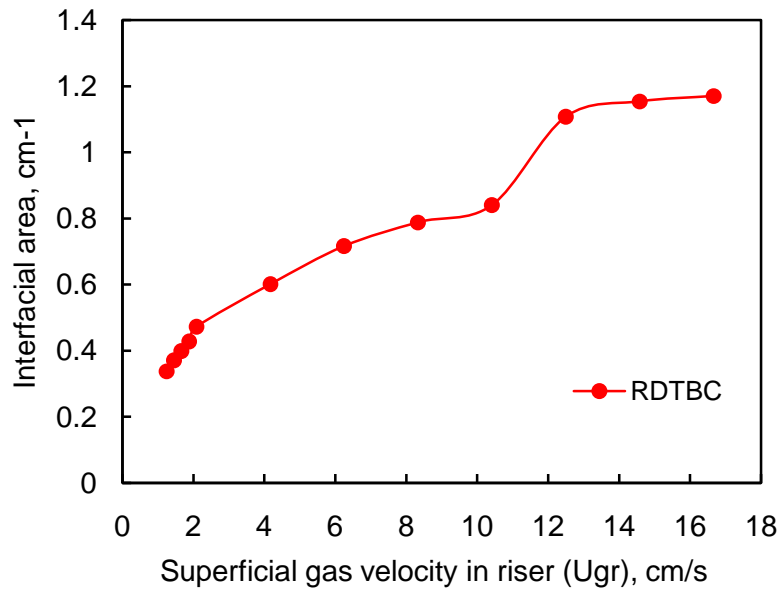


Fig. 4.22 Prototype interfacial area profile in RDTBC

(DT height = 70 cm)

Fig.4.22 shows the prototype profile of interfacial area in RDTBC. The trend of increase of interfacial area with U_{gr} was very much similar to that of the increase in gas holdup with U_{gr} . Like gas holdup the growth in interfacial area with increasing superficial gas velocities was always greater in the homogeneous region at low values of gas flow rates than in the heterogeneous regimes at higher flow rates. This pattern is attributed to the formation of larger bubbles in the heterogeneous regime due to increased bubble coalescence at higher flow rates, while the numerous small sized bubbles moving without much interaction with other bubbles were responsible for higher interfacial area at low gas flow rates in homogeneous regime.

Since interfacial area is directly proportional to the gas holdup $a = \frac{6 \varepsilon_g}{d_s}$ therefore factors contributing to an increase in gas holdup will directly contribute to increase in interfacial area. Interfacial area is also inversely proportional to Sauter mean bubble diameter, d_s which leads to the decrease in the rate of enhancement of interfacial area in heterogeneous regime where bubble size increases due to increased coalescence at higher gas flow rates.

Subsequently runs to determine the specific interfacial area were conducted in all draft tube bubble column devices developed in this investigation and the effect of geometrical shape, scale of operations etc. were discerned and are discussed in the following sections.

4.2.1 Effect of draft tube height on interfacial area for RDTBC

Influence of draft tube height on gas holdup was detailed in section 4.1.4, on the same lines effect of draft tube height on specific interfacial areas was studied by using two draft tubes of heights 60 cm and 70 cm in rectangular draft tube bubble columns. These devices were equipped with sparger C.

Specific gas-liquid interfacial areas were obtained by chemical method, for both cases over a range of values of U_{gr} , as shown in Fig. 4.23. Although both devices show similar pattern of increasing interfacial areas with increase in superficial gas velocity, U_{gr} but the interfacial area decreases with a decrease in draft tube height from 70 cm to 60 cm. Such decrease in interfacial area is the combined effect of decrease in total gas holdup and formation of larger bubbles as explained earlier.

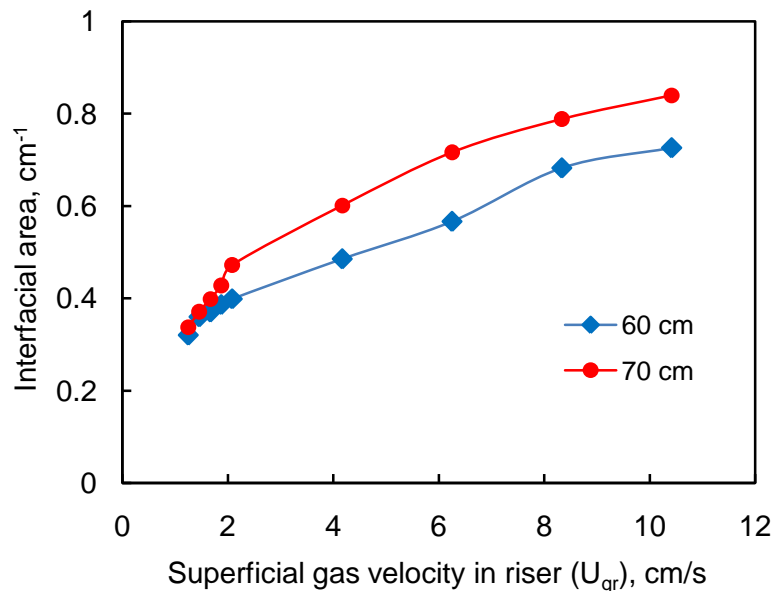


Fig. 4.23 Effect of draft tube height on interfacial area for RDTBC

Comparing the rate of enhancement of gas holdup as well as interfacial areas when the 60 cm draft tube was replaced by the 70 cm draft tubes it was observed that the enhancement for gas holdup was more in comparison with the interfacial areas at identical values of U_{gr} . This feature stems from the different dependencies of bubble volume and its surface area on bubble diameter. Thus, draft tube bubble columns with 70 cm draft tube height were used for further investigations and for applications because of its superior characteristics including higher gas holdup and interfacial area than the device with 60 cm draft tube.

4.2.2 Effect of draft tube on interfacial area

Profile of interfacial areas obtained in RDTBC were compared with that obtained in Rectangular Bubble Columns (RBC) at identical gas rates, both columns were equipped with sparger C. Table 4.2 presents the significant results at identical conditions of gas flow rates. It becomes necessary to invoke gas flow rates because the major point of departure in RDTBC and RBC is the flow path of the gas in these devices. In draft tube bubble columns the gases flow through the draft tube which occupies only a small fraction of the entire column cross section while in a bubble column the gases flow through the entire cross section. Hence at same gas flow rates there is considerable variation in the superficial gas velocity U_g for bubble column and U_{gr} for the draft tube system due to the decline in the cross-section area of the gas flow path in the presence of the draft tube in the draft tube bubble column even when the external dimension of the main column could be the same.

Table 4.2 Comparison of interfacial area of RBC and RDTBC

Air flow rate, LPM	RDTBC			RBC	
	Draft tube c.s. area = 8 cm ²			c.s. area = 42.8 cm ²	
	Unaerated liquid height = 75cm				
	U _{gr} (cm/s)	Height of draft tube		U _g (cm/s)	Interfacial area, a, cm ⁻¹
70 cm		60 cm			
		Interfacial area, a, cm ⁻¹			
3	6.25	0.716	0.566	1.168	0.386
4	8.33	0.788	0.682	1.558	0.542
5	10.42	0.840	0.726	1.947	1.057
8	16.67	1.170	0.914	3.115	2.107

It was observed in Table 4.2 that at low flow rates up to a certain gas flow rate the draft tube bubble column generated significantly larger specific interfacial areas in comparison with the rectangular bubble column, but as the gas flow rate increased there was a sharp increase in the interfacial areas in bubble columns while in the case of draft tube bubble columns the increase in interfacial area was gradual. The gas flow in draft tube columns is axial plug flow in nature while in a bubble column back mixed random flow is prevalent. At high gas flow rates the flow in the bubble column approaches plug flow behavior resulting in an increase in the interfacial area. At high gas flow rates the flow in the draft tube retains its plug flow nature but since the cross sectional area of the draft is much smaller, the magnitude of increase of interfacial area is not as significant as that of the bubble column.

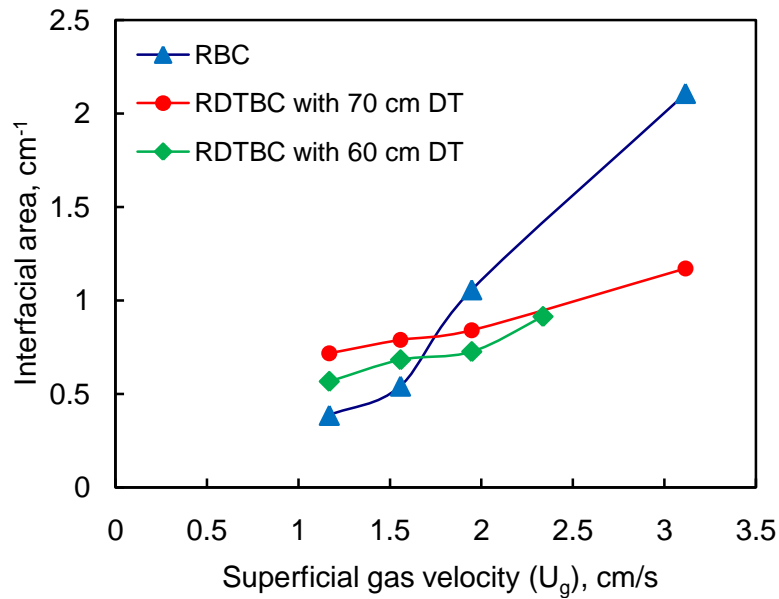


Fig. 4.24 Effect of draft tube on interfacial area for rectangular columns

Fig. 4.24 depicts the effect of the presence of draft tube in a column on the interfacial area. The comparison of the RBC, RDTBC with 70 cm draft tube height and RDTBC with 60 cm draft tube height is based on superficial gas velocity determined over the entire column cross-sectional area. It was noticeable from this figure that the draft tube columns provide very stable flow patterns and return interfacial areas that vary narrowly over a wide range of superficial velocity, at high gas flow rates, the performance of draft tube bubble column in terms of specific interfacial area available for mass transfer was inferior to that of a bubble column.

It appears that it is preferable to operate draft tube bubble column at low gas flow rates. DTBC are equipments of choice when stable flow is desired providing a narrow range of changes over a wide range of parametric variations, beyond a certain velocity not much advantage can be obtained from this device in mass transfer terms.

4.2.3 Effect of geometrical shape of draft tube bubble column on interfacial area

Specific gas-liquid interfacial areas at varying superficial gas velocities obtained in rectangular and circular draft tube bubble columns is shown in Fig. 4.25. Both these columns have identical draft tube cross sectional area ($\sim 8 \text{ cm}^2$), draft tube height (70 cm) and number and diameter of holes in sparger ($N_h = 4$).

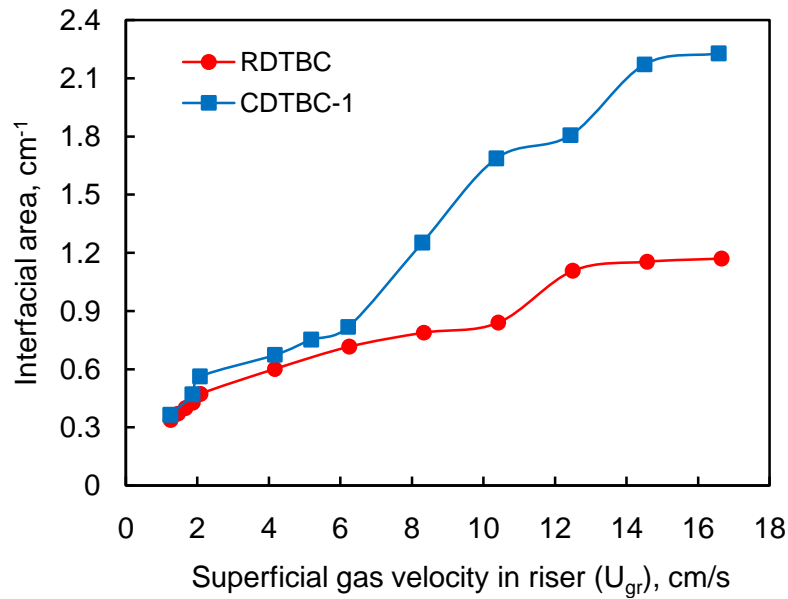


Fig. 4.25 Effect of geometrical shape of DTBC on interfacial area

(DT height = 70 cm; $N_h = 4$ in sparger; $A_r = 8 \text{ cm}^2$)

Since the cross sectional area of both the columns is identical the superficial velocity remains same for both columns at same gas rate. It is seen that except for very low gas velocities corresponding to ~ 2 LPM gas flow rate the interfacial area obtained was always more for CDTBC-1 than the rectangular RDTBC. The real divergence of the interfacial area profiles gets initiated beyond 6 cm/s superficial gas velocity corresponding to ~ 3 LPM gas flow rate, beyond this velocity the interfacial area in the CDTBC-1 increases drastically.

The RDTBC provided a rather narrow range of interfacial areas compared to CDTBC-1, it was visually observed at identical gas flow rates that in case of CDTBC at higher flow rates above 3 LPM, numerous small bubbles of circular shape and uniform size existed in the annulus space and was flowing downward with the circulating liquid, while in RDTBC in the annular space tiny bubbles adhered to the surface of the draft tube.

The large increase in interfacial areas at higher gas rates in CDTBC-1 is reminiscent of the sharp increase in interfacial area observed in rectangular bubble columns in comparison with RDTBC at the same gas flow rates discussed in Section 4.2.2. There is insufficient information available to analyze this behavior in the present context, it appears to stem from liquid circulation problems that are more uniform in circular columns. CFD analysis would certainly be able to throw more light on this behavior.

4.2.4 Effect of scale of operations on interfacial area

The effect of scale of operation on interfacial area was investigated in cylindrical draft tube bubble columns of different sizes. Column CDTBC-1 had a column ID of 6.4 cm and draft tube ID of 3.2 cm, the cross-sectional area of draft tube was 8.042 cm^2 , while column CDTBC-2 had an ID of 14 cm and draft tube ID of 8 cm, the cross-sectional area of draft tube was 50.3 cm^2 . The height of column and draft tube in both the devices was 1 meter and 70 cm respectively. The unaerated liquid height was kept 75 cm in both cases that corresponded to a liquid capacity of 2.2 lit in CDTBC-1 and 10.5 lit in CDTBC-2. Gas was sparged in CDTBC-1 through a four hole sparger while in CDTBC-2 a 8 hole sparger was used, the sparger hole diameter in both spargers was 1 mm.

The interfacial area profile in both these columns is shown in Fig. 4.26. The pattern of increase of interfacial area with an increase in superficial velocities is nearly similar, up to $U_{gr} \sim 6 \text{ cm/s}$ no difference in interfacial area is observed in both these devices, however, beyond this velocity the interfacial areas obtained in CDTBC-2 are almost 20% lower than that observed in CDTBC-1 but again at high U_{gr} the interfacial area values become almost similar.

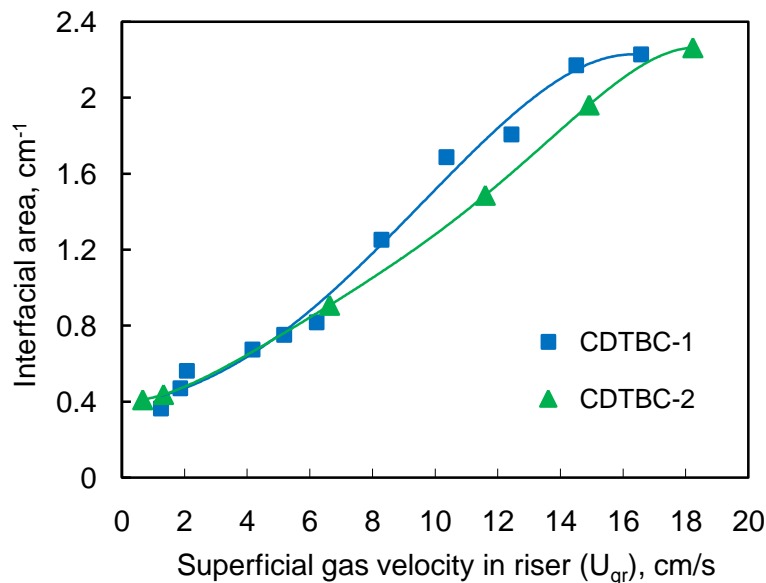


Fig. 4.26 Effect of scale of operation on interfacial area

(DT height = 70 cm; A_r of CDTBC-1 = 8.42 cm^2 ; A_r of CDTBC-2 = 50.3 cm^2)

The air flow rate required for attaining $U_{gr} \sim 6 \text{ cm/s}$ in CDTBC-1 was only 3 LPM, while in CDTBC-2 it was as high as 20 LPM, due to the large difference in the cross-sectional area of draft tubes in these columns. But even at flow rates of 3 LPM, the superficial gas velocities obtained in CDTBC-1 are sufficient to establish a liquid flow pattern that involved circulation of gas bubbles between draft tube and annulus and this gas and

liquid circulation goes on increasing with gas flow rates as shown in the snapshots of CDTBC-1 in Fig. 4.27.

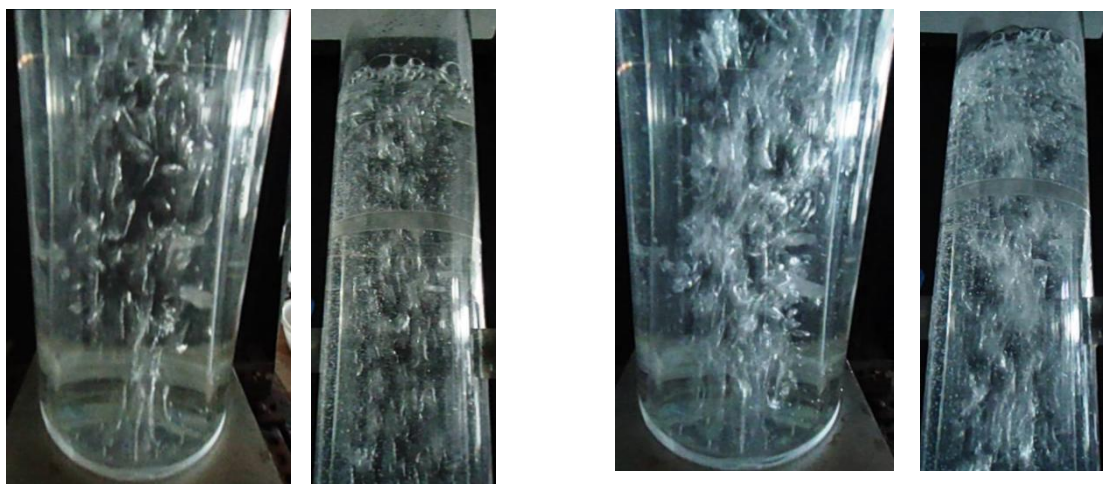


3 LPM

8 LPM

Fig. 4.27 Snapshots of bubble patterns in CDTBC-1 ($A_r = 8.042 \text{ cm}^2$, $A_d = 20.83 \text{ cm}^2$)

The greater value of interfacial area obtained in CDTBC-1 is attributed to the presence of gas bubbles in both the compartments of the device, due to gas phase circulation at gas flow rate 3 LPM onwards, while in CDTBC-2 even at gas rate of 20 LPM ($U_{gr} \sim 6 \text{ cm/s}$) the liquid circulatory flow is not sufficiently developed to create downward flow of bubbles in the annulus with circulating liquid due to large annulus cross-sectional area of 90.4 cm^2 . Therefore, the flow of bubbles remains confined to only the draft tube as shown in snapshots of CDTBC-2 in Fig. 4.28. Absence of bubbles in annulus restricts the interfacial area values.



3 LPM

8 LPM

Fig. 4.28 Snapshots of bubble patterns in CDTBC-2 ($A_r = 50.3 \text{ cm}^2$, $A_d = 90.4 \text{ cm}^2$)

It was visually observed that in CDTBC-2 at higher gas flow rates the gas bubbles emerging out from the sparger tend to coalesce in the sparger region perhaps due to high bubbling rate (79618 bubbles/sec corresponding to $U_{gr} \sim 6$ cm/s). It was observed that the liquid circulation pattern developed in this device induces the movement of gas bubbles towards the center of draft tube that enhances the possibility of coalescence of gas bubbles throughout its passage through the draft tube. The increase in bubble size because of this increased coalescence may also be attributed to lower interfacial area in CDTBC-2 without affecting the values of gas holdup which were higher in CDTBC-2 at higher gas flow rates.

4.3 MASS TRANSFER COEFFICIENTS

The mass transfer coefficients $k_L a$ and k_L are the parameters that define gas-liquid interaction in gas-liquid contactors. The individual liquid phase mass transfer coefficient k_L quantifies the nature of interaction and depends on the local turbulence created by the flow profile while the volumetric mass transfer coefficient ($k_L a$) is the key design parameter of gas-liquid contactors, $k_L a$ of the draft tube bubble columns was determined using dynamic gassing-in method.

All $k_L a$ experiments were conducted using deaerated water filled in the columns to get initial unaerated liquid height of 75 cm at ambient temperature and pressure in the draft tube bubble columns, gas was sparged through a 4 hole sparger having $d_h = 1$ mm in RDTBC and CDTBC-1. The effect of superficial gas velocity, height of draft tube and geometry of column on mass transfer coefficients in draft tube bubble columns is discussed in the following sections:

4.3.1 Effect of superficial gas velocity on $k_L a$

The volumetric mass transfer coefficient $k_L a$ is a product of two parameters k_L and a and both these parameters increases with an increase in the superficial gas velocity in gas-liquid contacting devices, therefore, $k_L a$ is bound to increase with superficial gas velocity. However, the functional dependence of $k_L a$ on the superficial gas velocities is expected to be quite different from the parameters that constitute it because while the specific surface area depends directly on the superficial gas velocities the value of k_L is not directly affected by the superficial gas velocity in the column and depends on the turbulence created in the liquid phase by the moving bubbles.

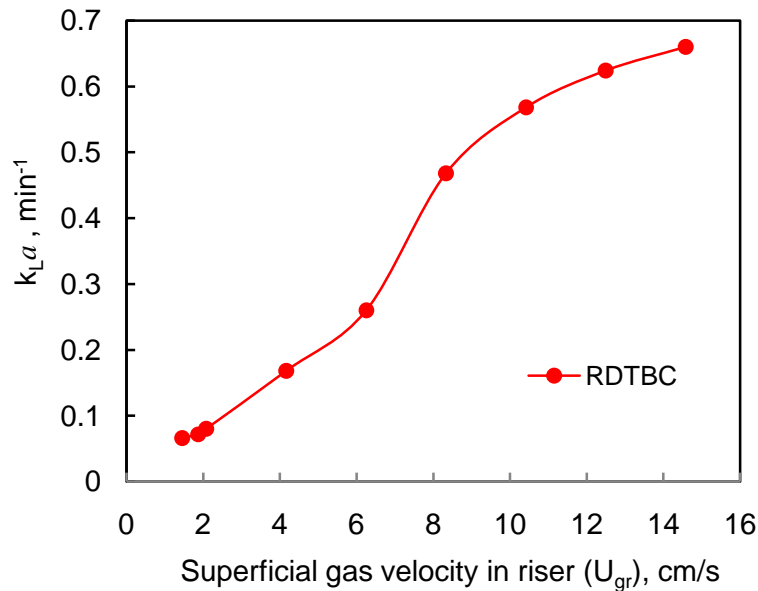


Fig. 4.29 Effect of superficial gas velocity on k_{La} in RDTBC

(DT height = 70 cm)

The effect of increasing superficial gas velocity on k_{La} for air-water system was obtained for rectangular as well as cylindrical draft tube bubble column device developed in the present investigation under identical set of conditions. The variation of liquid phase volumetric mass transfer coefficient (k_{La}) with U_{gr} is shown in Fig. 4.29 for RDTBC with 70 cm draft tube, it is observed that initially k_{La} increases linearly with U_{gr} but above a superficial gas velocity of 6 cm/s there is a sudden upsurge in k_{La} with increase in superficial gas velocities. This enhancement in k_{La} continues up to $U_{gr} = 12$ cm/s and thereafter tends to level of. Higher values of U_{gr} in the heterogeneous regime lead to bubble coalescence in the DTBC particularly in the upper zone and formation of larger bubbles that arrests the growth of interfacial area with U_{gr} leading to flattening of the a as well as k_{La} profiles.

4.3.2 Effect of geometrical shape of draft tube bubble columns on k_{La}

The effect of geometrical shape of column on volumetric mass transfer coefficients was investigated by conducting experiments at varying superficial gas velocities in rectangular and cylindrical draft tube bubble columns having identical cross sectional area of draft tubes $\sim 8 \text{ cm}^2$ and draft tube height of 70 cm (RDTBC and CDTBC-1). In both cases gas was introduced through a sparger having $N_h = 4$, $d_h = 1$ mm.

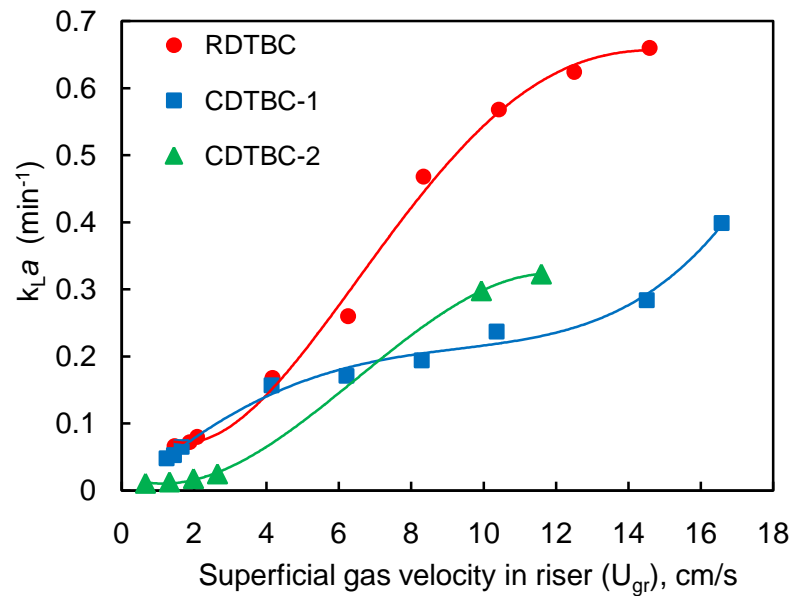


Fig. 4.30 Effect of geometrical shape of draft tube bubble columns on $k_L a$
(DT height = 70 cm)

Fig. 4.30 shows the increase of volumetric mass transfer coefficient with U_{gr} for cylindrical and rectangular shapes of the column. The profiles are distinctly different they appear like mirror images. At low values of superficial velocity (U_{gr}) the increase of $k_L a$ with U_{gr} is linear thereafter the $k_L a$ values in the RDTBC are concave downwards while in CDTBC-1 under similar conditions $k_L a$ values are concave upwards.

The interfacial area in CDTBC-1 increases more rapidly than RDTBC under identical conditions therefore it seems that the k_L component is responsible for this difference in profiles. *But why should k_L decrease with increasing U_{gr} ?* To reconfirm the results runs were repeated at a number of flow rates in both RDTBC and CDTBC-1 the results obtained were nearly similar. Incidentally the annulus area in RDTBC (27 cm^2) was greater than that of CDTBC-1 (20.8 cm^2), hence dramatic decline in k_L due to damping of turbulence in the annular region was a remote possibility.

A deeper analysis reveals that the problem is more complex than what it appears to be at the surface. It is very likely a measurement problem. The specific interfacial area ' a ' was evaluated by the chemical method and contributes to a global value for the whole column and not for any specified location while $k_L a$ was measured in the annulus at the centre of the column. The annulus as it is relatively unaerated region compared to draft tube. *Will the data obtained at a specific location by a physical method operating over a narrow range of measurement be representative for the entire device?* The gassing in technique for $k_L a$ determination was adopted by a number of investigators in DTBC, however there

is little scope to validate the results and establish its efficacy. There is enough scope for future work in this area of measurements.

With the larger draft tube column CDTBC-2, the type of profile obtained is as shown in the Fig.4.30, in this case the draft tube cross sectional area as well as the annular space was significantly larger than the other two devices, therefore $k_L a$ begins at extremely low values but then picks up at higher values of U_{gr} . However, the $k_L a$ profile obtained shows tendency of saturation at $U_{gr} = 12$ cm/s and its progress with U_{gr} is consistently lower than the RDTBC but becomes equivalent and exceeds the CDTBC-1 above 7 cm/s.

4.3.3 Effect of draft tube height on $k_L a$

The draft tube height significantly affected the holdup as well as interfacial areas. Shorter draft tubes led to greater extent of bubble coalescence in Region 2 above the draft tube and as a consequence reduced both ε_g and a . It was anticipated that on the same lines $k_L a$ also would get affected by change of draft tube height. To quantify this effect the rectangular draft tube bubble column that provided the most representative $k_L a$ measurements as shown in the previous section was used with the four holed sparger C and measurements were taken using two draft tubes of 60 cm and 70 cm height under otherwise identical conditions.

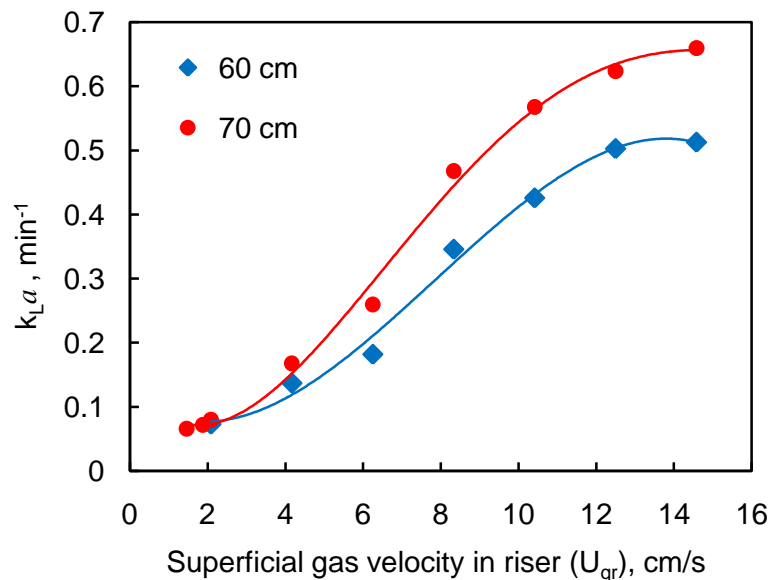


Fig. 4.31 Effect of draft tube height on $k_L a$ for RDTBC

There was not much of difference in the values of $k_L a$ obtained for the two draft tubes up to $U_{gr} = 2$ cm/s, but with an increase in U_{gr} the values of $k_L a$ obtained for the 70 cm draft tube progressively exceeded the values of $k_L a$ for the 60 cm draft tube under otherwise identical conditions as shown in Fig. 4.31. Above U_{gr} values of 13 cm/s the $k_L a$ plots for

the both the draft tubes flattens out indicating that no further advantage is gained by increasing the U_{gr} beyond this limit.

Similarity of the $k_L a$ profile pattern in both these cases in a way establishes the efficacy of the measurements in the RDTBC. It is worthwhile to note that the sampling point for fitting the DO probe used for $k_L a$ measurement was placed along the width of the column and the flow rate of the circulating fluid in this region is expected to be quite rapid leading to well mixed conditions.

The decline in $k_L a$ values with decline in the height of the draft tube is primarily attributed to the decline in a at identical flow conditions as seen in Fig. 4.23. Almost 10-15 % decline in ' a ' values are observed when 60 cm draft tube replaces the 70 cm draft tube under otherwise similar conditions. In the $k_L a$ measurements the decline is of the order of 20% and more at higher velocities when the shorter draft tube is used. It suggests that this decline in $k_L a$ results also from a decline in k_L , which could be caused by the chaotic backmixing taking place in the free space above the draft tube.

4.3.4 Prediction of $k_L a$ in draft tube bubble columns

A number of correlations have been developed over a period of time to predict the volumetric mass transfer coefficient in draft tube bubble columns as listed in Table 2.4. The correlations developed by Chisti et al. (1987) and Popovic and Robinson (1984) listed below are the most generalized ones depending only on superficial gas velocity and geometric parameters without involving any other parameters like liquid circulation rate etc. that are difficult to determine with precision.

Popovic and Robinson:

$$k_L a = 1.911 \times 10^{-4} U_{gr}^{0.525} \left[1 + \frac{A_d}{A_r} \right]^{-0.853} \mu_{ap}^{-0.89}$$

Chisti et al.:

$$k_L a = (0.349 - 0.102 C_s) U_{gr}^{0.837} \left[1 + \frac{A_d}{A_r} \right]^{-1}$$

Where, C_s i.e. Concentrations of solids were taken as zero and μ_{ap} i.e. apparent viscosity of liquid (water). In these equations, A_d and A_r are downcomer and riser cross-sectional areas respectively.

Efficacy of the above mentioned correlation as well as the correlation by Li et al. was checked with reference to the experimental data obtained in this investigation.

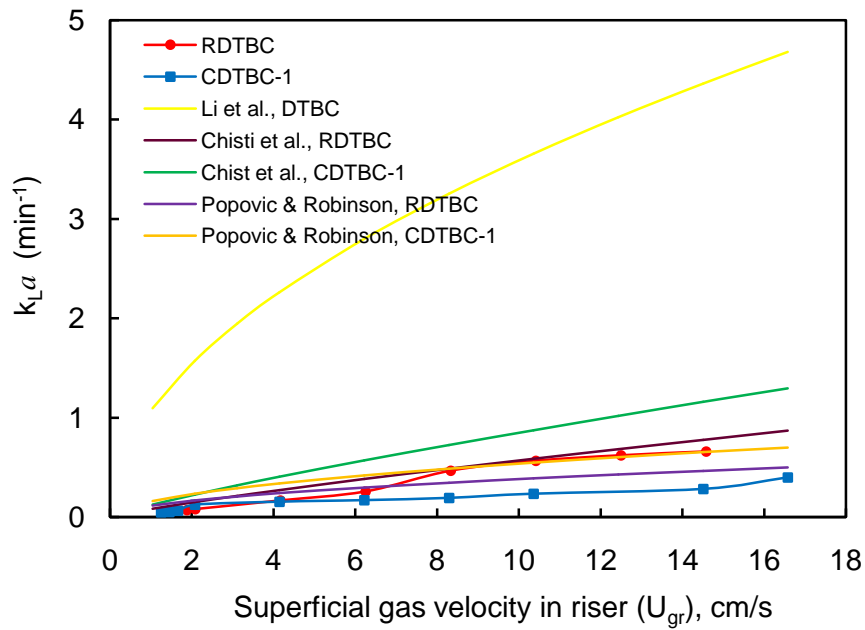


Fig. 4.32 Prediction of $k_L a$ in RDTBC and CDTBC-1

Fig. 4.32 depicts the extent of agreement observed between the experimental and the predicted values of $k_L a$. It is seen that there is no agreement between the experimental data and the correlation by Li et al. (1995)

$$k_L a = 0.0343 U_{gr}^{0.524} \mu_{ap}^{-0.255}$$

This pattern was expected because correlation by Li et al. did not involve geometric parameters.

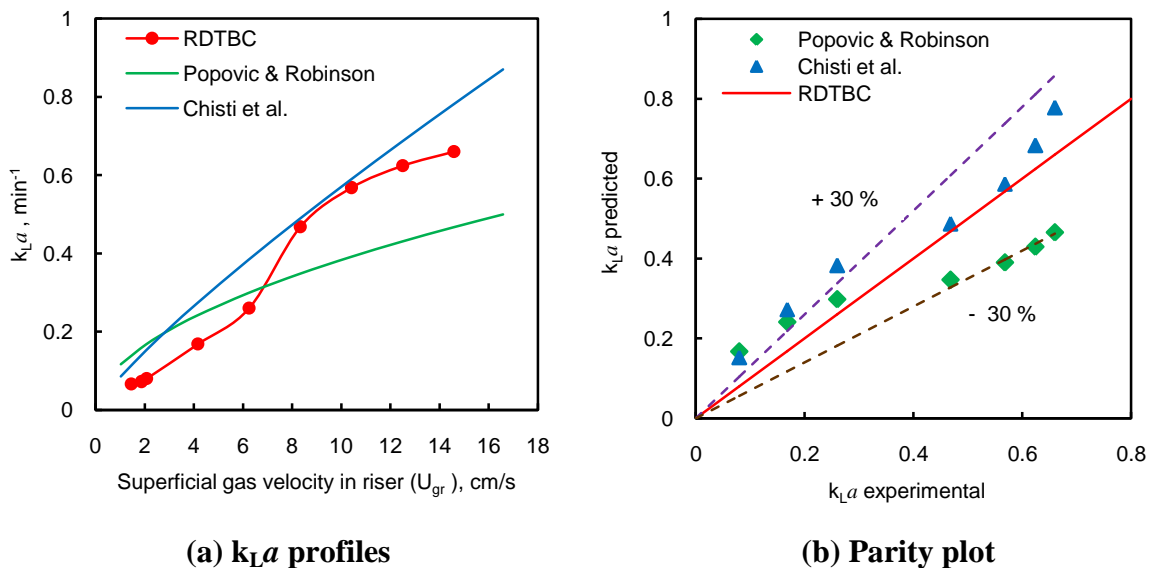


Fig. 4.33 Comparison of predicted and experimental $k_L a$ of RDTBC

(DT height = 70 cm; Sparger C, $A_d = 34.8 \text{ cm}^2$ and $A_r = 8 \text{ cm}^2$)

The $k_L a$ profiles observed for RDTBC and the predicted profiles by correlations of Chisti et al. and Popovic and Robinson are shown in Fig. 4.33(a), the parity plot is shown in Fig. 4.33(b). It is observed that the $k_L a$ data obtained over the entire range of superficial velocities is predicted by these correlations with an accuracy of $\pm 30\%$, at low superficial velocities the $k_L a$ values are predicted with greater degree of error by both correlations. The Popovic and Robinson correlation initially over predicts the $k_L a$ values and at higher U_{gr} values tends to under predict with errors of 30%, while the Chisti correlation consistently over predicts the $k_L a$ values but at higher values of U_{gr} it predicts more closely with most of the data being predicted with an accuracy of 15%. Although both these correlations were developed for flow in external loop systems they turn out to be good correlations also for internal loop draft tube columns. The absolute errors obtained with Chisti correlation turn out to be 33.6% while with Popovic and Robinson correlation the absolute error turns out to be 40.8%.

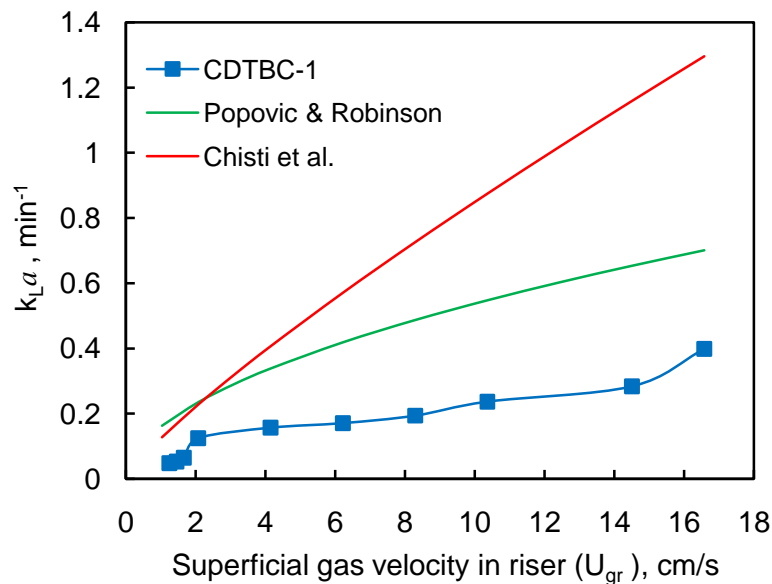


Fig. 4.34 Comparison of predicted and experimental $k_L a$ profiles of CDTBC-1

(DT height = 70 cm; Sparger with $N_h = 4$, $A_d = 20.83 \text{ cm}^2$ and $A_r = 8.042 \text{ cm}^2$)

The experimental values of $k_L a$ obtained for CDTBC-1 were considerably lower than the values obtained in RDTBC, necessarily the correlations over predicted the $k_L a$ values for the CDTBC-1 as is apparent from Fig. 4.34. The percentage absolute error by Popovic and Robinson correlation was 126.8 % while with Chisti et al., it was 221 %. These results indicate that the CDTBC-1 returned lower values of $k_L a$ during experiments, hence poor predictions by the correlations. The plausible cause for this behavior is already discussed earlier. However, there is still sufficient scope to develop new predictive correlations for $k_L a$.

4.3.5 True mass transfer coefficient, k_L in RDTBC

The true liquid side mass transfer coefficient is a parameter of significant importance in gas-liquid systems and devices. Experimental determination of k_L is a difficult task and often investigators have to resort to techniques developed by Danckwerts and coworkers (Danckwerts et al., 1963; Danckwerts and Sharma, 1966) to get an estimate of k_L . Although in physical absorption systems k_L is not a design parameter (while $k_L a$ is) but in reactive systems k_L and 'a' are independently required for design of contactors. Never the less k_L data if available yields deep insight on the mass transfer behavior of the system.

In this investigation both the parameters 'a' and $k_L a$ were determined under identical conditions in various devices, particularly the rectangular draft tube bubble column yielded $k_L a$ values that were representative of the total column dynamics at specified values of U_{gr} , thus comparing Fig. 4.23 and Fig. 4.31, it was realized that data for k_L could be generated by dividing the experimentally obtained values of $k_L a$ by the experimental values of the interfacial area 'a' at specific U_{gr} values. Hence, an estimate of the true liquid side mass transfer coefficients was obtained for RDTBC with both the draft tubes of 60 cm and 70 cm height and is presented in Table 4.3.

Table 4.3 Calculation of k_L for RDTBC

U_{gr} (cm/s)	$k_L a$ (min^{-1})		a (cm^{-1})		k_L (cm/min)	
	60 cm DT	70 cm DT	60 cm DT	70 cm DT	60 cm DT	70 cm DT
2	-	0.065	0.39	0.45	-	0.144
4	0.115	0.155	0.53	0.61	0.217	0.254
6	0.21	0.29	0.58	0.69	0.362	0.42
8	0.31	0.41	0.63	0.77	0.492	0.532
10	0.4	0.53	0.65	0.82	0.615	0.646

It is appropriate to mention that $k_L a$ data was obtained with air-water system while 'a' data was obtained by sulfite oxidation technique. The difference in the viscosity and surface tensions between water and sodium sulfite solution (0.5 M) was marginal hence these effects were neglected. The k_L values thus obtained for RDTBC were plotted versus U_{gr} for the 60 cm as well as 70 cm long draft tubes and are presented in Fig. 4.35.

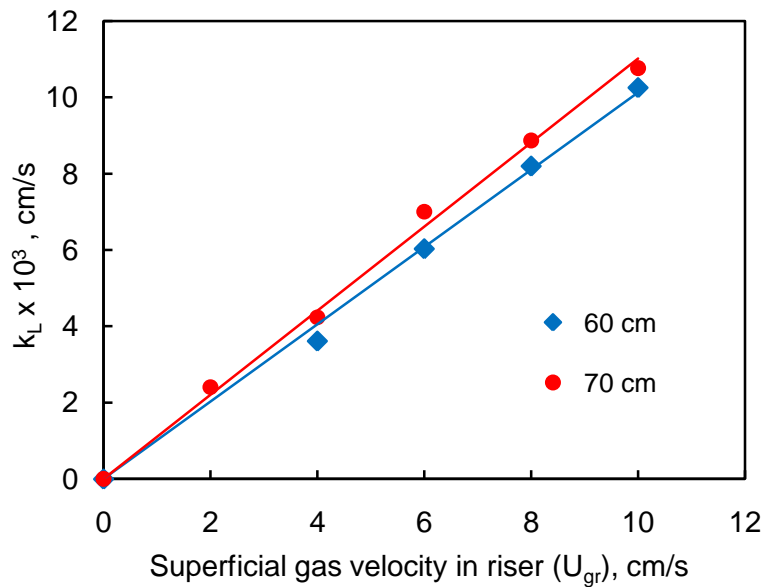


Fig. 4.35 Effect of draft tube heights on k_L at varying U_{gr} for RDTBC

The high degree of linearity of k_L with U_{gr} in a way validates the veracity of data over the entire device. The effect of draft tube height on k_L cannot be overlooked, the k_L values obtained for the 70 cm draft tubes are more than that obtained for 60 cm draft tubes under otherwise identical conditions implying that the degree of turbulence is more in case of 70 cm draft tube.

The gas flow through the draft tube primarily induces a liquid circulation pattern between the draft tube and the annulus caused by the density difference between the gas-liquid dispersion in the draft tube and the clear liquid in the annulus it is this liquid flow that contributes to k_L . In a shorter draft tube the momentum gained by the liquid because of rising bubbles gets considerably dissipated in the region above the draft tube where the fluids expand thereby failing to establish the liquid circulation pattern as vigorously as in a longer draft tube thereby causing a decline in k_L .

The dependencies of k_L on U_{gr} turns out to be $k_L = 1.102 \times 10^{-3} U_{gr}$ for 70 cm draft tube while $k_L = 1.013 \times 10^{-3} U_{gr}$ for 60 cm draft tube which shows greater dependency of k_L on U_{gr} for 70 cm draft tube than 60 cm draft tube in RDTBC.

4.4 CONCLUSIONS

The objective of this work was to study the hydrodynamic and mass transfer characteristic of draft tube bubble column and to establish the efficacy of rectangular draft tube bubble columns with reference to its hydrodynamic and mass transfer

behavior. Macro scale investigations yielded results and provided insight not only on the behavior of these devices but also on their plausible field applications. The conclusions drawn from this investigation are summarized as follows:

- The gas holdups in draft tube columns were studied in the range of U_{gr} from 0 to 17 cm/s and ε_g ranged from 0 to 10% in general ε_g was higher than bubble columns at corresponding superficial gas velocities. Sparger arrangement and design did not appear to affect the gas holdup prominently. The number of holes in the sparger, number of rows of holes and pitch of holes did not much effect the gas holdup, however, the size of holes appear to affect the gas holdup. In such situations a sparger that provides stable gas flow in the column should be used thus a four hole sparger was selected that gave stable flow pattern.
- The initial rise of gas holdup is rapid in homogeneous regime at low gas flow rates in DTBC, while at higher gas flow rates in heterogeneous regime a more gradual increase of gas holdup is observed, because bubble coalescence increased with increasing bubble population in the liquid that consequently led to the formation of larger bubbles which travel upwards with higher velocity resulting in a decrease in the rate at which total gas holdup increases with gas flow rate. Hence, the pattern of variation of interfacial area as well as volumetric mass transfer coefficient with superficial gas velocities was same as that of gas holdup.
- An attempt was also made in this investigation to explain and quantify the effect of draft tube height on ε_g , a , $k_L a$ and k_L for RDTBC.
 - The decrease in ε_g with decrease in draft tube height is attributed to the larger clearance between top of draft tube and dispersed liquid height and a corresponding decline of the residence time in the riser. Increase in this upper clearance increases the coalescence of bubbles leading to formation of large size bubbles that escape quickly from the system.
 - On the same lines, it was found that the longer draft tube yielded greater interfacial areas in comparison with the shorter draft tube under otherwise identical conditions.

- $k_L a$ and k_L was also found to increase with an increase in draft tube reflecting the trend observed in interfacial area.
- At low gas flow rates, the hydrodynamic and mass transfer characteristics obtained in rectangular draft tube bubble column (RDTBC) is superior to that of rectangular bubble columns. The liquid circulation pattern between draft tube and annulus is initiated, developed and governed by flow of gas phase through the draft tube it creates a stable flow pattern in comparison with ordinary bubble column. The crowding of gas bubbles in the space between the draft tube and dispersed liquid level occurs because quick disengagement does not take place in the column, it enhances the gas holdup in draft tube bubble columns without significantly affecting other parameters.
- Higher specific interfacial areas in draft tube bubble columns at low gas rates is attributed to the plug flow behaviour of gas phase through draft tube even at low gas flow rates compared to ordinary bubble columns where the flow patterns is quite chaotic. But at higher gas flow rates the interfacial areas of bubble columns supersedes that of draft tube bubble columns. Hence, it is advisable to operate draft tube bubble columns at low gas flow rates while bubble columns at higher gas flow rates to acquire benefits of their hydrodynamic and mass transfer features.
- No significant effect of geometric shape of column whether rectangular or cylindrical was observed on gas holdup in draft tube bubble columns. However, the interfacial area obtained in cylindrical draft tube bubble columns was significantly higher than rectangular one particularly at higher flow rates. Again the volumetric mass transfer coefficients obtained in rectangular shaped DTBC were higher than that of cylindrical geometries, this behavior was attributed to the rapid circulation of fluid in rectangular draft tube bubble column which made the $k_L a$ measurement more representative of the whole column dynamics.
- Increasing the size and operational scale of draft tube bubble column led to substantial increase in gas holdup particularly at higher velocities but this trend was not reflected in both interfacial area and volumetric mass transfer coefficient reinforcing the idea that all of gas holdup in columns do not contribute effectively

to ' a ' as well as $k_L a$ but more robust investigation is required before any definitive conclusion is arrived at.

- It was observed that generalized correlations usually did not give very good fit to the experimental data obtained in this work. Holdup could be best predicted with an absolute error of 37.3% by Popovic and Robinson correlation while $k_L a$ was best predicted by Chisti correlation with an absolute error of 33.6%. Thus, there is ample scope to develop meaningful correlations for DTBC to predict the design parameters.

CHAPTER 5

WASTEWATER TREATMENT

IN DRAFT TUBE

BUBBLE COLUMNS

5.1 INTRODUCTION

Nutrient removal has become a research focus in wastewater treatment with the occurrence of severe eutrophication problems, especially in closed water environment such as bays, lakes and ponds. The removal of nutrients like nitrogen and phosphorus compounds is essential to depress the eutrophication. Nitrogen removal has been achieved by biological methods, ion exchange, reverse osmosis and chemical methods. Among the variety of treatment systems proposed so far, the biological method is considered the most promising from an economical viewpoint. Biological nitrogen removal from organic wastewater using activated sludge consists of two stages, namely, the aerobic stage (ammonification and nitrification) and the anaerobic stage (denitrification). It is also known that uptake of phosphorus in microorganisms named PAO- Phosphate Accumulating Organisms, gets enhanced when the activated sludge is placed under an aerobic condition after the anaerobic one.

Conventional treatment systems for nutrient removal thus requires separate aerobic and anaerobic tanks leading to requirement of large area for installation of these treatment systems and it often leads to additional need for facilities such as energy and maintenance. The establishment of such facilitated treatment process is quite difficult in crowded downtown areas and neither is the network of sewer pipes fully equipped in developing areas or depopulated areas to transport the sewage to central facility. Therefore, there exists a need to develop compact, economical and efficient apparatus where aerobic and anaerobic conditions coexist in a single vessel for onsite continuous treatment of wastewater. This requirement can be fulfilled by using a draft tube bubble column. The draft tube bubble column provides both aerated and unaerated compartments in the same vessel which serve for the aerobic and anaerobic processes. The operation of draft tube bubble column requires relatively low energy input when compared stirred tank, since there is no need for mechanical circulating devices, which makes the system attractive as an alternative treatment process.

In the present study, the performance of rectangular bubble column and rectangular draft tube bubble column (RDTBC) were evaluated for ammoniacal nitrogen ($\text{NH}_3\text{-N}$) and phosphorus ($\text{PO}_4^{3-}\text{-P}$) removal from sewage wastewater using activated sludge method. Investigations were carried out to study the influence of air flow rates, draft tube height, shape of draft tube and main column as well as the scale of operations on nutrient removal from sewage water using activated sludge process. Experiments were also

performed using synthetic wastewaters having identical nutrient concentration as that of sewage water to test the efficacy and pattern of nutrients removal from streams having lesser degree of complexity using draft tube bubble columns

5.2 LITERATURE SURVEY

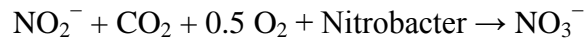
5.2.1 The necessity of nutrient removal from wastewater

Wastewater from rural areas contain high level of nitrogen and phosphorus because of excessive use of fertilizers, while in urban areas these nutrient levels are high due to domestic and industrial wastes. The buildup of these nutrients in environment is called eutrophication. Thus, the grey water discharged to rivers and lakes without treatment has caused a serious problem of eutrophication, which in turn encourage the overgrowth of various types of algae. This causes a rapid growth in the population of algae. The algae numbers are unsustainable and eventually die. The decomposition of the algae by bacteria uses up so much oxygen from the water that most of the marine life forms die this creates more organic matter for the bacteria to decompose. In addition to causing deoxygenation, some algae species produce toxins that contaminate drinking water supplies. Hence, to avoid these ill effects and for environmental sustainability different treatment processes are inevitably required to remove nitrogen and phosphorus from wastewater. The biological method for removal of these nutrient pollutants from organic wastewater has received wide attention in literature.

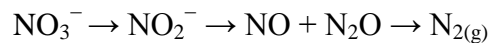
5.2.2 Mechanisms of removal of nitrogen and phosphorus from wastewater using activated sludge

Biological nitrogen removal from organic wastewater using activated sludge occurs in two stages, namely, aerobic stage wherein the steps of ammonification and nitrification occurs, and the other stage is anaerobic one where denitrification is carried out. Organic nitrogen is transferred to ammonia (NH_3) at the stage of ammonification, while in the nitrification step, biological oxidation of ammonia with oxygen into nitrite (NO_2^-) occurs in the presence of organisms such as *nitrosomonas* and *nitrosococcus*, followed by the oxidation of these nitrites into nitrates (NO_3^-) facilitated by bacteria of the genus *nitrobacter*. Nitrate and nitrite is finally converted to nitrogen gas (N_2) by the denitrifying bacteria such as *Paracoccus denitrificans*, *Pseudomonas denitrificans*, *Thiobacillus denitrificans*, etc... under the anaerobic condition.

The nitrifying organisms use carbon dioxide as their carbon source for growth. Thus, together with ammonification, nitrification forms a mineralization process which leads to the complete decomposition of organic material, with the release of available nitrogen compounds in waste water. Thus, nitrification is a process of nitrogen compound oxidation or effectively, loss of electrons from the nitrogen atom to the oxygen atoms and the chemistry of the process can be written as



Denitrification is a microbially facilitated process of nitrate reduction that may ultimately produce molecular nitrogen (N_2) through a series of intermediate gaseous nitrogen oxide products. This process reduces oxidized forms of nitrogen in response to the oxidation of an electron donor such as organic matter and use nitrate as the electron acceptor. The preferred nitrogen electron acceptors in order of most to least thermodynamically favourable include: nitrate (NO_3^-), nitrite (NO_2^-), nitric oxide (NO), and nitrous oxide (N_2O). Generally several species of bacteria as mentioned earlier are involved in the complete reduction of nitrate to molecular nitrogen. Thus, denitrification occurs under special conditions where oxygen, a more energetically favourable electron acceptor, is depleted, and bacteria respire nitrate as a substitute terminal electron acceptor, i.e. denitrification only takes place in anaerobic environments where oxygen consumption exceeds the rate of oxygen supply. Thus, denitrification generally proceeds through some combination of the following intermediate forms:



The complete denitrification process can be expressed as a redox reaction:



Carlson et al. (1997) have reported high removal of phosphorus from wastewater in the anaerobic – aerobic operation using activated sludge process. Under these conditions, a group of bacteria called polyphosphate accumulating organisms (PAO) are selectively enriched in the bacterial community within the activated sludge, these bacteria

accumulate large quantities of polyphosphate within their cells and the removal of phosphorus from wastewater is enhanced over the conventional activated sludge systems. Generally speaking, all bacteria contain a fraction (1-2%) of phosphorus in their biomass due to its presence in cellular components, therefore as bacteria in a wastewater treatment plant consume nutrients in the wastewater, they grow and phosphorus is incorporated into the bacterial biomass. When PAOs grow they not only consume phosphorus for cellular components but also accumulate large quantities of polyphosphate within their cells. Thus, the phosphorus fraction of phosphorus accumulating biomass is 5-7%. Separation of biomass from treated water at the end of the process removes the phosphorus. Thus, if PAOs are selectively enriched by the presence of an anaerobic zone prior to the aerobic region, then considerably more phosphorus is removed, compared to the relatively poor phosphorus removal in conventional activated sludge systems.

It has been reported by Barnard (1973) and Argaman & Brener (1986) that an additional anaerobic operation in addition to the aerobic one was effective for the enhancement of nitrogen removal from wastewater using the activated sludge process. The use of draft tube bubble column for wastewater treatment was pioneered by Hano et al. (1992) they removed nitrogen using the activated sludge method. The draft tube functioned as an aerobic region and the annulus as an anaerobic zone to enhance the nitrogen removal. Later Bando et al. (1999) used draft tube bubble columns, for the removal of nitrogen and phosphorus in wastewater treatment using activated sludge and noted the enhancement of removal in draft tube bubble columns over the ordinary bubble columns. These investigators also studied the effect of geometry and examined the contribution of anaerobic region volume on the nutrient removal and found that maximum removal of nitrogen and phosphorus occurs when the volume fraction of anaerobic region was 40-60%.

Yoo et al. (1999) developed an intermittently aerated and decanted single-reactor process for wastewater treatment and proposed key control parameters for nitrogen removal from two types of synthetic wastewater by simultaneous nitrification and denitrification (SND) via nitrite. In this work under optimal conditions nitrogen removal efficiency was found above 90%. for both types of wastewater In this process, nitrification (1st step of nitrification) was induced but nitratation (2nd step of nitrification) was effectively suppressed and denitrification was carried out using nitrite.

Meng et al. (2004 a) used rectangular airlift bubble column for wastewater treatment in a continuous mode, a partition plate segregated the column into anaerobic and aerobic regions. They investigated the effect of equipment size and operational conditions on gas holdup, liquid phase volumetric mass transfer coefficient, and liquid circulation flow rate on the biological nitrogen removal. They observed that removal of total nitrogen was maximized when the volume fraction of anaerobic region was about 0.5. In a subsequent work these investigators (Meng et al. 2004 b) used cellulose particles as immobilizing carrier in the airlift bubble column and observed that the volume fraction of the anaerobic region and the concentration of the immobilizing particles strongly affected the nitrogen removal from waste water.

Further, Meng et al. (2004 c) devised a unique method for retaining the microorganisms in the bubble column by installing polypropylene ring lace as a support system for the microorganisms to grow. The aim of using these support material was to immobilize nitrifying and denitrifying bacteria in the aerobic and anaerobic regions respectively and prevent them from washing out with effluent from the column. They reported considerable enhancement of nitrogen removal in this apparatus in comparison to conventional airlift bubble columns.

A packed bed external loop airlift bioreactor was proposed for the removal nitrogen compounds from wastewater by Silapakul et al. (2005). Their column consisted of aeration and non-aeration zones, both of which were packed with plastic bioballs to enhance the surface area for the attachment of bacteria and to achieve complete removal of all nitrogen compounds with simultaneous nitrification and denitrification.

The literature survey presented above as well as in Chapter 2 reveals that although draft tube bubble columns have been investigated for their hydrodynamic and mass transfer behavior but their application for wastewater treatment is only sparingly investigated. Further, it was observed that while some information on nitrogen removal was available but information on biological phosphorous removal using activated sludge process in draft tube bubble columns was very scarce. It was also noted that most of the investigations involved the use of synthetic wastewater rather than sewage wastewater for nutrient removal experiments.

In order to establish the efficacy of draft tube bubble columns for removal of nitrogen and phosphorus from waste waters using the activated sludge process and address some of the issues discussed above, draft tube bubble columns were used for water purification

in the semi-batch mode (air continuous). Effect of geometrical shape of draft tube bubble column, height of draft tube, scale of operations, and effect of process parameters on nutrient removal were investigated. This experimental investigation therefore, focuses primarily on these uncultivated areas of wastewater treatment for nitrogen and phosphorus removal using activated sludge.

5.3 MATERIALS AND METHODS

5.3.1 Sewage water and its composition

Sewage water for the experiments was obtained from downstream of Athamiya River, beneath an over bridge on Kalawad road, near village Motamava, Rajkot, Gujarat as shown in Fig.5.1 and Fig. 5.2. This sewage water contains adequate amount of nutrients such as nitrogen and phosphorus since village Motamava and some small scale industrial units are located on the upstream side of the river. This sewage water was filtered to remove large suspended physical impurities before adding to the column for treatment. Typical analytical composition of this sewage water is given in Table 5.1.

Table 5.1 Analytical composition of sewage wastewater

Parameter	Concentration (mg/L)
BOD (Biological Oxygen Demand)	225
COD (Chemical Oxygen Demand)	450
SS (Suspended Solids)	250
Ammoniacal Nitrogen	49.7
Phosphorus	4.56
Sulphates	110
Alkalinity	85
Chlorides	200

5.3.2 Activated sludge and its preparation

Activated sludge having very high concentration of microorganisms responsible for activities of both nitrification and denitrification was obtained from the sewage water treatment plant, RMC (Rajkot Municipal Corporation), Madhapar near Rajkot. This dry activated sludge was procured from sludge bed/lagoon area of plant situated after tertiary treatment process of wastewater.

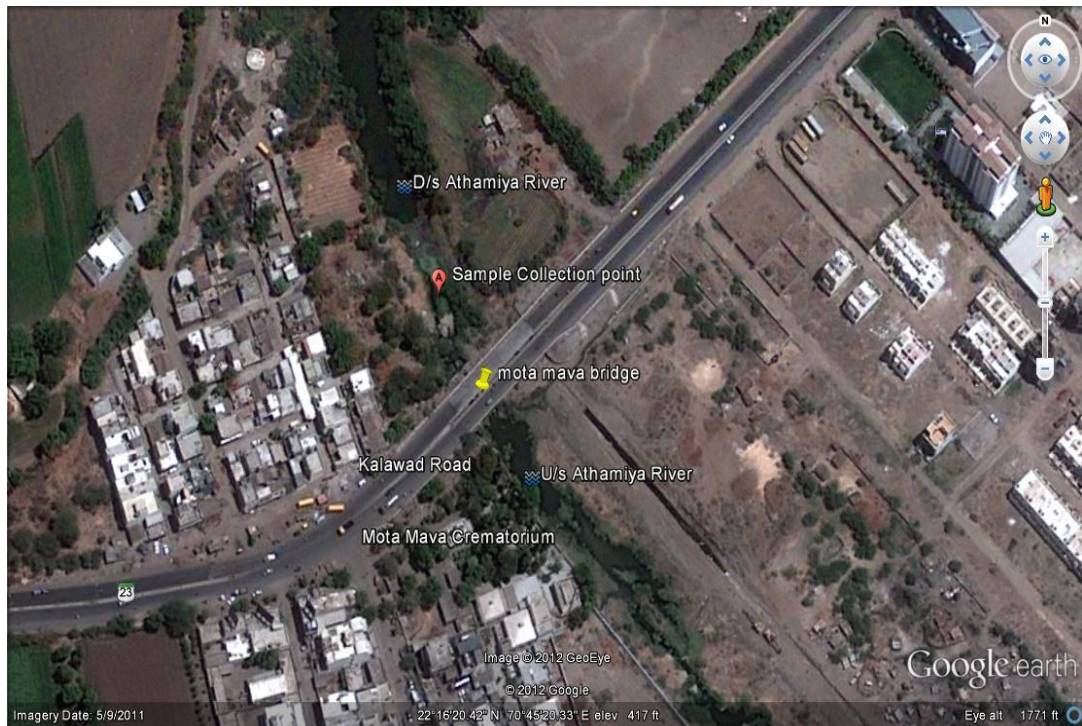


Fig. 5.1 Sample collection point of sewage water in downstream of Athamiya river
(courtesy from Google earth)



Fig. 5.2 Location of sewage water sample collection

Dry sludge was crushed to small size by pestle and mortar in laboratory and then screened to remove physical impurities. The required amount of activated sludge for various experiments was then acclimated over a month in feed sewage water by adding appropriate amount of sewage water in it to maintain its semi-solid form.

5.3.3 Chemicals and glassware

The chemicals used for all the wastewater experiments to measure ammoniacal nitrogen concentrations by manual phenate method, such as phenol (purity $\geq 89\%$), methyl alcohol ($\geq 99\%$), sodium nitroprusside (99%), trisodium citrate (99-100%), sodium hydroxide (98%, dry basis), sodium hypochlorite solution (4% w/v), and ammonium sulfate (98%) were of analytical reagent grade quality and procured from Merck India Pvt. Ltd.

Similarly, the chemicals used in another colorimetric ascorbic acid method for estimation of phosphorus, such as concentrated H_2SO_4 (98%), potassium antimonyl tartrate, $\text{K}(\text{SbO})\text{C}_4\text{H}_4\text{O}_6 \cdot \frac{1}{2}\text{H}_2\text{O}$ (purity $\geq 99\%$), ammonium molybdate, $(\text{NH}_4)_6\text{Mo}_7\text{O}_{24} \cdot 4\text{H}_2\text{O}$ (98%), ascorbic acid (99%), potassium dihydrogen phosphate, KH_2PO_4 (98%), phenolphthalein indicator solution (1%), and HCl ($\geq 35\%$) diluted for washing etc. were also of analytical grade and procured from Merck India Pvt. Ltd. Deionized water was used for preparing the solutions.

Synthetic wastewater using tap water was prepared using chemicals such as glucose, polypeptone, ammonium chloride, potassium dihydrogen phosphate (98%), and sodium bicarbonate (99.7%) etc. were also of analytical grade and also procured from Merck India Pvt. Ltd. Glassware used for the experiments such as measuring cylinders, beakers, volumetric flasks, amber bottles, pipettes, stirring rods, glass-stoppered bottles etc. were procured from Borosil Pvt. Ltd.

5.3.4 Synthetic wastewater and its composition

The synthetic wastewater for experiments was prepared in a fashion that the initial concentration of ammoniacal nitrogen (49.7 mg/L) and phosphorus (4.56 mg/L) was identical to that of the sewage water. It composed of glucose as a main carbon source, polypeptone and ammonium chloride (NH_4Cl) as nitrogen sources, Potassium dihydrogen phosphate (KH_2PO_4) as a phosphorus source along with some inorganic nutrients added in the tap water. Composition of the synthetic wastewater is given in Table 5.2.

Table 5.2 Composition of synthetic wastewater

Component	Concentration (mg/L)
Polypeptone	160
KH ₂ PO ₄	20
Glucose	350
NH ₄ Cl	190
NaHCO ₃	100

(Ammoniacal nitrogen = 49.7 mg/L; Phosphorus = 4.56 mg/L)

5.3.5 Operational methodology

Wastewater experiments were carried out in draft tube bubble columns and bubble columns as well. Effect of presence of draft tube, draft tube height, shape of column, column capacity and air flow rates on nitrogen and phosphorous removal was investigated. All the experiments performed at ambient temperature and pressure, the initial concentration of ammoniacal nitrogen, phosphorus, and activated sludge was maintained 49.7 mg/L, 4.56 mg/L and 3.33 kg/m³ respectively in the experiments. Total duration of experiments was about 7 hrs.

Water samples from the column was collected every hour after start-up of experiment and centrifuged (Biolab, 120 D) at 5000 rpm for 10 minute duration and then analyzed for nutrients. The manual Phenate method 4500-NH₃ F, APHA (1998) was used to determine the concentration of ammoniacal nitrogen and the Ascorbic acid method 4500-P E, APHA (1998) was used to determine the concentration of phosphates in the wastewaters. These methods are described in detail in the section 5.3.6 of analytical techniques. Since, both these methods involve colorimetric measurements; a spectrophotometer Hach, DR/2400 with 400 to 800 nm wavelength range and linear photometric range of - 2.000 to + 2.000 absorbance was used in the present investigation.

5.3.6 Analytical techniques

5.3.6.1 Ammoniacal nitrogen estimation

In wastewater the forms of nitrogen of greatest interest are, in order of decreasing oxidation state, nitrate, nitrite, ammonia, and organic nitrogen. Among these, ammonia is present naturally in surface and wastewaters. Ammoniacal nitrogen, NH₃-N concentrations in some wastewaters at concentration levels greater than 30 mg/L is quite

common. The two major factors that influence selection of the method to determine ammoniacal nitrogen are concentration and presence of interferences. Titrimetric method, ammonia selective electrode methods, phenate method and its variants are the usual methods available to determine ammoniacal nitrogen in wastewaters.

The titrimetric method is used only for samples that have been subjected to distillation step, to eliminate interferences excessively present in wastewaters. Due to this step additional requirements arise that enhance cost and time of the analysis. Other methods for ammoniacal nitrogen measurement can be used without this preliminary distillation step.

Although ammonia-selective electrode methods are applicable in the range from 0.03 to 1400 mg NH₃-N/L, these methods require a specific ion meter and ammonia selective pH electrode. The automated phenate method is applicable over the range of 0.02 to 2 mg NH₃-N/L but, these methods require sophisticated ammonia manifold analytical equipment, flow injection analysis equipments and data acquisition system.

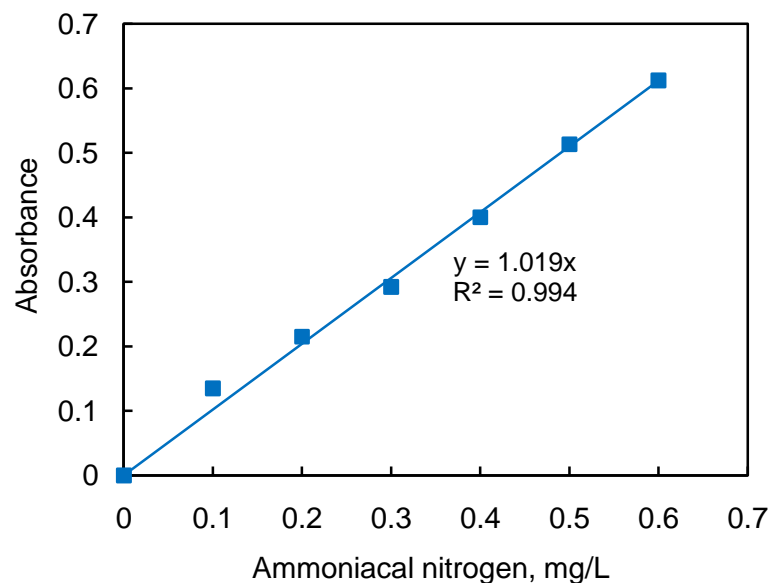


Fig. 5.3 Calibration curve of absorbance Vs ammoniacal nitrogen concentration

The colorimetric manual phenate method (Appendix-5) does not require preliminary distillation step and is applicable over 0 - 0.6 NH₃-N mg/L. This method was used in the present investigation to determine ammoniacal nitrogen in wastewaters. In the present work, it was required to dilute the sample of wastewater from column by hundred fold of the initial concentration of 50 mg/L of ammoniacal nitrogen. A standard calibration curve was generated by plotting absorbance readings of standard solutions versus known ammoniacal nitrogen concentration of standards as shown in Fig.5.3. The standard

calibration curve was used to obtain the ammoniacal nitrogen concentration of the diluted samples which were then normalized to account for the dilution.

5.3.6.2 Phosphorus estimation

Phosphorus occurs in wastewaters almost solely as phosphates. These are classified as orthophosphates, condensed phosphates (pyro-, meta-, and other polyphosphates), and organically bound phosphates. They occur in wastewaters, in particles or detritus, or in the bodies of aquatic organisms. These forms of phosphate arise from a variety of sources. Small amounts of orthophosphate or certain condensed phosphates are added to some water supplies during treatment. Larger quantities of the same compounds may be added when the water is used for laundering or other cleaning, because these materials are major constituents of many commercial cleaning preparations. Phosphates are used extensively in the treatment of boiler waters. Orthophosphates applied to agricultural or residential cultivated land as fertilizers are carried into surface waters with storm runoff. Organic phosphates are formed primarily by biological processes and they are contributed to sewage by body wastes and food residues, and also may be formed from orthophosphates in biological treatment processes or by receiving water biota.

Phosphorus analyses embody two general procedural steps: (a) conversion of the phosphorus form of interest to dissolved orthophosphate, and (b) colorimetric determination of dissolved orthophosphate. Phosphates that respond to colorimetric tests without preliminary hydrolysis or oxidative digestion of the sample is termed "reactive phosphorus" and it occurs in both dissolved and suspended forms, reactive phosphorus is largely a measure of orthophosphates present in wastewaters as phosphorus compounds. In the present investigation reactive phosphorous was determined using the direct colorimetric method without digestion treatment.

Three colorimetric methods of orthophosphate determination in wastewaters are available namely- the vanadomolybdophosphoric acid method, the stannous chloride method, and the ascorbic acid method. Selection of appropriate method among the available methods depends largely on the concentration range of orthophosphate. The vanadomolybdophosphoric acid method is most useful for routine analysis in the range of 1 to 20 mg P/ L, while the stannous chloride method and the ascorbic acid method is more suited for the range of 0.01 to 6 mg P/ L.

The ascorbic acid method as described in Appendix-6 was used to determine phosphorus concentration in wastewaters. A calibration curve of absorbance versus phosphate concentration was obtained as shown in Fig. 5.4.

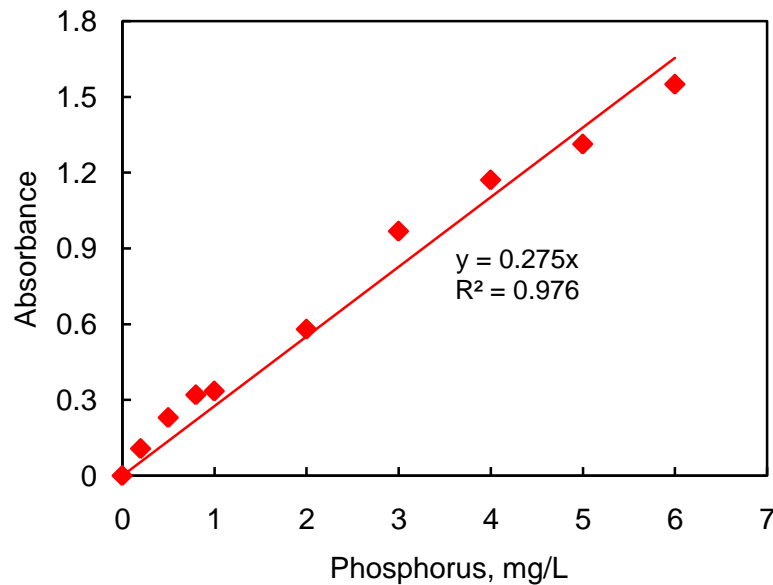


Fig. 5.4 Calibration curve of absorbance Vs phosphorus concentration

5.4 RESULTS AND DISCUSSION

5.4.1 Sewage wastewater treatment using activated sludge

Removal of nutrients - nitrogen and phosphorus from sewage wastewater using activated sludge was performed in bubble columns and draft tube bubble columns. The decline in the concentration of nitrogen and phosphorus with time was noted for total treatment duration of seven hours for all the variations studied. The performance of various column geometries on nutrient removal was compared with each other and the configuration that gave the best performance was identified.

5.4.1.1 *Effect of draft tube in a rectangular bubble column on nitrogen and phosphorus removal*

The decrease in concentration of ammoniacal nitrogen and phosphates from sewage water using activated sludge was observed in both Rectangular bubble column (RBC) as well as Rectangular draft tube bubble column (RDTBC) having column specifications detailed in Table 3.1,

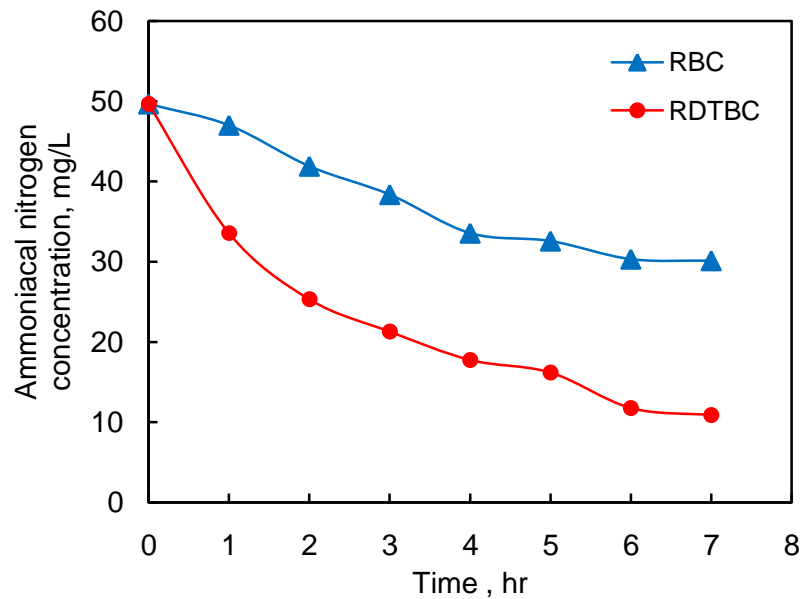


Fig. 5.5 Effect of draft tube on ammoniacal nitrogen removal in RBC

(Air flow rate = 2 LPM; DT height = 70 cm; Sparger C)

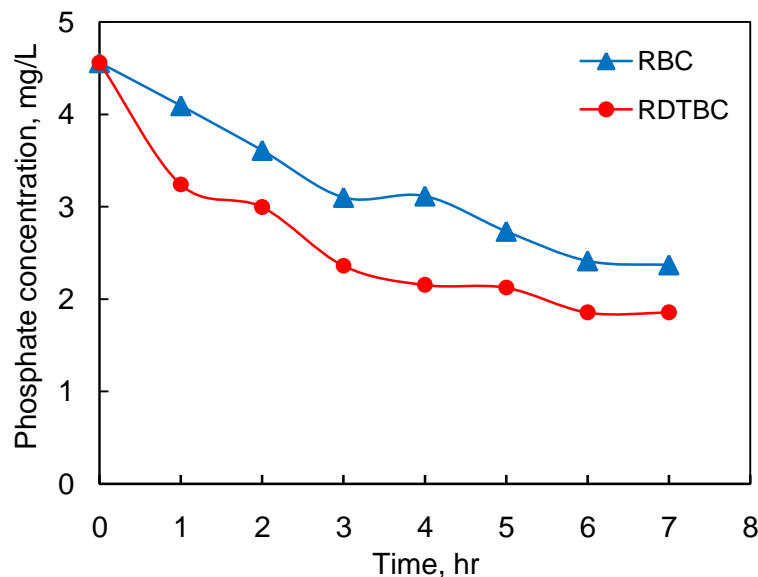


Fig. 5.6 Effect of draft tube on phosphorus removal in RBC

(Air flow rate = 2 LPM; DT height = 70 cm; Sparger C)

RDTBC was equipped with draft tube of 70 cm height. Sparger C having four holes of 1 mm diameter each and pitch of 20 mm was used in both the devices. The operating conditions were identical for both cases the initial concentration of nitrogen in sewage water was 49.7 mg/L and the air flow rate was maintained at 2 LPM, after 7 hrs of experiment the final concentration in RBC was 30.1 mg/L while that in RTDBC was 10.9 mg/L as shown in Fig.5.5, indicating a decline of ammoniacal nitrogen to the tune of 40% and 80% in RBC and RDTBC respectively. This result brings forward the singular advantage obtained by using RDTBC for nitrogen removal from wastewaters.

Similarly, starting with the same initial feed phosphorus concentration of 4.56 mg/L in RBC as well as RDTBC, the final phosphorous concentration obtained after seven hrs of aeration was 2.37 mg/L and 1.855 mg/L in RBC and RDTBC respectively, as shown in Fig.5.6. Thus the removal of phosphorus from wastewater was also more in RDTBC than in RBC throughout the run duration at identical flow rates of 2 LPM, accounting for phosphorus removal of 48 % and 60% in RBC and RDTBC respectively.

At 2 LPM air flow rate, which corresponds with U_g of 0.78 cm/s, in RBC, the gas holdup observed from Fig. 4.11 is 0.017 while in an RDTBC the gas holdup is 0.034 that is twice that of RBC. The corresponding values of specific gas-liquid interfacial area are 0.601 cm^{-1} for RDTBC ($U_{gr} = 4.167 \text{ cm/s}$) and $\sim 0.3 \text{ cm}^{-1}$ for RBC as shown in Fig. 4.22 and Fig. 4.24, which returns $k_L a$ of 0.168 min^{-1} in RDTBC. The enhanced decrease of ammoniacal nitrogen and orthophosphates from sewage water in RDTBC compared with RBC is attributed to not only superior aeration that is apparent from the parametric values of gas holdup, interfacial area and mass transfer coefficient reported above but also due to, and perhaps to a greater extent on the presence of aerobic and anaerobic regions in RDTBC through which the liquid flows sequentially on account of formation of circulatory flow patterns arising out of density difference between the draft tube and the annulus. The annulus region is largely anaerobic in nature while the draft tube through which the air is sparged operated as aerobic region. Thus the combination of both regions- aerobic and anaerobic is solely the feature of RDTBC, while in RBC only aerobic region exists. These aspects have been investigated earlier (Hano et al., 1992; Bando et al., 1999) as described in the section 5.2.2 of literature survey.

The flow rate of 2 LPM in draft tube bubble column marked the beginning of heterogeneous region; it was selected to take advantage of greater liquid circulation between draft tube and annulus and at the same time to maintain conditions such that air bubbles were not dragged into downcomer with circulating liquid, thus the entire downcomer could be considered anaerobic zone, while the whole riser functioned as aerobic region. Thus, enhanced removal of nitrogen as well as phosphorus from sewage water was achieved in RDTBC compared to RBC, since both nitrification and denitrification get facilitated in draft tube bubble columns. Hence, it is concluded that by simply inserting a draft tube in the bubble column added the anaerobic region and thus resulted in the increase of nutrient removal of draft tube bubble column compared to ordinary bubble column.

5.4.1.2 Effect of draft tube height on nutrient removal in RDTBC

The influence of draft tube height on nutrient removal efficiency of RDTBC was assessed by changing draft tube height from 70 cm to 60 cm; this resulted in increasing, Region 2 (Fig. 4.15), the liquid height above the draft tube. Runs were performed under identical conditions of initial nutrients concentration and temperature (30⁰ C) at flow rates of 2 LPM, the initial unaerated liquid height in the column was maintained at 75 cm.

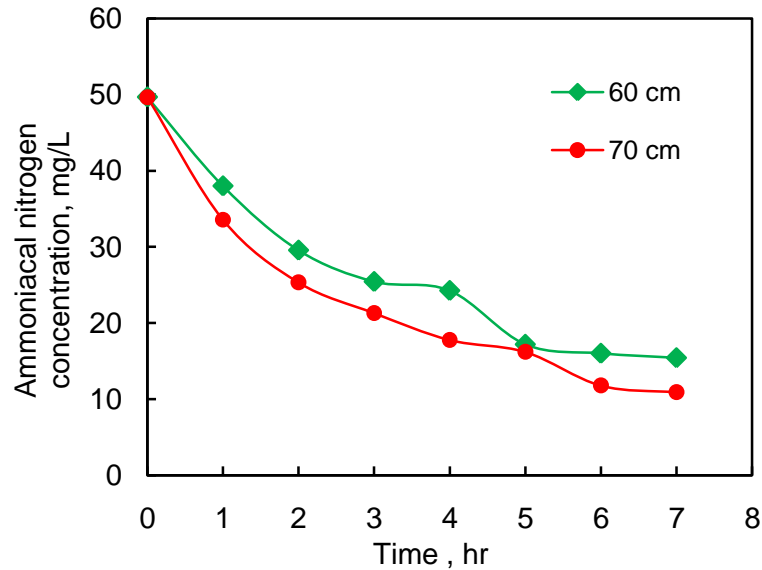


Fig. 5.7 Effect of draft tube height on ammoniacal nitrogen removal in RDTBC (Air flow rate = 2 LPM; Sparger C)

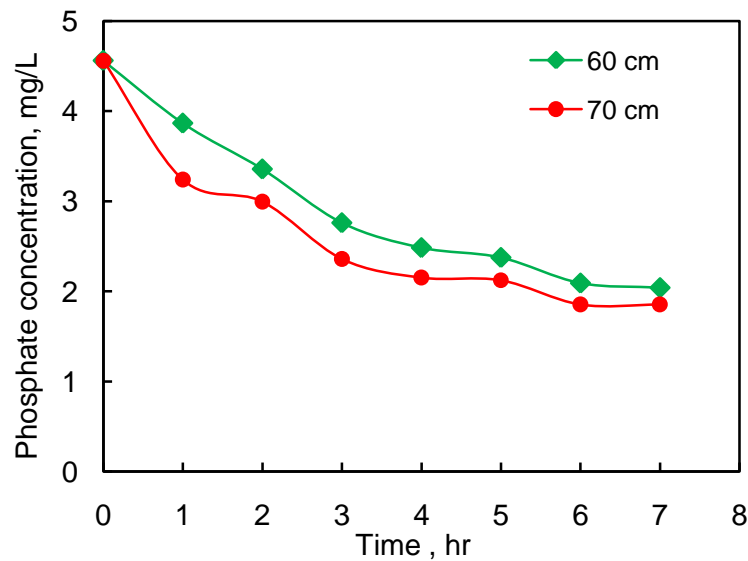


Fig. 5.8 Effect of draft tube height on phosphorus removal in RDTBC (Air flow rate = 2 LPM; Sparger C)

The extent of removal of ammoniacal nitrogen as well as phosphorous was consistently more in RDTBC with 70 cm draft tube in comparison with the 60 cm draft tube column as shown in Fig. 5.7 and 5.8. In case of nitrogen removal the difference between the performances of the two devices was ~ 15 % but for phosphorous removal it was ~ 25%. Phosphorous removal was very steep in the initial hours while nitrogen removal was more gradual. The principal reason for greater removal of N and P compounds in RDTBC with 70 cm draft tube compared with 60 cm draft tube was the increase of gas holdup, specific interfacial area and volumetric mass transfer coefficient as observed earlier in Fig. 4.13, Fig. 4.23 and Fig. 4.31 respectively. The relative values of these parameters at the specified operating conditions of 2 LPM air flow rate, corresponding to U_{gr} of 4.167 cm/s are listed in the Table below:

Column	ϵ_g	a (cm ⁻¹)	$k_L a$ (min ⁻¹)
RDTBC with 70 cm draft tube	0.0335	0.601	0.168
RDTBC with 60 cm draft tube	0.0209	0.480	0.137

Decreasing the height of draft tube in the column increases the liquid height above the draft tube, this region behaves like an ordinary bubble column with intense backmixing, further decrease in draft tube height reduces the fraction of the anaerobic region of the annulus that adversely affects the degree of removal of nitrogen and phosphorus compounds from sewage water. It was noted that reduction in the draft tube height increases the liquid circulation rate in RDTBC, increase in Region 2 facilitates coalescence of gas bubbles that results in substantial reduction in gas holdup and other mass transfer parameters that contribute to the decline of the performance of the aerobic region of the RDTBC.

The relative variation in the extent of removal of the nutrients between the two RDTBC with different draft tube heights was attributed to both these factors, the decline in factors influencing aeration of the water and also to the suppression of denitrification and other anaerobic mechanisms. Consequently, only draft tube with 70 cm height was chosen for further work in all draft tube bubble columns for sewage wastewater treatment using activated sludge.

5.4.1.3 Effect of air flow rate on nitrogen and phosphorus removal in RDTBC

The effect of air flow rate on removal of nitrogen and phosphorus from sewage water in RDTBC was investigated at air flow rates of 2, 4 and 6 LPM corresponding to U_{gr} of

4.167, 8.333 and 12.5 cm/s respectively. The activated sludge was in the suspended state at these flow rates. The extent of removal of ammoniacal nitrogen and orthophosphate decreased with increasing air flow rate; the removal of nitrogen was 80%, 45% and 38% at flow rates of 2, 4 and 6 LPM respectively in a time span of seven hours, similarly the orthophosphate concentrations declined and registered a removal of 60%, 50% and 46% at 2, 4 and 6 LPM respectively.

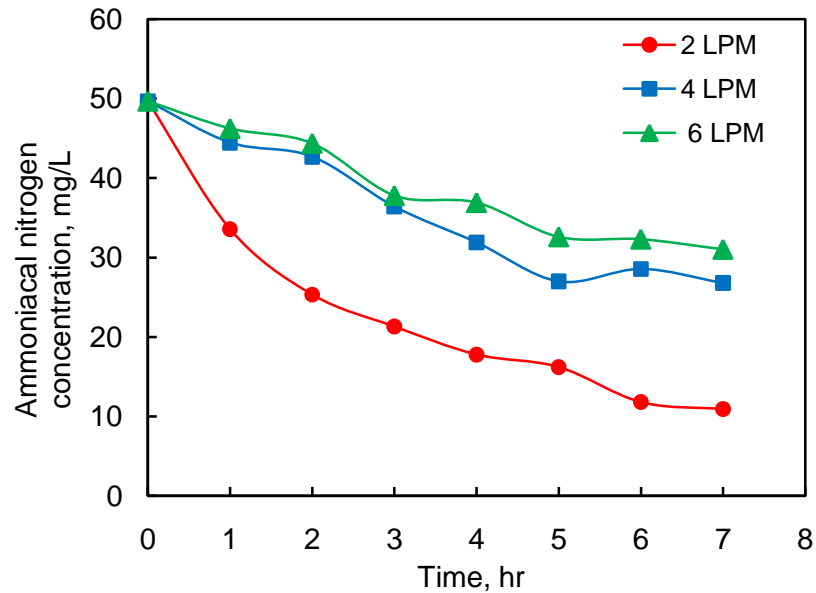


Fig. 5.9 Effect of air flow rate on ammoniacal nitrogen removal in RDTBC
(DT height = 70 cm; Sparger C)

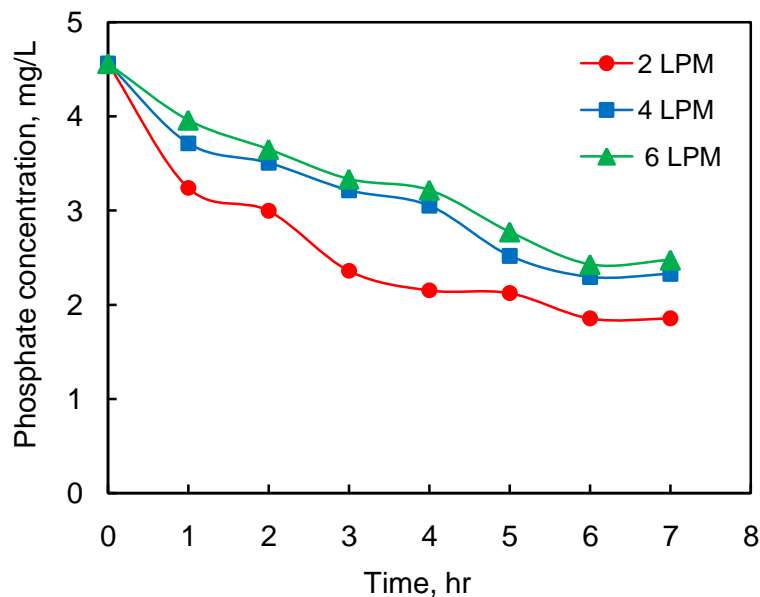


Fig. 5.10 Effect of air flow rate on phosphorus removal in RDTBC
(DT height = 70 cm; Sparger C)

Fig. 5.9 and 5.10 show the removal profiles of nitrogen and orthophosphate respectively in RDTBC at the varying flow rates. It is interesting to note from Fig. 5.10 that the maxima of removal of phosphate takes place in 6 hours time span. The decline in the nutrient removal is attributed to enhanced aeration of the water mass in the RDTBC. Runs performed earlier at 2 LPM flow rate corresponding to U_{gr} of 4.17 cm/s were designed to have controlled liquid circulation so that the liquid circulation rate does not drag air bubbles into the annulus and disturb its anaerobic nature. At flow rates of 4 and 6 LPM many air bubbles were entrained in the downcomer by the accelerated liquid circulation owing to increased air flow through the riser.

These results give credence to the model that DTBC, at modulated flow rates, comprise of aerobic and relatively anaerobic zones that support the enhanced removal of nutrients as expressed by Barnard (1973) & Argaman and Brener (1986). Interestingly it is observed that at elevated gas flow rates of 6 LPM, the circulation rates become so large that the entire DTBC become aerobic behaving just as an ordinary bubble column resulting in nearly same extent of removal of phosphorous (~47%) and nitrogen (~40%) in seven hours duration. Thus, it was observed that the fraction of anaerobic region in the column decreased with increasing air flow rate resulting in the suppression of anaerobic steps, leading to decline of nitrogen and phosphorus removal. Therefore, to achieve enhanced nutrient removal during wastewater treatment, the fractions of anaerobic and aerobic regions in the column must be well balanced not only in terms of draft tube height but also by modulating the liquid circulation rates by adjusting air flow rate.

5.4.1.4 Effect of geometrical shape of draft tube bubble column on nutrient removal

The effect of geometrical shape of draft tube bubble column on the nutrient removal pattern from sewage water using activated sludge was investigated by using a cylindrical DTBC (CDTBC-1) having equivalent cross-sectional area of draft tube as that of the RDTBC and comparing the results. Both the draft tube columns (CDTBC-1 and RDTBC) had draft tube height of 70 cm and spargers with same number of holes ($N_h = 4$) and were operated at air flow rate of 2 LPM, which corresponds to U_{gr} of 4.15 cm/s.

The removal of ammoniacal nitrogen from sewage water under otherwise identical conditions in CDTBC-1 and RDTBC in the runtime duration of seven hours is shown in Fig. 5.11 and that of phosphorus compounds is shown in Fig. 5.12.

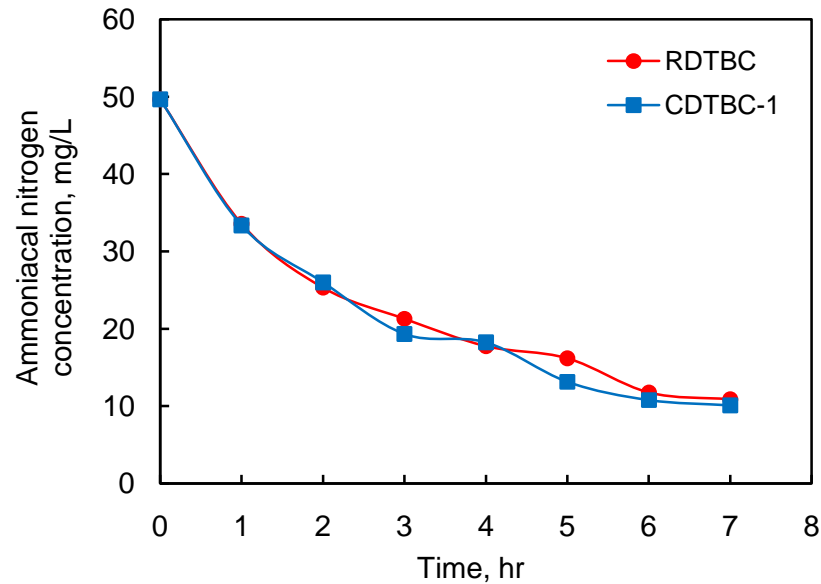


Fig. 5.11 Effect of shape of DTBC on ammoniacal nitrogen removal

(Air flow rate = 2 LPM; DT height = 70 cm; Sparger with $N_h = 4$; $A_r = 8 \text{ cm}^2$)

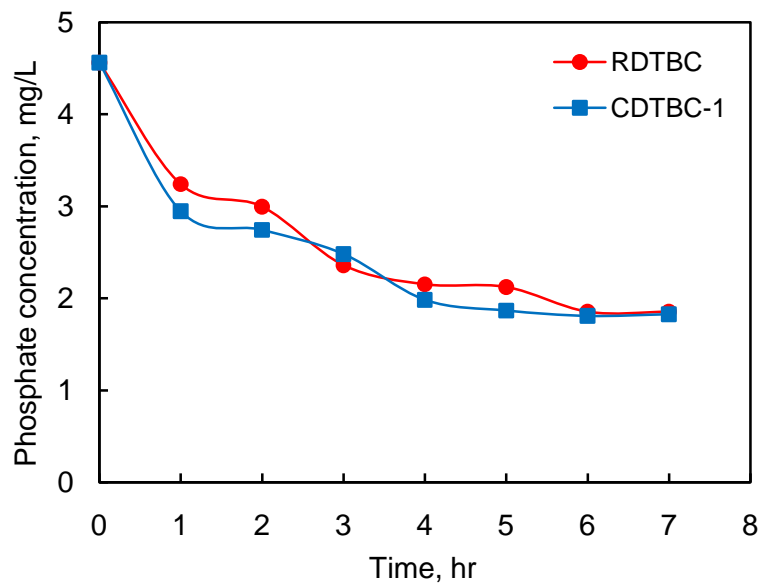


Fig. 5.12 Effect of shape of DTBC on phosphorus removal

(Air flow rate = 2 LPM; DT height = 70 cm; Sparger with $N_h = 4$; $A_r = 8 \text{ cm}^2$)

It is seen in Fig. 5.11 that the nitrogen removal profiles observed in RDTBC and CDTBC-1 almost superimpose due to almost similar values of gas holdup, interfacial area and mass transfer coefficients in both these columns at 2 LPM air flow rate, as shown in Fig. 4.16, Fig. 4.25 and Fig. 4.30, The specific values of these parameters at 2 LPM air flow rate which corresponds to U_{gr} of 4.15 cm/s, are listed in the following Table:

Column	ϵ_g	a (cm ⁻¹)	$k_L a$ (min ⁻¹)
RDTBC	0.0335	0.601	0.168
CDTBC-1	0.0385	0.674	0.157

The orthophosphate removal profiles are also quite close but jerky that may be attributed to external effects. Thus, no significant effect of the cross-sectional shape-whether rectangular or circular on the nutrient removal capacities of these draft tube bubble columns at 2 LPM was observed since at the specified air flow rate with 70 cm draft tube height in RDTBC and CDTBC-1, the fraction of aerobic and anaerobic regions are well balanced.

5.4.1.5 Effect of scale of operation in CDTBC on nutrients removal

The effect of scale of operation on removal of ammoniacal nitrogen and phosphorus compounds from sewage water was investigated by performing experiments under identical conditions in cylindrical draft tube bubble columns of different diameters. Column CDTBC-1 had a column ID of 6.4 cm and draft tube ID of 3.2 cm the cross-sectional area of draft tube was 8.042 cm², while column CDTBC-2 had an ID of 14 cm and draft tube ID of 8 cm the cross-sectional area of draft tube was 50.3 cm². In CDTBC-1 sparger with 4 holes of 1 mm diameter while for CDTBC-2 a sparger with 8 holes of 1 mm diameter was used. The height of column in both the cases was 1 meter and draft tube height was 70 cm.

Runs were performed by filling the sewage water in the columns up to initial unaerated liquid height of 75 cm that corresponded to wastewater volume of 2.2 liter in CDTBC-1, and 10.5 liter in CDTBC-2. Since earlier experiments were performed in CDTBC-1 and RDTBC at gas flow rate of 2 LPM that was equivalent to U_{gr} of 4.14 cm/s hence experiments were performed in CDTBC-2 at identical U_{gr} , which corresponded to 12.5 LPM air flow rate due to enhancement of draft tube cross-sectional areas of this column.

The extent of removal of ammoniacal nitrogen and orthophosphates from sewage water in CDTBC-2 at 12.5 LPM air flow rates were 86% and 64% respectively in a time span of seven hours, in comparison with 80 % and 60 % removal observed in CDTBC-1. The extent of nutrient removal was higher in CDTBC-2 compared to CDTBC-1 at U_{gr} of 4.14 cm/s, as shown in Fig 5.13 and Fig. 5.14. The better performance of CDTBC-2 could be attributed to a number of reasons, which are not easy to quantify.

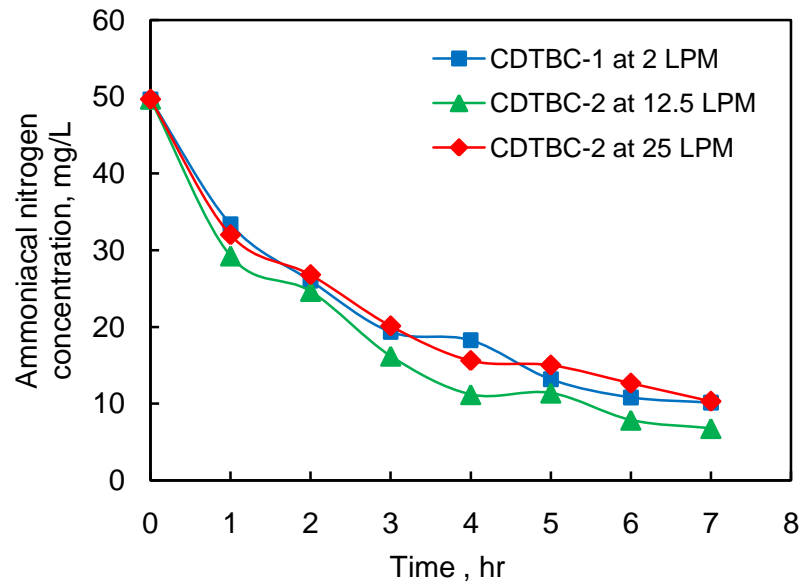


Fig. 5.13 Effect of scale of CDTBC on nitrogen removal at varying air flow rates

(DT height = 70 cm; of A_r of CDTBC-1 = 8.042 cm²; A_r of CDTBC-2 = 50.3 cm²)

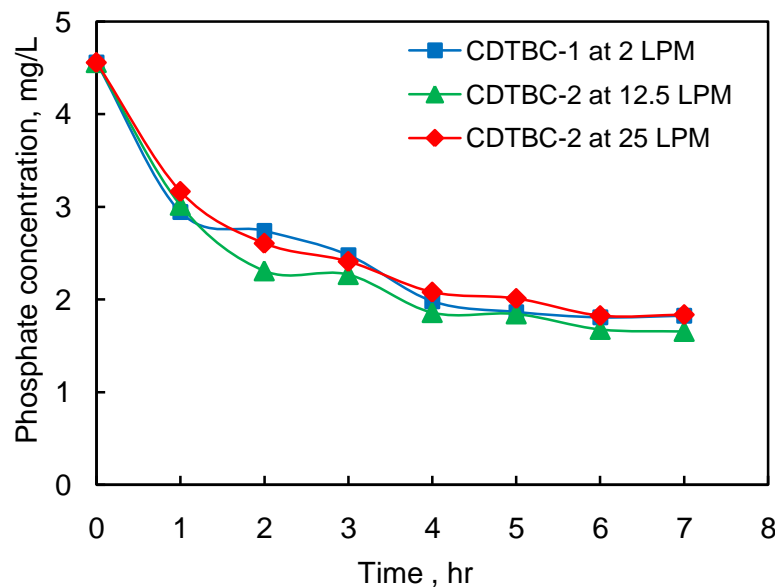


Fig. 5.14 Effect of scale of CDTBC on phosphorus removal at varying air flow rates

(DT height = 70 cm; of A_r of CDTBC-1 = 8.042 cm²; A_r of CDTBC-2 = 50.3 cm²)

The gas holdup at U_{gr} of 4.14 cm/s in CDTBC-1 and CDTBC-2 were 0.0385 and 0.033 respectively, while specific interfacial area in CDTBC-2 was 0.8 cm⁻¹ while in CDTBC-1, it was 0.674 cm⁻¹ as shown in Fig. 4.26. The above data indicates that the extent of aeration in both the columns is nearly identical however, the volumetric mass transfer coefficients was found to be 0.157 min⁻¹ in CDTBC-1 and 0.09 min⁻¹ in CDTBC-2, from which it can be inferred that k_L in CDTBC-2 was quite low; this result is however expected in view of larger size of the column and lesser degree of turbulence created by circulatory flows.

Another aspect contributing to superior performance of CDTBC-2 is the enhanced fraction of the anaerobic region in this column. The annulus cross-sectional area of CDTBC-2 was 90.4 cm^2 in comparison with 20.8 cm^2 in CDTBC-1 accounting for a 4.34 fold increase in annulus volume. Therefore, there was no constraint of space for the anaerobic processes at the specified gas velocities.

The effect of air flow rate on removal of nitrogen and phosphorus from sewage water was also investigated in CDTBC-2 at 12.5 LPM and 25 LPM as shown in Fig.5.13 and Fig.5.14 respectively. Increasing air flow rate had deleterious effect on removal of both the nutrients- nitrogen and phosphorus in the larger scale operations, in almost a similar fashion as observed in RDTBC. The decrease in the removal of nutrients from sewage water at higher air flow rate is again attributed to increased liquid circulation causing entrainment of air bubbles in the annulus zone, leading to suppression of anaerobic mechanisms thus causing inferior performance of the column at high air velocities.

Further it is observed that the removal profile of nutrients from CDTBC-2 at 25 LPM air flow rate ($U_{gr} = 8.28 \text{ cm/s}$) matched closely to that obtained in CDTBC-1 at 2 LPM air flow rate having $U_{gr} = 4.14 \text{ cm/s}$. Moreover, CDTBC-2 at $U_{gr} = 4.14 \text{ cm/s}$ (12.5 LPM air flow rate) returned marginally superior nutrient removal profiles compared to CDTBC-1 and RDTBC at the same superficial velocity of $U_{gr} = 4.14 \text{ cm/s}$ obtained at 2 LPM air flow rates as seen in Fig. 5.13 and 5.14. This behavior is largely attributed to the presence of larger anaerobic zone in CDTBC-2; it also reinstates the observation that at relatively higher air flow rates the performance of draft tube bubble column falters for nutrient removal.

These results illustrate some important characteristic of DTBC with respect to nutrient removal they are the following:-

- Device geometry has almost no effect on overall device performance
- Large annular space in DTBC generally favors nutrient removal and does not hamper overall performance of the devices
- Superficial velocities are key performance parameters and changes of scale of operation maintaining the superficial gas velocity will return almost identical removal profiles.

5.4.2 Synthetic wastewater treatment using activated sludge in rectangular columns

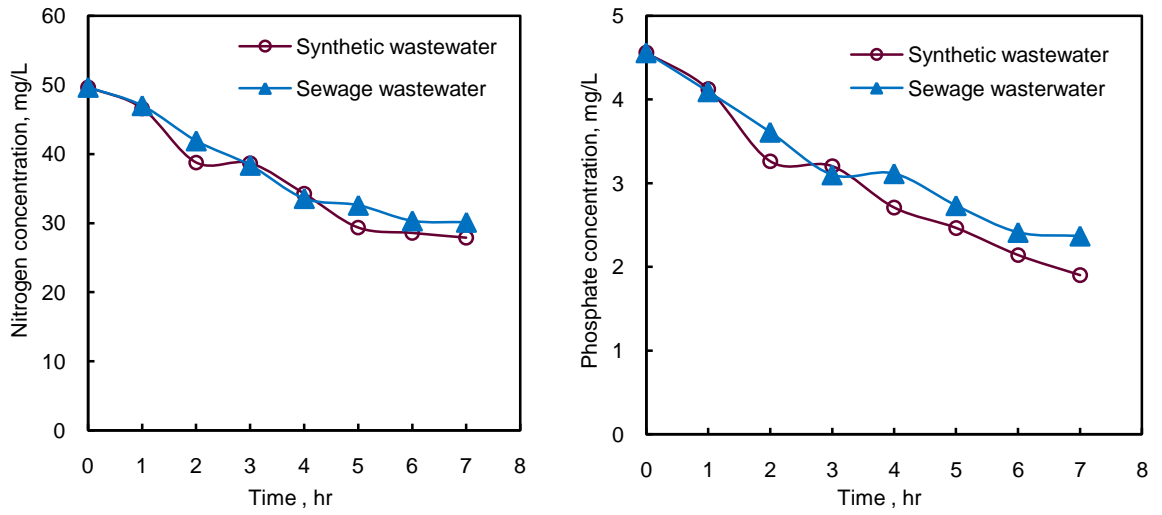
Rectangular draft tube bubble columns (RDTBC) as well as rectangular bubble columns were also used for the removal of ammoniacal nitrogen and orthophosphates from synthetic wastewaters, prepared in laboratory, using activated sludge. The objective of this investigation was to check the efficacy of the data obtained in laboratory with actual field data.

The composition of synthetic wastewater was adjusted to exactly match with the initial concentration of ammoniacal nitrogen (49.7 mg/L) and phosphorus (4.56 mg/L) of the sewage water so that the nutrient removal profiles from these two wastewaters could be meaningfully compared. Table 5.2 gives the components and composition of the wastewater synthesized in the laboratory. All the experimental runs with synthetic wastewater were performed in rectangular columns; both the draft tubes (70 cm height as well as 60 cm height) were used at airflow rates of 2 LPM corresponding to U_{gr} of 4.167 cm/s in draft tube columns, the unaerated liquid height was kept 75 cm. The total duration of the runs were seven hours similar to the run time for sewage waste water.

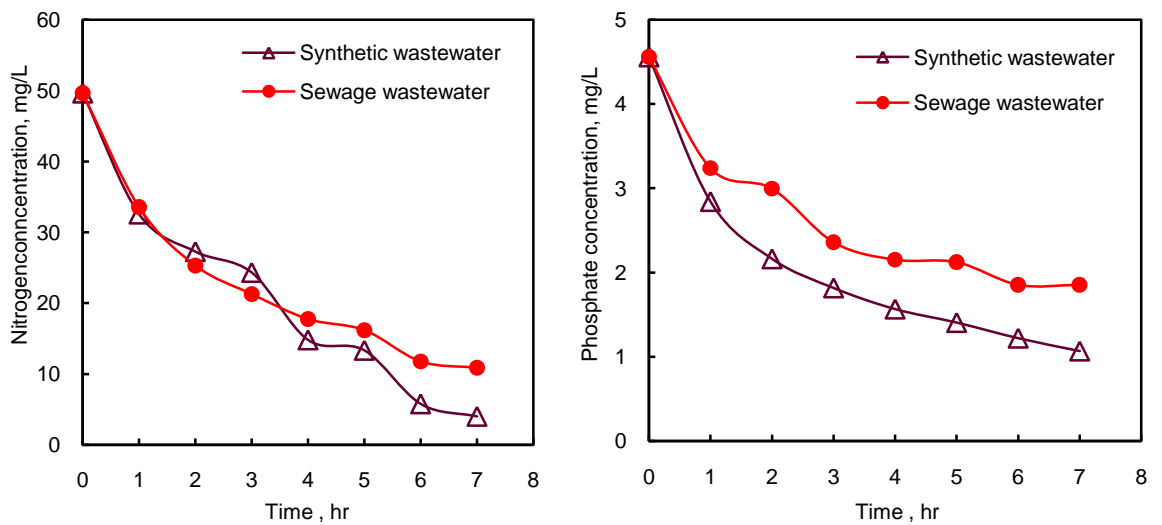
The nitrogen and phosphorus removal profiles of synthetic waste water and sewage waste water in three different devices rectangular bubble column and rectangular draft tube bubble columns are shown in Fig 5.15 at a fixed gas flow rate of 2 LPM. The removal profiles of nitrogen in both waste waters in bubble columns intermingle closely while in RDTBC with 70 cm draft tube also the removal profiles are quite close up to 5 hrs thereafter the curves diverge out, same is the case with 60 cm draft tube.

Phosphorous removal from synthetic waste waters in DTBC was substantially larger than from sewage waste water, in 70 cm DT column the final extent of removal was 77% for synthetic waste water and 60% for sewage waste water while in 60 cm draft tube phosphorous removal was 70% and 55% respectively for synthetic and sewage wastewaters. In bubble columns as well the extent of phosphorus removal achieved from synthetic wastewater was 58% while from sewage wastewater it was just 48% under identical conditions.

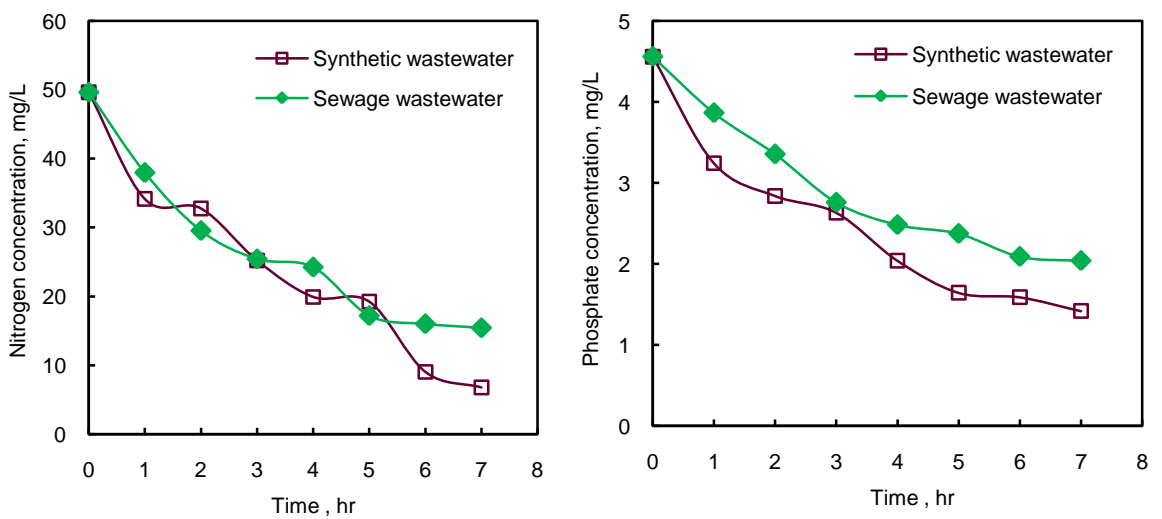
The greater extent of phosphorus removal from synthetic waste water is attributed to the relatively simple phosphorus compound present in synthetic wastewater vis-à-vis the sewage water.



(a) RBC ($U_g = 0.78$ cm/s)



(b) RDTBC with 70 cm draft tube ($U_{gr} = 4.167$ cm/s)



(c) RDTBC with 60 cm draft tube ($U_{gr} = 4.167$ cm/s)

Fig. 5.15 Comparison of synthetic wastewater and sewage water for nitrogen and phosphorus removal in rectangular columns. (Air flow rate = 2 LPM; Sparger C)

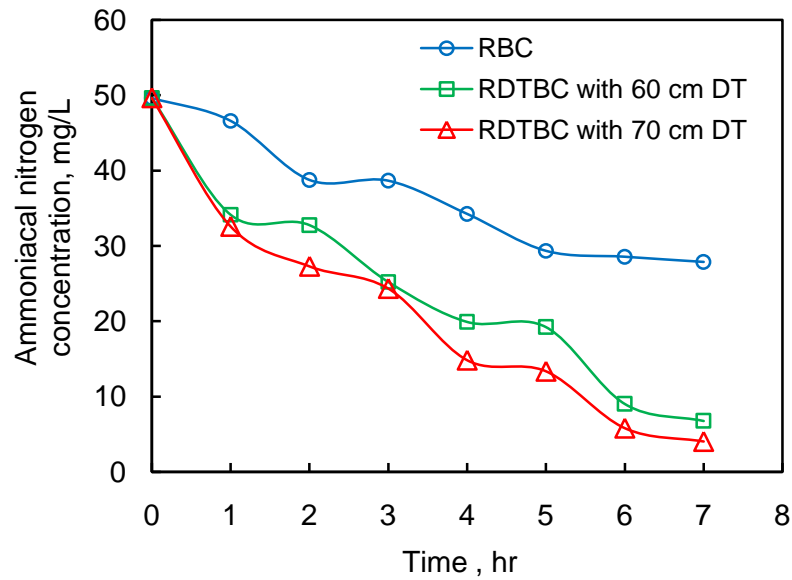


Fig. 5.16 Ammoniacal nitrogen removal from synthetic wastewater in RBC and RDTBC (Air flow rate = 2 LPM; Sparger C)

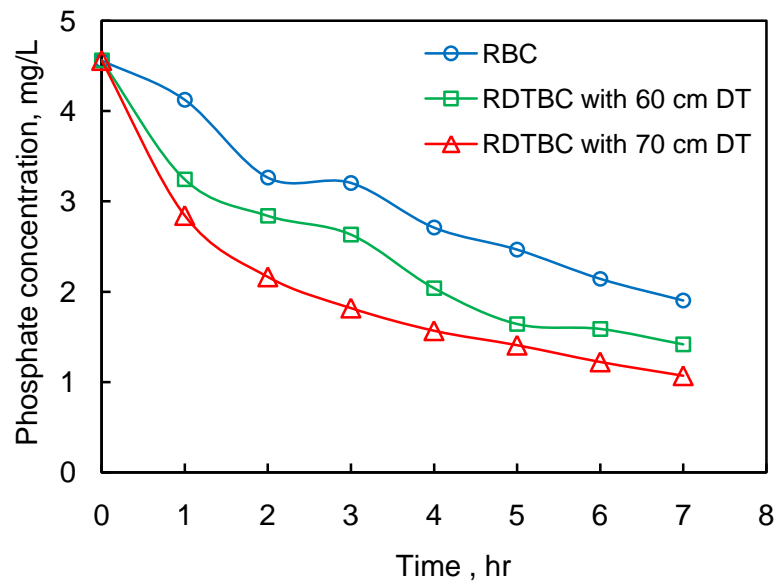


Fig. 5.17 Phosphorus removal from synthetic wastewater in RBC and RDTBC (Air flow rate = 2 LPM; Sparger C)

The relative performance of the three devices - the rectangular bubble column, the rectangular draft tube bubble column with 70 cm draft tube and one with 60 cm draft tube- for removal of nitrogen and phosphorous based nutrients from the synthetic wastewater are shown in Fig 5.16 and Fig 5.17. It is observed that the device performance followed the order RDTBC > RBC, in RDTBC the draft tube with 70 cm height outperformed the RDTBC with 60 cm height. Similar results were obtained earlier with sewage waste water as well; the cause for such performance is elaborated earlier in sections 5.4.1.1 and 5.4.1.2. One interesting departure that was noticed was that unlike

sewage wastewater the depletion profile of phosphorus in synthetic wastewater was relatively smooth and gradual. The net removal of nitrogen and phosphorus from both wastewaters after seven hours operation in the three devices are listed in the Table 5.3 below.

Table 5.3 Comparison of nutrient removal from synthetic and sewage wastewater

Column	Synthetic wastewater		Sewage water	
	% N removal	% P removal	% N removal	% P removal
RBC	44	58	40	48
RDTBC with 70 cm draft tube	92	77	80	60
RDTBC with 60 cm draft tube	86	70	70	55

These results home in the point that device specific data portability is possible between laboratory developed synthetic wastewater systems and sewage wastewaters without substantial loss of information but such data transfer across devices such as bubble column to draft tube bubble columns is not advisable without appropriate scaling.

5.5 CONCLUSIONS

The significant conclusions drawn from this investigation on wastewater treatment using activated sludge in draft tube bubble columns are as under:

- The draft tube bubble column proved to be a superior device for the biological removal of nitrogen and phosphorous compounds from wastewater in comparison to the bubble column. These results validate the hypothesis forwarded by Barnard (1973) that aerobic and anaerobic regions are required for enhanced biological treatment of nitrogen and phosphorus compounds from waste water.
- The geometric shape of the column did not influence the removal rates of N and P when design and operational parameters in different geometries were nearly identical.
- Superficial velocities are key performance parameters and changes of scale of operation maintaining the superficial gas velocity returns almost identical removal profiles.

- Height of draft tube influenced the rates of N and P removal from wastewater. Draft tube height needs to be optimized for specific applications, it was observed that lower draft tube height made the DTBC device more like a bubble column reducing the specific interfacial area and mass transfer coefficient, that had a bearing on the overall removal rates.
- Annular region in the DTBC functions as the anaerobic zone, large annular space generally favors nutrient removal and does not hamper overall performance of these devices.
- Nitrogen and phosphorus removal from sewage waste water and synthetically prepared waste water show similar removal patterns although the extent of removal from sewage water is about 10% less which is expected in view of the relative complexity of molecular species involved in sewage water.
- Results indicate that device specific data portability is possible between field data and laboratory data developed based on synthetic wastewater systems without substantial loss of information but data transfer across devices such as bubble column to draft tube bubble columns is not advisable without appropriate scaling.
- The draft tube bubble column turns out to be a simple, compact and effective device for nutrient removal from wastewaters and is a tool for process intensification.

CHAPTER 6

FERMENTATION OF BAKER'S YEAST IN DRAFT TUBE BUBBLE COLUMNS

6.1 INTRODUCTION

A large part of the earth's population is malnourished, due to poverty and inadequate supply of food. Scientists are concerned whether the food supply can keep up with the world population increase, with the increasing demands for energy, the ratio of land area required for global food supply or production of bioenergy, the availability of raw materials, as well as the maintenance of wild biodiversity (Zhuang, 2004). Therefore, the production of microbial biomass for food consumption is a major concern for the industry and the scientific community.

The *Saccharomyces cerevisiae* biomass, mainly in the form of baker's yeast, represents the largest bulk production of any single-cell microorganism in the world. Several million tons of fresh baker's yeast cells are produced yearly for human food use (Walker, 1998) and other applications in food industries. Baker's yeast is also one of the oldest products of industrial fermentation that was used traditionally. It is still one of the most important in industries based on its use for bread-making, a staple food for large section of world's population. Today, the scientific knowledge and technology allows the isolation, construction and industrial production of baker's yeast strains with specific properties to satisfy the demands of the baking and fermentation industry (Phaff, 1990). The significance of baker's yeast in food technology as well as in human nutrition, as an alternative source of protein to cover the demands in a world of low agricultural production and rapidly increasing population makes the production of baker's yeast extremely important (Bekatorou et al., 2006).

Baker's yeast is usually produced starting from a small quantity of *S. cerevisiae* added to a liquid solution of essential nutrients, at suitable temperature and pH using batch fermentation. Batch culture/fermentation is a closed system which contains an initial, limited amount of nutrient. In the course of the entire fermentation, nothing is added except oxygen (in a form of air), an antifoam and acid/base to control the pH. Composition of the batch culture medium, biomass, and metabolite concentration change continuously as a result of cell metabolism. Most fermentation processes use batch fermentation for not only its simplicity, ease of operation, superior baking quality, favorable economics, constant specific growth rate and well tested design, but for prevention of contamination as well. However, the productivity for many types of fermentation can be enhanced using continuous and fed-batch fermentation (Whitaker et al., 1995).

Baker's yeast production is aerobic fermentation process whose efficiency is strongly dependent on the transfer of oxygen and nutrients to the microorganisms. Sugar cane molasses/juice is an inexpensive and commonly used raw material in the manufacture of baker's yeast. It is the fed carbon/energy source, with sucrose as the main sugar constituent. The most important requisites in the commercial production of baker's yeast are rapid growth and high biomass yield. The production of baker's yeast requires a high oxygen supply rate, in order to avoid the undesirable alcoholic metabolism under anoxia condition. Under this metabolism, the microorganisms will be inhibited and have a poor growth rate.

Choosing a proper type of bioreactor is a key step in achieving maximum yield. In the case of microbial cultivation, the fermentation environment and conditions provided by the bioreactor will have to match the specific needs of the microorganisms, in order to get higher productivity and specific growth rate. The critical aspect of fermenter design is to satisfy the need of gas-liquid mass transfer. In this context, the bubble columns usually are the most economical bioreactors for baker's yeast production.

Bubble columns and its variant the draft tube bubble columns are commonly used in aerobic fermentation processes because of their simple construction, lack of moving parts, effective mixing without high shear force, greater oxygen transfer efficiencies and ease of maintenance. In addition, in the bubble column reactor cells are not exposed to large variations in shear forces and thus are able to grow in a more stable physical environment. In contrast, in stirred tank reactors, high shear conditions will arise near the impeller, causing cell damage or cell stress and thus lowering productivity.

In the present investigation, batch cultivation of *S. cerevisiae* was carried out in a shake flask, rectangular bubble column, rectangular draft tube bubble column and cylindrical draft tube bubble columns of different sizes and their relative performances were evaluated based on biomass concentration and sugar depletion, the two critically needed measurements in fermentation investigations. The influence of size and shape of fermentator geometries, air flow rates, presence of a draft tube in bubble column and height of draft tube on the cell biomass production, specific growth rate and sugar depletion from fermentation broth was also evaluated.

6.2 LITERATURE SURVEY

6.2.1 General characteristics of fermentation process

Fermentation is a process in which an organism is cultivated in a controlled manner to produce the organism cell mass itself, or a product produced by the cell. Baker's yeast is one of the microbial biomass which has been produced by fermentation process. Regardless of the type of fermentation an established fermentation process may be divided into six basic components parts:

- i. The formulation of media to be used in culturing the process organism during the development of the inoculum and in the production fermenter.
- ii. The sterilization of the medium, fermenters and ancillary equipment.
- iii. The production of an active, pure culture in sufficient quantity to inoculate the production vessel.
- iv. The growth of the organism in the production fermenter under optimum conditions for product formation.
- v. The extraction of the product and its purification.
- vi. The disposal of effluents produced by the process.

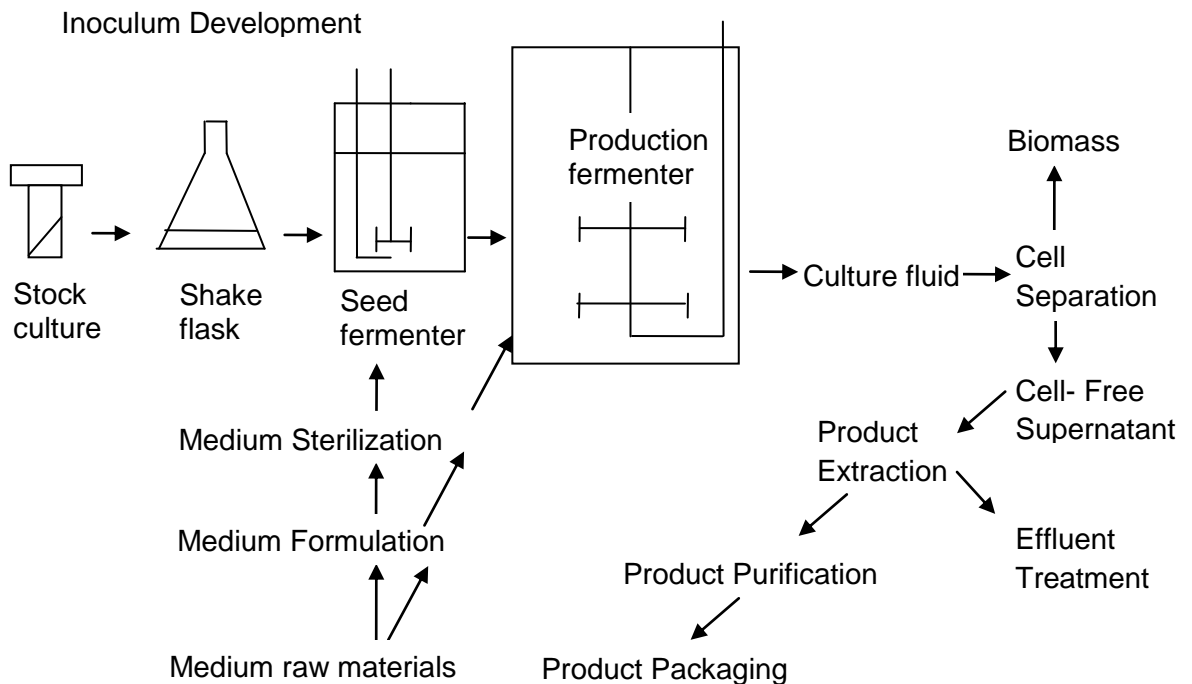


Fig. 6.1 A generalized schematic representation of a typical fermentation process,

adopted from Whitaker (1995)

The interrelationships between the six component parts are illustrated in Fig. 6.1, which shows the flow of steps in a development of product which is designed to gradually improve the overall efficiency of the fermentation.

6.2.2 Kinetics of batch fermentation

In batch fermentation, inoculated culture will pass through a number of phases, as illustrated in Figure 6.2. After inoculation there is a period during which it appears that no growth takes place; this period is referred to as the *lag phase* and may be considered as a time of adaption.

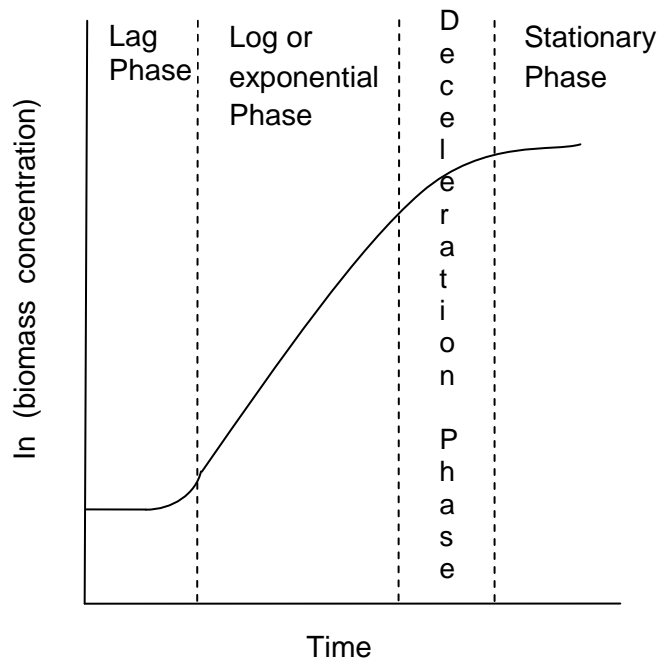


Fig. 6.2 Typical batch growth curve

In a commercial process the length of lag phase should be reduced as much as possible and this may be achieved by using a suitable inoculum. Following a period during which the growth rate of the cells gradually increases, the cells grow at a constant, maximum, rate and this period is known as the *log*, or *exponential phase*. In exponential growth phase, the progressive doubling of cell number results in a continually increasing rate of growth in the population. The growth rate, $\frac{dx}{dt}$ at any particular time is proportional to the concentration of biomass (x) of yeast cell at that time. Thus, the exponential phase may be described by the equation:

$$\frac{dx}{dt} = \mu x \quad (6.1)$$

where, x is the concentration of microbial biomass at any time, t is time (hours) and μ is known as specific growth rate (h^{-1}). Integration of above equation gives:

$$x = x_0 e^{\mu t} \quad (6.2)$$

where, x_0 is the initial biomass concentration. On taking natural logarithms, above equation becomes:

$$\ln x = \ln x_0 + \mu t \quad (6.3)$$

Thus, a plot of the natural logarithm of biomass concentration ($\ln x$) against time (t) should yield a straight line, the slope of which would equal to μ . In addition to specific growth rate μ , cell growth rates are often expressed in terms of the doubling time t_d . An expression for doubling time can be derived from equation 6.2. Starting with a cell concentration of x_0 , the concentration at $t = t_d$ is $2x_0$. Substituting these values into equation 6.2,

$$2x_0 = x_0 e^{\mu t_d} \quad (6.4)$$

$$\therefore t_d = \frac{\ln 2}{\mu} \quad (6.5)$$

The maximum specific growth rate for yeast has been reported to be 0.6 h^{-1} , equivalent to a doubling time of 1.16 hour. During the exponential phase nutrients are in excess and the organism is growing at its maximum specific growth rate. As nutrients in the culture medium become depleted and/or inhibitory products accumulate, growth rate of culture decreases until growth ceases and the *stationary phase* is reached. Some culture exhibits a *death phase* as the cells lose viability or are destroyed by lysis (Doran, 1995).

6.2.3 Baker's yeast

Yeasts constitute one of the most important industrial sources of a great variety of fermentation products ranging from small molecules like ethanol to complex recombinant therapeutic proteins. Yeasts were used to raise bread in Egypt from 4000 BC, and fermented dairy products such as cheese and yogurt were developed early in history. Yeasts are also the most extensively used microorganisms in industry. They are cultured for cell mass, cell components, and products that they produced during the fermentation. Yeasts can be used in many industrial processes, such as the production of alcoholic beverages, biomass (baker's and fodder) and various metabolic products. Industrial production of yeast cells for their biomass and production of alcohol by yeast are two quite different processes. The first process is aerobic process, requires oxygen

for maximum production of cell, whereas the alcoholic fermentation process is anaerobic and takes place only in the absence of oxygen. The yeast widely used for both industrial and domestic processes is baker's yeast.

Baker's yeast has a significant role in food technology. It is the most common food grade yeast, which is used worldwide for the production of bread and baking products. Baker's yeast is included in starter cultures, for the production of specific types of fermented foods like bread, sourdoughs, fermented meat and vegetable products, etc. It is also the most widely used yeast species, whose selected strains are used in breweries, wineries and distilleries for the production of beer, wine, distillates and ethanol.

Baker's yeast is composed of living cells of aerobically grown *Saccharomyces cerevisiae*. A selected strain of baker's yeast, *S.cerevisiae* has been extensively studied and applied widely both at laboratory and at industrial scale production. These strains are selected for stable physiological characteristics, vigorous sugar fermentation in dough and cellular dispersion in water, no autolysis during fermentation, rapid growth and high cell yields and easy maintenance during storage. Baker's yeast is produced utilizing molasses from sugar industry by-products as a raw material. The fermentation of baker's yeast has to produce a product with minimum variation in yeast performance, maximum yield on raw material, and minimum production of undesirable side products. Under aerobic conditions, *S. cerevisiae* uses sugars such as glucose to grow cell mass rather than produce alcohol.

6.2.4 Yeast metabolism

Yeasts are facultative anaerobes and can grow with or without oxygen. In the presence of oxygen, they convert sugars to CO₂, energy and biomass. In anaerobic conditions, as in alcoholic fermentation, yeasts do not grow efficiently and leads to Crabtree effect wherein sugars are converted to intermediate by-products such as ethanol, glycerol and CO₂ (Balls et al., 1925). Therefore, in yeast propagation, the supply of air is necessary to avoid Crabtree effect and for optimum biomass production.

The principal raw materials used in developing baker's yeast are the pure yeast culture and Cane molasses. Cane and beet molasses are used as the principal carbon sources to promote yeast growth and supplies all the sugar that yeast needs for growth and energy along with part of the needed nitrogen (John, 1954). Besides its high sugar content, molasses contains minerals, organic compounds and vitamins, which are valuable nutrients in fermentation processes.

Yeasts can metabolize variety of carbons sources such as glucose, fructose, mannose, galactose, sucrose, maltose and hydrolyzed lactose. The main carbon and energy source for most yeast is sucrose supplied from molasses, which is rapidly hydrolyzed by *yeast invertase*, giving a mixture of mainly glucose and fructose in the medium, which is subsequently converted to the glycolytic pathway by aerobic assimilation to pyruvate and by the Krebs cycle to anabolites and energy in the form of ATP.

Assimilable nitrogen for commercial baker's yeast production is supplied in the form of aqueous ammonia, ammonium salts (such as phosphate, sulfate, chloride, bicarbonate, carbonate, etc.) and urea. Occasionally, amino acid mixtures such as protein hydrolysates or autolysates may be added. Nitrate and nitrite are not assimilated by *S.cerevisiae* (Chen and Chiger, 1985). Elements such as P, K, Mg, Na, S, Fe, Cu and Zn are needed to be supplied in traces for proper yeast growth, while other elements such as B, Mn, Ca, Ti, Co, I and Sn have no effect on yeast growth. Phosphorus and sulphur are usually assimilated in the form of inorganic phosphates and sulphates, respectively.

6.2.5 Production of baker's yeast

Theoretical analysis of baker's yeast production with experimental verification in a laboratory scale bubble column fermenter in a fed-batch process was successfully implemented by Sweere et al. (1988; 1989). Fed batch culture of *Saccharomyces cerevisiae* was carried out in a bubble column and the airlift reactor with net draft tube by Wu and Wu (1991). They observed higher cell mass production that was attributed to the much higher oxygen transfer rates in the net draft tube airlift reactor in comparison to a conventional airlift reactor and bubble column. An airlift reactor with double net draft tubes was developed by Tung et al. (1997) for batch fermentation of *Saccharomyces cerevisiae*. The proposed reactor in this research had higher gas holdup and volumetric mass transfer coefficient and lower mixing time and cultivation time in comparison with those of the bubble column.

Comparison of baker's yeast process performance in laboratory and production scale for fed batch process with molasses as carbon source was carried out by George et al. (1998); they used a 215 m³ industrial bubble column reactor having 17.5 m height and 4 m diameter. Van Dijken et al. (1993) as well as Win et al. (1996) investigated the kinetics of growth of *Saccharomyces cerevisiae* in batch and/or fed batch processes at optimum temperature of 30⁰ C, pH of 5.5 and also focused on corresponding sugar consumption rates by yeasts.

Partial substitution of sugarcane molasses by cheese whey in the fed batch production of baker's yeast in a 3 liter stirred tank bioreactor was evaluated by Ferrari et al. (2001); they found no significant differences in biomass volumetric productivity, by-products yields and baking quality although there was slight decline in the biomass yield. The specific growth rate reported by these investigators ranged between 0.2 - 0.3 h⁻¹.

One of the major problems militating against the achievement of high yield and high volumetric productivity during fermentation of *Saccharomyces cerevisiae* for the production of baker's yeast at both laboratory and industrial scales is the conversion of a lot of the limiting substrate into ethanol even under aerobic conditions as soon as, a so called critical growth rate is exceeded. Consequently, most control strategies in baker's yeast fermentations are designed to eliminate ethanol production or at least minimize its production rate. Therefore, Ejiofor et al. (1994) have demonstrated a robust fed-batch feeding strategy to allow for an accurate optimal estimation of yield and critical growth rate for baker's yeast production.

Franco-lara et al. (2007) have carried out different case studies (including industrial production of baker's yeast in bubble columns) addressing the specification of system performance and estimation of optimal cultivation policies for different yeast cultivation systems. Modeling and/or simulation of kinetics and mass transfer studies for estimation of biomass concentration and specific growth rate of baker's yeast in industrial fermenters were carried out by many investigators (Szewczyk and Warsaw, 1989; Enfors et al., 1990; Yuan et al., 1993; Santacesaria et al., 2001; Karakuzu et al., 2006).

6.3 MATERIALS AND METHODS

6.3.1 Cane sugar solution

The sugarcane juice obtained by the milling of high grade sugarcane was used as the principal raw material. This sugar cane juice was filtered to remove suspended impurities. To achieve desired sugar concentration (7 % w/v), it was diluted with addition of appropriate amount of water and used for inoculum preparation and as a media for fermentation of baker's yeast.

6.3.2 Chemicals and glassware

Chemicals used in the experimental and analytical methods such as yeast extract, peptone, dextrose, agar, lactic acid (purity 88%), ammonium sulphate (99%), potassium dihydrogen phosphate (99.5%), magnesium sulfate (99.5%), methanol (99.5%),

NaOH(98%), concentrated HCl, sodium bicarbonate (99.7%), aqueous ferricyanide solution (99%), indicator methylene blue (95%), etc. were of reagent-grade quality and procured from Merck India Pvt. Ltd. Deionized water was used for all dilutions and preparing all aqueous solutions. Necessary glassware such as erlenmeyer flasks, conical flasks, petri dish, slant tubes, measuring cylinders, pipettes, beakers, quartz cuvette, centrifuge tubes, etc. were procured from Borosil Pvt. Ltd.

6.3.3 Experimental procedure

Batch fermentation protocol was developed in the present investigation considering the standard conventional technology of aerobic submerged fermentation, which involves preliminary development of inoculums and secondarily production of baker's yeast in different types of bioreactors under standardized physicochemical parameters of fermentation process.

6.3.3.1 Primary cultivation and preservation of baker's yeast

The strain of organism *S.cerevisiae* used in this study was obtained from the local sources in Rajkot and revived on YEPD broth (10 kg/m³ yeast extract, 10 kg/m³ peptone, 20 kg/m³ dextrose) in erlenmeyer flask under shaking condition using rotary shaker (REMI, RIS104) at 100 rpm and 30 ± 1°C for 24 hrs. After revival of baker's yeast, it was cultivated on YEPD agar (20 kg/m³) plates after 24 hrs of incubation at 30°C.



Fig. 6.3 Colonies of baker's yeast on YEPD agar plates

From the colonies obtained on YEPD agar plates as shown in Fig. 6.3, the colonies exhibiting larger size, i.e. more biomass were selected for further work and were preserved by periodic transfer on YEPD slant tubes at refrigerated temperature.

6.3.3.2 Medium design, optimization and sterilization

Media formulation is an essential stage in the design of successful laboratory experiments, pilot-scale development and manufacturing processes. In most practical industrial fermentation processes, the choice of culture media is based on the cost, requirement of nutrients and the ease of preparation of nutrients.

In the present investigation, sugar cane juice after filtration was used as the carbon source and ammonium salt was selected as assimilable nitrogen for baker's yeast production. Yeast extract was selected to stimulate the growth of organism. Elements such as K, P, Mg, S etc. were supplied in trace amounts in the form of their salts such as KH_2PO_4 and MgSO_4 . For maximum growth of baker's yeast, initial pH was adjusted to 5.5 using lactic acid. Groundnut oil was used as an antifoam agent during fermentation.

The media optimization was conducted in a series of experiments changing composition of one of the nutrients while keeping other parameters constant at specified set of conditions. Two parameters namely concentrations of carbon source (C) and nitrogen source (N) were chosen for optimization in order to obtain higher productivity of baker's yeast. Sugar cane juice, as a carbon source was varied from a concentration of 50 kg/m^3 to 110 kg/m^3 with ammonium sulphate as a nitrogen source the ratio of these compounds were adjusted to give C: N as 7:1 (Chen and Chiger, 1985).

Table 6.1 Optimization of carbon content in fermentation broth

(C: N = 7:1)

Time (hr)	Concentration of sugar cane juice (kg/m^3)						
	50	60	70	80	90	100	110
	<i>Optical density</i>						
0	0.09	0.087	0.095	0.088	0.091	0.098	0.1
1	0.115	0.105	0.128	0.108	0.114	0.126	0.126
2	0.143	0.138	0.143	0.129	0.139	0.140	0.137
3	0.176	0.166	0.181	0.164	0.179	0.180	0.177
4	0.239	0.246	0.247	0.235	0.241	0.238	0.243
5	0.313	0.301	0.354	0.326	0.335	0.342	0.337

As shown in Table 6.1 the optical density of these fermentation broths was measured every hour for a period of 5 hours of fermentation in a 500 ml shake flask on rotary shaker at 100 rpm and 30°C . The sugar cane juice concentration of 70 kg/m^3 ,

consistently returned the highest optical density every hour and resulted in the maximum biomass concentration after 5 hrs, hence this concentration of juice was considered optimal and used for all runs in this investigation. For evaluation of the most appropriate concentration of nitrogen source, different concentrations of ammonium sulphate ranging from 1 kg/m³ to 12 kg/m³ were employed with the optimized carbon source of 70 kg/m³ as shown in Table 6.2, again, the optimized ammonium sulfate concentration of 10 kg /m³, which resulted in the highest optical density after 5 hrs was used in all the runs in the present investigation.

Table 6.2 Optimization of nitrogen content in fermentation broth

(Sugar cane juice concentration = 70 kg/m³)

Time (hr)	Concentration of ammonium sulfate (kg/m ³)						
	1	2	4	6	8	10	12
	<i>Optical density</i>						
0	0.093	0.086	0.098	0.088	0.1	0.095	0.095
1	0.103	0.126	0.132	0.119	0.136	0.128	0.125
2	0.136	0.141	0.140	0.132	0.152	0.143	0.139
3	0.168	0.178	0.184	0.176	0.183	0.181	0.180
4	0.203	0.216	0.226	0.236	0.245	0.247	0.234
5	0.217	0.268	0.297	0.328	0.342	0.354	0.346

The optimized media having concentration of sugar cane juice and ammonium sulfate as 70 kg/m³ and 10 kg/m³ respectively and other components as specified in Table 6.3 was used for preparation of inoculum and as a production media for fermentation of baker's yeast. The medium was sterilized at 121°C and 15 psi for 15 minutes in an autoclave (Nova, 8533) prior to its use.

Table 6.3 Optimized media for baker's yeast production

Component	Concentration (kg/m ³)
Sugar cane juice	70
Ammonium sulphate, (NH ₄) ₂ SO ₄	10
Yeast extract	5.0
Potassium dihydrogen phosphate, KH ₂ PO ₄	2.0
Magnesium sulphate, MgSO ₄	4.0

6.3.3.3 Inoculum preparation

The strain of *S.cerevisiae* from a slant tube was inoculated in a 500 ml erlenmeyer flask containing appropriate quantity of sterilized inoculum medium on a rotary shaker at 100 rpm and 30°C for 24 hrs as shown in Fig.6.4. The inoculum broth 10% v/v of total production medium was inoculated in the fermenter. The relative proportions of all the ingredients in production medium were the same as inoculum medium to shorten the lag phase duration.



Fig. 6.4 Inoculum on a rotary shaker

6.3.3.4 Experiment using shake flask

Preliminary growth study of baker's yeast was carried out in a sterilized inoculated media in a 500 ml erlenmeyer flask on rotary shaker at 100 rpm and 30°C for 10 hrs. Samples were taken from shake flask under aseptic conditions at an interval of every one hour for total fermentation duration of 8 hrs.

6.3.3.5 Trial run using small bubble column

Preliminary batch experiment on yeast biomass production was carried out in a small bubble column having an inner diameter of 69 mm and height of 33.5 cm made from 3 mm thick transparent Perspex[®] sheet as shown in Fig.6.5 (a). An acrylic circular sparger with 37 holes of 1 mm diameter as shown in Fig.6.5 (b) was used in this column. A hemispherical chamber at the bottom of the column as shown in Fig.6.5(c) was provided for effective distribution of air through sparger. The effective working volume of the

column was only 0.8 liter. The entire assembly of column was sterilized using methanol. A 0.2 micron bacteria filter as shown in Fig.6.5 (d) was used to sterilize air before entering into the column. Preliminary batch fermentation was carried out in this column for eight hours.



Fig. 6.5 Snapshots of the small bubble column assembly and its parts

6.3.3.6 Production of baker's yeast in bubble columns and draft tube bubble columns

After trial runs in the small bubble column runs were carried to compare the performance of baker's yeast production in bubble columns and draft tube bubble columns of rectangular and cylindrical geometries that were already characterized for their mass transfer behavior and used for waste water treatment. Runs were carried out at varying air flow rates at ambient pressure and temperature, at different scales of operation depending on fermenter capacity. Methanol wash was given to the entire assembly of the column to sterilize the fermenter before its use. A 0.2 micron bacteria filter earlier used in the small CBC was also used in these column configurations for sterilization of inlet air.

In all fermentations, after sterilization of equipment, sterilized production medium was transferred aseptically into the fermenter and inoculated with about 10% of inoculum. The optical density of inoculum was set to 1.0 at 600 nm, pH of fermentation broth was measured by a pH meter (Biocraft Scientific system, NIG334 coupled to a pH electrode with an automatic temperature compensation probe) and was controlled at 5.5 by adding 4 N NaOH. Fermentation studies were continued for maximum eight hours in these columns. Samples were withdrawn from sampling valve at every hour and analyzed off-line for growth of biomass and sugar consumption.

6.3.3.7 Measurement of optical density, calculation of biomass concentration and specific growth rate

Broth culture samples obtained every hour from fermenters were diluted appropriately to obtain a linear response range of absorbance. The optical density of the diluted sample was measured at 600 nm using spectrophotometer (Hach, DR/2400). Freshly prepared, uninoculated, sterile media was used as a blank for zeroing. Measured optical densities were converted to dry cell mass concentration (x) using calibration curve of optical density versus biomass concentration (x) developed as described in the following section. Finally, specific growth rate, μ was calculated by non-linear regression analysis of Equation 6.2.

- ***Calibration curve of optical density versus biomass concentration***

Centrifuge tubes of 15 ml capacities were marked and dried to constant weight. The strain of *S.cerevisiae* was grown up to the end of logarithmic phase. 10 ml of this culture was pipetted into a pre-weighed centrifuge tube and the cells were separated by centrifugation using Biolab, 120 D centrifuge and after three washings with sterile deionized water, the cells were re-suspended in the sterile deionized water and the volume made up to 10 ml. Using this cell suspension, series of dilutions were made and the optical density of each one was determined. After obtaining the necessary dilutions, the cell suspensions were centrifuged at 5000 rpm for 15 minutes. The supernatant was removed carefully without loss of cells from the tubes and the washed cells were dried to constant weight in oven (Biotech) at 70⁰C and then each tube was weighed again. The difference in weight in each tube was the measure of total dry cell biomass weight in the suspension present in that tube. Finally, the calibration curve of optical density versus

biomass concentration, x (gm/ml) was obtained and used to calculate biomass concentration, x for each sample.

6.3.3.8 Estimation of total sugar consumption

Cell free supernatant obtained after centrifugation of the sample was used for the analysis of total sugar in % w/v of the sample. Cole's method (Appendix-7) was used for determination of total sugar i.e. sucrose concentration in the fermentation broth media containing sugar cane juice.

6.4 RESULTS AND DISCUSSION

Batch fermentation of *S.cerevisiae* was carried out in a shake flask, in a small bubble column for trial run, in RBC, in RDTBC with draft tubes of 70 cm and 60 cm height as well as in CDTBC of different sizes at different air flow rates to evaluate the performance of these devices. Cell biomass concentration, specific growth rate and sugar depletion in fermentation broth were the parameters for comparing production of baker's yeast in these column fermenters used in this investigation. Increase in optical density of fermentation broth corresponding to the increase in cell biomass concentration with time and the decline in the sugar concentration of fermentation broth with time was obtained during batch cultivation of baker's yeast in all these fermenters. Different extent of increase in biomass concentration and sugar depletion was observed for shake flask, bubble columns and draft tube bubble columns over a maximum cultivation period of 10 hours. The performance and scale up aspects of these fermenters were assessed and are elaborated in the following sections.

6.4.1 Effect of aeration and agitation on growth of baker's yeast

Preliminary batch studies on the production of baker's yeast revealed the effect of aeration and agitation on the growth of biomass and on sugar depletion rate. This data was obtained in a 500 ml shake flask and in the small bubble column at 4 LPM air flow rate. The increase in biomass concentration with cultivation time and the corresponding decrease in total sugar concentration with time during the trial runs in these fermenters are shown in Fig.6.6 and Fig.6.7.

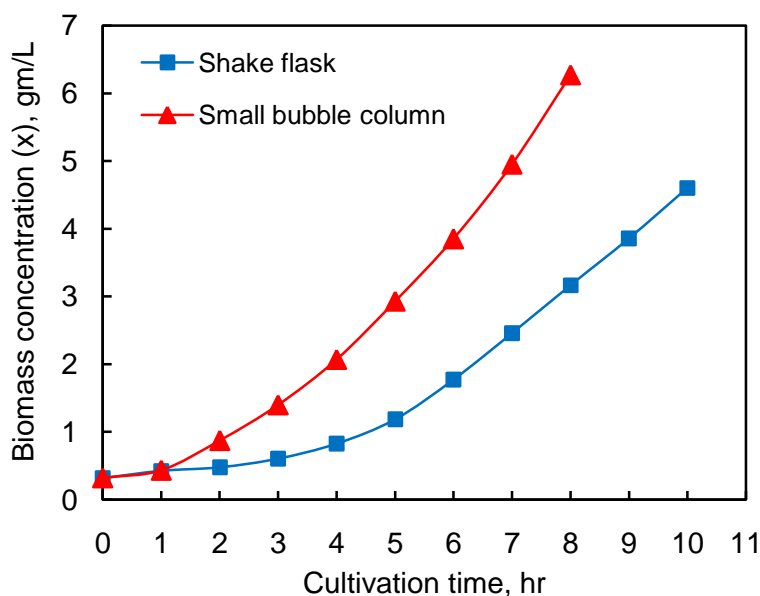


Fig. 6.6 Effect of aeration and agitation on growth rate of biomass

(Air flow rate in bubble column = 4 LPM)

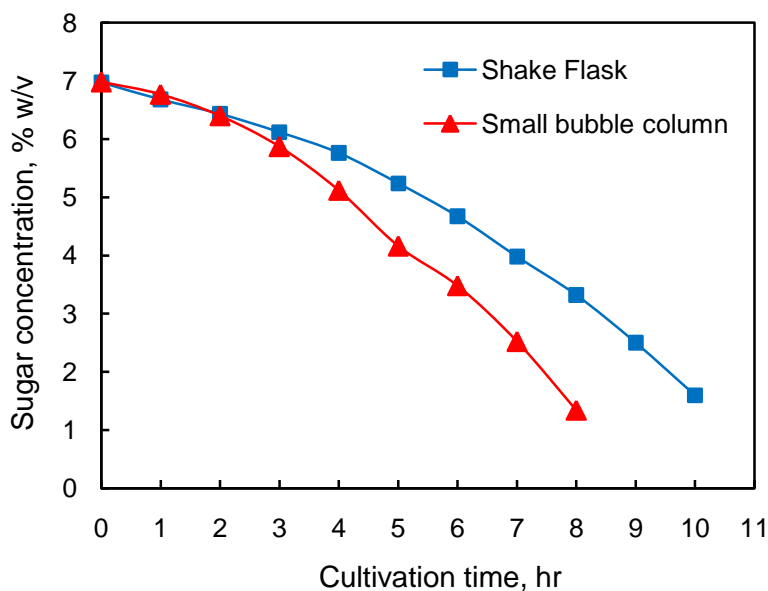


Fig. 6.7 Effect of aeration and agitation on sugar depletion rate

(Air flow rate in bubble column = 4 LPM)

It was observed that the growth rate of biomass as well as the rate of sugar depletion was significantly higher for bubble column compared to the shake flask. It is also observed in Fig.6.6 that the ultimate growth of yeast obtained in shake flask after 10 hr of cultivation time was obtained in just ~ 6.5 hr in small bubble column. The specific growth rates obtained in the shake flask was 0.285 h^{-1} compared to 0.38 h^{-1} obtained in the small bubble column. Hence, the performance of the shake flask was much poorer than the bubble column.

The superior performance of bubble column is attributed to greater extent of pneumatic aeration and agitation in bubble column. This aspect however is difficult to quantify but qualitatively it is rather obvious. Aeration supplies the necessary oxygen to the microorganisms, and agitation maintains uniform conditions within the fermenter altogether, the aeration and agitation are of prime importance for promoting effective mass transfer to liquid medium in the fermenter.

The production of baker's yeast being aerobic fermentation process requires high oxygen supply rate for the growth of cells. In shake flask, aeration and agitation are accomplished by the rotary or reciprocating action of the shaker apparatus, the oxygen supply in this device is restricted therefore the undesirable alcoholic metabolism sets in, this leads to a poor growth rate of the biomass, while in pneumatically agitated bubble columns, ample oxygen is supplied through sparger by compressed air with sufficient pneumatic agitation of fermentation broth for efficient growth of biomass.

Additionally, in the bubble column fermenters the agitation is accomplished pneumatically compared to mechanical agitation by agitators in conventional stirred tank fermenters, therefore the cells are not exposed to large variations in shear forces and are able to grow in a more stable physical environment, while in stirred tank reactors high shear conditions will arise near the impeller, causing cell damage and lower the productivity of biomass.

6.4.2 Effect of draft tube in a bubble column on cell biomass yield

Batch cultivation of *S.cerevisiae* was carried out in rectangular bubble column and rectangular draft tube bubble column to assess their performance for cell biomass yield and corresponding sugar depletion. Both these columns were operated at identical air flow rate of 4 LPM and using sparger C ($N_h = 4$, $d_h = 1$ mm, $P_t = 20$ mm) for aeration. The RDTBC was equipped with the 70 cm draft tube. Cultivation of baker's yeast in the RDTBC demonstrated relatively superior performance than RBC by reducing the cultivation time for achieving specific biomass concentration as shown in Fig. 6.8. It also led to more rapid depletion of sugar concentration achieving the targeted final sugar concentration almost an hour earlier as shown in Fig. 6.9.

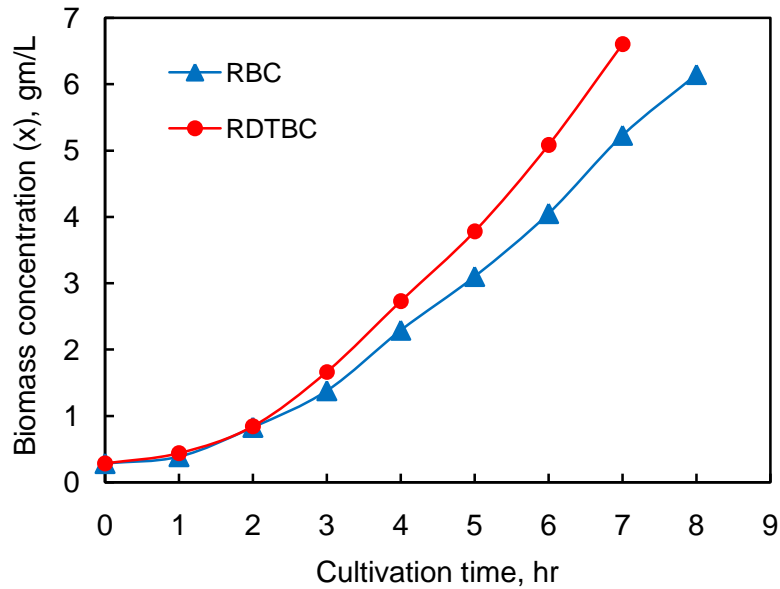


Fig. 6.8 Effect of insertion of draft tube on biomass production for RBC

(Air flow rate = 4 LPM; DT height = 70 cm; Sparger C)

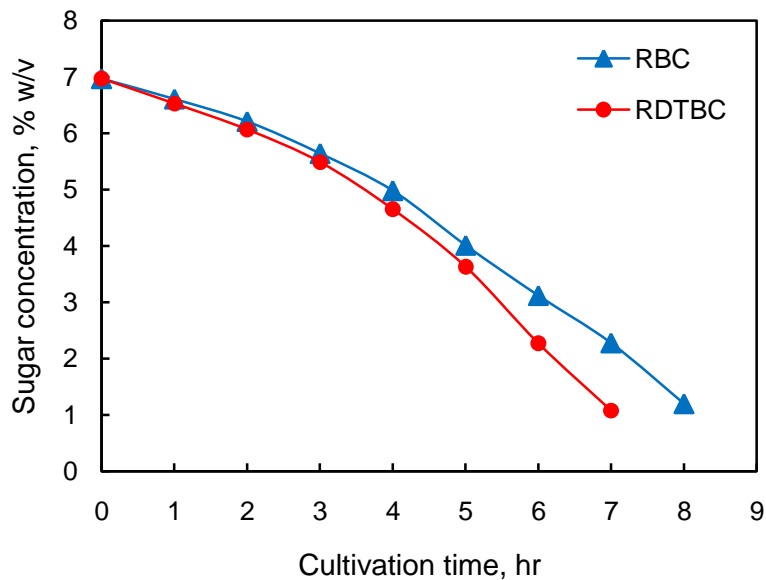


Fig. 6.9 Effect of insertion of draft tube on reducing sugar concentration for RBC

(Air flow rate = 4 LPM; DT height = 70 cm; Sparger C)

The superior performance of the draft tube column is attributed to the patterned gas flow in the device which induces a plug flow behavior in the gas as well as in the liquid although the riser region in the draft tube is more aerated in comparison to the annular region. Air flow rate of 4 LPM corresponds with superficial gas velocity U_g of 1.56 cm/s in bubble column under these conditions the gas holdup observed from Fig. 4.11, is 0.034 while in an RDTBC the gas holdup at the same flow rate turns out to be 0.06.

The corresponding values of specific gas-liquid interfacial area at U_g of 1.56 cm/s were 0.788 cm^{-1} for RDTBC and 0.542 cm^{-1} for RBC as shown in Fig. 4.24, while the $k_L a$ value turns out to be 0.468 min^{-1} in RDTBC. Thus the hydrodynamic and mass transfer characteristics of draft tube bubble column were superior to the bubble column which led to improved performance of the DTBC compared to ordinary bubble column.

The values of specific growth rates obtained for RBC was 0.401 h^{-1} , while that for RDTBC was 0.467 h^{-1} under otherwise similar conditions. It is noteworthy that the specific growth rates in rectangular draft tube bubble columns was 15% more than rectangular bubble column under identical conditions. Hence, it can be concluded that insertion of a draft tube in the bubble column enhances the growth of biomass and nutrient depletion due to its superior hydrodynamic and mass transfer characteristics.

6.4.3 Effect of draft tube height on specific growth rate in RDTBC

The effect of draft tube height on biomass production and total sugar consumption rates in RDTBC was obtained by conducting experimental runs in draft tube bubble columns with draft tube of 70 cm as well as 60 cm height. Fermentation in these devices was compared at identical air flow rate of 4 LPM ($U_{gr} = 8.33 \text{ cm/s}$), initial unaerated liquid height of 75 cm using sparger C. It can be seen from the Fig.6.10 that the final cell concentration after seven hours of fermentation in RDTBC with 70 cm draft tube was 20% greater than for RDTBC with 60 cm draft tube.

In Fig. 6.11, it is observed that the curves of sugar depletion for both these columns almost superimpose up to four hrs of cultivation time and then they diverge. The rate of sugar depletion in RDTBC with 70 cm draft tube was more rapid than that with the 60 cm draft tube. It shows that the draft tube height has a small effect on the overall performance of the column. The reason of better performance of RDTBC with 70 cm draft tube is attributed to the superior hydrodynamic and mass transfer characteristics observed with the longer draft tube at 4 LPM air flow rate as shown in Table below:-

Column	ϵ_g	$a \text{ (cm}^{-1}\text{)}$	$k_L a \text{ (min}^{-1}\text{)}$
RDTBC with 70 cm draft tube	0.0602	0.788	0.468
RDTBC with 60 cm draft tube	0.0409	0.682	0.346

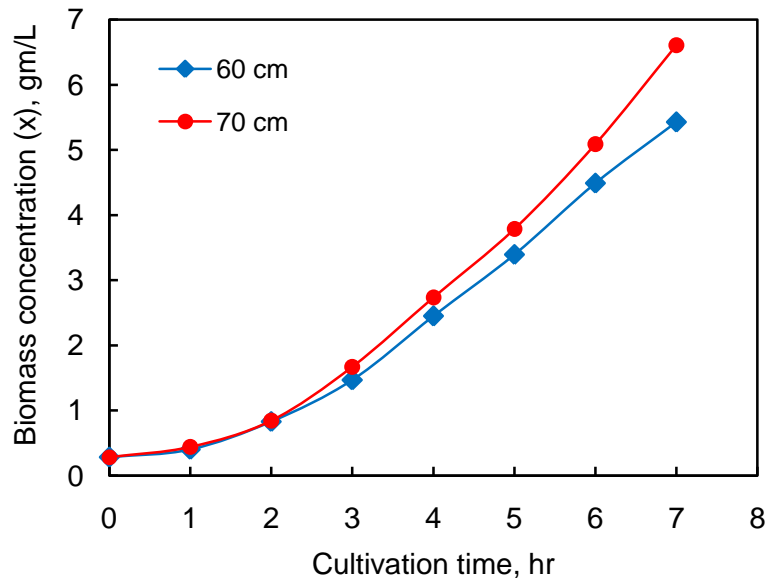


Fig. 6.10 Effect of draft tube height on biomass production rate in RDTBC

(Air flow rate = 4 LPM; Sparger C with $N_h = 4$)

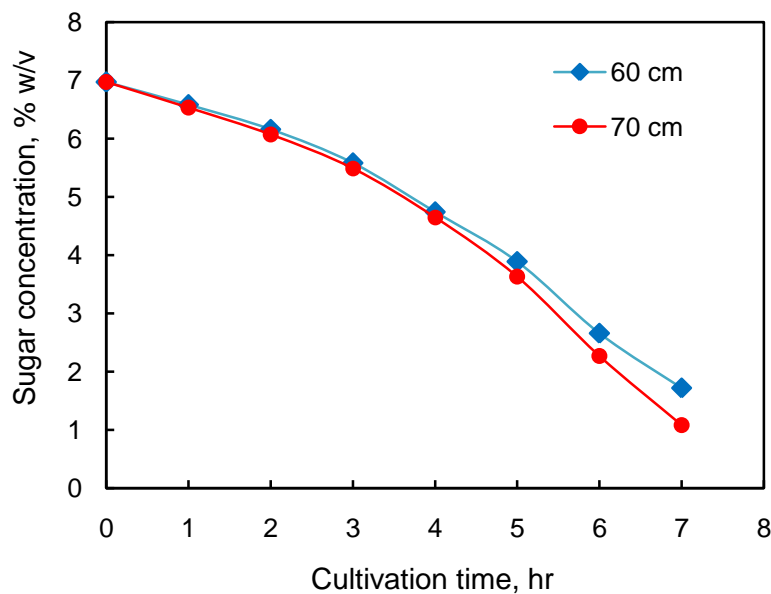


Fig. 6.11 Effect of draft tube height on total sugar consumption in RDTBC

(Air flow rate = 4 LPM; Sparger C with $N_h = 4$)

These factors primarily affect the aeration and mass transfer in these fermenters. The specific growth rate obtained for RDTBC with 70 cm draft tube and RDTBC with 60 cm draft tube were 0.467 h^{-1} and 0.445 h^{-1} respectively. Since, the value of specific growth rate for RDTBC with 60 cm draft tube height is greater than that of RBC (0.401 h^{-1}) but, lower than that of RDTBC with 70 cm draft tube, it indicates that RDTBC with 70 cm draft tube is superior among the three fermenters at identical air flow rate of 4 LPM.

Consequently, only the 70 cm draft tube was used for further investigation on baker's yeast production.

6.4.4 Effect of air flow rate on baker's yeast production in RDTBC

The effect of air flow rate on the biomass yield during baker's yeast fermentation and corresponding sugar consumption rate in RDTBC was investigated at three air flow rates, 2, 4 and 6 LPM corresponding to U_{gr} of 4.167, 8.333 and 12.5 cm/s respectively, using the four holed sparger C. The unaerated liquid height was kept 75 cm in the RDTBC and fermentation continued over a period of seven hours.

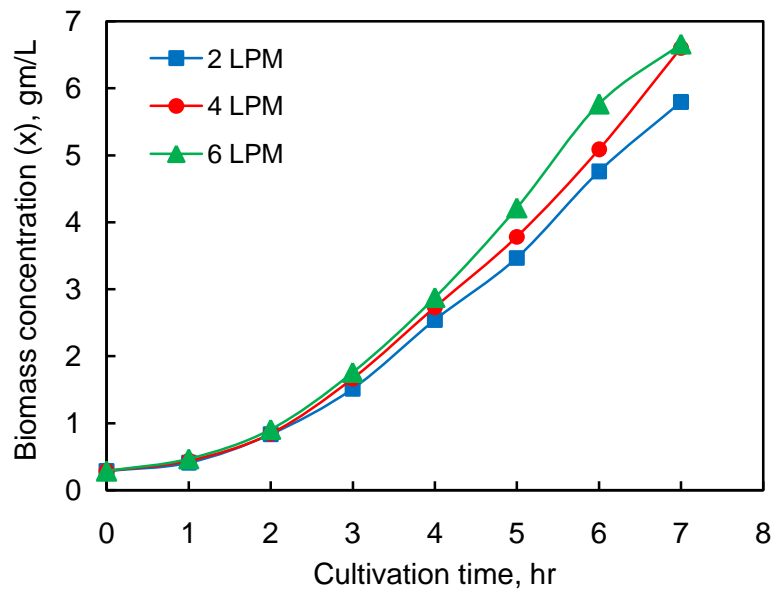


Fig. 6.12 Effect of air flow rate on biomass yield for RDTBC

(DT height = 70 cm; Sparger C with $N_h=4$)

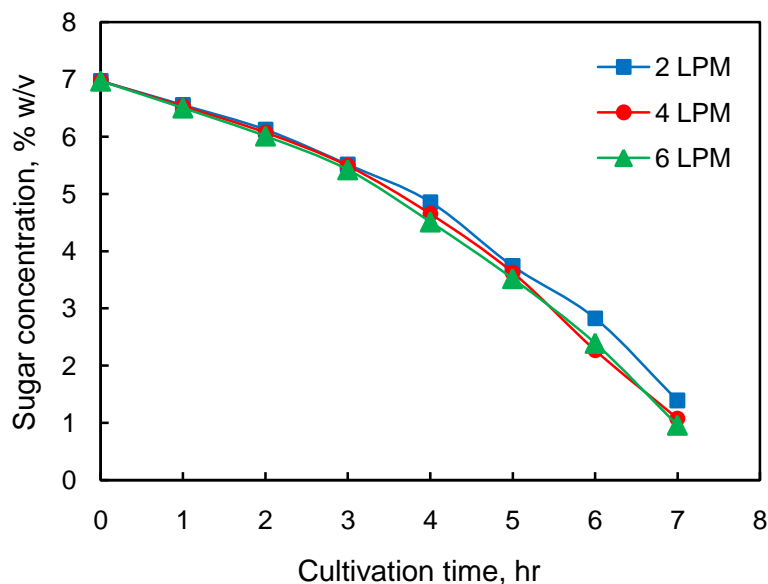


Fig. 6.13 Effect of air flow rate on sugar consumption rate for RDTBC

(DT height = 70 cm; Sparger C with $N_h=4$)

Increase in the gas flow rate caused a moderate increase in the biomass yield that became noticeable after four hours cultivation time as seen in Fig. 6.12. The values of specific growth rates were 0.454 h^{-1} , 0.467 h^{-1} and 0.472 h^{-1} for 2 LPM, 4 LPM and 6 LPM respectively. It is well known that the growth of *S. cerevisiae* depends on sufficient substrate supply and oxygen transfer under aerobic condition. Therefore, increase in specific growth rate of baker's yeast production with air flow rate was obviously due to supply of more oxygen in the fermenter.

The increase in air flow rate did not improve the cell production exceptionally as anticipated. This behavior of the fermentor during batch cultivation of baker's yeast is attributed to the continuous increase of cell mass concentration with time and the corresponding decrease of substrate concentration in the fermentation broth – processes governed by the oxygen transfer capability of the fermenter system. The decline in sugar concentration during fermentation is shown in Fig. 6.13. The depletion rates of sugar at gas rates of 4 LPM and 6 LPM are almost the same while at gas rate of 2 LPM the depletion rate of sugar is slightly less.

As the cell mass increases with increased aeration, the requirement for oxygen to sustain its growth increases but the oxygen transfer capability of the device does not keep pace with the rate of cell growth, as a result the yeast productivity approaches the limit of oxygen transfer capability thereby restricting the growth of biomass. In this situation the aerobic metabolic pathway tends to shift toward anaerobic pathways that result in formation of ethanol. Thus much advantage cannot be acquired in terms of cell productivity by increasing air flow rate in batch fermentation of *S. cerevisiae*. Hence, it is preferred to operate the fermenter at an air flow rate that is able to sustain the growth of yeast without being limited by the oxygen transfer capacity of the system. In this context the DTBC turns out to be a superior device than a bubble column since it provides larger gas holdups and interfacial areas than bubble columns at significantly lower aeration rates that eventually lead to greater oxygen transfer rates at lower gas velocities.

6.4.5 Effect of shape of draft tube bubble column on biomass production

The effect of geometrical shape of draft tube bubble column on the biomass productivity was determined by using a cylindrical shaped DTBC (CDTBC-1), having draft tube cross-sectional area similar to the rectangular draft tube ($\sim 8 \text{ cm}^2$) used in the RDTBC for the production of baker's yeast and comparing the results in both the devices. Both

the columns had 70 cm draft tubes, unaerated liquid height of 75 cm and spargers with four holes. The columns were operated at optimized air flow rate of 4 LPM, which corresponds to U_{gr} of 8.33 cm/s.

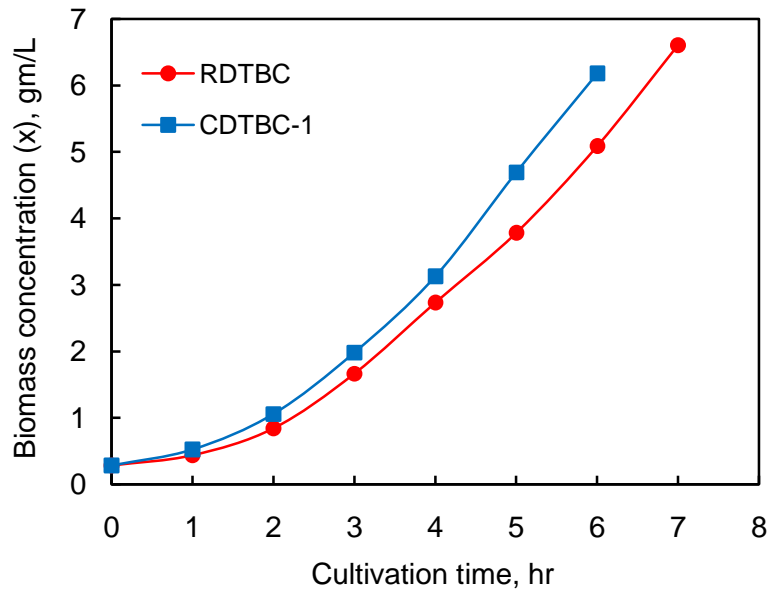


Fig. 6.14 Effect of geometrical shape of DTBC on baker's yeast production rate

(Air flow rate = 4 LPM; DT height = 70 cm; $A_r \sim 8 \text{ cm}^2$)

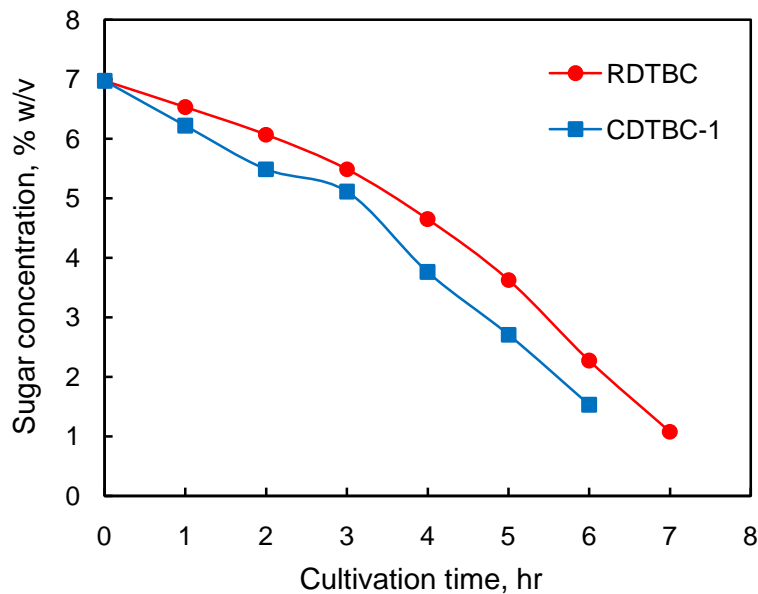


Fig. 6.15 Effect of geometrical shape of DTBC on reducing sugar of fermentation

broth (Air flow rate = 4 LPM; DT height = 70 cm; $A_r \sim 8 \text{ cm}^2$)

Fig. 6.14 shows rates of biomass production in both these devices and we find that the CDTBC-1 scores better, in the sense that the biomass growth rate is faster under identical conditions. Similarly, the drop in total sugar concentration in fermentation broth was greater in CDTBC-1 compared to RDTBC, as observed in Fig.6.15. Specific growth

rates obtained in these draft tube bubble columns 0.524 h^{-1} and 0.472 h^{-1} for cylindrical and rectangular geometries respectively.

The better performance of the cylindrical device over the rectangular one is contributed by the superior aeration conditions achieved in CDTBC-1. The key parameters contributing to this affect at 4 LPM ($U_{gr} = 8.33 \text{ cm/s}$) air flow rate are listed in the Table below:

Column	ϵ_g	$a \text{ (cm}^{-1}\text{)}$
RDTBC	0.0602	0.788
CDTBC-1	0.066	1.252

6.4.6 Effect of scale of operation in CDTBC on biomass productivity

The effect of scale of operation on production of baker's yeast was investigated by performing batch cultivation experiments under identical conditions in cylindrical draft tube bubble columns of different capacities. Column CDTBC-1 had a column ID of 6.4 cm and draft tube ID of 3.2 cm, the cross-sectional area of draft tube was 8.042 cm^2 , while column CDTBC-2 had an ID of 14 cm and draft tube ID of 8 cm the cross-sectional area of draft tube was 50.3 cm^2 . The height of column in both the cases was 1 meter and draft tube height was 70 cm. The unaerated liquid height was kept 75 cm in both cases which corresponded to a liquid capacity of 2.2 lit for CDTBC-1 and 10.5 lit for CDTBC-2.

In view of the much larger diameter of CDTBC-2, the aeration rates were scaled in a linear fashion. Since superficial gas velocity $U_{gr} = 8.33 \text{ cm/s}$ (flow rate of 4 LPM) gave optimal performance for biomass growth in RDTBC and the same was also used in CDTBC-1, hence experiments were performed in CDTBC-2 also at the same superficial gas velocities, which corresponded to 25 LPM air flow rate in CDTBC-2.

Under identical set of conditions, the rate of biomass production as well as sugar depletion was somewhat greater in CDTBC-2 than CDTBC-1 over fermentation duration of 6 hours, as shown in Fig. 6.16 and Fig. 6.17. Calculated specific growth rates for CDTBC-1 at 4 LPM and CDTBC- 2 at 25 LPM were 0.524 h^{-1} and 0.538 h^{-1} respectively. The slightly improved performance of CDTBC- 2 was attributed to higher total gas holdup in CDTBC- 2 in comparison with CDTBC-1 which were 0.082 and 0.066 respectively at $U_{gr} = 8.33 \text{ cm/s}$ (Fig. 4.18).

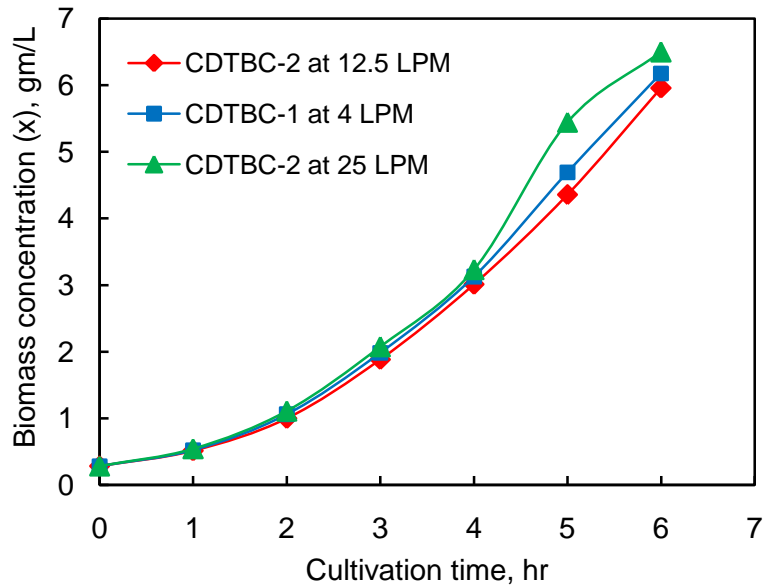


Fig. 6.16 Effect of scale of CDTBC on biomass production at varying air flow rates

(DT height = 70 cm; A_r of CDTBC-1 = 8.042 cm²; A_r of CDTBC-2 = 50.3 cm²)

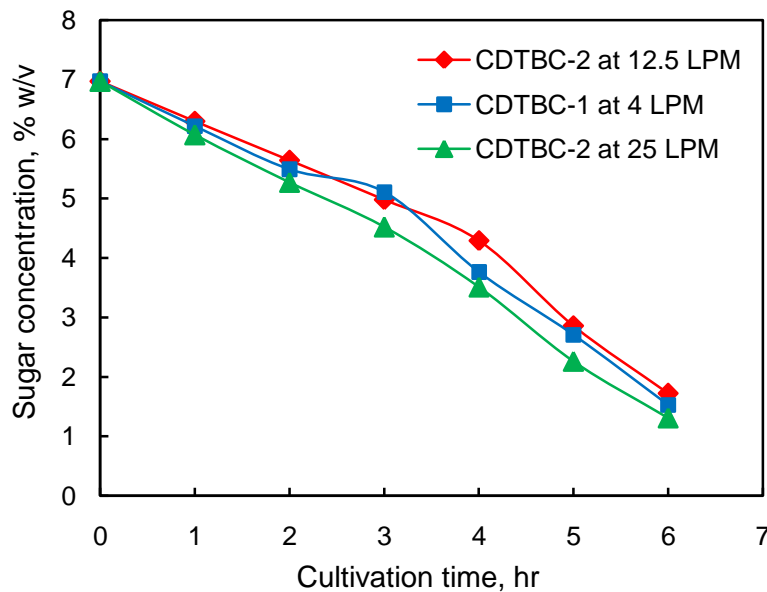


Fig. 6.17 Effect of scale of CDTBC on sugar depletion at varying air flow rates

(DT height = 70 cm; A_r of CDTBC-1 = 8.042 cm²; A_r of CDTBC-2 = 50.3 cm²)

The effect of air flow rate on biomass concentration in fermentation broth for production of baker's yeast was also investigated in CDTBC-2. Comparing the results obtained for $U_{gr} = 8.33$ cm/s and $U_{gr} = 4.14$ cm/s corresponding to air flow rates of 25 LPM and 12.5 LPM respectively as shown in Fig. 6.16 and Fig. 6.17, we observed the effect of decreasing air flow rate on cell productivity of baker's yeast in CDTBC-2, which turns out to be marginal in the same manner as observed earlier for RDTBC in section 6.4.4.

There was a slight decline in overall performance of CDTBC-2 by decreasing air flow rate as suggested by the values of specific growth rates that were 0.538 h^{-1} and 0.518 h^{-1} for 25 LPM and 12.5 LPM air flow rates respectively. This behaviour in large scale column is attributed to the aeration pattern and liquid circulations arising out of them.

6.5 CONCLUSIONS

Selection of appropriate fermenter is a key step in achieving maximization of biomass yield in cell cultivation. In this context, draft tube bubble column was found to be an efficient bioreactor for baker's yeast production due to its superior hydrodynamic and mass transfer characteristics particularly at relatively low superficial gas velocities. This work establishes the superiority of DTBC over bubble columns and shaking devices and comments on the efficacy of DTBC devices of different shapes and configurations.

The specific growth rates of exponential growth phase of these devices showed the pattern of

- Shake flask \ll RBC $<$ RDTBC $<$ CDTBC

The higher values of specific growth rates in bubble columns and draft tube bubble columns compared to shake flask is attributed to greater extent of pneumatic aeration in these columns. Between draft tube bubble column and bubble columns under identical conditions, DTBC gives greater growth rate due to greater gas holdup and interfacial areas in DTBC. Decreasing the draft tube height in DTBC resulted in the lower specific growth rates because the behaviour of DTBC approached bubble column behavior in the shorter draft tube device.

The specific growth rates of baker's yeast in DTBC at varying superficial velocities showed the following pattern:

- RDTBC : $12.5 \text{ cm/s (6 LPM)} > 8.333 \text{ cm/s (4 LPM)} > 4.167 \text{ cm/s (2 LPM)}$
- CDTBC-2 : $8.333 \text{ cm/s (25 LPM)} > 4.167 \text{ cm/s (12.5 LPM)}$.

CHAPTER 7

SUMMARY AND CONCLUSIONS

7.1 INTRODUCTION

Draft tube bubble columns offer numerous advantages over the conventional stirred tank reactor and bubble columns but their application in industries is not widespread. They were mostly used for single cell protein production but when the SCP project was commercially unsuccessful, this device was also nearly written off. Recently the use of DTBC was explored to some extent by environmental engineers for wastewater treatment. It is time not only to salvage the utility and applicability of this versatile device but to find new avenues for its use and proliferation.

A major cause for the current non applicability of this contactor stems from the ignorance of its behavior and dynamics. The objective of this work therefore was to investigate the hydrodynamics and mass transfer aspects of draft tube bubble columns so as to aid in the understanding of the behavior of DTBC, also to investigate the efficacy of a rectangular shaped device in comparison to the conventional cylindrical shaped ones for reasons listed in *Chapter1: Introduction*.

This thesis is oriented in a fashion that initially preliminary information of DTBC would be acquired with reference to key parameters like gas holdup, interfacial area and volumetric mass transfer coefficient, in relation with factors associated with design, geometry and operational conditions of these devices. Subsequent to this, the use of DTBC is focused on wastewater treatment and fermentation processes which are the most plausible candidate processes for DTBC applications.

The summary of the experimental work and significant conclusions drawn from these investigations are listed below:

7.2 EXPERIMENTAL

One rectangular and two cylindrical draft tube bubble columns were designed and fabricated for studying the effect of geometrical and operational parameters on hydrodynamics and mass transfer. These columns were made from transparent acrylic material to facilitate the observation of flow pattern of bubbles. The relevant column dimensions and areas are as follows:

Column	Parts	Specifications, cm		
		W	D	H
RDTBC $(A_r = 8 \text{ cm}^2, A_d = 26.96 \text{ cm}^2)$	Outer column	10.7	4	100
	Draft tube -1	8	1	70
	Draft tube - 2	8	1	60
		ID	OD	H
CDTBC-1 $(A_r = 8.042 \text{ cm}^2, A_d = 20.83 \text{ cm}^2)$	Outer column	6.4	7	100
	Draft tube	3.2	3.8	70
CDTBC-2 $(A_r = 50.3 \text{ cm}^2, A_d = 90.4 \text{ cm}^2)$	Outer column	14	15	100
	Draft tube	8	9	70

Volume expansion method was used for gas holdup measurements. The chemical method of sulfite oxidation was used for determination of interfacial area. The physical method of dynamic gassing in technique was used to evaluate volumetric mass transfer coefficients.

7.3 CHARACTERIZATION OF DRAFT TUBE BUBBLE COLUMNS

The significant findings of *Chapter 4: Hydrodynamic and mass transfer characteristics of draft tube bubble columns* are summarized as below:

- Visual observations in RDTBC revealed that sparger C having four holes each of 1 mm diameter and a pitch of 2 cm gave the most uniform distribution of gas bubbles over the entire cross-sectional area of the draft tube and throughout the travel path. Hence, sparger C was selected for further investigation. It was found that sparger design in general did not have much influence on gas holdup only variation of size of holes had significant effect.
- Draft tube height was found to be a key parameter influencing holdup, interfacial area and mass transfer coefficients, In general the DTBC is conceived to be made up of two regions, Region 1 extended from base up to the upper edge of draft tube and Region 2 extended between the upper edge of draft tube and dispersed liquid level. Shorter draft tube contributed to a large Region 2 where bubble column like behavior was prevalent. It was observed that shorter the draft tube more the DTBC resembled bubble column like behavior.

- At low gas flow rates bubble columns gave low holdup and interfacial areas in comparison with DTBC but at higher gas flow rates the behaviour was contrary to this as shown in Table 4.2.
- Cylindrical DTBC having same draft tube cross-sectional area as rectangular units at identical gas velocities resulted in nearly similar gas holdup but much larger interfacial areas indicating that gas holdups are more effective in CDTBC than RDTBC. Enhancing scale of operations at identical gas velocities resulted in larger holdup in the bigger column, but at the same time interfacial area was more in the smaller column, this was attributed to greater degree of bubble coalescence and clustering in the bigger column which handled large gas loads for attaining the same superficial velocities.
- Volumetric mass transfer coefficients in cylindrical columns appeared to be point specific in contrast in rectangular columns where the value of $k_L a$ appeared to be representative of the unit, perhaps because the liquid circulation in RDTBC was relatively rapid. Therefore the $k_L a$ profiles obtained in the RDTBC were used to get the values of k_L under identical conditions. The true mass transfer coefficient was correlated to superficial gas velocity as $k_L = 1.102 \times 10^{-3} U_{gr}$ for RDTBC with 70 cm draft tube.
- Existing correlations for gas holdup and $k_L a$ were fitted to the experimental data, the best fit for gas holdup was by the correlation of Popovic and Robinson, which gave an absolute error of 37.3 % and for $k_L a$ the best fit was by Chisti that gave an absolute error of 33.6%.

7.4 DTBC FOR WASTEWATER TREATMENT

Sewage water obtained from downstream of Athamiya River near village Motamava, Rajkot, contains fair amount of nutrients such as nitrogen and phosphorus. Typical analytical composition of this sewage water is as follows: Ammoniacal nitrogen - 49.7 mg/L, Phosphorus - 4.56 mg/L, BOD - 225 mg/L, COD - 450 mg/L, and SS - 250 mg/L etc. Nutrient removal from this water was attempted in draft tube bubble columns using activated sludge obtained from the sewage water treatment plant of Rajkot Municipal Corporation.

The manual phenate method 4500-NH₃ F, APHA (1998) was used to determine the concentration of ammoniacal nitrogen and the ascorbic acid method 4500-P E, APHA (1998) was used to determine the concentration of phosphates in the wastewaters.

The investigation on wastewater treatment using activated sludge in adequately characterized draft tube bubble columns reveals the following:

- The extent of removal of ammoniacal nitrogen using RDTBC with 70 cm draft tube is almost double (~ 80 %) in comparison to RBC (~ 40 %). Similarly, the enhancement in the removal of orthophosphate is 25 % more in RDTBC (~ 60 %) compared to RBC (~ 48 %). This improvement in DTBC is attributed to the sequential movement of liquid through two separate compartments - riser and annulus, which function as the aerobic and relatively anaerobic regions respectively for enhanced removal of nitrogen and phosphorus compounds from wastewaters as suggested by Barnard.
- The 70 cm draft tube height gave better results all through, difference in the RDTBC with 70 cm and 60 cm draft tube height was ~15 % for nitrogen removal and ~ 25% for phosphorus removal. The extent of nutrients removal decreased with increasing air flow rate; the removal of nitrogen was 80%, 45% and 38% at flow rates of 2, 4 and 6 LPM respectively. Similarly orthophosphate removal was 60%, 50% and 46% at gas rates of 2, 4 and 6 LPM respectively. This behavior is due to the enhanced aeration of annular space at higher gas flow rates that disturbs its anaerobic nature. Thus the draft tube height and superficial gas velocity are the governing parameters for enhanced removal of nutrients from sewage wastewater.
- Change of scale of operation from CDTBC-1 to the bigger sized CDTBC-2, while maintaining the same superficial gas velocity returns almost identical removal profiles, it is observed that the larger annulus space of CDTBC-2 induces better overall performance.
- It was found that synthetically prepared wastewaters of identical concentration as the sewage water gave similar results for nutrient removal in the RDTBC, suggesting device specific portability between field and laboratory data systems without substantial loss of information. However, data transfer across devices such as bubble column to draft tube bubble columns is not advisable without appropriate scaling.

7.5 DTBC – AS A FERMENTOR

The draft tube bubble columns that were appropriately characterized were employed for production of baker's yeast by fermentation. Cane sugar solution was used as the raw material. Batch fermentation protocol was developed in this investigation which involves preliminary development of inoculums, medium design and optimization, sterilization and secondarily production of baker's yeast in different columns. Biomass concentration of broth culture samples were obtained by measuring its absorbance, while sugar consumption was traced by using Cole's method.

The main function of a properly designed fermenter is to provide a controlled environment to achieve optimal product formation in the specific cell system employed. Successful commercial production of baker's yeast necessitates rapid growth and high biomass yield that can be achieved if the fermenter satisfies the requirements of adequate supply of oxygen and nutrients to the microorganisms and efficient gas-liquid mass transfer conditions at low shear.

The significant findings drawn from this investigation of production of baker's yeast in draft tube bubble columns are summarized as under:

- In preliminary studies bubble column gave higher specific growth rates (0.38 h^{-1}) than shake flask (0.285 h^{-1}) due to greater extent of pneumatic aeration.
- The specific growth rate in rectangular DTBC with 70 cm draft tube (0.467 h^{-1}) was 15% more than rectangular bubble column (0.401 h^{-1}), and is attributed to the superior hydrodynamic and mass transfer characteristics of DTBC. On the same lines, RDTBC with 60 cm draft tube resulted in specific growth rates (0.445 h^{-1}) intermediate between bubble column and DTBC with 70 cm draft tube. CDTBC-1 gave higher specific growth rates (0.524 h^{-1}) than RDTBC (0.467 h^{-1}) because of greater values of gas holdup and interfacial area at identical superficial gas velocities.
- The values of specific growth rates obtained in RDTBC were 0.454 h^{-1} , 0.467 h^{-1} and 0.472 h^{-1} for 2 LPM, 4 LPM and 6 LPM respectively, which indicates slight increase in baker's yeast production with air flow rate. This behavior is attributed to the limited oxygen transfer capability of RDTBC to cope up with substrate requirement of increased biomass at higher air flow rates in batch cultivation.

- Specific growth rates obtained for CDTBC-1 at 4 LPM and CDTBC- 2 at 25 LPM were 0.524 h^{-1} and 0.538 h^{-1} respectively. The slightly improved performance of CDTBC- 2 was attributed to higher total gas holdup in CDTBC- 2 in comparison with CDTBC-1 at identical superficial gas velocities.
- There was a slight decline in overall performance of CDTBC-2 by decreasing air flow rate as suggested by the values of specific growth rates that were 0.538 h^{-1} and 0.518 h^{-1} for 25 LPM and 12.5 LPM air flow rates respectively. This behaviour in large scale column was attributed to the aeration pattern and liquid circulations arising out of them.

Thus, this work establishes the superiority of DTBC over bubble columns and shaking devices and comments on the efficacy of DTBC devices of different shapes and configurations. It also establishes the operating conditions of draft tube bubble columns for the growth of baker's yeast. DTBC turns out to be an excellent candidate for such fermentation processes. The results of this investigation would help not only in selection of a fermenter but also for scale up of baker's yeast production at commercial scale.

7.6 SCOPE FOR FUTURE WORK

This investigation on draft tube bubble columns was undertaken with the objective to understand this device with respect to its hydrodynamic, mass transfer and application aspects. While providing information on these aspects this work also raises many questions that expand the scope of work in future. Some grey areas that need to be addressed in the future are the following:

- Role of draft tube height with reference to the unaerated liquid level in the device needs to be explored further.
- Effectiveness of the gas holdup in enhancing mass transfer in the device needs further investigation to understand the role of bubbles in the liquid above the draft tube. CFD analysis of draft tube bubble column could be a means to acquire appropriate information in this regard.
- How liquid circulation patterns differ in rectangular and cylindrical draft tube bubble columns? needs to be investigated experimentally as well by CFD analysis.

- In the course of the present investigation it was found that DTBC have a rather narrow range of interfacial area while the bubble column has a much wider range of interfacial area under the same set of operating conditions this aspect needs to be explored in greater detail. Similarly why cylindrical columns provide higher interfacial areas in the same set of conditions also needs to be explored.
- In spite of repetitive experiments it was observed that the nature of $k_L a$ profiles in rectangular and cylindrical DTBC were considerably different, the reason for this difference has to be sorted out.
- In addition to the dynamic gassing technique employed in this study other techniques such as sulfite oxidation, sodium dithionite oxidation etc. need to be investigated to check the efficacy of $k_L a$ measurements.
- Viscosity effects need to be investigated to gain deeper insight of column behavior during fermentation processes that lead to enhancement of viscosities, the entire hydrodynamic and mass transfer study using non-newtonian fluids may be investigated to get deeper insight into the actual fermentation behaviour.
- Effect of solids present on the behaviour of draft tube bubble column warrants to be explored, that will provide valuable information on three phase slurry draft tube bubble columns.
- Predictive correlations for holdup, interfacial area and mass transfer coefficients have to be developed or refined in light of new data.
- Application based design protocols need to be developed.

REFERENCES

- Akita K, Yoshida F. Gas holdup and volumetric mass transfer coefficients in bubble columns. *Ind Eng Chem Proc Des Dev.* 1973;12:76–80.
- Akita K, Yoshida F. Bubble size, interfacial area and liquid-phase mass transfer coefficient in bubble columns. *Ind Eng Chem Proc Des Dev.* 1974;12:76–80.
- Akita K, Kawasaki M. *Proceedings of the 48th Meet of Chem Engrs Jpn* Kyoto, Japan, 122–126, 1983.
- Alper E, Abu-Sharkh B. Kinetics of absorption of oxygen into aqueous sodium sulfite: order in oxygen. *AIChE J.* 1988;34(8):1384-1386.
- Andre G, Moo-Young M, Robinson CW. Improved method for the dynamic measurement of mass transfer coefficient for application to solid–substrate fermentation. *Biotechnol Bioeng.* 1981;23:1611-1622.
- APHA (American Public Health Association), *Standard Methods for the Examination of Water and Wastewater*, 20th ed. American Water Works Association and Water Environment Federation, Washington, DC, 1998.
- Argaman Y, Brener A. Single sludge nitrogen removal: modeling experimental results. *J Water Pollut Control Fed.* 1986;58:853-860.
- Astarita G, Marrucci G, Gioia F. The influence of carbonation ratio and total amine concentration on carbon dioxide absorption in aqueous monoethanolamine solutions. *Chem Eng Sci.* 1964;19(2):95-103.
- Balls A, Brown J. Studies in yeast metabolism - I. *J Biol Chem.* 1925;62:789-821.
- Bando Y, Nishimura M, Sota H, Suzuki S. Flow characteristics of counter current bubble column with perforated draft tube. *Chem Eng Sci.* 1992;47:3371-3378.
- Bando Y, Kato K, Yasuda K, Sakurai Y, Nakamura M. Wastewater treatment by anaerobic-aerobic activated sludge method in bubble column with draft tube. *J Chem Eng Jpn.* 1999;32(6):770-775.

- Barnard JL. Biological denitrification. *Water Pollut Control*. 1973;72:705-720.
- Barron CH, O'Hern HA. Reaction kinetics of sodium sulfite oxidation by the rapid-mixing method. *Chem Eng Sci*. 1966;21:397-404.
- Baykara ZS, Ulbrecht J. Gas-liquid mass transfer in bubble columns with aqueous polymer solutions. *Biotechnol Bioeng*. 1978;20(2);287-291
- Behkish A, Men Z, Inga RJ, Morsi BI. Mass transfer characteristics in a large scale slurry bubble column reactor with organic liquid mixtures. *Chem Eng Sci*. 2002;57:3307-3324.
- Bekatorou A, Psarianos C, Koutins A. Production of food grade yeasts. *Food Technol Biotech*. 2006;44:407-415.
- Bello RA. *A characterization study of airlift contactors for applications to fermentations*. Ph.D. thesis, University of Waterloo, Canada, 1981.
- Bello RA, Robinson CW, Moo-Young M. Gas holdup and overall volumetric oxygen transfer coefficient in airlift contactors. *Biotechnol Bioeng*. 1985a;27(3):369-381.
- Bello RA, Robinson CW, Moo-Young M. Prediction of the volumetric mass transfer coefficient in pneumatic contactors. *Chem Eng Sci*. 1985b;40(1):53-58.
- Bhattacharya BC, Ghosh TK, Maiti BR. Studies on mass transfer characteristics of a modified airlift fermenter. *Bioprocess Eng*. 1993;9:239-244.
- Blakebrough N, Shepherd PG, Nimmons I. Equipment for hydrocarbon fermentation. *Biotechnol Bioeng*. 1967;9:77-89.
- Botton R, Cosserrat D, Charpentier JC. Mass transfer in bubble columns operating at high gas throughputs. *The Chem Eng J*. 1980;20:87-94.
- Bouaifi M, Hebrard G, Bastoul D, Roustan M. A comparative study of gas holdup, bubble size, interfacial area and mass transfer coefficients in stirred gas-liquid reactors and bubble columns. *Chem Eng Process*. 2001;40:97-111.
- Bui-Dinh TT, Choi S. Application of image processing techniques in air/water two-phase flow. *Mech Res Commun*. 1999;26(4):463-468.

- Bukur DB, Daly JG. Gas holdup in bubble columns for Fischer–Tropsch synthesis. *Chem Eng Sci.* 1987;42:2967–2969.
- Buwa VV, Ranade VV, Dynamics of gas–liquid flow in a rectangular bubble column: experiments and single/multi-group CFD simulations. *Chem Eng Sci.* 2002;57:4715–4736.
- Cai J, Nieuwstad TJ, Kop JH. Fluidization and sedimentation of carrier material in a pilot-scale airlift internal loop reactor. *Water Sci Technol*, 1992;26(9-11):2481-2484.
- Carlsson H, Aspegren H, Lee N, Hilmer A. Calcium phosphate precipitation in biological phosphorous removal systems. *Wat Res.* 1997;31(5):1047-1055.
- Chakravarty M, Singh HD, Baruah JN, Lyengar MS. *Indian Chem Eng.* 1974;16:17-22.
- Chen SL, Chiger M. Production of baker's yeast. *Comprehensive Biotechnology: Vol. 3*,(Moo-Young M, Blanch HW, Drew S, Wang DIC,editors), New York: Elsevier. 1985:429-461.
- Chen NY. The design of airlift fermentors for use in biotechnology. *Biotechnol Genet Eng.* 1990;8:379-396.
- Chisti MY, Fujimoto K, Moo-Young M. Hydrodynamic and oxygen mass transfer studies in bubble columns and airlift bioreactors. *Biotechnology Processes: Scale-up and Mixing*, (Ho CS, Oldshue JY., editors), AIChE Publication. 1987:72-81.
- Chisti MY, Moo-Young M. Airlift reactors: characteristics, applications and design considerations. *Chem Eng Commun.* 1987;60:195-242.
- Chisti MY, Halard B, Moo-Young M. Liquid circulation in airlift reactors. *Chem Eng. Sci.* 1988; 43(3): 451-457.
- Chisti MY, Moo-Young M. Gas holdup in pneumatic reactors. *The Chem Eng J.* 1988;38:149-152.
- Chisti MY, Moo-Young M. Hydrodynamic and oxygen transfer in pneumatic bioreactor devices. *Biotechnol Bioeng.* 1988;31:487-494.
- Chisti MY. *Airlift Bioreactors*, New York: Elsevier, 1989.

Chisti Y, Kasper M, Moo-Young M. Mass transfer in external-loop airlift bioreactors using static mixers. *Can J Chem Eng.* 1990;68:45-50.

Chisti Y, Choi KH, Moo-Young M. Influence of the gas-liquid separator design on hydrodynamic and mass transfer performance of split-channel airlift reactors. *J Chem Tech Biotechnol.* 1995;62:327-332.

Cooper CM, Fernstrom GA, Miller SA. Performance of agitated gas-liquid contactors. *Ind Eng Chem.* 1944;36(6):504-509.

Daly JG, Bukur DB. Measurement of gas holdups and sauter mean bubble diameter in bubble column reactors by dynamic gas disengagement method. *Chem Eng Sci.* 1992; 47:3647-3654.

Danckwerts PV, Kennedy AM, Roberts D. Kinetics of CO₂ absorption in alkaline solutions-II: absorption in a packed column and tests of surface-renewal models. *Chem Eng Sci.* 1963;18:63-72.

Danckwerts PV, Sharma MM. Absorption of carbon dioxide into solutions of alkalis and amines. *The Chem Eng CE.* 1966;244-280.

Danckwerts PV. *Gas-Liquid reactions.* New York: McGraw-Hill, 1970.

De Waal, KJA, Okeson, JC. The oxidation of aqueous sodium sulphite solutions. *Chem Eng Sci.* 1966;21:559-572.

Deckwer WD, Burckhart R, Zoll G. Mixing and mass transfer in tall bubble columns. *Chem Eng Sci.* 1974;29:2177-2188.

Deckwer WD, Louisi Y, Zaidi A, Ralek M. Hydrodynamic properties of the Fisher-Tropsch slurry process. *Ind Eng Chem Proc Des Dev.* 1980;19:699-708.

Deckwer WD, Nguyen-Tien K, Schumpe A, Serpemen Y. Oxygen mass transfer into aerated CMC solutions in a bubble column. *Biotechnol Bioeng.* 1982;24:461-481.

Deckwer WD. *Bubble Column Reactors.* Chichester: Wiley, 1992.

Deen NG, Mudde RF, Kuipers JAM, Zehner P, Kraume M. Bubble columns. *Ullmann's Encyclopedia of Industrial Chemistry*, 7th ed. Wiley Publication. 2007.

- Doraiswami LK, Sharma MM. *Heterogeneous reactions: Vol. II*. New York: Wiley, 1984.
- Doran PM. *Bioprocess Engineering Principles*. San Diego: Elsevier, 1995.
- Eissa SH, Schugerl K. Holdup and backmixing investigations in concurrent and countercurrent bubble columns. *Chem Eng Sci*. 1975;30:1251-1256.
- Ejiofor AO, Poston CH, Solomon BO, Deckwer WD. A robust fed-batch feeding strategy for optimal parameter estimation for baker's yeast production. *Bioprocess Eng*. 1994;11:135-144.
- El-Temtamy SA, Khalil SA, Nour-El-Din AA, Gaber A. Oxygen mass transfer in a bubble column bioreactor containing lysed yeast suspensions. *Appl Microbiol Biotechnol*. 1984;19: 376-381.
- Enfors SO, Hedenberg J, Olsson K. Simulation of the dynamics in the baker's yeast process. *Bioprocess Eng*. 1990; 5:191-198.
- Erickson LE, Patel SA, Glasgow LA, Lee CH. Effect of viscosity and small bubble segregation on mass transfer in airlift fermenters. *Process Biochem*. 1983;18(3):16-19.
- Fair JR, Lambright AJ, Anderson JW. Heat transfer and Gas holdup in a sparged contactor. *Ind Eng Chem Proc Des Dev*. 1962;1:33-36.
- Fan LS, Matsuura A, Chern SS. Hydrodynamic characteristics of a gas-liquid-solid fluidized bed containing a binary mixture of particles. *AIChE J*. 1985;31:1801-1810.
- Farizoglu B, Keskinler B. Influence of draft tube cross-sectional geometry on $k_L a$ and ε in jet loop bioreactors. *Chem Eng J*. 2007;133:293-299.
- Ferrari MD, Bianco R, Froche C, Loperena ML. Baker's yeast production from molasses/cheese whey mixtures. *Biotechnol Lett*. 2001;23:1-4.
- Franco-Lara E, Krull R, Hempel DC, Haarstrick A. Specification and supervision of system performance in yeast bioprocesses. *Chem Biochem Eng Q*. 2007;21(4):335-344.
- Fukuma M, Muroyama K, Morooka S. Properties of bubble swarm in a slurry bubble column. *J Chem Eng Jpn*. 1987;20:28-33.

- Gallo T, Sandford DS. The application of deep shaft technology to the treatment of high-strength industrial waste water. *86th National Meeting of AIChE*, Houston, Texas; 1-5 April, 1979.
- Gasner LL. Development and application of the thin channel rectangular airlift mass transfer reactor to fermentation and waste-water treatment systems. *Biotechnol Bioeng*. 1974;16:1179-1195.
- George S, Larsson G, Olsson K, Enfors SO. Comparison of the baker's yeast process performance in laboratory and production scale. *Bioprocess Eng*. 1998;18:135-142.
- Godbole SP, Honath MF, Shah YT. Holdup structure in highly viscous newtonian and non-newtonian liquids in bubble columns. *Chem Eng Commun*. 1982;16:119-134.
- Gouveia ER, Hokka CO, Badino jnr AC. The effects of geometry and operational conditions on gas holdup, liquid circulation and mass transfer in airlift reactor. *Braz J Chem Eng*. 2003;20:363-374.
- Govindarao VMH. On the dynamics of bubble column slurry reactors. *Chem Eng J*. 1975;9:229-240.
- Graen-Heedfeld J, Schlueter S. Gas circulation in internal airlift loop reactors. *Chem Eng Technol*. 2000;23(12):1051-1055.
- Grover GS, Rode CV, Chaudrai RV. Effect of temperature on flow regimes and gas holdup in a bubble column. *Can J Chem Eng*. 1986;64:501-504.
- Han P, Tang L, Huang Y, Ouyang P. Experimental study on the hydrodynamics and mass transfer characteristics of ultrasonic loop airlift reactor. *Can J Chem Eng*. 2005;83:204-211.
- Hano T, Matsumoto M, Kuribayashi K, Hatate Y. Biological nitrogen removal in a bubble column with a draft tube. *Chem Eng Sci*. 1992;47(13/14):3737-3744.
- Hatch RT, Cuevas C, Wang DIC. Oxygen absorption rates in airlift fermentors: laboratory and pilot studies. *Paper presented at the 158th National American Chemical Society Meeting*. New York; 8 September 1969.

- Hatch RT. Fermentor design. *Single Cell Protein*, II, (Tannenbaum SR, Wang DIC, editors), The MIT press, Cambridge. 1975;2:46-68.
- Heijnen JJ, Van't Riet K. Mass transfer, mixing and heat transfer phenomena in low viscosity bubble column reactors. *Chem Eng J*. 1984;28:B21-B42.
- Hikita H, Kikukawa H. Liquid phase mixing in bubble columns: effect of liquid properties. *Chem Eng J*. 1974;8:191-197.
- Hikita H, Asai S, Tanigawa K, Segawa K, Kitao M. Gas holdup in bubble column. *Chem Eng J*. 1980;20:59-67.
- Hikita H, Asal S, Kikukawa H, Zalke T, Ohue M. Heat transfer coefficient in bubble column. *Ind Eng Chem Proc Des Dev* 1981;20:540-545.
- Hills JH. The operation of a bubble column at high throughputs - I. Gas holdup measurements. *Chem Eng*. 1976;12:89-99.
- Hines DA, Bailey M, Ousby JC, Roesler FC. The ICI deep shaft aeration process for effluent treatment. *ICHEME Conference*, York, England; 16-17 April, 1975.
- Ho CS, Erickson LE, Fan LT. Modeling and simulation of oxygen transfer in airlift fermentors. *Biotechnol Bioeng*. 1977;19:1503-1522.
- Hofmann H. Packed up-flow bubble columns. *Chem Ing Techn*. 1982;54:865-876.
- Hsiun DY, Wu WT. Mass transfer and liquid mixing in an airlift reactor with a net draft tube. *Bioprocess Eng*. 1995;12:221-225.
- Hsu KH, Erickson LE, Fan LT. Oxygen transfer to mixed cultures in tower systems. *Biotechnol Bioeng*. 1975;17:499-514.
- Huang SY, Yeh MC, Liou KT. Performance in mixing in cell mass propagation of air lift fermentor. pp. 668 *Abstracts: Fifth International Fermentation Symposium*, Berlin; 1976.
- Hughmark GA. Holdup and mass transfer in bubble columns. *Ind Eng Chem Proc Des Dev*. 1967;6:218-220.

- Hyndman CL, Larachi F, Guy C. Understanding gas-phase hydrodynamics in bubble columns: a convective model based on kinetic theory. *Chem Eng Sci.* 1997;52:63–77.
- Jhaveri AS, Sharma MM. Kinetic of absorption of oxygen in aqueous solutions of cuprous chloride. *Chem Eng Sci.* 1967;22(1):1-6.
- Jhaveri AS, Sharma MM. Absorption of oxygen in aqueous alkaline solutions of sodium dithionite. *Chem Eng Sci.* 1968;23:1-8.
- Jin B, Lant P. Flow regime, hydrodynamics, floc size distribution and sludge properties in activated sludge bubble column, airlift and aerated stirred reactors. *Chem Eng Sci.* 2004;59:2379-2388.
- John W. *Yeast Technology*. New York: McGraw-Hill, 1954.
- Joshi JB, Sharma MM. A Circulation cell model for bubble columns. *Trans Inst Chem Eng.* 1979;57:244–251.
- Joshi JB, Vitankar VS, Kulkarni AA, Dhotre MT, Ekambara K. Coherent flow structures in bubble column reactors. *Chem Eng Sci.* 2002;57(16):3157-3183.
- Joshi JB, Kulkarni AA. Simultaneous measurement of flow pattern and mass transfer coefficient in bubble columns. *Chem Eng Sci.* 2004;59:271-281.
- Joshi JB, Ekambara K, Dhotre MT. CFD simulations of bubble column reactors: 1D, 2D and 3D approach. *Chem Eng Sci.* 2005;60:6733-6746.
- Kang Y, Cho YJ, Woo KJ, Kim SD. Diagnosis of bubble distribution and mass transfer in pressurized bubble columns with viscous liquid medium. *Chem Eng Sci.* 1999;54:4887-4893.
- Kara S, Kelkar BG, Shah YT, Carr NL. Hydrodynamics and axial mixing in a three-phase bubble column. *Ind Eng Chem Proc Des Dev.* 1982;21:584–594.
- Karakuzu C, Turker M, Ozturk S. Modeling, on-line state estimation and fuzzy control of production scale fed-batch baker's yeast fermentation. *Control Eng Pract.* 2006;14:959-974.

- Kastnek F, Zahradnik J, Kratochvil J, Cermak J. *Chemical Reactors for Gas-Liquid Systems*, Prague: Academia, 1993.
- Kawagoe M, Nakao K, Otake T. Liquid-phase mass transfer coefficient and bubble size in gas sparged contactors. *J Chem Eng Jpn.* 1975;8:254-256.
- Kawase Y, Moo-Young M. Influence of non-newtonian flow behavior on mass transfer in bubble columns with and without draft tubes. *Chem Eng Commun.* 1986a;40:67-83.
- Kawase Y, Moo-Young M. Mixing and mass transfer in concentric-tube airlift fermenters: Newtonian and non-newtonian media. *J Chem Technol Biot.* 1986b;36:527-553.
- Kawase Y, Halard B, Moo-Young M. Theoretical prediction of volumetric mass transfer coefficients in bubble columns for newtonian and non-newtonian fluids. *Chem Eng Sci.* 1987;42:1609-1617.
- Kawase Y, Moo-Young M. Heat transfer in bubble column reactors with Newtonian and non-Newtonian fluids. *Chem Eng Res Des.* 1987;65:121-126.
- Kawase Y, Moo-Young M. Volumetric mass transfer coefficients in aerated stirred tank reactors with newtonian and non-newtonian media. *Chem Eng Res Des.* 1988;66:284-288.
- Kawase Y, Umeno S, Kumagai T. The prediction of gas holdup in bubble column reactors: newtonian and non-newtonian fluids. *Chem Eng J.* 1992;50(1):1-7.
- Kawase Y, Tsujimura M, Yamaguchi T. Gas holdup in external-loop airlift bioreactors. *Bioproc Eng.* 1995;12:21-27.
- Kelkar BG, Shah YT, Carr NL. Hydrodynamics and axial mixing in a three phase bubble column: Effects of slurry properties. *Ind Eng Chem Proc Des Dev.* 1984;23:308-313.
- Kilonzo PM, Margaritis A, Bergougnou MA, Yu J, Ye Q. Effects of geometrical design on hydrodynamics and mass transfer characteristics of a rectangular-column airlift bioreactor. *Biochem Eng J.* 2007;34:279-288.
- Koenig B, Seewald C, Schugerl K. Penicillin production in a bubble column airlift loop reactor. *Adv Biotechnol.* 1981;1:573-579.

- Koide K, Morooka S, Ueyama K, Matsuura A. Behavior of bubbles in large scale bubble column. *J Chem Eng Jpn.* 1979;12:98–104.
- Koide K, Kurematsu K, Iwamoto S, Iwata Y, Horibe K. Gas holdup and volumetric liquid-phase mass transfer coefficient in bubble column with draught tube and with gas dispersion into tube. *J Chem Eng Jpn.* 1983;16(5):413-419.
- Koide K, Sato H, Iwamoto S. Gas holdup and volumetric liquid phase mass transfer coefficient in bubble column with draught tube and with gas dispersion into annulus. *J Chem Eng Jpn.* 1983a;16(5):407-413.
- Koide K, Takazawa A, Komura M, Matsunga H. Gas holdup and volumetric liquid phase mass transfer coefficient in solid-suspended bubble column. *J Chem Eng Jpn.* 1984;17:459–466.
- Koide K, Horibe K, Kawabata H, Ito S. Gas holdup and volumetric liquid-phase mass transfer coefficient in solid-suspended bubble column with draught tube. *J Chem Eng Jpn.* 1985;18(3):248-254.
- Koide K, Yamazoe S, Harada S. Effects of surface-active substances on gas holdup and gas-liquid mass transfer in bubble column. *J Chem Eng Jpn.* 1985;4:287-292.
- Koide K, Kimura M, Nitta H, Kawabata H. Liquid circulation in bubble column with draught tube. *J Chem Eng Jpn.* 1988;21(4):393-399.
- Kojima H, Okumara B, Nakamura A. Effect of pressure on gas holdup in bubble column and a slurry bubble column. *J Chem Eng Jpn.* 1991;24:115-117.
- Krishna R, De Stewart JWA, Ellenberger J, Martina GB, Maretto C. Gas holdup in slurry bubble columns: Effect of column diameter and slurry concentration. *AIChE J.* 1997;43:311-316.
- Kulkarni AA, Joshi JB, Ravikumar V, Kulkarni BD. Simultaneous measurement of holdup profiles and interfacial area using LDA in bubble columns: predictions by multiresolution analysis and comparison with experiments. *Chem Eng Sci.* 2001;56:6437-6445.

- Kumar A, Dageleesan TE, Ladda GS. Bubble swarm characteristics in bubble columns. *Can J Chem Eng.* 1976;54:503–508.
- Laari A, Kallas J, Palosaari S. Gas–liquid mass transfer in bubble columns with a T– Junction nozzle for gas dispersion. *Chem Eng Technol.* 1997;20:550-556.
- Ladha SS, Danckwerts PV. Reaction of CO₂ with ethanalamines: kinetics from gas-absorption. *Chem Eng Sci.* 1981;36(3):479-482.
- Li GQ, Yang SZ, Cai ZL, Chen JY. Mass transfer and gas-liquid circulation in an airlift bioreactor with viscous non-newtonian fluids. *Chem Eng J.* 1995;56:B101-B107.
- Li H, Prakash A. Heat transfer and hydrodynamics in a three-phase slurry bubble column. *Ind Eng Chem Res.* 1997;36:4688–4694.
- Li H, Prakash A. Influence of slurry concentration on bubble population and their rise velocities in three phase slurry bubble column. *Powder Technol.* 2000;113:158-167.
- Linek V. The oxidation of aqueous sulphite solutions. *Chem Eng Sci.* 1971;26:491-494.
- Linek V, Vacek V. Chemical engineering use of catalyzed sulfate oxidation kinetics for the determination of mass transfer characteristics of gas-liquid contactors. *Chem Eng Sci.* 1981;36(11):1747-1768.
- Linek V, Vacek V, Benes P. A critical review and experimental verification of the correct use of the dynamic method for the determination of oxygen transfer in aerated agitated vessels to water, electrolyte solution and viscous liquids. *Chem Eng.* 1987;34:11-34.
- Lockett MJ, Kirkpatrick RD. Ideal bubbly flow and actual flow in bubble columns. *Trans Inst Chem Eng.* 1975;53:267–273.
- Lu X, Ding J, Wang Y, Shi J. Comparison of the hydrodynamics and mass transfer characteristics of a modified square airlift reactor with common airlift reactors. *Chem Eng Sci.* 2000;55:2257-2263.
- Luo X, Lee DJ, Lau R, Yang G, Fan L. Maximum stable bubble size and gas holdup in high pressure slurry bubble columns. *AIChE J.* 1999;45:665–685.

- Maclean GF, Erickson LE, Hsu KH, Fan LT. Oxygen transfer and axial dispersion in an aeration tower containing static mixers. *Biotechnol Bioeng.* 1977;19:493-505.
- Malfait JL, Wilcox DJ, Mercer DG, Barker LD. Cultivation of a filamentous mold in a glass pilot scale fermentor. *Biotechnol Bioeng.* 1981;23:863-877.
- Markl H, Bronnenmeier R, Wittek B. Hydrodynamic stress resistance of microorganisms. *Chem Ing Techn.* 1987;59:907-917.
- McManamey WJ, Wase DJ. Relationship between the volumetric mass transfer coefficient and gas holdup in airlift fermenters. *Biotechnol Bioeng.* 1986;28:1446-1448.
- Medic L, Cehovin A, Koloini T, Pavko A. Volumetric gas-liquid mass transfer coefficients in a rectangular bubble column with rubber aeration pad. *The Chem Eng J.* 1989;41:B51-B54.
- Meng L, Bando Y, Nakamura M. Dissolved oxygen distribution in a rectangular airlift bubble column for biological nitrogen removal. *J Chem Eng Jpn.* 2004a;37(8):1005-1011.
- Meng L, Tsuno N, Bando Y, Nakamura M. Enhancement of nitrogen removal in a rectangular airlift bubble column having aerobic and anaerobic regions by adding an immobilizing carrier. *J Chem Eng Jpn.* 2004b;37(3):399-405.
- Meng L, Bando Y, Nakamura M. Development of rectangular airlift bubble column installed with support material for enhancement of nitrogen removal. *J Biosci Bioeng.* 2004c;98(4):269-273.
- Merchuk JC. Hydrodynamics and holdup in air-lift reactors. *Encyclopedia of Fluid Mechanics*, (Cheremisinoff NP., editor), Gulf Publishing, Houston. 1986;3:1485-1511.
- Merchuk JC, Ben-zvi S. A novel approach to the co-relation of mass transfer rates in bubble columns with non-newtonian liquids. *Chem Eng Sci.* 1992;47:3517-3523.
- Merchuk JC, Ladwa N, Cameron A, Bulmer M, Pickett A. Concentric-tube airlift reactors: effects of geometrical design on performance. *AIChE J.* 1994;40(7):1105-1117.
- Miller DN. Interfacial Area, bubble coalescence and mass transfer in bubble column reactors. *AIChE J.* 1983;29:312-319.

- Miyahara T, Hamaguchi M, Sukeda Y, Takehashi T. Size of bubbles and liquid circulation in a bubble column with draught tube and sieve plate. *Can J Chem Eng.* 1986;64:718-725.
- Moresi M. Optimal design of airlift fermenters. *Biotechnol Bioeng.* 1981; 23: 2537-2560.
- Mouza AA, Dalakoglou GK, Paras SV. Effect of liquid properties on the performance of bubble column reactors with fine pore spargers. *Chem Eng Sci.* 2005;60:1465-1475.
- Mouza AA, Kazakis NA, Papadopoulos ID. Bubble columns with fine pore sparger operating in the pseudo-homogeneous regime: Gas holdup prediction and a criterion for the transition to the heterogeneous regime. *Chem Eng Sci.* 2007;62:3092-3103.
- Muller FL, Davidson F. On the effects of surfactants on mass transfer to viscous liquids in bubble columns. *Chem Eng Res Des.* 1995;73:291.
- Nakanoh M, Yoshida F. Gas absorption by newtonian and non-newtonian liquids in a bubble column. *Ind Eng Chem Proc Des Dev.* 1980;19:190-195.
- Nakanoh M, Yoshida F. Transient characteristics of oxygen probes and determination of k_{La} . *Biotechnol Bioeng.* 1983;25:1653-1654.
- Ozturk SS, Schumpe A, Deckwer WD. Organic liquids in a bubble column: holdups and mass transfer coefficients. *AIChE J.* 1987;33:1473-1480.
- Phaff HJ. Isolation of yeasts from natural sources. *Isolation of Biotechnological organism from nature*, (Labeda DP editor), New York, McGraw-Hill, 1990:53-79.
- Piggott AM. *Mass transfer and mixing in airlift columns*. MASC Thesis, University of Waterloo, Ontario. 1985.
- Pino LZ, Solari RB, Siquier S, Estevez LA, Yopez MM. Effect of operating conditions on gas holdup in slurry bubble columns with a foaming liquid. *Chem Eng Commun.* 1992;117:367-382.
- Pironti FF, Medina VR, Calvo R, Saez AE. Effect of draft tube position on the hydrodynamics of a draft tube slurry bubble column. *The Chem Eng Biochem Eng J.* 1995;60:155-160.

- Polli M, Stanisalo MD, Bagatin R, Bakr EA, Masi M. Bubble size distribution in the sparger region of bubble columns. *Chem Eng Sci.* 2002;57:197-205.
- Popovic M, Robinson CW. Estimation of some important design parameters for non newtonian liquids in pneumatically-agitated fermenters. *Proceedings of the 34th Canadian Chemical Engineering Conference*, Quebec City, Canada, 258-264, 1984.
- Popovic M, Robinson CW. The specific interfacial area in external-circulation-loop airlifts and a bubble column-I: aqueous sodium sulphite solution. *Chem Eng Sci.* 1987;42(12): 2811-2824.
- Prakash A, Margarities A, Li H. Hydrodynamics and local heat transfer measurement in bubble column with suspension of yeast. *Biochem Eng.* 2001;9:155-163.
- Prasher BD, Wills GB. Mass transfer in an agitated vessel. *Ind Eng Chem Proc Des Dev.* 1973;12(3):351-354.
- Redman J. Deep shaft treatment for sewage. *The Chemical Engineer.* 1987;October: pp.12-13.
- Reilley IG, Scott DS, De Bruijin T, Jain A, Piskorz J. A correlation for gas holdup in turbulent coalescing bubble columns. *Can J Chem Eng.* 1986;64:705-717.
- Roy NK, Guha DK, Rao MN. Fractional gas holdup in two-phase and three-phase batch-fluidized bubble-bed and foam-systems. *Indian Chem Eng.* 1963;27-31.
- Royse S. Scaling up for mammalian cell culture. *The Chemical Engineer.* 1987; November: pp. 12-13.
- Ruzicka MC, Drahos J, Fialova M, Thomas NH. Effect of bubble column dimensions on flow regime transition. *Chem Eng Sci.* 2001;56:6117-6124.
- Sada E, Katoh S, Yoshil H. Performance of the gas liquid bubble column in molten salt systems. *Ind Eng Chem Proc Des Dev.* 1984;23:151-154.
- Sada E, Kumazawa H, Lee CH, Narukawa H. Gas-liquid interfacial area and liquid-side mass transfer coefficient in a slurry bubble column improving mass transfer coefficient. *Ind Eng Chem Res.* 1987;26:112-116.

- Santacesaria E, Serio MD, Tesser R. A kinetic and mass transfer model to simulate the growth of baker's yeast in industrial bioreactors. *Chem Eng J*. 2001;82:347-354.
- Saxena SC, Rao NS, Saxena AC. Heat transfer and gas holdup studies in bubble column: air-water-glass bead system. *Chem Eng Commun*. 1990;96:31-55.
- Schluter S, Steiff A, Weinspach PM. Modeling and simulation of bubble column reactors. *Chem Eng Process*. 1992;31:97-117.
- Schultz JS, Gaden EL. Sulfite oxidation as a measure of aeration effectiveness. *Ind Eng Chem*. 1956;48(12):2209-2212.
- Schumpe A, Grund G. The gas disengagement technique for studying gas holdup structure in bubble columns. *Can J Chem Eng*. 1986;64:891-896.
- Schumpe A, Deckwer WD. Viscous media in tower bioreactors: hydrodynamic characteristics and mass transfer properties. *Bioprocess Eng*. 1987;2:79-94.
- Schumpe A, Grund G, Deckwer WD. Gas-liquid mass transfer in a bubble column with organic liquids. *Chem Eng Sci*. 1992;47:3509-3516.
- Seipenbusch R, Birckenstaedt JW, Blenke H, Schindler F. Optimization of oxygen and substrate supply for paraffin-based fermentation in a loop reactor. *Pp. 65, Abstracts: Fifth International Fermentation Symposium*, Berlin; 1976.
- Shah YT, Godbole SP, Deckwer WD. Design parameters estimations for bubble column reactors. *AIChE J*. 1982;28:353-379.
- Shamlou PA, Pollard DJ, Ison AP. Volumetric mass transfer coefficient in concentric – tube airlift bioreactors. *Chem Eng Sci*. 1995;10:1579-1590.
- Shivaji K, Murty GSRN. Kinetics of sulfite oxidation reaction. *Ind Eng Chem Fundam*. 1982;21:344-352.
- Siegel MH, Merchuk JC, Schugerl K. Airlift reactor analysis: Interrelationships between riser, downcomer and gas-liquid separator behavior, including gas recirculation effects. *AIChE J*. 1986;32:1585-1596.

- Siegel MH, Merchuk JC. Mass transfer in air–lift reactors: effects of gas recirculation. *Bioreactors and Biotransformations*. (Moody GW, Baker PB., editors), Elsevier Publication. 1987: 350-362.
- Silapakul S, Powtongsook S, Pavasant P. Nitrogen compounds removal in a packed bed external loop airlift bioreactor. *Korean J Chem Eng*. 2005;22(3):393-398.
- Sinclair CG, Ryder DN, Lehrer IH. Application of Lehrer's technique to the calculation of mass transfer in a bubble column fitted with a draught tube. *Chem Eng Sci*. 1971;26(3):489-491.
- Sinha VT, Butensky MW, Hyman D. Three phase fluidization of polydisperse beads. *AIChE Symp Ser*. 1984;80(241):176-185.
- Smart NJ, Fowler MW. An airlift column bioreactor suitable for large-scale cultivation of plant cell suspensions. *J Exp Bot*. 1984;35:531-537.
- Smith DN, Fuchs W, Lynn RJ, Smith DH, Hess M. Bubble behavior in a slurry bubble column reactor model, chemical and catalytic reactor modeling. *ACS Symp Ser*. 1984;237:125.
- Sobotka M, Prokop A, Dunn IJ, Einsele A. Review of methods for the measurement of oxygen transfer in microbial systems. *Annual Reports on Fermentation Process*. (Tsao GT., editor) Academic Press(London).1982:127-210.
- Sweere APJ, Van Dalen JP, Kishoni E, Luyben KChAM, Kossen NWF, Renger RS. Theoretical analysis of the baker's yeast production: An experimental verification at a laboratory scale, part-1: liquid mixing and mass transfer. *Bioprocess Eng*. 1988;3:165-171.
- Sweere APJ, Van Dalen JP, Kishoni E, Luyben KChAM, Kossen NWF, Renger RS. Theoretical analysis of the baker's yeast production: An experimental verification at a laboratory scale, part-2: fed batch fermentations. *Bioprocess Eng*. 1989;4:11-17.
- Szewczyk KW, Warsaw. A model for baker's yeast growth. *Bioprocess Eng*. 1989;4:261-264.

- Thorat BN, Joshi JB. Regime transition in bubble columns: experimental and predictions. *Exp Therm Fluid Sci.* 2004;28:423–430.
- Tung HL, Chiou SY, Tu CC, Wu WT. An airlift reactor with double net draft tubes and its application in fermentation. *Bioprocess Eng.* 1997;17:1-5.
- Tung HL, Tu CC, Chang YY, Wu WT. Bubble characteristics and mass transfer in an airlift reactor with multiple net draft tubes. *Bioprocess Eng.* 1998;18:323-328.
- Van Dijken JP, Weusthuis RA, Pronk JT. Kinetics of growth and sugar consumption in yeasts. *Antonie van Leeuwenhoek.* 1993;63: 343-352.
- Van't Riet K. Review of measuring methods and results in nonviscous gas–liquid mass transfer in stirred vessels. *Ind Eng Chem Proc Des Dev.* 1979;18:357-364.
- Vatai G, Tekis MN. Effect of pseudo plasticity on hydrodynamic characteristics of airlift loop contactor. *Rheol Acta.* 1986;26:271.
- Vazquez G, Cancela MA, Riverol C, Alvarez E, Navaza JM. Determination of interfacial areas in bubble column by different chemical methods. *Ind Eng Chem Res.* 2000;39:2541-2547.
- Verlaan P, Tramper J. Hydrodynamics, axial dispersion and gas–liquid oxygen transfer in an airlift loop bioreactor with three-phase flow. *Bioreactors and Biotransformations.* (Moody GW, Baker PB., editors), Elsevier Publication. 1987: 363-373.
- Walker GM. *Yeast Physiology and Biotechnology.* Chichester, UK: Wiley, 1998.
- Wallis GB. *One Dimensional Two-Phase Flow.* New York: McGraw-Hill, 1969.
- Wang DIC, Hatch RT, Cuevas C. Engineering aspects of single-cell protein production from hydrocarbon substrates: the airlift fermenter. In: *Proceedings of the 8th World Petroleum Congress.* 1971;5:149-166.
- Wei C, Xie B, Xiao H. Hydrodynamics in internal loop airlift reactor with a convergence-divergence draft tube. *Chem Eng Technol.* 2000;23(1):38-45.
- Weiland P, Onken U. Differences in the behavior of bubble columns and airlift loop reactors. *Ger Chem Eng.* 1981;4:174-181.

- Weiland P. Influence of draft tube diameter on operational behaviour of air lift loop reactors. *Ger Chem Eng.* 1984;7:374–385.
- Westerterp KR. Design of agitators for gas-liquid contacting. *Chem Eng Sci.* 1963;18(8):495-502.
- Westlake R. Large Scale continuous production of single cell protein. *Chem Ing Techn.* 1986;58:934-937.
- Whitaker A, Stanbury PF, Hall SJ. *Principles of Fermentation Technology*, 2nd ed. New York: Elsevier, 1995.
- Win SS, Impoolsup A, Noomhorm A. Growth kinetics of *Saccharomyces cerevisiae* in batch and fed-batch cultivation using sugarcane molasses and glucose syrup from Cassava starch. *J Ind Microbiol.* 1996;16:117-123.
- Wood PJ, Wiest EG. Assay of Sodium Hydrosulfite. In: *Proceedings of the American Association of Textile Chemists and Colorists; American Dyestuff Reporter:* 1957;443-447.
- Wood LA, Thompson PW. Application of air lift fermenter. pp. 157-172, In: *Proceedings of international conference on Bioreactor Fluid Dynamics*, Cambridge, England, 15-17 April, 1986.
- Wu JU, Wu WT. Fed-batch culture of *Saccharomyces cerevisiae* in an airlift reactor with net draft tube. *Biotechnol Progr.* 1991;7:230-233.
- Wu WT, Hsiun WT. Oxygen transfer in airlift reactor with multiple net draft tubes. *Bioprocess Eng.* 1996;15:59-62.
- Yagi H, Yoshida F. Gas absorption by newtonian and non–newtonian fluids in sparged agitated vessels. *Ind Eng Chem Proc Des Dev.* 1975;14:488-493.
- Yamashita F. Effect of ratio of aerated area of partition plates on gas holdup in bubble columns with partition plates. *J Chem Eng Jpn.* 1994;27:418-420.
- Yoo H, Ahn KH, Lee HJ, Lee KH, Kwak YJ, Song KG. Nitrogen removal from synthetic wastewater by simultaneous nitrification and denitrification (SND) via nitrite in an intermittently-aerated reactor. *Wat Res.* 1999;33(1):145-154.

- Yoshida F, Ikeda A, Imakawa S, Miura Y. Oxygen absorption rates in stirred gas-liquid contactors. *Ind Eng Chem*. 1960;52(5):435-438.
- Yoshida F, Miura Y. Effective interfacial area in packed columns for absorption with chemical reaction. *AIChE J*. 1963;9:331-337.
- Yoshimoto M, Suenaga S, Furumoto K, Fukunaga K, Nakao K. Gas-liquid interfacial area, bubble size and liquid-phase mass transfer coefficient in a three-phase external loop airlift bubble column. *Chem Biochem Eng*. 2007;21(4):365-372.
- Yuan JQ, Bellgardt KH, Deckwer WD, Jiang WS. Modification and verification of the dynamic cell cycling model for baker's yeast. *Bioprocess Eng*. 1993; 9:173-182.
- Zaruba A, Krepper E, Prasser H, Reddy M, Vanga BN. Experimental study on bubble motion in a rectangular bubble column using high speed video observations. *Flow Meas Instrum*. 2005a;16:277-287.
- Zaruba A, Krepper E, Prasser H, Schleicher H, Vanga BN. Measurement of bubble velocity profiles and turbulent diffusion coefficients of the gaseous phase in rectangular bubble column using image processing. *Exp Therm Fluid Sci*. 2005b;29:851-860.
- Zhao B, Li Y, Tong H, Zhuo Y, Zhang L, Shi J, Chen C. Study on the reaction rate of sulfite oxidation with cobalt ion catalyst. *Chem Eng Sci*. 2005;60:863-868.
- Zhuang J. *Economic analysis of cellulose production by Clostridium thermocellum in solid state and submerged fermentation*. M. S. thesis, University of Kentucky, Lexington, United states, 2004.
- Zlokarnik M. Sorption characteristics for gas-liquid contacting in mixing vessels. *Adv Biochem Eng*. 1978;8:133-151.
- Zou R, Jiang X, Li B, Zu Y, Zhang L. Studies on gas holdup in a bubble column operated at elevated temperatures. *Ind Eng Chem Res*. 1988;27:1910-1916.

APPENDIX - I

IODOMETRIC TITRATION

The Iodometric titration used to determine the decrease in sodium sulfite concentration during sulfite oxidation technique of interfacial area determination is as under:

a) Preparation of 0.1N Iodine Solution

- i. Dissolve 20 gm of Potassium Iodide (KI) in 300 ml distilled water.
- ii. Add 13 gm of ground iodine powder in above prepared 300 ml KI solution.
- iii. Swirl the solution until the powder iodine get dissolved into the KI solution.
- iv. Filter the above prepared solution through glass wool.
- v. Washing the glass wool with distilled water and make the final volume 1000 ml using distilled water.
- vi. The solution thus prepared is approximately 0.1N iodine solution.

b) Analytical Procedure

- i. Collect about 5-6 ml solution from column through sampling valve in a measuring cylinder.
- ii. Take 2 ml solution from above measuring cylinder in a 250 ml conical flask.
- iii. Add about 2-3 drops of 1% starch solution as an indicator in above flask.
- iv. Titrate it against 0.1N iodine solution.
- v. Add 0.1N iodine solution till color changes to dark blue.
- vi. Note down the reading.
- vii. Repeat the above procedure and take other readings.
- viii. Find out the sulfite concentration of the sample by conventional titrimetric calculations.

APPENDIX - II

PREDICTION OF DIFFUSIVITY OF OXYGEN

In the determination of interfacial area determination using sulfite oxidation method, Diffusivity of oxygen (D_A) in water was estimated by the most comprehensive Wilke-Chang equation as follows:

$$D_A = 7.4 \times 10^{-8} \frac{(x M_B)^{1/2} T}{\eta_B V_A^{0.6}}$$

Where,

D_A is the diffusivity of oxygen, cm^2/s

M_B is the molecular weight of solvent (water) = 18

T is temperature = 303 K

x is the association factor of solvent (water) = 2.6

η_B is viscosity of solvent (water) = 1 cP

V_A is the molar volume of the solute (O_2) at normal boiling point = $25.6 \text{ cm}^3/\text{mol}$

APPENDIX-III

JUSTIFICATIONS OF ASSUMPTIONS IN DYNAMIC GASSING IN METHOD

The dynamic gassing in technique used in the present investigation for determination of volumetric mass transfer coefficient in draft tube bubble columns, assumed a constant gas phase composition, a “well mixed” liquid and a negligible effect of the dynamics of the dissolved oxygen electrode, justified briefly as below:

- **The constant gas phase composition**

The positional variations in the gas phase composition can affect the saturation concentration C^* of oxygen in the liquid and thereby influence the apparent $k_L a$. For the transfer of a sparingly soluble gas such as oxygen the gas phase mixing is of negligible importance. However, numerous theoretical and experimental demonstrations of this fact are available (Deckwer et al., 1974; Govindarao, 1975). The reason for this observation is that even at the maximum values of $k_L a$ in pneumatically mixed air – water dispersions (no chemical reaction), less than 0.01% of the oxygen in the total air input of the reactor is transferred to the liquid. For practical purposes, the oxygen partial pressure in the gas phase remains unchanged and the assumption of a constant gas phase composition applies.

- **A “well – mixed” liquid**

Although no gas-liquid contactor of any significant dimensions can be considered “well-mixed” in liquid, the “well-mixed” assumptions can be justified for the mass transfer work for large vessels containing highly viscous (and relatively poorly mixed) fluids. Because the typical $k_L a$ measurements are reproducible to about $\pm 10\%$, agreement of $k_L a$ values from two or more properly located sampling points to within $\pm 10\%$ may be taken as an indication of fully mixed behavior. This is even more so when the mass transfer rates are relatively low (i.e. $k_L a \leq 0.1 \text{ s}^{-1}$). Many investigators (Siegel and Merchuck, 1987; Verlaan and Tramper, 1987) also regard the insignificant impact of liquid mixing on mass transfer and on $k_L a$ calculations for draft tube bubble columns. The fluid (air-water) mixing and the gas-phase mixing considerations are unimportant

from $k_L a$ calculation viewpoint especially when a sparingly soluble gas such as oxygen is involved and the liquid hydrodynamics are in the range of typical pneumatically agitated reactors. It should be noted, however, that in external loop draft tube bubble columns the liquid flow tends more toward plug flow and the mixing tends to be somewhat poorer than in the internal loop draft tube bubble columns as use in the present investigation.

- **The negligible influence of DO electrode dynamics**

In the transient technique the dynamics of the oxygen electrode itself may influence the $k_L a$ results. The electrode delays, which are a function of the fluid hydrodynamics near its measuring surface, may be satisfactorily accounted for by the first- order model (Nakanoh and Yoshida, 1980; El-Temtamy et al., 1984; Chisti et al., 1987)

$$\frac{C^* - C_L}{C^* - C_{L0}} = \left(\frac{e^{-t k_L a}}{t_E} - k_L a e^{-\frac{t}{t_E}} \right) \frac{t_E}{1 - t_E k_L a}$$

Where t_E is the electrode time lag. For $t \gg t_E$ above equation reduces to,

$$\frac{C^* - C_L}{C^* - C_{L0}} = \frac{e^{-t k_L a}}{1 - t_E k_L a}$$

$$\ln \left(\frac{C^* - C_{L0}}{C^* - C_L} \right) = \ln \left(\frac{1 - t_E k_L a}{e^{-t k_L a}} \right)$$

$$\ln \left(\frac{C^* - C_{L0}}{C^* - C_L} \right) = k_L a t + \ln (1 - t_E k_L a)$$

Thus, a plot of $\ln \left(\frac{C^* - C_{L0}}{C^* - C_L} \right)$ against time, t yields a straight line of slope $k_L a$ and intercept $\ln (1 - t_E k_L a)$ from which the time delay may be obtained.

The maximum response time of the DO electrodes used was almost always under 10 seconds, which was in keeping with the manufacturer's data. Care should be taken to ensure that the C_L values from C_L Vs t curves were read at least 20 seconds after the start of the initial operation. This will ensure that the complete development of the hydrodynamics, and furthermore, the condition that $t \gg t_E$ was also satisfied. Nakanoh and Yoshida (1983) found that the $k_L a$ calculated by taking the probe response into account did not differ significantly from the values obtained by assuming instantaneous

response ($t_E = 0$) for $k_L a$ values $\leq 0.1 \text{ s}^{-1}$. They subsequently ignored the probe response in their calculation of $k_L a$. The same observation was reported by Yagi and Yoshida (1975) in quite viscous Newtonian and non-Newtonian fluids. Van't Riet (1979) showed that ultimate error in $k_L a$ to be $< 6\%$ as long as the DO electrode response time (63% of full scale) was $\leq 1/k_L a$. Thus, the $k_L a$ data determined by taking the electrode dynamics into consideration and that determined by ignoring the probe delays did not differ much, so the effects of dynamics of DO electrodes can be neglected in $k_L a$ calculations.

APPENDIX - IV

CALIBRATION OF DO PROBE

The stepwise procedure for calibration of DO Probe in water saturated air, used in the dynamic gassing-in method for determining volumetric mass transfer coefficient in draft tube bubble columns, in the present investigation is as follows: (DO probe with its parts is shown in Fig.3.7 of chapter-3)

1. Remove the membrane protector from the membrane cap. Do not cover the small hole on the protector with fingers during removal of the protector.
2. Hold the membrane cap in a vertical position, open-end up.
3. Fill the membrane cap about 2/3 full with Dissolved Oxygen Electrolyte Filling Solution.
4. While holding the DO probe vertically with the tip pointing down, gently screw the module cap onto the tip. Electrolyte should leak out of the thread (Note: If electrolyte does not leak out of the threads, air may remain inside the module cap. To ensure accurate results, repeat this procedure using more filling solution).
5. Attach the DO probe cable connector to the meter.
6. With the probe in the calibration and storage chamber, observe the mg/L dissolved oxygen concentration after the probe has been polarized for the appropriate period of time. Calibration may be performed when the display is stable for several minutes.
7. Secure the probe cable to the calibration and storage chamber by wrapping cable through the bottom of the chamber lid before filling with water.
8. Prepare the calibration and storage chamber by holding it under water and squeezing it a couple of times to pull a small amount of water into the lower chamber through the inlet. Alternately, open the bottom of the chamber and insert a water-soaked sponge. (Note: Avoid completely filling the lower part of the calibration chamber with water).
9. Insert the DO probe into the calibration and storage chamber. The tip of the probe must not be flooded with water or be holding a drop of water on the membrane.
10. Allow at least ten minutes for the atmosphere in the chamber to reach a steady state. (Note: Gently squeezing the lower chamber a couple of times to force water-saturated air into the probe chamber will speed up stabilization. Avoid

squeezing liquid water into the chamber). (Note: Keep the DO probe at a uniform temperature. When holding the probe, do not touch the metallic button on the side of the probe. The button is a thermistor that senses temperature. An inaccurate calibration will result if the temperature of the thermistor is different from the probe membrane).

11. Press the DO key to put the meter in DO Reading mode.
12. Press the CAL key located in the lower left corner of the keypad to initiate calibration.
13. The display will show 100%. Press the ENTER key. The stabilizing icon will appear while the meter completes the calibration.
14. When the calibration is complete, the meter will return to the reading mode. Press the EXIT key during the calibration sequence to back out of the calibration routine, one screen at a time, without completing a calibration. (Note: If the Cal and ? icons flash after calibration, the calibration failed and needs to be repeated).

APPENDIX-V

MANUAL PHENATE METHOD

The reagents used and the stepwise procedure of the manual phenate method used for nitrogen estimation in wastewaters is discussed below:

- **Reagents:**

- i. ***Phenol solution:*** Mix 11.1 ml liquefied phenol ($\geq 89\%$) with 95% v/v methyl alcohol to a final volume of 100 ml. Prepare this solution weekly. (Caution: Wear gloves and eye protection when handling phenol; use good ventilation to minimize all personnel exposure to this toxic volatile substance).
- ii. ***Sodium nitroprusside, 0.5% w/v:*** Dissolve 0.5 gm sodium nitroprusside in 100 ml deionized water. Store in amber bottle for up to 1 month.
- iii. ***Alkaline citrate:*** Dissolve 20 gm trisodium citrate and 1 gm sodium hydroxide in deionized water. Dilute to 100 ml.
- iv. ***Sodium hypochlorite, commercial solution, about 5%:*** This solution slowly decomposes once the seal on the bottle cap is broken. Replace about every 2 months.
- v. ***Oxidizing solution:*** Mix 100 ml alkaline citrate solution with 25 ml sodium hypochlorite. Prepare fresh daily.
- vi. ***Stock ammonium solution:*** Dissolve 4.714 gm of anhydrous $(\text{NH}_4)_2\text{SO}_4$ in deionized water and dilute to 1 liter. So, this stock solution is having 1000 mg of $\text{NH}_3\text{-N/L}$ of solution.
- vii. ***Standard ammonium sulfate solution:*** For obtaining a calibration curve, prepare a series of standard solutions in the appropriate range of the concentrations of the samples such as 0(blank), 0.1, 0.2, 0.3, 0.4, 0.5 and 0.6 mg $\text{NH}_3\text{-N/L}$ of solution by stepwise dilution from stock solution of 1000 mg/L to 100 mg/L to 10 mg/L to 1 mg/L and so on.

- **Procedure:**

1. To a 25-ml sample in a 50-ml erlenmeyer flask, add, with thorough mixing after each addition, 1 ml phenol solution, 1 ml sodium nitroprusside solution, and 2.5 ml oxidizing solution.
2. Cover samples with plastic wrap or paraffin wrapper film. Let color develop at room temperature in subdued light for at least 1 h. An intensely blue compound, Indophenol, is formed by the reaction of ammonia, hypochlorite, and phenol catalyzed by sodium nitroprusside. Color is stable for 24 hr.
3. Measure absorbance at 640 nm wavelength in spectrophotometer (Hach, DR/2400) with a light path of 1 cm or greater using quartz cuvette.
4. Treat all standard solutions the same as samples.

APPENDIX - VI

ASCORBIC ACID METHOD

The reagents used and the stepwise procedure of the ascorbic acid method used for phosphorus estimation in wastewaters is discussed below:

- **Reagents:**

- i. **Sulfuric acid, H_2SO_4 , 5N:** Dilute 70 ml concentrated H_2SO_4 to 500 ml with distilled water.
- ii. **Potassium antimonyl tartrate solution:** Dissolve 1.3715 gm $K(SbO)C_4H_4O_6 \cdot \frac{1}{2} H_2O$ in 400 ml distilled water in a 500-ml volumetric flask and dilute to volume. Store in a glass- stoppered bottle.
- iii. **Ammonium molybdate solution:** Dissolve 2 gm $(NH_4)_6Mo_7O_{24} \cdot 4H_2O$ in 500 ml distilled water. Store in a glass- stoppered bottle.
- iv. **Ascorbic acid:** Dissolve 1.76 gm ascorbic acid in 100 ml distilled water. The solution is stable for about 1 week at 4°C.
- v. **Combined reagent:** Mix the above reagents in the following proportions for 100 ml of the combined reagent: 50 ml 5N H_2SO_4 , 5 ml potassium antimonyl tartrate solution, 15 ml ammonium molybdate solution, and 30 ml ascorbic acid solution. Mix after addition of each reagent. Let all reagents reach room temperature before they are mixed and mixed in the order given. If turbidity forms in the combined reagent, shake and let stand for a few minutes until turbidity disappears before proceeding. The reagent is stable for 4 hr.
- vi. **Stock phosphate solution:** Dissolve 0.2195 gm of anhydrous KH_2PO_4 in distilled water and dilute to 1 liter. So, this stock solution contains 50 mg/L of PO_4^{3-} - P (phosphorus as phosphates).
- vii. **Standard phosphate solution:** To obtain a calibration curve, prepare a series of standard solutions of 0(blank), 0.2, 0.5, 0.8, 1, 2, 3, 4, 5 and 6 mg/L of P as PO_4^{3-} by appropriate dilution of the stock phosphate solution.

- **Procedure:**

1. Pipet 50 ml sample into a clean, dry test tube or 125-ml erlenmeyer flask. Add 0.05 ml (1 drop) phenolphthalein indicator. If a red color develops add 5N H₂SO₄ solution dropwise to just discharge the color.
2. Add 8 ml combined reagent and mix thoroughly. Ammonium molybdate and potassium antimonyl tartrate react in acid medium of combined reagent with orthophosphate to form a heteropoly acid - phosphomolybdic acid - that is reduced to intensely colored molybdenum blue by ascorbic acid.
3. After at least 10 min but not more than 30 min, measure absorbance of each sample at 880 nm wavelength in spectrophotometer (Hach, DR/2400) with a light path of 1 cm using quartz cuvette and with reagent blank as reference solution.
4. Treat all standard phosphate solutions the same as samples and use a distilled water blank with the combined reagent to make photometric readings for the calibration curve.

Note: Use acid-washed glassware for determining concentrations of phosphorus by the ascorbic acid method. Phosphate contamination is common because of its absorption on glass surfaces. Avoid using commercial detergents containing phosphate. Clean all glassware with hot dilute HCl and rinse well with distilled water. Preferably, reserve the glassware only for phosphate determination and after use, wash and keep filled with water until needed. If this is done, acid treatment is required only occasionally.

APPENDIX - VII

COLE'S METHOD

The stepwise procedure of the Cole's method used for total sugar estimation in fermentation broth is discussed below:

1. Concentrated hydrochloric acid in the ratio of 1: 20 is added to the supernatant (cell free sample after centrifugation) for inversion of sugar present in it. Keep it on boiling water bath for 20 minutes.
2. Cool it and make up total volume to 21 ml with distilled water.
3. To neutralize the acidity, sodium bicarbonate was added till the effervescence come out from the hydrolyzed sample.
4. Measure 20 ml of 1% w/v aqueous ferricyanide solution and 5 ml of 2.5 N sodium hydroxide solutions in 100 ml flask. Place it on wire gauze over a flame.
5. Heating should be arranged in such a way that the mixture begins to boil within 2 minutes. As soon as the mixture boils, the flame can be lowered. Active boiling should be maintained during the whole titration.
6. Add 2 – 3 drops of 1% methylene blue.
7. Titrate with the hydrolyzed sample. Sugars having free –CO and –CHO groups, when heated in alkaline solution, these keto or aldehyde group is converted to form enediol. This has more reducing power and reduces $K_3Fe(CN_6)^{-3}$ to $K_4Fe(CN_6)^{-4}$ and sugars are oxidized to complex mixture of acids. The amount of ferricyanide reduced depends upon the concentration of sugar.
8. The end point is reached when the solution is decolorized.
9. Note down the titration reading (X ml) and calculate the amount of sugar according to following formula:

$$\text{Sucrose} = 19.2 + (0.065 X) \text{ mg} / X \text{ ml}$$

10. Divide above value with 10 to get total sugar % in w/v of the sample.